

**Primary metabolism and its regulation in the human
cell line AGE1.HN – application of metabolic flux
analysis for improved biopharmaceutical production**

Dissertation
zur Erlangung des Grades
des Doktors der Ingenieurwissenschaften
der Naturwissenschaftlich-Technischen Fakultät III
Chemie, Pharmazie, Bio- und Werkstoffwissenschaften
der Universität des Saarlandes

von
Jens Niklas

Saarbrücken

2011

Tag des Kolloquiums: 23.03.2012
Dekan: Prof. Dr. Wilhelm F. Maier
Berichterstatter: Prof. Dr. Elmar Heinzle
Prof. Dr. Manfred Schmitt
Prof. Dr. An-Ping Zeng
Vorsitz: Prof. Dr. Wilhelm F. Maier
Akad. Mitarbeiter: Dr. Gert-Wieland Kohring

“Rien ne sert de courir; il faut partir à point.”

Jean de La Fontaine

Table of contents

Table of contents.....	4
Abstract.....	5
Zusammenfassung.....	6
Aim and outline of the thesis	7
1 General introduction – metabolic flux analysis in mammalian cells	9
2 Quantitative characterization of metabolism and metabolic shifts during growth of the new human cell line AGE1.HN using time resolved metabolic flux analysis.....	28
3 Metabolite channeling and compartmentation in the human cell line AGE1.HN determined by ¹³ C labeling experiments and ¹³ C metabolic flux analysis.....	48
4 Primary metabolism in the new human cell line AGE1.HN at various substrate levels: increased metabolic efficiency and α_1 -antitrypsin production at reduced pyruvate load.....	63
5 Metabolic flux rearrangement in the amino acid metabolism reduces ammonia stress in the α_1 -antitrypsin producing human AGE1.HN cell line	82
6 Metabolism and metabolic burden by α_1 -antitrypsin production in human AGE1.HN cells.....	102
7 Quercetin treatment changes fluxes in the primary metabolism and increases culture longevity and recombinant α_1 -antitrypsin production in human AGE1.HN cells	121
8 Outlook and future prospects.....	135
Summary	139
References.....	143
Supplementary material	157
Acknowledgements	165
Curriculum vitae	167

Abstract

This thesis focused on generating a detailed understanding of the primary metabolism and its regulation in the novel human cell line AGE1.HN and the application of the acquired knowledge to improve biopharmaceutical production. The different issues that were addressed include (i) metabolic shifts during cultivation, (ii) metabolite channeling and metabolic fluxes during overflow metabolism, (iii) primary metabolism at various substrate levels and the effect of different substrate feeding on cell culture process and metabolism, (iv) adaptation of the metabolism to ammonia stress, (v) metabolism and metabolic burden imposed by recombinant α_1 -antitrypsin production, and (vi) improvement of metabolism and biopharmaceutical production in AGE1.HN. Several types of metabolic network modeling and metabolic flux analysis (MFA) were applied. A time resolved MFA approach was developed to analyze metabolic shifts over time. Stationary MFA using mass balances was used extensively to identify alterations in the metabolism induced by physiological perturbations. ^{13}C tracers and ^{13}C MFA were applied to get in-depth insights into metabolite channeling and compartmented fluxes in the metabolism. The presented results provide valuable guidance for improvement of AGE1.HN, in particular, and of the biopharmaceutical production in mammalian cells in general. Additionally, this thesis contributes to an improved understanding of metabolic regulation in human cells.

Zusammenfassung

In dieser Arbeit wurden der Primärmetabolismus und dessen Regulation in der humanen Zelllinie AGE1.HN analysiert, wobei der Fokus auf der Anwendung des erworbenen Wissens zur Verbesserung der biopharmazeutischen Produktion lag. Folgende Aspekte wurden untersucht: (i) Veränderungen des Metabolismus im Kultivierungsverlauf, (ii) metabolische Flüsse unter Überflussbedingungen, (iii) Metabolismus und α_1 -Antitrypsin-Produktion bei verschiedenen Substratkonzentrationen, (iv) Anpassung des Metabolismus an Ammonium-Stress, (v) zelluläre und metabolische Adaptation an die Produktion von rekombinantem α_1 -Antitrypsin und (vi) Verbesserung des Metabolismus und der biopharmazeutischen Produktion in AGE1.HN. Verschiedene Arten der Modellierung von metabolischen Netzwerken sowie der metabolischen Flussanalyse (MFA) wurden hierbei angewendet. Eine dynamische MFA Methode wurde zur Analyse metabolischer Veränderungen entwickelt. Stationäre MFA wurde verwendet um Anpassungen des Metabolismus zu charakterisieren. ^{13}C Markierungsexperimente sowie ^{13}C MFA wurden genutzt um detaillierte Einsichten in das *Channeling* von Metaboliten sowie in die metabolischen Flüsse innerhalb und zwischen verschiedenen Kompartimenten zu erlangen. Die Ergebnisse stellen eine wertvolle Basis zur weiteren Verbesserung der biopharmazeutischen Produktion in AGE1.HN sowie in anderen Säugerzellen dar. Die vorliegende Arbeit trägt zusätzlich zu einem besseren Verständnis der Metabolismus-Regulation in humanen Zellen bei.

Aim and outline of the thesis

The work described in this thesis was imbedded in the BMBF project SysLogics – Systems biology of cell culture for biologics. This project aimed at the development and refinement of system biological methods for the analysis of metabolic and regulatory processes in mammalian cells. Additionally, these methods were applied for an in-depth characterization of the physiology of the novel human cell line AGE1.HN which was developed for the production of challenging glycoproteins requiring complex human-type glycostructures. A thorough knowledge of the dynamics of cellular metabolism and related regulatory processes is mandatory for setting up models that might eventually allow the performance of the cells under varying conditions to be predicted.

The pre-defined goals of this thesis were (i) the development and refinement of methods for metabolic flux analysis in industrially relevant, mammalian cell culture processes and (ii) the application of these methods to study the central metabolism in the AGE1.HN cell line and derived producer clones.

A general introduction to metabolic flux analysis and its significance for system biological research in mammalian cells is provided in **chapter 1**. Additionally, application examples of metabolic flux analysis in different mammalian cells are reviewed.

When we started to work with the new cell line AGE1.HN, almost nothing was known about the metabolism in these cells. In **chapter 2**, the first characterization of the AGE1.HN cell line concerning growth, metabolic profiles, and intracellular metabolism is presented. For an improved analysis of the metabolic shifts that were observed during cultivation, we additionally developed a flexible metabolic flux analysis method, called time resolved metabolic flux analysis, which is suitable for analyzing fluxes in industrially relevant cell culture processes in which the cellular metabolism has to adapt to a changing environment. Metabolism and metabolic shifts during batch cultivation of AGE1.HN were analyzed by this dynamic method and compared to flux estimates obtained by stationary metabolic flux analysis. We were able to identify the main events triggering alterations in the metabolism.

Very detailed insights into the metabolism of AGE1.HN during overflow conditions were obtained by employing labeling experiments using ^{13}C labeled substrates and by performing ^{13}C metabolic flux analysis. The data are presented in **chapter 3**. We were able to verify connections between different metabolite pools and the activity of central metabolic pathways was unraveled. Additionally, the results were useful to get further hints for an optimization of the cell line and its cultivation. One finding which was particularly interesting was the observed low connectivity between cytosolic pyruvate and mitochondrial pyruvate pools during overflow conditions.

The adaptation of the primary metabolism of AGE1.HN to various substrate levels was analyzed in a following study which is presented in **chapter 4**. An important finding of this analysis was an increasingly inefficient metabolism with increasing pyruvate load. We were able to show in cultivations of an α_1 -antitrypsin producing cell clone, AGE1.HN.AAT, applying different feeding profiles that reduction of pyruvate load improves metabolic efficiency and increases α_1 -antitrypsin production.

The accumulation of toxic waste products during cell culture processes is still a factor that limits the productivity. **Chapter 5** focuses on the detailed analysis of the effects of elevated ammonia concentrations on growth, metabolism, and α_1 -antitrypsin production in AGE1.HN.AAT cells. We were able to unravel the adaptation mechanism of this cell line to high ammonia conditions which is accomplished by global flux rearrangement in the amino acid metabolism leading to increased fixation of free ammonia in specific amino acids.

What are the specific cellular properties responsible for high-level glycoprotein production in selected producer clones? This question is addressed in **chapter 6** by comparing the high producing cell line AGE1.HN.AAT with the parental cell population. By analyzing dynamics of biomass constituents, metabolic differences, and by modeling and simulation of the metabolic burden imposed by glycoprotein production, we were able to identify important properties of the producer. The data pointed to further interesting targets for improvement of biopharmaceutical production not only in the AGE1.HN cell line but also in mammalian cells in general.

Optimization of biopharmaceutical production can be performed, e.g., by genetic engineering of cell lines or media optimization. Based on the previous detailed studies, it was possible to design an engineering strategy for improving the metabolic phenotype of AGE1.HN. Besides the modification of substrate concentrations in the medium, as applied in the study in chapter 4, addition of specific substances having selected beneficial effects on cell physiology, primary metabolism, protein production, and product yields represents a promising strategy that is addressed in **chapter 7**. It is shown that addition of the flavonoid quercetin remarkably improves the overall performance of the cells and, eventually, the final product titer. Using the available analytical and developed metabolic flux analysis tools, we were able to show that quercetin treatment results in specific dose-dependent changes in the primary metabolism of this human cell line. Additionally, we were able to contribute to an improved understanding of quercetin action on human cells.

In **chapter 8** possible future prospects are presented and discussed.

Systems biology has become an increasingly exciting field in biological science. An increasing number of research institutions and groups are focusing on this field, and various public and private funding agencies and companies are substantially supporting research in this field. The major reason for this substantial investment is the anticipated increase in understanding the functioning of biological systems that is expected to strongly support the creation of new and improved therapies, drugs, as well as biotechnological processes (Alberghina and Westerhoff 2005; Choi 2007). The enormous booming of this area is heavily driven by the breathtaking progress in molecular biology combined with the development of large-scale experiments whose data collection and analysis only became possible with the new bioinformatic methods and tools. Bioinformatics has made it possible to store relevant data on databases that are quickly accessible by everybody at any time on a global scale. In parallel, techniques of mechanistic modeling are evolving that permit structured development of mathematical models and their solution on a larger scale. It is primarily these models that are essential in the process of conceptual clarification and that allow testing the power of prediction.

Mammalian cells are model organisms that are used to help understanding diseases like cancer or neurological diseases (Villoslada et al. 2009) and identifying suitable drug targets. Mammalian cells, particularly human cells, are of increasing relevance for testing the metabolism and toxicity of drug candidates (Beckers et al. 2010; Niklas et al. 2009; Noor et al. 2009). Another major application of mammalian cells is in the production of biopharmaceuticals (O'Callaghan and James 2008), in particular of proteins such as antibodies, but also of vaccines and viral carriers for gene therapy (Genzel and Reichl 2009; Wurm 2004). Hereby, a solid systems understanding will assist in improving product quality, e.g., correct human glycosylation, and product titers, e.g., by systems-supported media design or model-driven genetic modifications. Engineering of producing cells will be supported by a new discipline, synthetic biology, that helps designing new biological systems or elements thereof, e.g., new promoters, switches, or sensors (Koide et al. 2009; Weber and Fussenegger 2007). In order to understand and improve production processes or to understand toxic effects, methods are needed that can describe the different phenotypes of the cells under different conditions. Metabolic fluxes or intracellular reaction rates represent an endpoint of a metabolic network reflecting all types of network events including regulation at different levels, i.e., gene, protein, and metabolic interactions (Niklas et al. 2010; Sauer 2006), making it a very powerful method for systems biology research (Fig. 1-1).

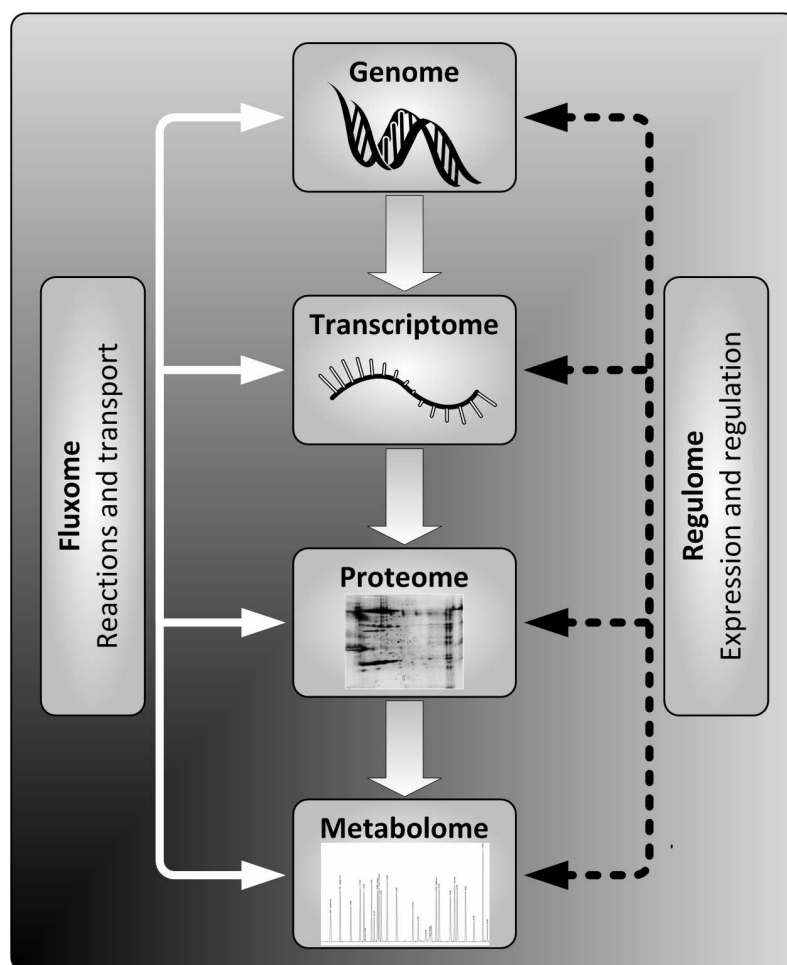


Fig. 1-1 Interactions on the various levels of the cellular hierarchy (Niklas and Heinzle 2011).

The analysis of metabolic fluxes has been employed extensively in the past to understand, design, and optimize a number of cell types and biological processes (Boghigian et al. 2010; Niklas et al. 2010; Quek et al. 2010). Metabolic flux analysis (MFA) provides a quantitative description of *in vivo* intracellular reaction rates in metabolic networks describing activities of intracellular enzymes and whole pathways (Wittmann 2007). Fluxes can be quantified either by using metabolite balancing, often also called flux balance analysis (FBA), or by ^{13}C MFA, which involves the use of ^{13}C isotope-labeled substrates (Wiechert and de Graaf 1996).

Flux analysis using metabolite balancing for microorganisms was described as early as 1978 (Aiba and Matsuoka 1978). It has been and still is the most commonly applied method for the analysis of the metabolism of mammalian cells (Bonarius et al. 1996; Niklas et al. 2009; Quek et al. 2010; Sidorenko et al. 2008). The accuracy of flux estimates can be improved compared to pure metabolite balancing by using ^{13}C tracers in metabolic flux studies and later incorporation of the resulting labeling information stored in the metabolites into the flux calculation. Different mathematical methods that have been developed in the past have significantly contributed to the applicability of ^{13}C flux analysis. Zupke and Stephanopoulos introduced the concept of atom mapping matrices (AMM) for the modeling of isotope distributions in metabolic networks (Zupke and Stephanopoulos 1994). A following important advancement was the introduction of isotopomer mapping matrices (IMM) by Schmidt et al. (Schmidt et al. 1997), which

allowed using the complete information of the isotopomer distributions of metabolites and the elegant use of matrices for solving complex isotopomer models. Another method is based on local isotopomer balances and allows the estimation of local flux split ratios (Fischer et al. 2004; Nanchen et al. 2007; Sauer et al. 1997). This method is generally very suitable for high-throughput because of its easy calculation. Flux split ratios can be used directly and interpreted biologically, or can serve as additional constraints for FBA. Metabolic flux screening on a miniaturized scale using mass spectrometry was shown to be a promising method for high-throughput analysis of cellular phenotypes (Velagapudi et al. 2007). Whereas earlier labeling patterns were mostly analyzed by NMR (Sonntag et al. 1993; Zupke and Stephanopoulos 1995), in the late 1990s, GC-MS was proposed as a possible competitive technique and mass isotopomer distributions obtained from GC-MS measurements can be sufficient for detailed analysis of metabolic fluxes (Wittmann and Heinzle 1999). In 1999 Wiechert et al. provided an elegant procedure for solving isotopomer balances and introduced the concept of cumulative isotopomers (cumomers) (Wiechert et al. 1999). Another significant improvement for flux calculation was presented by Antoniewicz et al. (Antoniewicz et al. 2007). They introduced an efficient decomposition algorithm that identifies the minimum amount of information needed to simulate the isotopic labeling in a reaction network. This so-called elementary metabolite unit (EMU) framework significantly reduces the computation time needed for flux estimation. Another milestone, in particular, for studying compartmented systems is the introduction of specific fluorescence resonance energy transfer (FRET) techniques (Nüttläe et al. 2009). The determination of individual compartmental concentrations by using FRET nanosensors that can be combined with ^{13}C flux analysis might allow studying even fluxes between compartments and different cells, providing deeper insights into metabolic compartmentation in eukaryotic cells in future studies. As can be seen in the literature, MFA was mostly applied in biotechnology to increase the productivity of producing microorganisms (Becker et al. 2005; Kiefer et al. 2004; Wittmann and Heinzle 2002). In mammalian cells, it is still less established owing to their higher complexity, particularly, concerning compartmentation, complex medium requirements, and unbalanced growth behavior. However, there have been a number of interesting studies applying MFA in the past, mainly in the areas of cell culture technology and toxicology/medicine (Forbes et al. 2006; Maier et al. 2009; Niklas et al. 2009; Srivastava and Chan 2008; Vo and Palsson 2006). These studies are mostly performed under the assumption of metabolic steady state, which is a prerequisite for stationary MFA. In mammalian cells the question remains whether a true steady state and balanced growth behavior can be achieved. In particular, in batch cultures in which the medium composition changes and the cellular metabolism has to adapt to a changing environment, true metabolic steady state will not be achieved. Mammalian cells change their metabolism as a response to different substrate concentrations, e.g., low and high glucose concentrations (Sanfeliu et al. 1997). There are different possibilities to deal with this challenge of usually unbalanced growth. In most cases mean fluxes are calculated for the exponential growth phase of the cells, and during this phase metabolic steady state is assumed, which is often a fair assumption (Niklas et al. 2009; Sidorenko et al. 2008). Another possibility is to examine metabolism and flux distributions over time using dynamic approaches (Llaneras and Pico 2007; Niklas et al. 2011d). If specific short time effects on the metabolism

are to be investigated, e.g., effects of certain compounds, transient ^{13}C flux analysis would be an interesting but still very sophisticated method (Maier et al. 2009). For reliable ^{13}C metabolic profiling in mammalian cell culture processes, which usually takes several days, a special medium design could be an option to come close to metabolic and isotopic steady state allowing stationary ^{13}C flux analysis (Deshpande et al. 2009). Different flux estimation methods applied to mammalian cells are depicted and compared in Fig. 1-2.

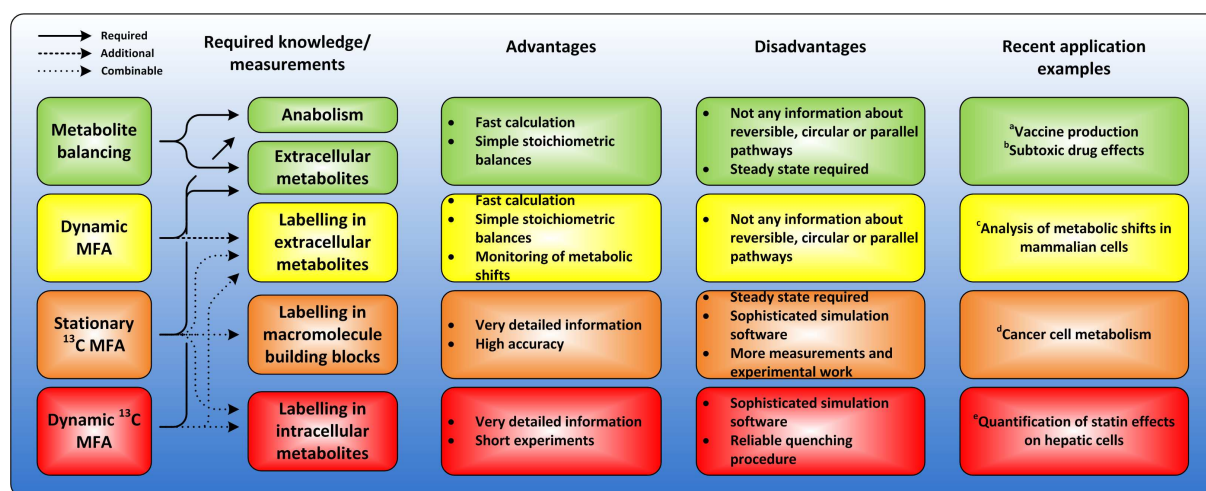


Fig. 1-2 Methods of whole cell metabolic flux distribution measurement in mammalian cell systems with required knowledge and measurements and their advantages and disadvantages. ^a(Sidorenko et al. 2008), ^b(Niklas et al. 2009), ^c(Niklas et al. 2011d), ^d(Metallo et al. 2009), ^e(Maier et al. 2009). This figure was published in Niklas et al. (Niklas et al. 2010).

1.1 Theoretical aspects: methods for MFA

Different MFA methods are available as discussed before. A typical workflow of a stationary ^{13}C MFA is depicted in Fig. 1-3. If metabolite balancing is applied without the use of any tracers, only the measurement of labeling patterns would be excluded from the workflow. Another main difference between metabolite balancing methodology and ^{13}C MFA is computation. Flux calculations can be straight forward using metabolite balancing as described in section 1.1.1 In ^{13}C MFA (1.1.2), metabolite balancing is extended by carbon isotopomer balances resulting in a nonlinear least squares problem. This can be solved, e.g., by using efficient numerical optimization techniques (Weitzel et al. 2007; Yang et al. 2008).

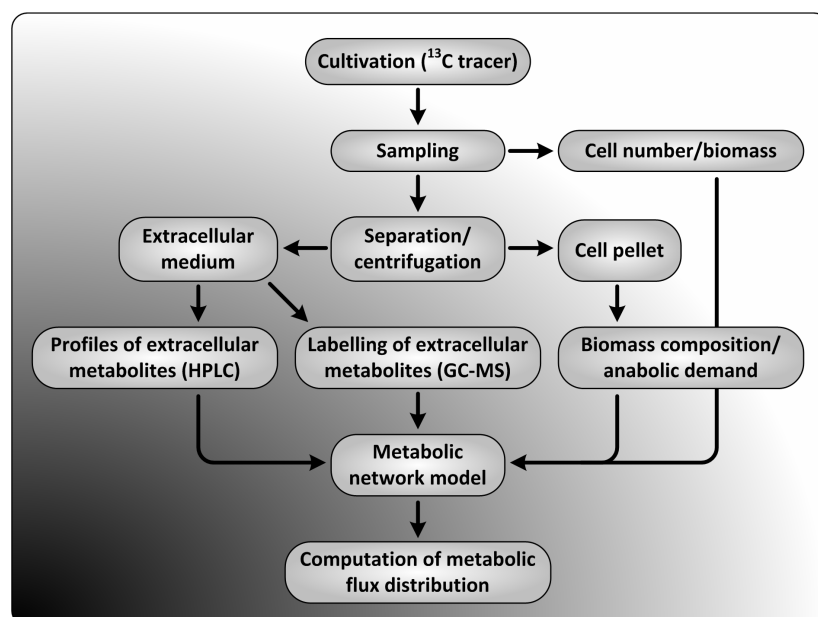


Fig. 1-3 Exemplary workflow of an experiment for metabolic flux analysis (Niklas and Heinzle 2011).

1.1.1 Stoichiometric models and metabolite balancing in mammalian cells

The metabolite balancing or flux balancing technique is the MFA method that has been applied most often for the analysis of animal cell metabolism. The stoichiometric models used for flux balancing can also be applied for *in silico* prediction of network characteristics (e.g., maximal yields, optimal pathways, minimum substrate requirements) (Fong et al. 2005; Kromer et al. 2006; Wahl et al. 2008) or prediction of optimal genetic modifications using different algorithms (Melzer et al. 2009; Patil et al. 2005; Segre et al. 2002; Suthers et al. 2007; Trinh et al. 2009). The importance of these targeted optimization approaches is rapidly increasing, which is also caused by an increasing availability of genomic information as well as genome-scale models of different mammalian species (Duarte et al. 2007; Quek and Nielsen 2008; Selvarasu et al. 2010). The general metabolite balancing methodology is depicted in Fig. 1-4. The first step is to set up a network that describes the part of the metabolism to be investigated. Metabolic network models of the central metabolism of mammalian cells have been described and applied in a number of studies (Niklas et al. 2009; Quek et al. 2010; Sidorenko et al. 2008; Srivastava and Chan 2008; Wahl et al. 2008). As an example, a model of the human central metabolism is presented in Fig. 1-5. An important database that can be used to set up metabolic networks is the Kyoto Encyclopedia of Genes and Genomes (KEGG) pathway database (<http://www.kegg.com>). If a metabolic network consists of N fluxes and M internal metabolites, it has $F = N - M$ degrees of freedom, meaning that F fluxes have to be measured to determine all remaining fluxes (Nielsen 2003). The calculation of metabolic fluxes in an overdetermined network (more measurements than necessary) results in a set of calculated fluxes that represents a least squares solution. In this case, it can also be checked if measurements are consistent meaning that the balance around each metabolite is zero. The network is underdetermined if not enough measurements are available, which can also be seen by calculating the rank of the stoichiometric matrix. If the rank is lower than the number of internal metabolites, the network is underdetermined. In this case the network has to be simplified or specific fluxes must be assumed *a priori*. If insufficient fluxes are

measured, this can sometimes be easily solved by measuring extra rates. Other options exist to calculate fluxes in underdetermined parts of the network which would extend the metabolite balancing method. Thermodynamic constraints can be used indicating that certain reactions do not take place or can only proceed in one direction (Beard et al. 2004). Expression data or measurements of *in vitro* enzyme activities can be used to exclude specific reactions in the network (Akesson et al. 2004; Korke et al. 2004; Vriezen and van Dijken 1998; Wahl et al. 2008). Another possibility is to use specific objective functions such as, e.g., maximizing energy production to find flux distributions that optimize the applied objective function (Savinell and Palsson 1992a, 1992b). Probably, the best possibility is the use of labeled substrates (^{13}C tracers) and analysis of resulting labeling patterns in metabolites providing additional information about cellular metabolism. The labeling of specific metabolites can be used, for example, to get information about fluxes at branch points like the glycolysis/pentose phosphate pathway (PPP) split (Lee et al. 1998). ^{13}C MFA is further explained in the next paragraph.

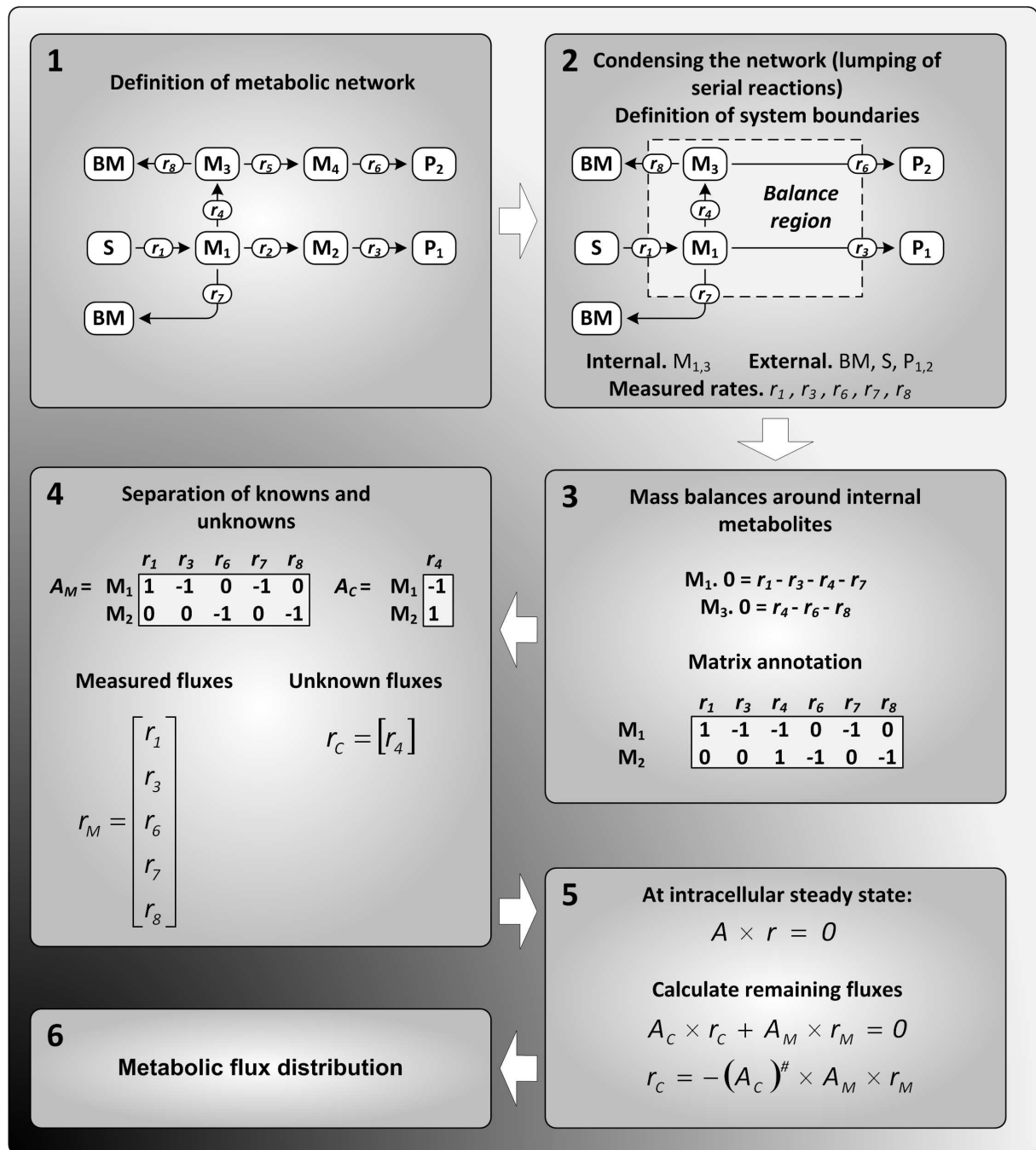


Fig. 1-4 Procedure of metabolic flux analysis using the metabolite balancing technique. *BM* biomass, *M* metabolite, *S* substrate, *P* product, *r* reaction rates, *A* stoichiometric matrix, $(A)^\#$ pseudo inverse of the matrix (Niklas and Heinzle 2011).

The metabolic network model in Fig. 1-5 for flux balancing in human cells and general aspects of modeling metabolic networks in mammalian cells will be explained in this section. The metabolic network can be divided into the following parts:

Central energy metabolism The main pathways of the energy metabolism are represented, i.e., glycolysis, oxidative decarboxylation, TCA-cycle, electron transport chain, and oxidative phosphorylation. Since it is not known for some reactions in the model whether NADH or NADPH take part and due to possible activity of nicotinamide nucleotide transhydrogenases, NADH and NADPH were lumped together. The

excess of NAD(P)H and FADH₂ considering their consumption and production in all reactions permits the estimation of the total ATP excess. However, the P/O ratio which is the amount of ATP formed per NADH oxidized is usually not exactly known. In the literature, different P/O values were assumed or estimated (Martens 2007; Miller et al. 1987; Wahl et al. 2008; Xie and Wang 1996a). The calculated ATP excess in the presented model example (Fig. 1-5) represents an estimate of the amount of ATP that is needed in the cell, e.g., for maintenance and transport reactions but also for so-called substrate or futile cycles (Russell 2007).

Pentose phosphate pathway The PPP consists of an oxidative and a nonoxidative branch. The split between glycolysis and PPP and the reversible reactions of the non-oxidative part cannot be resolved by metabolite balancing alone. Therefore, PPP is usually assumed to be responsible only for nucleic acid synthesis in pure metabolite balancing studies and the nonoxidative part is neglected. However, there are possibilities for obtaining some information concerning the glycolysis/PPP split by using additional ¹³C tracer experiments (Lee et al. 1998), which can be included in the metabolic flux calculation.

Amino acid metabolism The metabolism of proteinogenic amino acids is usually modeled by selected degradation pathways. Where several pathways are possible the most probable and suitable pathway can be chosen or additional experiments (e.g., enzyme activity measurements) can be performed to evaluate this. Since metabolite balancing can only be used to calculate net fluxes, there are no data concerning reversibility as for example in the synthesis and degradation of nonessential amino acids such as alanine and glutamate. The degradation flux of essential amino acids should usually be close to zero or higher, but never below zero. Values below zero would indicate that there are errors in the metabolite measurement or in the applied anabolic demand.

Further reactions The reactions catalyzed by the enzymes malic enzyme (cytosolic and mitochondrial), phosphoenolpyruvate carboxykinase, and pyruvate carboxylase represent parallel or reversible pathways and also cannot be distinguished by pure metabolite balancing. Again this can be solved by assuming activities for some of these enzymes, by taking data from other experiments, or by lumping all these reactions together into one reaction representing the sum of all these fluxes converting malate/oxaloacetate to pyruvate as was done in the model in Fig. 1-5.

Synthesis of biomass Fluxes to biomass can be represented as five fluxes to the major macromolecules of the cell, i.e., proteins, carbohydrates, DNA, RNA, and lipids. Hereby, the lipid fraction also contains the cholesterol part of the cells. These anabolic fluxes are calculated using the specific anabolic demand of the cells, which is derived from the biomass composition of the cells. In most flux studies, the biomass composition is assumed constant. However, in detailed studies concerning cellular biomass dynamics, it was shown that this composition and also the total biomass of the cells (e.g., dry weight) can vary during cultivation or at different growth conditions (Jang and Barford 2000; Nielsen et al. 1997). The methods that are usually used to determine cellular macromolecules are, however, time-consuming and require relatively large quantities of sample material making it usually not possible to determine the biomass composition in every flux analysis experiment which would, strictly speaking, be required.

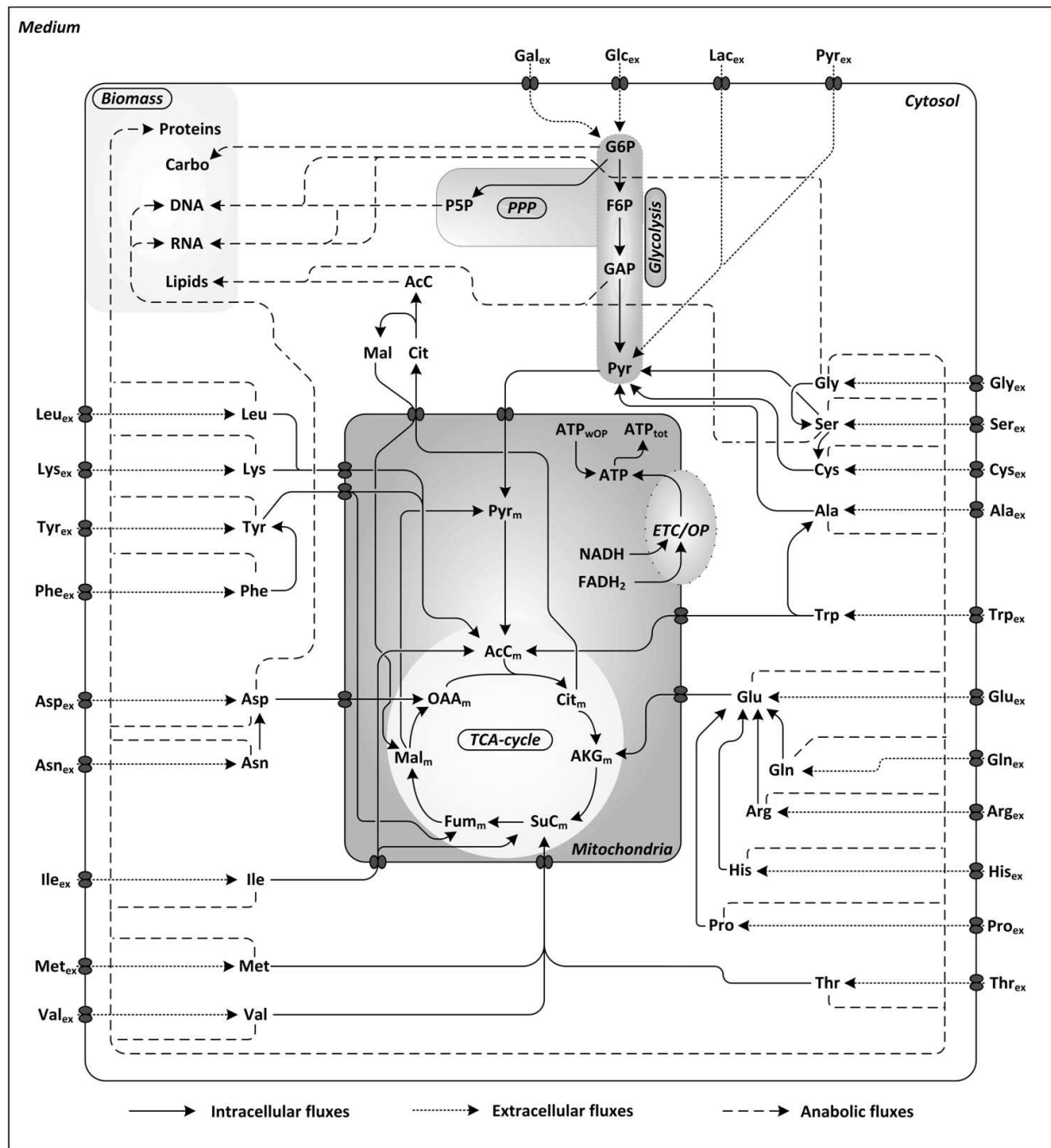


Fig. 1-5 Exemplary stoichiometric metabolic network model of a human cell (Niklas and Heinzle 2011). *ETC* electron transport chain, *OP* oxidative phosphorylation, *PPP* pentose phosphate pathway, *TCA* tricarboxylic acid, *AcC* acetyl coenzyme A, *AKG* a-ketoglutarate, *ATP* adenosine triphosphate, *ATP_{tot}* total ATP, *ATP_{wOP}* ATP without oxidative phosphorylation, *Carbo* carbohydrates, *Cit* citrate, *F6P* fructose 6-phosphate, *FADH₂* flavin adenine dinucleotide, *Fum* fumarate, *G6P* glucose 6-phosphate, *GAP* glyceraldehyde 3-phosphate, *Gal* galactose, *Glc* glucose, *Lac* lactate, *Mal* malate, *NADH* nicotinamide adenine dinucleotide, *OAA* oxaloacetate, *P5P* pentose 5-phosphate, *Pyr* pyruvate, *SuC* succinyl coenzyme A, standard abbreviations for amino acids. Indices: *m* mitochondrial, *ex* extracellular.

1.1.2 ^{13}C Metabolic Flux Analysis

In mammalian cells, relevant information can already be obtained by the metabolite balancing methodology since the number of measurable uptake and production fluxes of metabolites is large. However, there are several cases in which the balancing technique is insufficient. In particular, certain circular pathways, reversible reactions, and alternative pathways cannot be resolved (Fig. 1-6). Most important underdetermined parts in the metabolic network of mammalian cells are typically the PPP split, the anaplerotic/gluconeogenic fluxes around pyruvate/phosphoenolpyruvate/malate/oxaloacetate, and reversibility of uptake and production of substrate metabolites. Specific metabolic compartmentations, such as, e.g., different intracellular pools of metabolites as suggested for pyruvate (Zwingmann et al. 2001), are other parts that cannot be resolved just by balancing. In some situations, it might be possible to use well-defined constraints to solve some underdetermined parts. Mass balances of cofactors, e.g., ATP and NAD(P)H, irreversibility of reactions, or specific objective functions have been proposed and reviewed as additional constraints (Bonarius et al. 1997). However, balancing of the energy metabolites (ATP, NAD(P)H) does not seem generally applicable since this would require knowing all energy-producing and -consuming reactions as well as all conversion reactions between the energy metabolites (Wiechert 2001). In addition, the P/O ratio can vary and can usually not be determined precisely (Sauer and Bailey 1999), substrate or futile cycles might impair results, e.g., in the anaplerosis (Petersen et al. 2000), and for some reactions it is just not known which co-metabolite, NADH or NADPH, is used. E.g., malic enzyme and isocitrate dehydrogenase enzymes can utilize NADH or NADPH (<http://www.kegg.com>). In case of PPP split, it would be possible to get some estimates about its activity by balancing NADPH. However, transhydrogenation reactions can occur in the cells transferring reducing equivalents between NADPH and NADH, which would falsify PPP estimates. In a study comparing results obtained by metabolite balancing with those from ^{13}C MFA, discrepancies were found concerning PPP split (Schmidt et al. 1998). All the shortcomings and limitations of the metabolite balancing method can be overcome by getting more information through application of isotopically labeled ^{13}C tracers. These tracers are ^{13}C labeled substrates that are taken up by the cell, and the labeled carbon atoms are distributed through the cellular metabolism in a clearly defined way (Fig. 1-7). Depending on the activity of enzymes and metabolic pathways, this will result in specific labeling patterns in metabolites. These chemically identical compounds with different isotope composition are referred to as isotopomers. As depicted in Fig. 1-7, labeling in extracellular and intracellular metabolites can be measured but also the labeling in macromolecule building blocks, e.g., amino acids in proteins, provides equivalent information. Extracellular metabolites can be easily measured since these are directly present in the medium, usually, in high abundance.

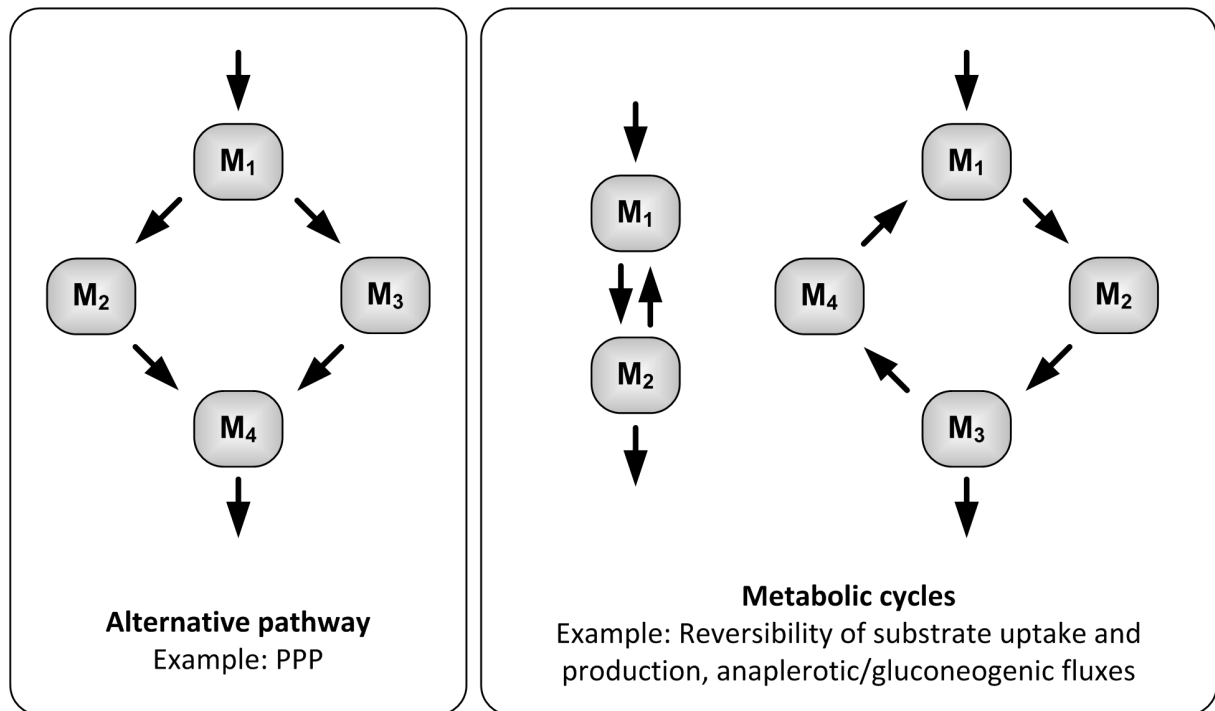


Fig. 1-6 Cases in which the metabolite balancing technique is limited and examples in the metabolism (Niklas and Heinzle 2011). *M* metabolite.

However, measurement of intracellular metabolites requires reliable quenching of the metabolism and appropriate extraction methods. This is fairly established for adherent cells (Hofmann et al. 2008; Maier et al. 2008) but still much more complicated for suspension cells (Dietmair et al. 2010). Measurement of the labeling in monomers of macromolecules, as is often done in studies on prokaryotes (Becker et al. 2005), is usually not suitable for flux analysis in mammalian cells. This is because mammalian cells generally have much lower growth rates than microorganisms and, therefore, slow macromolecule turnover and slow labeling incorporation.

The measurement of labeling patterns in metabolites can be performed by nuclear magnetic resonance (NMR) measurements, gas chromatography mass spectrometry (GC-MS), liquid chromatography mass spectrometry (LC-MS), (Sauer et al. 1997; Wittmann 2007; Wittmann and Heinzle 1999; Christensen and Nielsen 1999; Des Rosiers et al. 2004; Kelleher 2001; Maaheimo et al. 2001; Matsuda et al. 2003; Wittmann et al. 2002), matrix-assisted laser desorption ionization-time of flight mass spectrometry (MALDI-ToF MS) (Wittmann and Heinzle 2001a, 2001b), capillary electrophoresis MS (Toya et al. 2007), or membrane inlet MS (Yang et al. 2006b). Recently, it was demonstrated that gas chromatography combustion-isotope ratio mass spectrometry (GC-C-IRMS) is another interesting method for labeling quantification in ^{13}C MFA with a low labeling degree of tracer substrate, which is interesting for performing MFA in larger scale cultivations like industrial pilot scale fermentations (Heinzle et al. 2008; Yuan et al. 2010). Compared to NMR, MS seems to be more attractive, which is mainly due to higher sensitivity and rapid data accumulation (Wittmann 2002). Certain potential problems of MS that would impair flux analysis, like isotope effects or naturally occurring isotopes particularly in atoms other than carbon, can be solved efficiently using specific correction methods (Dauner and Sauer 2000; Heinzle et al.

2008; Moseley 2010; van Winden et al. 2002; Wahl et al. 2004; Wittmann and Heinzle 1999; Yang et al. 2009).

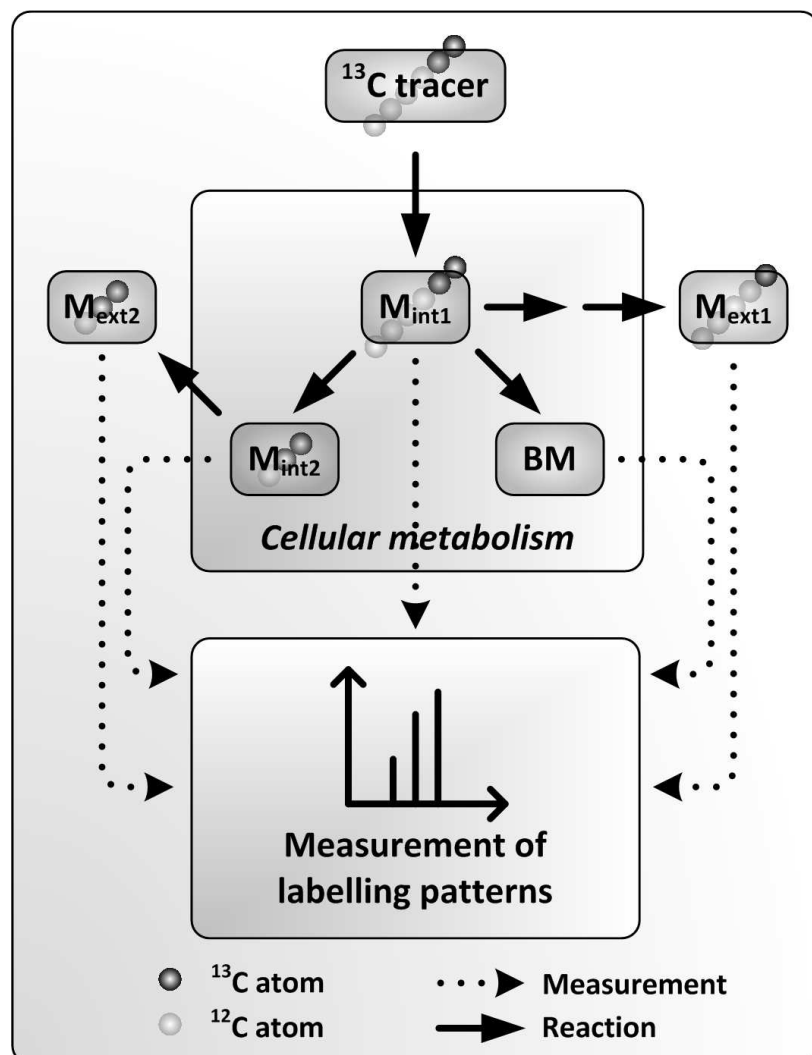


Fig. 1-7 ^{13}C tracer experiment (Niklas and Heinzle 2011). The labeling of the tracer is distributed through the metabolism resulting in specifically labeled intracellular metabolites (M_{int}), extracellular metabolites (M_{ext}), and biomass (BM) components. Measurement of labeling patterns can be performed directly in intracellular or extracellular metabolites but also in macromolecule building blocks of biomass constituents.

For ^{13}C MFA, the carbon atom transitions in the metabolic network of the cell have to be modeled. The concept of AMM, which is a systematic formulation of atom transfers (Zupke and Stephanopoulos 1994), was further expanded by the IMM concept (Schmidt et al. 1997). This allowed calculating mass and NMR spectra directly from isotopomer abundance (Wittmann and Heinzle 2008). The introduction of cumomers (Wiechert et al. 1999) and later EMUs (Antoniewicz et al. 2007) improved computation of fluxes. The computational part in ^{13}C MFA can be performed by using available software packages (Quek et al. 2009; Wiechert et al. 2001; Zamboni et al. 2005). Further description of ^{13}C MFA can also be found in several review articles (Sauer 2006; Wittmann 2007; Sauer 2004; Wiechert 2001; Wittmann and Heinzle 2008). ^{13}C MFA can be further divided into stationary and dynamic approaches, which both have been applied successfully in mammalian cells (Goudar et al. 2010; Maier et al. 2008; Metallo et al. 2009; Niklas et al. 2011c). Metabolic steady state is a prerequisite for stationary ^{13}C MFA. This is still a challenge, in particular, for suspension cells used in industrial production. Appropriate medium design can be an option

also enabling detailed ^{13}C MFA in suspension cells during exponential growth (Deshpande et al. 2009). For adherent cells, the problem of instationarity can be overcome by using transient ^{13}C MFA as demonstrated on hepatic cells (Hofmann et al. 2008; Maier et al. 2009; Maier et al. 2008). The tracers that are mostly applied in ^{13}C MFA on mammalian cells are different glucose and glutamine tracers since these metabolites are the main substrates of mammalian cells (Eagle 1959). Depending on the question of the study and the applied metabolic network structure, different tracers or combinations of tracers will be best suitable (Metallo et al. 2009).

1.2 Application of MFA in systems biology of mammalian cells

1.2.1 Optimization of cell culture processes

Mammalian cells are extensively used for the production of vaccines (Genzel and Reichl 2009) and therapeutic proteins requiring specific post-translational glycosylation (Seth et al. 2006; Wurm 2004). The number of biopharmaceuticals available for treatment of severe diseases as well as the quantity produced is steadily growing (Pavlou and Reichert 2004). Therapeutic proteins are mainly expressed in Chinese hamster ovary (CHO) cells, but also other cell lines are commonly employed, such as murine myeloma, hybridoma, baby hamster kidney (BHK), or human embryo kidney cells (HEK-293) (Chu and Robinson 2001; Wurm 2004). New, engineered human cell lines also represent very promising production systems, e.g., the cell lines AGE1.HN (Niklas et al. 2011d) and PER.C6 (Pau et al. 2001). Vaccine production is conventionally carried out in embryonated chicken eggs. However, especially in the last decade, several cell culture-derived vaccines have been established (Genzel and Reichl 2009). Much effort has been made to optimize cell culture processes to increase productivity and product quality. This includes on the one hand optimization of the cultivation and on the other hand targeted engineering of the cell. Different cellular pathways that are associated with superior characteristics concerning cell growth and production were engineered. This includes central metabolism, protein synthesis and secretion, protein glycosylation, post-translational modifications, cell cycle control, and apoptosis (Godia and Cairo 2002; Lim et al. 2010; Seth et al. 2006). Optimization of the metabolism of the producer cell is mandatory for different reasons. On the one hand efficient energy metabolism is important. In particular, the production of recombinant proteins requires a great deal of energy. On the other hand final product titers are directly dependent on integral viable cell density and lifespan of the culture, which can be increased when the substrate usage of the cell is very efficient. In an ideal scenario this would mean that the cell does not accumulate toxic waste products, which would decrease the lifespan of the culture, and substrates are taken up just to fulfill the cellular demand. Analyses of the metabolism and metabolic flux studies have significantly contributed in the past to understanding and optimizing the metabolism of mammalian cells. In this section metabolic flux studies in hybridoma and myeloma cells, CHO cells, and cell lines that are used for vaccine production are reviewed.

1.2.1.1 MFA in hybridoma and myeloma cells

Hybridoma and myeloma cells are widely employed for the production of monoclonal antibodies (Chu and Robinson 2001). In many studies, MFA was used to understand the metabolism of these cells. Savinell and Palsson (Savinell and Palsson 1992a, 1992b) applied linear optimization theory to understand the influences of fluxes on overall cell behavior and to analyze limitations. They concluded that neither antibody production nor maintenance demand for ATP limited cell growth. Medium design represents one of the most important issues in optimizing cell culture processes, which is also reflected by many metabolic flux studies in this area. Xie and Wang (Xie and Wang 1996b, 1997) presented a balancing approach to design culture media for fed-batch cultures that integrated substrates, products, pH, osmolarity, and cell growth. They also estimated stoichiometric ATP production in batch and fed-batch cultures of hybridoma cells (Xie and Wang 1996a). Another interesting study focused on regulation of fluxes in the central metabolism of myeloma cells (Vriezen and van Dijken 1998). By determining fluxes and enzyme activities in the central metabolism, the regulation of metabolic fluxes could be shown to occur mainly through modulation of enzyme activity. Determination of metabolic fluxes for multiple steady states in hybridoma continuous culture indicated that the performance could be improved by inducing specific cellular metabolic shifts leading to favourable flux distribution (Follstad et al. 1999). Europa et al. performed fed-batch cultivations that were then switched to continuous mode (Europa et al. 2000). This approach enabled reaching a more desirable steady state with higher concentrations of cells and product. Additionally, from analyses of hybridoma cells at different physiological states, it was reported that the amino acid metabolism is very important in reducing lactate production (Gambhir et al. 2003). In an earlier metabolite balancing study using additional constraints to resolve underdetermined parts in the metabolic network, Bonarius et al. found that around 90% of the glucose was channeled through PPP, which was very surprising (Bonarius et al. 1996). In a following study using ^{13}C mass spectrometry in combination with ^{13}C lactate NMR spectroscopy and metabolite balancing, it was found that just 20% is channeled through PPP (Bonarius et al. 2001). This shows that different methods can yield very different results. As mentioned before, cofactor balance constraints must be used very carefully. In particular for estimation of PPP, constraints based on ^{13}C labeling might be much more realistic since the labeling measurement is usually very accurate and carbon transition in the reactions is exactly determined. Another interesting aspect that was analyzed by Bonarius et al. using MFA was the cellular response to oxidative and reductive stress (Bonarius et al. 2000). They reported that particularly dehydrogenase reactions producing NAD(P)H were decreased under oxygen limitation. In a recent study, it was reported that antibody production in hybridoma cells could be increased by enhancing specific fluxes through the addition of specific metabolites to the medium (Omasa et al. 2010). Fluxes between malate and pyruvate were increased by the addition of the intermediates pyruvate, malate, and citrate, resulting in increased ATP and antibody production. This is a good example showing how metabolic flux data can be used to improve the metabolic phenotype in a cell culture process. Another important step is the construction of mathematical models that can be used to predict growth, metabolism, and product

formation during the cultivation. Dorka et al. utilized an approach based on MFA to model batch and fed-batch cultures of hybridoma cells (Dorka et al. 2009). Genome-scale modeling and *in silico* simulations for fed-batch cultures of hybridoma cells were recently carried out suggesting that the applied methodology might serve as a valuable tool for targeted optimization in the future (Selvarasu et al. 2009b).

1.2.1.2 MFA in CHO cells

CHO cells (Puck et al. 1958) represent the main workhorse for the industrial production of biopharmaceuticals (Chu and Robinson 2001). In several studies, the metabolism of these cells under different conditions was analyzed. CHO cells are often cultured in media supplemented with specific hydrolysates that contain many peptides, which makes MFA more complicated. Nyberg et al. (Nyberg et al. 1999b) reported that these potential substrates must be balanced for accurate metabolic flux estimates. In another study, metabolic effects on the glycosylation of recombinant protein were reported. Particularly glutamine limitation seemed to influence glycosylation remarkably (Nyberg et al. 1999a). Altamirano et al. published several results on medium design and favourable fed-batch strategies for CHO (Altamirano et al. 2006; Altamirano et al. 2001; Altamirano et al. 2004). MFA was performed, in particular, to understand lactate consumption in CHO cells grown on galactose. It was found that lactate was not used as a fuel in the TCA cycle (Altamirano et al. 2006). A very important aspect in mammalian cell culture processes is the optimization of the bioreactor operation. Goudar et al. presented an approach for quasi real-time estimation of metabolic fluxes (Goudar et al. 2006). Cellular physiology and metabolism can be monitored by combining on-line and off-line data to calculate metabolic fluxes. This methodology can help in optimizing the cultivation process. Recently, the same group analyzed metabolic fluxes of CHO cells in perfusion culture by applying metabolite balancing and 2D-NMR spectroscopy (Goudar et al. 2010). Flux data obtained by metabolite balancing in this case corresponded well with flux information from 2D-NMR spectroscopy. Recently, a study was published in which MFA was performed for the late non-growth phase in CHO cultivation (Sengupta et al. 2010). In this case a combination of metabolite balancing and isotopomer analysis was used. The most surprising finding in this study was that almost all of the consumed glucose was channeled through PPP. This result is in contrast with several publications that determined different flux distributions in the growth phase of CHO or other cells (Goudar et al. 2010; Lee et al. 1998; Maier et al. 2008; Mancuso et al. 1994; Metallo et al. 2009; Vo and Palsson 2006).

1.2.1.3 MFA in cell lines for production of vaccines and viral vectors

Another promising and important application of mammalian cell culture is the production of vaccines (Audsley and Tannock 2008; Genzel and Reichl 2009). A number of cell lines were identified to be suitable for high-yield vaccine manufacturing (Genzel et al. 2010), e.g., madin darby canine kidney (MDCK) cells (Kessler et al. 1999), HEK-293 cells (Le Ru et al. 2010), or specifically engineered cell lines such as PER.C6 or AGE1.CR (Jordan et al. 2009; Pau et al. 2001). Optimization of cell culture processes for vaccine production is still mainly done by trial and error. Detailed metabolic studies might help substantially to understand cell culture based vaccine production (Ritter et al. 2010) and enable targeted optimization. Wahl et al. investigated an influenza vaccine production process in MDCK cells using a

segregated growth model for distinct growth phases in the batch process. Comparison of observed metabolic fluxes with theoretical minimum requirements revealed large optimization potential for this process (Wahl et al. 2008). Flux analysis of MDCK in glutamine-containing media and media in which glutamine was replaced by pyruvate was presented in another publication (Sidorenko et al. 2008). Ammonia and lactate release were remarkably reduced in a high pyruvate medium without further dramatic changes in the central metabolism. Henry and co-workers showed that MFA can provide a basis to develop a feeding strategy for perfusion cultures of HEK-293 cells for production of adenovirus vectors (Henry et al. 2005). Martinez et al. compared metabolic states of HEK-293 cells during growth and adenovirus production to optimize media according to the cellular demand (Martinez et al. 2010). Higher cell densities and increased adenovirus production were achieved.

1.2.2 MFA in medical research

MFA was mostly applied in the past by bioengineers to understand phenotypes of producer cells. But another very important field in which MFA can contribute substantially is the medical sector. Defects in mitochondrial function contribute to many physiological diseases. Ramakrishna et al. (Ramakrishna et al. 2001) stated that FBA of mitochondrial energy metabolism might be a useful methodology to characterize the pathophysiology of mitochondrial diseases. The strength of metabolic flux data, as mentioned in the beginning of this chapter and shown in Fig. 1-1, is the integration of all interactions at different levels of the cellular hierarchy. Therefore, specific flux patterns that reflect a certain physiological response might be indicators for specific diseases or genetic defects. Lee et al. proposed that MFA could be a very useful tool for tissue engineering (Lee et al. 1999). By applying MFA, it is possible to obtain a very comprehensive view of the metabolic state, and flux estimates under different conditions can be used to monitor and optimize tissue function. Forbes and co-workers described an interesting method that uses isotopomer path tracing to quantify fluxes in metabolic models containing reversible reactions and applied MFA to analyze the effects of estradiol on breast cancer cells (Forbes et al. 2001; Forbes et al. 2006). Metabolic fluxes were calculated from extracellular fluxes and isotope enrichment data generated by NMR. They observed that breast cancer cells are dependent on PPP and glutamine consumption for estradiol-stimulated biosynthesis and concluded that these pathways might be possible targets for estrogen-independent breast cancer therapy. Brain function and, in particular, physiological and pathophysiological regulation of neural metabolism were investigated in several metabolic studies. Zwingmann et al. investigated glial metabolism using ^{13}C -NMR (Zwingmann and Leibfritz 2003). They concluded that the observed metabolic flexibility of astrocytes might buffer the brain tissue against extracellular cytotoxic stimuli and metabolic impairments. In another study, the coupling between metabolic pathways of astrocytes and neurons was modeled and investigated by FBA (Cakir et al. 2007). By using the reconstructed model, effects of hypoxia could be fairly well predicted. This shows how stoichiometric models can be used in medical metabolic flux modeling. Teixeira et al. investigated the metabolism of astrocytes by combining ^{13}C -NMR spectroscopy and MFA (Teixeira et al. 2008). In a

subsequent study, the method was applied to analyze metabolic alterations induced by ischaemia in astrocytes (Amaral et al. 2010).

1.2.3 MFA in toxicology

The analysis of effects of drugs and chemicals on cellular metabolism is another very promising application of MFA and highly relevant for toxicological research. Toxicity of drugs is one of the leading causes of attrition at all stages of the drug development process (Kramer et al. 2007) and is mainly detected late in the pipeline where also most of the costs are incurred (Kola and Landis 2004). Identification of toxicity early in the drug development process would save a lot of money. Metabonomics is a system approach for studying *in vivo* metabolic profiles and has emerged in the last decade as a very powerful technique for studying drug toxicity, disease processes, and gene function (Nicholson et al. 2002; O'Connell and Watkins 2010; Winnike et al. 2010). MFA, which provides potentially more information than metabolic profiling, is, however, still not routinely used in toxicity studies, which might be mainly due to its presently low throughput. Some studies have focused on developing and adapting MFA methods and setups for high-throughput screening (Balcarcel and Clark 2003; Fischer et al. 2004; Hollemeyer et al. 2007; Sauer 2004; Velagapudi et al. 2007; Wittmann et al. 2004). Balcarcel et al. (Balcarcel and Clark 2003) presented a method called High-Throughput Metabolic Screening that can be used for faster screening of the overall activity of metabolic pathways in mammalian cells. In a recent study it was shown that MFA can be applied in a high-throughput setup to analyze subtoxic drug effects (Niklas et al. 2009). Several changes in the metabolism of Hep G2 cells could be detected upon exposure to subtoxic drug levels. In the future it might be possible to use MFA in a high-throughput format to detect specific metabolic signatures or flux patterns that are associated with specific toxicity mechanisms. Other studies analyzed effects of different compounds on cellular metabolism without focusing on high-throughput application of the applied methods. Srivastava and co-workers applied MFA to identify the toxicity mechanism of free fatty acids and metabolic changes in Hep G2 cells (Srivastava and Chan 2008). They observed that free fatty acid toxicity is associated with the limitation of cysteine import causing reduced glutathione synthesis. Another very promising MFA method was implemented by Maier et al. to quantify statin effects on hepatic cholesterol synthesis (Maier et al. 2009). Transient ^{13}C flux analysis was applied to study effects of atorvastatin at a therapeutic concentration.

Summarizing this section, it can be seen that there have been some interesting applications of MFA to identify toxicity mechanisms and metabolic effects of compounds. However, these methods must be applicable in high-throughput format to be attractive for larger scale toxicity screening. Additionally, the analysis has to be more detailed calling for improved analytical methods. Specific flux patterns and signatures for different toxicity mechanisms must be identified and clearly defined in the future, which would lead to a better understanding of toxicity at the metabolome level. Then it might be possible to elucidate possible side effects of compounds early in the drug development process.

1.3 Conclusions

MFA is a very important method for understanding the metabolism of mammalian cells under various conditions. The acquired knowledge can be used to optimize cell culture media and cellular phenotypes, to define favourable feeding strategies, as well as to understand mechanisms of toxicity and diseases. In suspension cells that are employed in industrial production, mainly MFA using metabolite balancing was applied. ^{13}C MFA cannot be directly applied in industrially relevant processes since metabolic steady state is not reached. As presented in some studies, continuous cultures are an option to enable detailed stationary ^{13}C flux studies. Dynamic methods are very promising tools to describe the dynamic and adaptive behavior of the cells during batch and fed-batch processes. Since they are still fairly complex and laborious, they are not yet widely applied. ^{13}C MFA is relatively established in tissues and adherent cells where the flux experiment can be performed at a short time scale and metabolic and isotopic steady state may be reached very fast. Transient ^{13}C flux analysis represents a very interesting method that may in many cases solve the problem of changing metabolism during cultivation of mammalian cells. The application examples presented in this chapter indicate that MFA can contribute significantly in many areas in which the metabolism of mammalian cells is of interest. However, MFA method development has to be intensified in the future to enable broader application in mammalian cell culture and to permit robust and realistic studies. Compartmentation of the metabolism is an issue that is often only rudimentarily considered in metabolic flux studies but is very important, especially, for ^{13}C MFA.

2 Quantitative characterization of metabolism and metabolic shifts during growth of the new human cell line AGE1.HN using time resolved metabolic flux analysis.

2.1 Abstract

For the improved production of vaccines and therapeutic proteins, a detailed understanding of the metabolic dynamics during batch or fed-batch production is requested. To study the new human cell line AGE1.HN, a flexible metabolic flux analysis method was developed that is considering dynamic changes in growth and metabolism during cultivation. This method comprises analysis of formation of cellular components as well as conversion of major substrates and products, spline fitting of dynamic data, and flux estimation using metabolite balancing. During batch cultivation of AGE1.HN, three distinct phases were observed, an initial one with consumption of pyruvate and high glycolytic activity, a second characterized by a highly efficient metabolism with very little energy spilling waste production, and a third with glutamine limitation and decreasing viability. Main events triggering changes in cellular metabolism were depletion of pyruvate and glutamine. Potential targets for the improvement identified from the analysis are (i) reduction of overflow metabolism in the beginning of cultivation, e.g., accomplished by reduction of pyruvate content in the medium, and (ii) prolongation of phase 2 with its highly efficient energy metabolism applying, e.g., specific feeding strategies. The method presented allows fast and reliable metabolic flux analysis during the development of producer cells and production processes from microtiter plate to large scale reactors with moderate analytical and computational effort. It seems well suited to guide media optimization and genetic engineering of producing cell lines.

This chapter was published as

Niklas J, Schröder E, Sandig V, Noll T, Heinzle E. Quantitative characterization of metabolism and metabolic shifts during growth of the new human cell line AGE1.HN using time resolved metabolic flux analysis. *Bioprocess Biosyst Eng.* 2011 Jun;34(5):533-45.

2.2 Introduction

Cell culture products represent currently the most important and most promising source for new biopharmaceuticals. The majority of recombinant biopharmaceuticals are produced by mammalian cell culture and this fraction is steadily increasing (Ferrer-Miralles et al. 2009; O'Callaghan and James 2008; Wurm 2004). The projected sales volume for therapeutic proteins by 2010 is USD 70 billion (Pavlou and Reichert 2004; Walsh 2006). Commonly employed production cell lines are, e.g., Chinese Hamster Ovary (CHO) cells or murine lymphoid cells. These production systems must be capable of generating high quantities of proteins to enable the administration of high doses required in clinical application (Dinnis and James 2005; Rose et al. 2008; Sandig et al. 2005). A number of approaches were applied to optimize product yields (Kumar et al. 2007), e.g., cell cycle arrest and control of apoptosis (al-Rubeai and Singh 1998; Fogolin et al. 2004; Trummer et al. 2006; Yoon et al. 2003) or addition of nutrient supplements (Eyer et al. 1995; Oh et al. 2005; Sung et al. 2004). However, there is still room for improvement. New production cell lines are entering the market due to demands for higher product quality (e.g., glycosylation), efficiency, productivity, and robustness. Cell lines created from primary cells represent promising new production systems. These cell lines overcome typical limitations of other cells, e.g., serum requirements or attachment dependence, and eliminate also the repeated safety testing required for each new batch of primary tissue (Jordan et al. 2009). Concerning manufacturing of therapeutic proteins, engineered human cell lines may have in particular another unique advantage over standard producer cell lines, as, e.g., CHO cells, because of their genuine human post-translational modification machinery. The cell line AGE1.HN represents such a new human cell line which was immortalized and engineered for apoptosis resistance and can be used for production of recombinant proteins but also for viruses and viral vectors. However, further targeted optimization would be promoted by a profound knowledge of growth and metabolism of the cells. In order to find optimized cultivation conditions and targets for metabolic engineering for improved production, metabolic flux analysis seems most suited since it represents the functional end point of genome, proteome, and metabolome interactions (Nielsen 2003; Sauer 2006). This methodology has revealed valuable insights into the metabolism of several mammalian cell systems (Balcarcel and Clark 2003; Bonarius et al. 1996; Niklas et al. 2009; Sidorenko et al. 2008; Wahl et al. 2008). A requirement for reliable stationary metabolic flux analysis is metabolic steady state that is usually not reached due to complex growth requirements. It seems generally possible to optimize the medium such that metabolic steady state is reached during a longer period (Deshpande et al. 2009). However, if the metabolism of cells in a conventional medium should be investigated, dynamic changes of the cellular metabolism commonly observed in cell culture have to be monitored and considered (Altamirano et al. 2006). One way to deal with this challenge is to focus just on the exponential growth phase of the cells where in some cases metabolic steady state can be observed (Niklas et al. 2009). Another possibility is to divide the growth of the cells in different metabolic phases and calculate the flux distribution for each phase (Altamirano et al. 2006). The third possibility is to compute instantaneous flux distributions during the whole cultivation (Llaneras and Pico 2007). Most detailed information can be obtained using ^{13}C -

substrate labeling techniques. This can be accomplished either by assuming intracellular steady state of metabolites (Bonarius et al. 2001) or by analyzing intracellular metabolite and isotopomer dynamics. The latter requires much more sophisticated analytical methods and is much more laborious both for analysis as well as modeling and computation (Hofmann et al. 2008; Maier et al. 2008). In this study, we quantitatively analyze dynamics of growth and metabolism of the new human cell line AGE1.HN using a dynamic flux analysis method. The presented method of metabolic flux analysis is well suited to monitor and investigate metabolic shifts caused by environmental changes that occur during batch cultivation of mammalian cells. It does not require any kinetic model and is, therefore, widely applicable. Estimated flux dynamics were compared to results obtained from stationary metabolic flux analysis in different metabolic phases. We analyzed parental AGE1.HN cells in this study to gain detailed quantitative knowledge and understanding of growth behavior, cellular metabolism, as well as its dynamics. The results are, therefore, expected to be useful for rational development of optimal growth media, for further optimization and engineering of the cell line to obtain higher cell densities in a process, for all derived producer cells, and for the design of other producer cell lines.

2.3 Materials and methods

2.3.1 Cell line.

The AGE1.HN cell line was developed from primary cells from a human brain tissue sample. The primary cells were immortalized with an expression plasmid containing the adenoviral E1 A and B genes of human adenovirus type 5 driven by the human pGK and the endogenous E1B promoter, respectively. While the E1A induces progression of the cell cycle, the E1B proteins prevent apoptosis caused by E1A through interaction with p53 and bax. The cell line was further modified to express the structural and regulatory protein pIX from human adenovirus type 5. This modification changes cell metabolism, enhances productivity for secreted proteins, and modulates susceptibility to a variety of viruses. The AGE1.HN cells express marker genes representative for cells of neuronal lineage and lack expression of glial markers. The cell line was adapted to robust growth in suspension in both serum/protein-free and chemically defined culture media and has been proven to grow efficiently in shaker, spinner, roller, and stirred tank bioreactors. The entire development work for the generation of the AGE1.HN line was carried out in a dedicated cell culture suite and the complete development history was recorded. The documentation for all media and supplements used in the AGE1.HN cell line development is in compliance with the stipulations of EMEA 410/01. The AGE1.HN cell line is proprietary to ProBioGen AG (Berlin, Germany) covered by patent application 06807777.5-2406.

2.3.2 Cell culture and experimental procedure.

The cells were cultured in baffled shake flasks (Corning, NY, USA) at 37°C on a shaker (2 inches orbit, ES-X, Kühner, Basel, Switzerland) enclosed in a 5% CO₂ supplied, humidified (80%) incubator (Mytron, Heilbad Heiligenstadt, Germany). The preculture was carried out in a 250 ml baffled shake flask in 42-

Max-UB-medium, which is serum-free and was especially developed for the AGE1.HN cell line. The medium composition is presented in Table S1. The cells were centrifuged (800 1/min, 7 min, 22°C, Megafuge, Heraeus Instruments, Hanau, Germany) and the supernatant discarded. The pellet was resuspended in 42-Max-UB-medium without glucose and glutamine. Four 125 ml baffled shake flasks were inoculated yielding an initial cell density of about 4×10^5 cells/ml. Glucose and glutamine were finally added. The final culture volume was 54 ml. Samples (1.6 ml) were taken every day. 500 μ l were directly used for cell counting. The rest was centrifuged (1,500 1/min, 5 min, 22°C, Megafuge, Heraeus Instruments, Hanau, Germany), the supernatant transferred into fresh tubes and frozen (-20°C). The analysis of several cultivation parameters was carried out using an automated cell culture analyzer (Cedex AS20, Innovatis, Bielefeld, Germany) which determines cell density, viability (Trypan Blue exclusion method), size, morphology, and aggregation rate. Dissolved oxygen was always above 80% in the applied setup, which was determined in an additional cultivation using the OXY-4 mini system (PreSens - Precision Sensing GmbH, Regensburg, Germany) described earlier (Deshpande and Heinzle 2009).

2.3.3 Quantification of metabolites.

Glucose, lactate, and pyruvate in the supernatant were analyzed using high-pressure liquid chromatography (HPLC) as described previously (Niklas et al. 2009). Quantification of proteinogenic amino acids was performed by another HPLC-method (Kromer et al. 2005). The measured metabolite concentrations as well as cell density were corrected for evaporation using (1). The determined evaporation rate k_E in the applied setup was 0.0356 h^{-1} .

$$c_{corr} = c_{meas} \times \frac{100}{(100 + t \times k_E)} \quad (1)$$

c_{corr} represents the corrected concentration and c_{meas} the measured concentration.

Glutamine hydrolysis was observed to be a first order process having a rate constant k_G of 0.00198 h^{-1} in the applied medium (pH 7.4, 37°C). The actual glutamine uptake rate r_{Gln} was calculated employing polynomials of degree 5 in Matlab 7.5 (The Mathworks, Natick, MA, USA) using

$$\frac{d[Gln]}{dt} = -(k_G \times [Gln] + r_{Gln}) \quad (2)$$

2.3.4 Metabolic network.

A metabolic network model (Fig. 2-1) was set up using the Kyoto Encyclopedia of Genes and Genomes (KEGG) pathway database for Homo sapiens as well as other published metabolic network information (Duarte et al. 2007). The enzymes that were included into the model are given in Table S4 of the supplementary material section. The stoichiometric matrix of the model had the dimensions 41×70 and a rank of 41. It is presented in the supplementary material (Table S5).

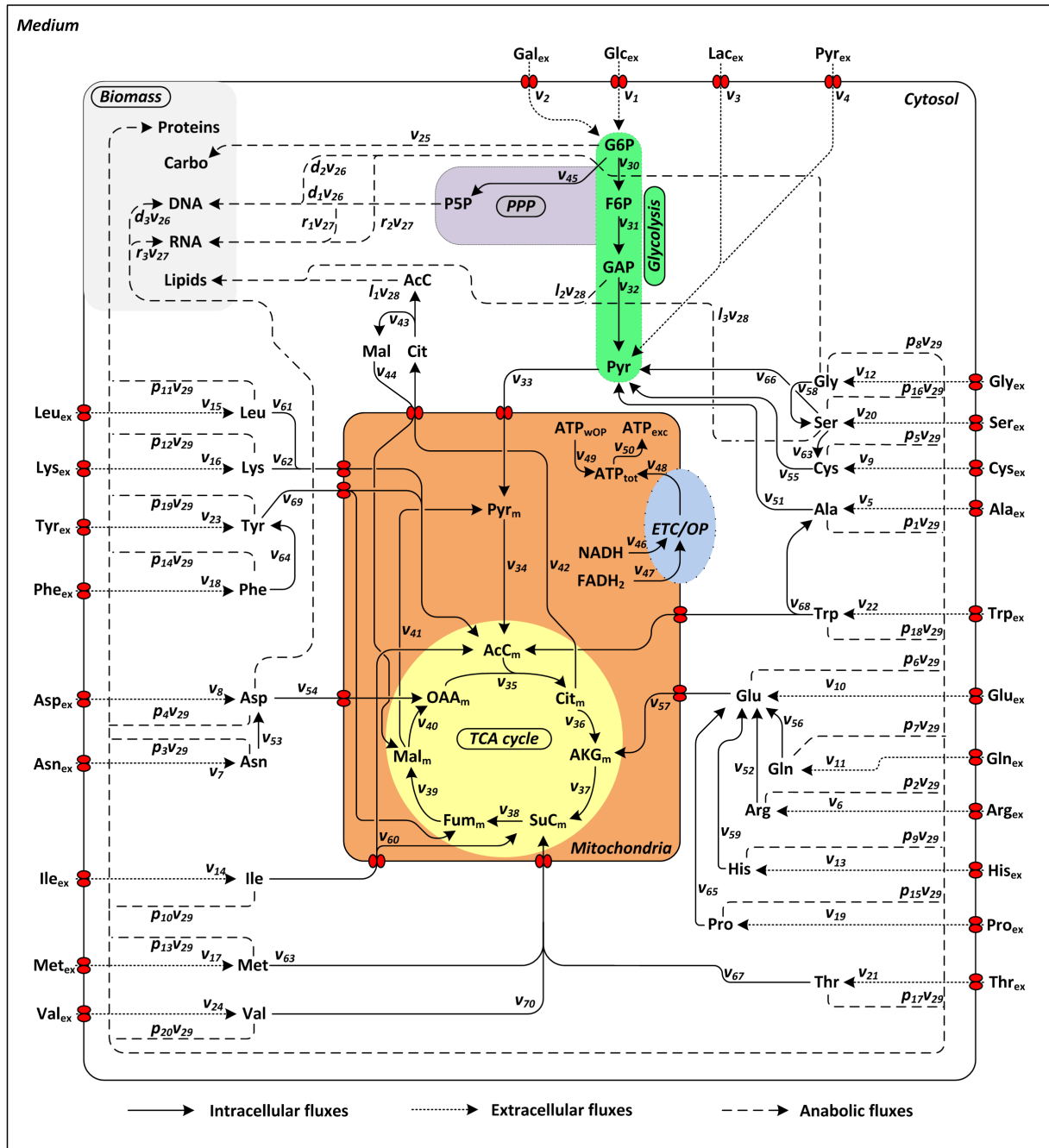


Fig. 2-1 Metabolic network used for metabolic flux analysis. *PPP* pentose phosphate pathway, *TCA* tricarboxylic acid, *ETC* electron transport chain, *OP* oxidative phosphorylation, *Carbo* carbohydrates, *Glc* glucose, *Gal* galactose, *Lac* lactate, *Pyr* pyruvate, *G6P* glucose 6-phosphate, *P5P* pentose 5-phosphate, *F6P* fructose 6-phosphate, *GAP* glyceraldehyde 3-phosphate, *AcC* acetyl coenzyme A, *Cit* citrate, *AKG* a-ketoglutarate, *SuC* succinyl coenzyme A, *Fum* fumarate, *Mal* malate, *OAA* oxaloacetate, *ATP* adenosine triphosphate, *ATP_{wOP}* ATP without oxidative phosphorylation, *ATP_{tot}* total ATP, *ATP_{exc}* ATP excess, *NADH* nicotinamide adenine dinucleotide, *FADH₂* flavin adenine dinucleotide, standard abbreviations for amino acids. Indices: *m* mitochondrial, *ex* extracellular.

Central energy metabolism. The main pathways of the energy metabolism, glycolysis, oxidative decarboxylation, TCA cycle, electron transport chain, and oxidative phosphorylation, are represented. Due to the possible action of nicotinamide nucleotide transhydrogenases and the fact that for some reactions it is not known whether NADH or NADPH take part, NADH and NADPH were lumped together. The

excess of NAD(P)H and FADH₂ from all reactions considered in the model was calculated. For oxidative phosphorylation, it was assumed that per NAD(P)H and FADH₂ 2.5 ATP and 1.5 ATP are produced, respectively. The excess of ATP (ATP_{tot}) was calculated considering the demand or production of all reactions. However, the energy needed for transport of metabolites and maintenance was not included in the ATP-balance.

Pentose phosphate pathway. Pentose phosphate pathway/glycolysis split can not be resolved by metabolite balancing alone and was assumed to be just responsible for nucleic acid synthesis.

Amino acid metabolism. The metabolism of proteinogenic amino acids is represented by selected degradation pathways. In cases where several pathways are possible, the most probable and suitable pathway was chosen (Table S4 of supplementary material and Fig. 2-1).

Other reactions. Since it is not possible to distinguish between the reactions catalyzed by the enzymes phosphoenolpyruvate carboxykinase, malic enzyme (malate dehydrogenase, oxaloacetate decarboxylating), and pyruvate carboxylase with the method applied in this study, just one reaction from malate to pyruvate was included which represents the sum of the fluxes through these enzymes.

Synthesis of biomass. The biomass fluxes are represented as five fluxes to the major macromolecules of the cell. Cytosolic acetyl coenzyme A, which is needed for the synthesis of fatty acids and lipids, is assumed to be solely derived from citrate that is transported through the citrate/malate shuttle and converted through the citrate lyase to acetyl coenzyme A and malate. Further precursors that were considered for the synthesis of lipids are glyceraldehyde 3-phosphate and serine. Carbohydrates were taken as polyglucose and are, therefore, derived from glucose 6-phosphate. The precursors considered for nucleic acid synthesis are ribose 5-phosphate, glycine, and aspartate. For proteins, a certain amount of each proteinogenic amino acid is needed per cell, which was calculated using the amino acid composition of total cellular protein determined in this study (described below).

Transport of metabolites. As mentioned above, the energy demand for transport was not included in the ATP balance. From calculated fluxes, a rough estimate could, however, be derived using literature knowledge, e.g., about amino acid transport (Hyde et al. 2003). The mitochondrial transporters included in the model are the pyruvate carrier, citrate/malate shuttle, glutamate/aspartate shuttle, and the ADP/ATP transporter (Berg et al. 2003; Kaplan 2001). For further metabolites entering the mitochondria, no specific transport mechanisms were assumed.

Anabolic demand of AGE1.HN. Macromolecules. The applied macromolecular composition of the cells was: Proteins, 70.6%; lipids, 9.2%; carbohydrates, 7.1%; DNA, 1.4%; RNA, 5.8%; rest/ash, 5.9%. The lipid composition was determined once using 4.9×10^8 cells, harvested at a cell density of 3.4×10^6 cells/ml (viability 97%) using a published protocol (Niklas et al. 2009). The other parts of the composition were taken from Bonarius et al. (1996).

Amino acid composition. The amino acid composition of total cellular protein was determined using samples of $1-2 \times 10^7$ cells that were washed twice with PBS to remove amino acids from the medium. For hydrolysis, 6 M HCl (280 μ l/ 10^7 cells) was used and incubated for 24 h at 110°C. The solution was neutralized using 6 M NaOH and the amino acid composition was determined using HPLC as described

above. The determined relative composition (n=4) was: aspartic acid/asparagine, $9.25 \pm 0.6\%$; glutamic acid/glutamine, $12.83 \pm 0.48\%$; serine, $6.19 \pm 0.12\%$; histidine, $2.18 \pm 0.12\%$; glycine, $9.45 \pm 0.67\%$; threonine, $4.94 \pm 0.1\%$; arginine, $5.19 \pm 0.23\%$; alanine, $8.06 \pm 0.09\%$; tyrosine, $1.9 \pm 0.04\%$; valine, $6.14 \pm 0.13\%$; phenylalanine, $3.56 \pm 0.08\%$; isoleucine, $4.49 \pm 0.09\%$; leucine, $8.71 \pm 0.1\%$; lysine, $7.5 \pm 0.17\%$; proline, $3.99 \pm 0.12\%$. Methionine, tryptophan, and cysteine are degraded by the applied hydrolytic method. Relative amounts for these amino acids were taken from literature (Savinell and Palsson 1992a): methionine, 1.7%; tryptophan, 1.1%; cysteine, 2.8%.

Cell dry weight estimation. The cell dry weight of mammalian cells in culture is not constant and increases with increasing growth rate (Frame and Hu 1990; Nielsen et al. 1997). It was shown, that the volume of cells is proportional to their dry weight and can be used as an indirect measure of the biomass concentration in the culture (Frame and Hu 1990). In this study, cell size was determined using an automated cell culture analyzer (Cedex AS20, Innovatis, Bielefeld, Germany) providing an accurate determination of the cell diameter. Assuming that the cells are spherical, the respective cell volume was calculated. The correlation between dry cell weight, DCW (pg), and cell volume, CV (μm^3), determined in a control experiment using the procedure described previously (Niklas et al. 2009), was $\text{DCW} = 0.25 \times \text{CV}$. This relationship was used for calculation of biomass concentrations. The anabolic demand of the cells is shown in Table 2-1.

Table 2-1 Anabolic demand of AGE1.HN.

Macromolecule	Anabolic demand [$\mu\text{mol}/\text{g}_{\text{biomass}}$]
Carbohydrates	438.3
DNA	45.3
RNA	180.3
Lipids	128.1
Proteins	6,433.0

2.3.5 Metabolic flux analysis.

The two different procedures applied for calculation of metabolic fluxes are depicted in Fig. 2-2. For the calculation of metabolic fluxes over time (dynamic method), splines were fitted to the measured data for biomass and extracellular metabolites (Supplementary Fig. S1) using Matlab 7.5 (The Mathworks, Natick, MA, USA). These were used to calculate specific rates (v) for each metabolite concentration M_i over time using

$$v_{M_i} = \frac{dM_i/dt}{B} \quad (3)$$

where B represents the respective biomass in the culture. Intracellular fluxes were calculated using

$$v_k = S_k^{-1} \times (-S_m \times v_m) \quad (4)$$

where v_m and v_k represent the measured and the calculated rate vectors. S_k and S_m are corresponding stoichiometric matrices.

For calculating stationary fluxes, growth was divided into different metabolic phases (Fig. 2-2). Average rates for each metabolite M_i were calculated assuming metabolic steady state for each phase using the estimated specific growth rate μ and metabolite yields:

$$v_{M_i} = \mu \frac{\Delta M_i}{\Delta B} \quad (5)$$

B represents the total biomass in the culture. The data was implemented into the metabolic network model and intracellular fluxes for each phase were subsequently calculated using equation (4).

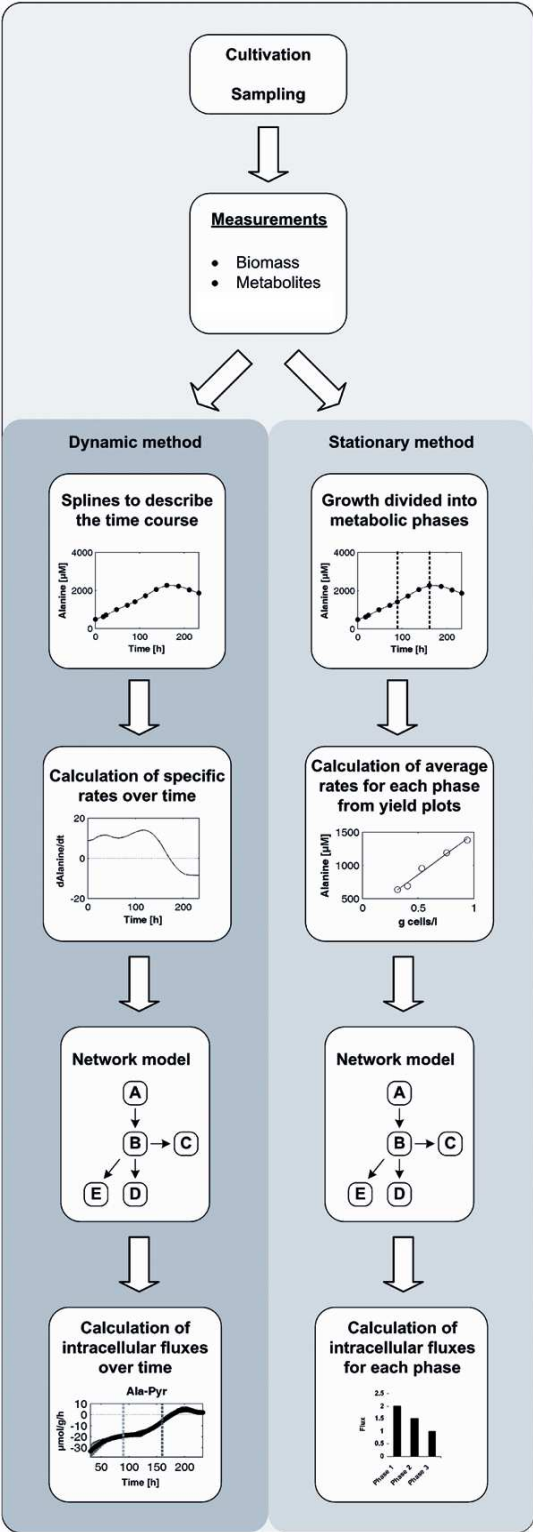


Fig. 2-2 Methods applied for metabolic flux analysis. Dynamic method for calculation of the time course of metabolic fluxes and stationary method for calculation of mean fluxes for different metabolic phases.

2.4 Results

2.4.1 Growth profile of AGE1.HN during batch cultivation.

During the initial growth period lasting up to 160 h, the viability remained high at about 95% (Fig. 2-3). At 160 h the viability started decreasing and the growth rate slowed down. The cell density at the end of the batch cultivation was about 7.5×10^6 cells/ml (Fig. 2-3). By plotting the logarithm of the cell density against time (not shown), distinct growth phases could be distinguished. The first lasted from 0 h to 90 h, the second from 90 h to 160 h, and the third from 160 h to 230 h having growth rates of 0.351 ± 0.055 d⁻¹, 0.279 ± 0.021 d⁻¹, and 0.056 ± 0.011 d⁻¹.

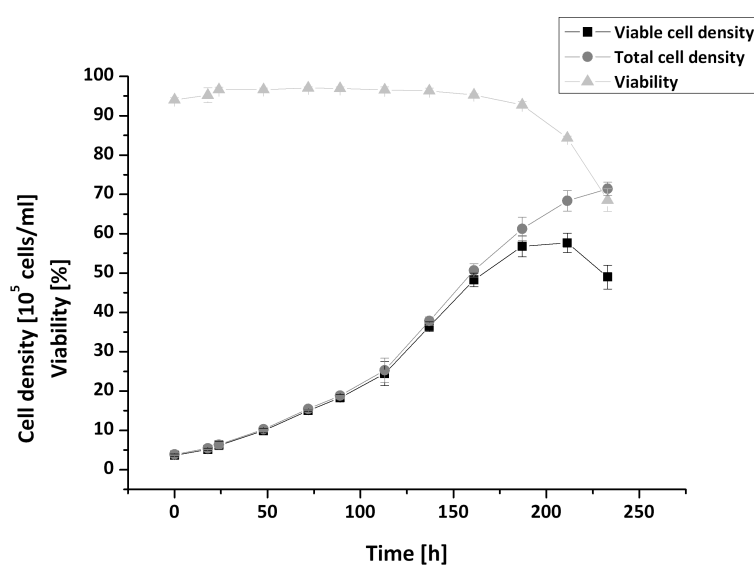


Fig. 2-3 Growth of AGE1.HN. Viable cell density, total cell density, and viability during batch cultivation. Mean values and standard deviations of four parallel cultivations.

2.4.2 Exometabolome analysis and extracellular fluxes.

The observed growth behavior is strongly linked to metabolite profiles (Fig. 2-4, Fig. S1). Pyruvate was consumed during the first 90 h of the cultivation (phase 1), and lactate, glutamate, alanine, and glycine were produced. The uptake rates of glucose and pyruvate as well as the production rate of lactate were highest in the beginning and dropped until 90 h (Fig. 2-5). The lactate production stopped with pyruvate depletion at about 90 h indicating a coupling of these reactions (Fig. 2-5). The glutamate production rate was decreasing during the first phase whereas the glutamine consumption rate remained at a constant high value in this phase (Fig. 2-5). For most other amino acids, the uptake or production rates were highest in phase 1 (Fig. S2, Table S2 and Table S3).

After 90 h (phase 2), when pyruvate was used up, lactate production stopped immediately and the cells started to consume glutamate as well as glycine (Fig. 2-4). The extracellular fluxes for most metabolites were significantly lower than in phase 1 (Fig. 2-6, Table S3). The glucose uptake rate, which was almost identical to the rate of glycolysis, was constant (Fig. 2-5), and the lactate production rate was very low (Fig. 2-5, Fig. 2-6). The glutamine uptake rate was decreasing (Fig. 2-5, Table S2). At the end of phase 2,

glutamine was nearly completely consumed and the cells started to consume glutamate (Fig. 2-5, Table S2). The production rate of alanine was decreasing (Fig. 2-5, Fig. S2 and Table S2). The rates for other amino acids remained nearly constant or were very low (Fig. S2).

After 160 h (phase 3), glutamine was used up which forced the cells to adapt their metabolism again. Glutamate consumption increased initially in this phase. Lactate production again increased slightly but was nevertheless very low compared to phase 1 (Fig. 2-5, Table S3). Alanine, which was constantly produced during phases 1 and 2, was now consumed. In addition, the cells stopped exponential growth and the viability dropped directly after glutamine depletion, which indicates the important role of glutamine as substrate for AGE1.HN. Almost all of the calculated mean extracellular fluxes (Fig. 2-6, Table S3) were significantly different compared to phase 1, and most of them were also significantly different compared to phase 2. Glutamate was completely exhausted at about 215 h (Fig. 2-4). The glucose consumption rate was constantly decreasing until glucose was completely depleted at the end of the cultivation at 230 h (Fig. 2-4 and Fig. 2-5).

In general, the standard errors for extracellular fluxes were high in the beginning and decreased with time (Fig. 2-5). This is due to the small differences in substrate concentrations in the beginning of the cultivation. The integral yield of cells per glucose was around 340 cells/nmol which is a favourable feature of AGE1.HN since it is higher compared to the corresponding yield in CHO cells which is typically ranging between 60 and 100 cells/nmol of glucose consumed (Deshpande et al. 2009; Kim and Lee 2007).

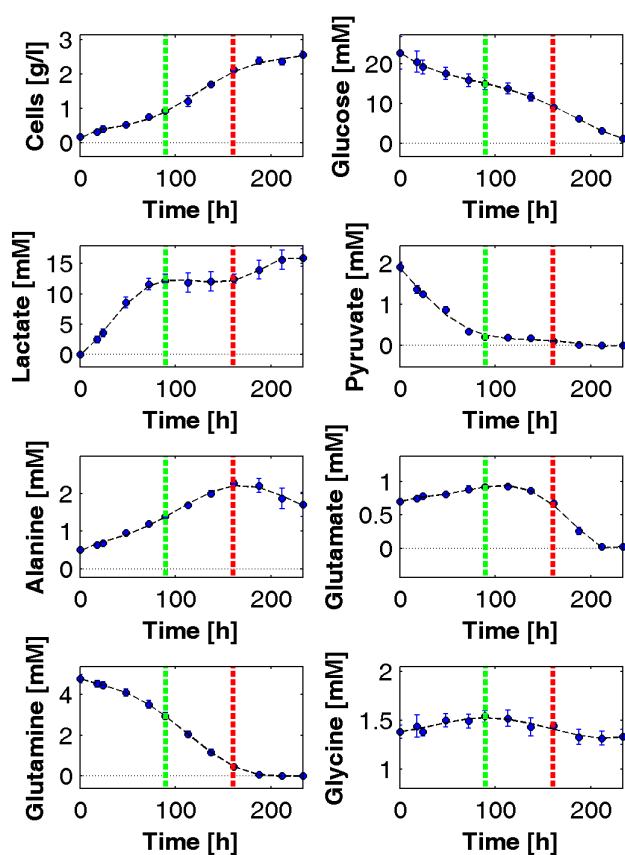


Fig. 2-4 Cultivation profile of AGE1.HN. Mean values and standard deviations for cell mass and selected metabolites of four parallel cultivations are depicted. Further metabolites are depicted in Fig. S1 of the supplementary material. The first line (90 h) indicates the end of the first metabolic phase when pyruvate is depleted, the second line (160 h) the end of the second metabolic phase when glutamine is depleted.

2.4.3 Metabolic flux analysis – intracellular fluxes.

Intracellular fluxes were calculated using the stoichiometric network model depicted in Fig. 2-1.

Glycolysis. The highest flux through the glycolytic pathway was observed in phase 1 (Fig. 2-6 and Table S3). Then it steadily decreased until 90 h (Fig. 2-5 and Fig. S2). In phase 2, glycolytic activity was significantly lower and remained nearly constant. In phase 3, glycolytic flux was slightly decreasing until the end of the cultivation (Fig. 2-5 and Fig. S2) but was not significantly different from phase 2 (Fig. 2-6 and Table S3).

Pyruvate dehydrogenase activity. The calculated fluxes through the pyruvate carrier (Pyr-Pyr_m, Fig. 2-5 and Fig. 2-6) and through the pyruvate dehydrogenase complex (Pyr_m-AcC_m) were low in the beginning, i.e., not significantly different from zero (Table S3) and increased in phase 1. In phase 2, pyruvate dehydrogenase activity remained constant and was significantly higher compared to phase 1 (Fig. 2-5, Fig. 2-6 and Table S3). Since lactate production was approximately 0 in phase 2, most of the pyruvate was entering the TCA cycle via pyruvate dehydrogenase. This flux was still high in phase 3 but slightly decreasing (Fig. 2-5).

TCA cycle and anaplerosis. The activity of the TCA cycle in phase 1 was significantly lower than in phases 2 and 3 (Fig. 2-5, Fig. 2-6 and Table S3). No lactate was produced from pyruvate in phase 2. Therefore, a large fraction of pyruvate entered the TCA cycle and fluxes through the upper part as well as the lower part of the TCA cycle were very high in this phase (Fig. 2-5, Fig. 2-6 and Table S3). The anaplerotic flux through the enzyme glutamate dehydrogenase (Glu-AKG_m) was decreasing during the cultivation matching the decrease in available extracellular glutamine (Fig. 2-5). The aspartate aminotransferase flux (Asp-OAA_m) was highest in phase 1 and decreased thereafter. During phase 2, this flux remained constant until it decreased again in phase 3 (Fig. S3). Fluxes through the TCA cycle in phase 3 were similar to those in phase 2 but decreasing towards the end (Fig. 2-5, Fig. 2-6 and Table S3). Glutamine was depleted and glutamate was taken up instead (Fig. 2-4). However, the flux through glutamate dehydrogenase was very low in phase 3 which shows that acetyl coenzyme A derived from pyruvate was by far the most important fuel for TCA cycle after glutamine depletion. The calculated flux from malate to pyruvate (Mal_m-Pyr_m) was very high in the beginning of phase 1. In the following phases, this flux dropped and was significantly lower (Fig. 2-5, Fig. 2-6 and Table S3). Interestingly, the TCA cycle was additionally fed by the degradation of the branched chain amino acids isoleucine, leucine, and valine during phase 1. In the other phases, degradation of these amino acids to form intermediates of TCA cycle was not significantly different from zero.

Electron transport chain/oxidative phosphorylation. In accordance to the time courses for FADH₂ and NAD(P)H production, the activity of the oxidative phosphorylation (ATP_{OP}) was low in phase 1 and then increased to a constant level during phase 2 until the middle of phase 3 and subsequently decreased (Fig. S3 and Table S3). The ATP-balance for all reactions included in the network without oxidative phosphorylation (ATP_{wOP}) indicates that the ATP demand was also highest in phases 1 and 2 and lowest in phase 3.

Amino acid metabolism. The fluxes through glutamine synthetase (Gln-Glu) and glutamate dehydrogenase (Glu-AKG_m) were almost constant in phase 1 and then decreased during the cultivation, since glutamine and glutamate were successively depleted (Fig. 2-5, Fig. 2-6 and Table S3). The glutamate pool was

additionally fed by degradation of arginine (Arg-Glu, Fig. S3 and Table S3). In phases 1 and 2 less asparagine was taken up than needed for protein synthesis which was then synthesized through the asparagine synthase from aspartate (Asn-Asp, Fig. S3 and Table S3). Aspartate was feeding into the TCA cycle during the whole cultivation through the aspartate aminotransferase catalyzed reaction leading to oxaloacetate (Asp-OAA_m). This flux was decreasing over time (Fig. S3). Since glycine was produced in phase 1 and then only slightly taken up (Fig. 2-4), it had to be produced via glycine hydroxymethyltransferase indicated by Gly-Ser in Fig. S3 and Table S3. This flux significantly decreased with time because glycine was taken up in phases 2 and 3 where, additionally, the anabolic demand decreased because of slower growth. The flux through serine dehydratase (Ser-Pyr) also significantly decreased (Fig. S3 and Table S3). In accordance with the time course of proline production (Fig. 2-5), the flux from glutamate to proline (Pro-Glu, Fig. S3 and Table S3) was highest in phase 1 and then decreased. Other degradation rates of amino acids were very low indicating that the uptake of these amino acids was just matching the anabolic demand of the cells.

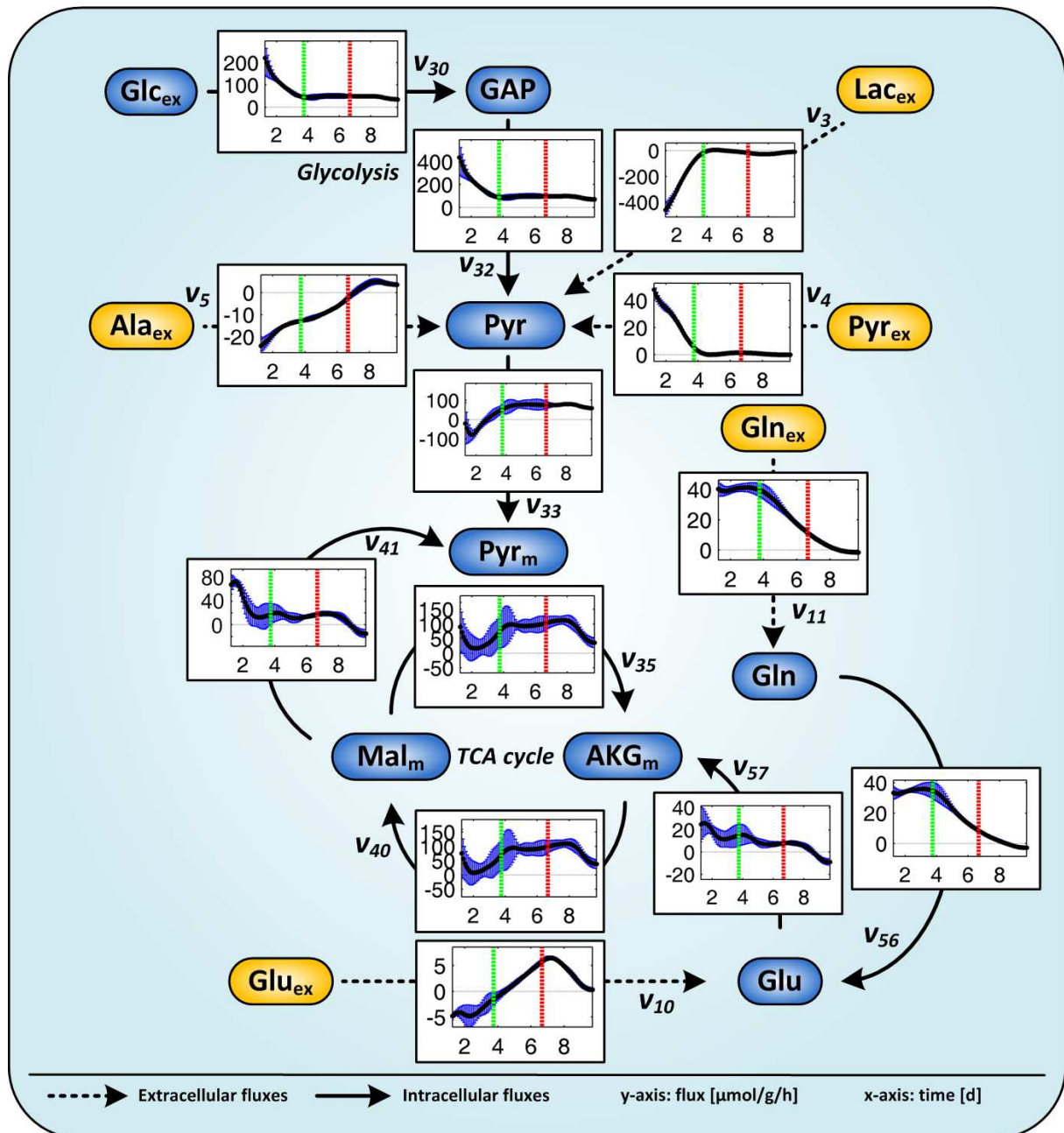


Fig. 2-5 Selected metabolic fluxes of AGE1.HN over time related to biomass. Mean values and confidence intervals (90%) of four parallel cultivations. The fluxes (y-axis) are given in $\mu\text{mol/g/h}$ and the time (x-axis) in days. The first line (90 h) indicates the end of the first metabolic phase when pyruvate is consumed, the second line (160 h) the end of the second metabolic phase when glutamine is consumed. Negative values indicate fluxes in the opposite direction of the arrow. Further extracellular and intracellular fluxes are depicted in Fig. S2 and Fig. S3 of the supplementary material.

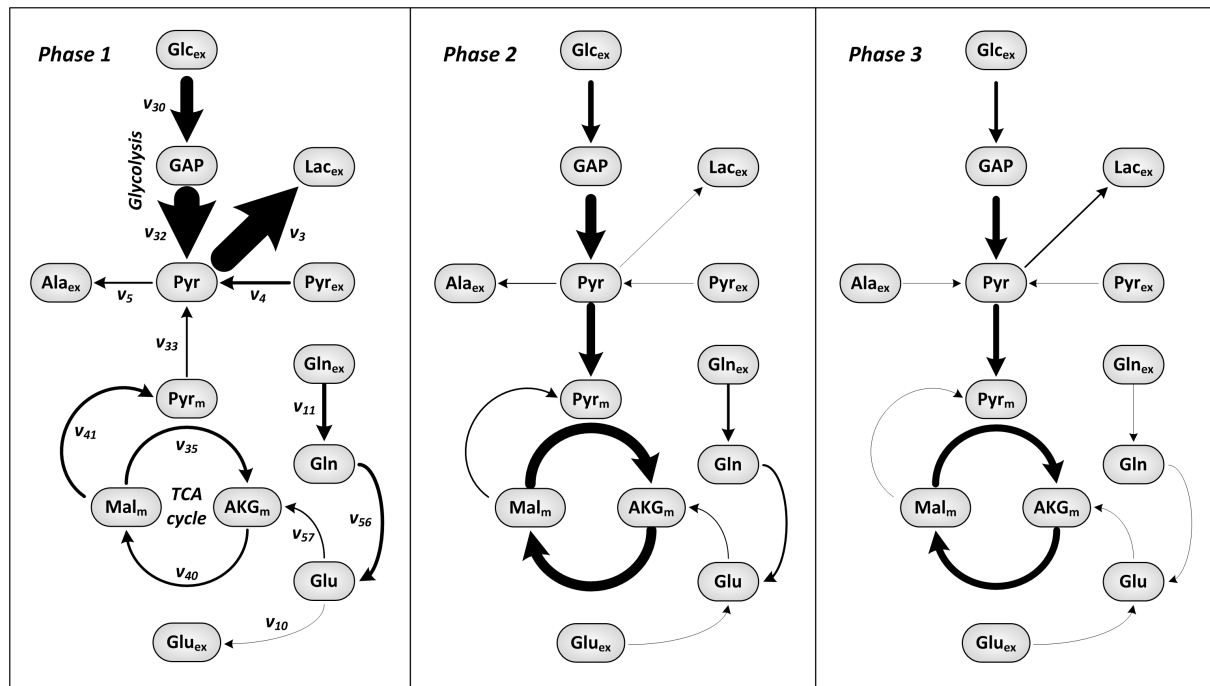


Fig. 2-6 Average metabolic flux distribution of AGE1.HN in each metabolic phase. Arrow width indicates flux strength. Flux symbols selected for this figure are shown in the flux map of phase 1 and are defined in the metabolic network (Fig. 2-1). Same experiment as shown in Fig. 2-5. Further data are provided in Table S3 of the supplementary material.

2.5 Discussion

2.5.1 Metabolism in AGE1.HN.

Metabolism and metabolic shifts of the new human cell line AGE1.HN were quantitatively analyzed in this study using time resolved metabolic flux analysis and stationary metabolic flux analysis in different phases during batch cultivation. Our results indicate that pyruvate uptake during phase 1 in combination with high levels of other substrates resulted in an inefficient metabolic phenotype characterized by overflow metabolism leading to waste product formation. In phase 2, the metabolism was switching to a most efficient state characterized by low substrate uptake rates and no lactate formation. The data indicate that a decrease in substrate levels occurring during the cultivation resulted in a slowdown of glycolysis during phase 1. Additional experiments using different pyruvate concentrations in the medium support the conclusion that there is a strong link between pyruvate in the medium and lactate production in AGE1.HN (Niklas et al. 2011b). Another possibility would be that the cells could secrete lactate only until a certain concentration is reached and would then stop the production. However, in other experiments that were performed using high lactate start concentrations (about 8 mM), it was observed that the cells were producing almost the same amount of lactate as in experiments where lactate start concentration was 0. This indicates that pyruvate depletion seems to be an important factor for cessation of lactate production. This particular phenotype was so far not observed in other mammalian cells (Altamirano et al. 2006; Gambhir et al. 2003; Niklas et al. 2009; Sidorenko et al. 2008).

During exponential growth of mammalian cells under non-limiting substrate levels, inefficient substrate utilization was reported for several other mammalian cell lines (Bonarius et al. 2001; Le Ru et al. 2010; Niklas et al. 2009; Sidorenko et al. 2008). Usually, only a small amount of intracellular pyruvate is entering the TCA cycle under these conditions, which is considered very unfavourable. Increasing flux through pyruvate dehydrogenase represents an optimization target for the cultivation of many mammalian cells, but the mechanisms and molecular reasons are still poorly understood (Modak et al. 2002; Zeng et al. 2002). In a recent study on HEK-293 cells, pyruvate dehydrogenase activity was reported to be around 22% of glycolytic activity (Le Ru et al. 2010). Very low or even no activity of the pyruvate dehydrogenase complex was reported in other studies on different mammalian cells (Neermann and Wagner 1996; Sidorenko et al. 2008). In AGE1.HN cells, this was observed only during the first phase. During phases 2 and 3, pyruvate dehydrogenase activity was high. In MDCK cells, it was found that an addition of pyruvate in a glutamine depleted medium resulted even in an increase in the flux from pyruvate into the TCA cycle (Sidorenko et al. 2008). In AGE1.HN, it seems that available pyruvate has an opposite effect triggering the conversion of pyruvate to lactate. High uptake rates of glucose and pyruvate, as observed in phase 1, might lead to an increase of the intracellular pyruvate pool triggering overflow metabolism into lactate/alanine, eventually resulting in an increased secretion of these waste metabolites. This might be changed by increasing reactions connecting TCA cycle and glycolysis, e.g., by stimulating pyruvate dehydrogenase and pyruvate carboxylase fluxes (Elias et al. 2003; Irani et al. 1999). However, the success of this strategy can not be predicted *a priori*. Increase of fluxes into the TCA cycle must be accompanied by an increase in oxidative phosphorylation activity, which might not always be possible. Another strategy that is working in the opposite direction would be decreasing the substrate uptake rates, e.g., by knock down of transporters (Paredes et al. 1999) or decreasing the lactate production, e.g., by knock down of lactate dehydrogenase (Kim and Lee 2007).

2.5.2 Comparison of selected metabolic fluxes in AGE1.HN with those in other cells.

Selected metabolic fluxes in AGE1.HN that were calculated by the stationary method for different phases are compared to fluxes published for other mammalian cells (Table 2-2). Glucose uptake and lactate production rates were generally lower in AGE1.HN than in other cells. Pyruvate represents an extracellular metabolite that was often neglected in other studies (Altamirano et al. 2006; Bonarius et al. 2001). However, as shown in this study and in MDCK cells (Genzel et al. 2005; Sidorenko et al. 2008) or CHO cells (Omasa et al. 2010), it is a very interesting metabolite that can induce huge changes in the metabolism. In AGE1.HN cells, pyruvate uptake rate was far lower than in MDCK cells that were grown in high pyruvate medium (Table 2-2, M2). However, the ratio of pyruvate uptake per glucose uptake was similar. The second phase in AGE1.HN showed a very efficient metabolism concerning substrate usage as already discussed before. The cells were proliferating without lactate production. Pyruvate dehydrogenase (PDH) activity was high. In all other cell lines, high lactate production was observed during the phases that were analyzed by MFA except for CHO cells in presence of galactose after glucose depletion. In

order to reach higher cell densities in cultivations of AGE1.HN, the second phase could be prolonged by feeding of glutamine. PDH activity in AGE1.HN was low in phase 1 and high in phases 2 and 3. A similar situation was observed in CHO cells (Altamirano et al. 2006) which exhibited low PDH activity and overflow metabolism during growth on glucose. After glucose depletion, these cells were consuming lactate in the presence of galactose having high PDH activity. No PDH activity was reported for MDCK cells in glutamine containing medium. In medium without glutamine and high pyruvate concentration, low PDH activity was found in these cells. The absolute flux through PDH was highest in continuously cultured hybridoma cells (Bonarius et al. 2001), but the metabolism was by far not as efficient as in phase 2 of AGE1.HN since there was high glucose consumption and waste product formation. Absolute glutamate dehydrogenase (GDH) activity of AGE1.HN during phases 1 and 2 was lower than in other cell lines, but the relative activity compared to the glucose uptake rate was quite similar in MDCK and CHO cultures. Upper and lower TCA cycle activity in phases 2 and 3 was comparable to the activity in CHO cells with glucose medium (S1 in Table 2-2) and in MDCK cells (M2 in Table 2-2) cultured without glutamine. For hybridoma cells, higher TCA cycle activity was reported.

Table 2-2 Comparison of selected metabolic fluxes in AGE1.HN during different metabolic phases (P1-3) with fluxes published for other mammalian cell lines.

	Flux [$\mu\text{mol g}^{-1} \text{h}^{-1}$]							
	AGE1.HN			MDCK ^a		CHO ^b		Hybridoma ^c
	P1	P2	P3	M1	M2	S1	S2	
Glc uptake	123.0	56.6	33.7	1,108.7	476.6	322.5	43.8 ^d	674.6
Pyr uptake	28.7	0.9	0.4	0.0	111.0	nd	nd	nd
Lac production	236.3	4.5	14.3	2,188.0	965.0	612.5	-68.8	1,030.0
Gln uptake	37.1	23.5	2.1	70.9	0.9	0.0	0.0	146.9
Glu production	4.0	-2.4	-2.9	-42.1	-22.1	-56.3	-56.8	1.2
PDH	12.2	88.1	56.8	0.0	33.1	35.5	174.6	355.7
GDH	13.2	8.3	1.7	64.7	42.8	28.1	14.0	110.1
Upper TCA	-4.0	66.4	57.7	-27.3	43.5	35.5	148.8	312.5
Lower TCA	9.2	74.7	59.3	54.3	63.0	78.9	195.8	441.1

Fluxes are given in $\mu\text{mol/g/h}$. Literature fluxes that were given per cell were normalized to biomass by assuming a cell dry weight of 800 pg/cell for MDCK cells (Wahl et al. 2008) and 400 pg/cell for CHO and hybridoma cells (Bonarius et al. 1996; Xie and Wang 1994). MDCK murine darby canine kidney, M1 glutamine containing medium, M2 medium with high pyruvate concentration and without glutamine, CHO chinese hamster ovary, S1 stage 1 of cultivation, S2 stage 2 of cultivation when glucose is exhausted, Glc glucose, Pyr pyruvate, Lac lactate, Gln glutamine, Glu glutamate, PDH pyruvate dehydrogenase, GDH glutamate dehydrogenase, upper TCA activity of the upper tricarboxylic acid cycle represented by the flux from citrate to α -ketoglutarate, lower TCA activity of the lower TCA cycle represented by the α -ketoglutarate dehydrogenase flux, nd not determined. ^aMDCK cell culture (Sidorenko et al. 2008), ^bCHO cell culture (Altamirano et al. 2006), ^cContinuous culture of hybridoma cells (Bonarius et al. 2001), ^dGalactose uptake.

The main differences between the metabolic phases of AGE1.HN are summarized in Fig. 2-7. The results indicate further targets for improving the metabolic phenotype of these cells to reach higher cell densities as well as to obtain a more efficient utilization of the nutrients. The high overflow metabolism in the beginning of the cultivation with channeling of pyruvate to lactate could be decreased. This could be accomplished by genetic engineering, e.g., by deletion of lactate dehydrogenase (Chen et al. 2001) or introduction of pyruvate carboxylase (Elias et al. 2003), further medium optimization, e.g., reduced concentrations of pyruvate, or by application of new feeding strategies (Omasa et al. 2010). The observed metabolism in phase 2 indicates the potential of this cell line to grow very efficiently having minimum formation of waste products and minimum energy spilling (Russell 2007). Therefore, it seems promising to change environmental conditions, i.e., media, substrate feeding, as well as enzyme expression such as to approach the efficient metabolic state of phase 2 during a process. Studies on enzyme expression and detailed labeling experiments in combination with ^{13}C metabolic flux analysis would provide additional hints for the best way to further improve the cell line.

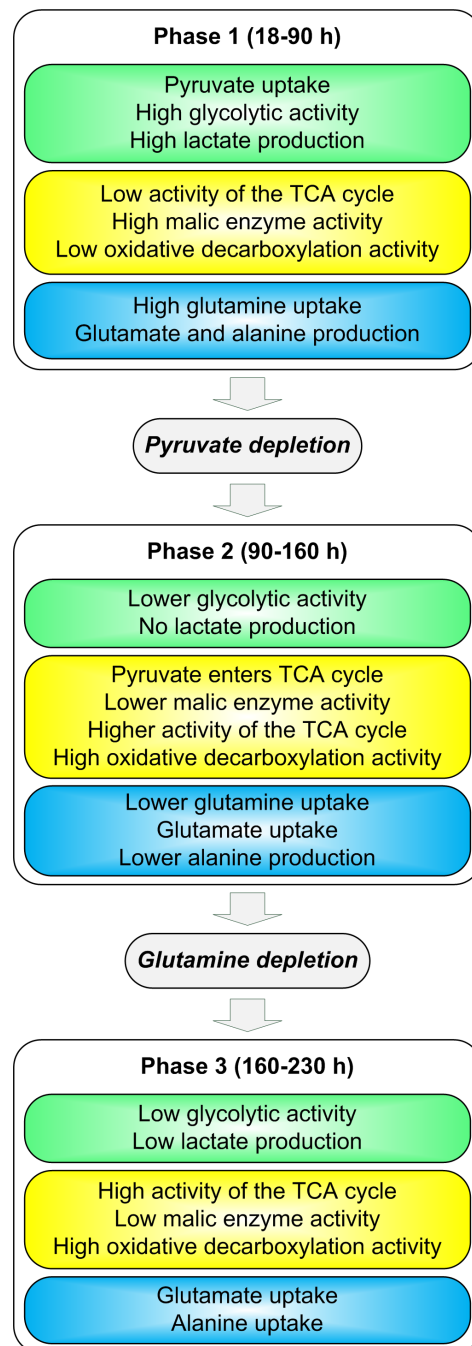


Fig. 2-7 Summary of metabolic shifts during batch cultivation of AGE1.HN.

2.5.3 Time resolved vs. stationary flux analysis.

The applied dynamic method is well suited to analyze and monitor metabolic shifts during the cultivation. Cell growth, cell size, extracellular, as well as intracellular fluxes of mammalian cells in a cell culture process are highly dynamic which is caused by environmental changes. Therefore, the presented method that is considering the dynamics of all included metabolites and biomass is best suited to understand and finally model the process. Stationary metabolic flux analysis, which was applied extensively in the past (Sidorenko et al. 2008; Xie and Wang 1996b), is only suited to describe the mean metabolism during a certain phase which is a significant disadvantage since changes during the phase considered are neglected (Niklas et al. 2010). However, if the pseudo steady state assumption during a phase is justified, it can give

a useful overview of its average metabolism (Quek et al. 2010). The information obtained by flux balance analysis can be validated (Zupke and Stephanopoulos 1995) or further enriched by specific labeling information (Bonarius et al. 1998b) to resolve reversible, cyclic, or parallel fluxes as, e.g., pentose phosphate pathway split (Lee et al. 1998; Velagapudi et al. 2007).

2.6 Concluding remarks

The application of a dynamic metabolic flux analysis method, as presented in this study, is well suited to describe the dynamic and adaptive behavior of the metabolism of mammalian cells during cultivation in industrially relevant media at any scale. Thus it supports the identification of targets for improved growth and substrate utilization based on derived metabolic flux distribution. Further improvement of the method could be achieved by including labeling information as, e.g., to monitor pentose phosphate pathway split. The presented dynamic method can be applied to almost any cultivation of a mammalian cell and could replace the widely applied but inflexible stationary MFA. In this study, metabolic shifts caused by changing environmental conditions during cultivation of AGE1.HN cells were described in detail (Fig. 2-7). This knowledge about the reaction of the cells to changes in the environment is a valuable basis for designing efficient feeding strategies and provides hints for genetic modifications. In the AGE1.HN cell line, major targets identified for improvement are as follows: (i) overflow metabolism during phase 1 should be reduced, e.g., by reduction of pyruvate content in the medium, (ii) phase 2 should be prolonged by specific feeding strategies, e.g., of glutamine. The dynamic metabolic flux data presented in this study are a contribution to the attempts at understanding this cell line at a systems level. Such an understanding is expected to eventually support the improvement of heterologous protein production in derived producers. Generally, the method represents a valuable option to support today and future improvement of cell culture media and processes.

2.7 Acknowledgements

This work has been financially supported by the BMBF project SysLogics - Systems biology of cell culture for biologics. We thank Michel Fritz for valuable support for the HPLC analysis as well as Christian Priesnitz, Averina Nicolae, and Judith Wahrheit for their supporting work and valuable suggestions.

2.8 Supplementary material

The supplementary material for this chapter is available online:

http://www.springerlink.com/content/b8373v8224272736/449_2010_Article_502_ESM.html.

3 Metabolite channeling and compartmentation in the human cell line AGE1.HN determined by ^{13}C labeling experiments and ^{13}C metabolic flux analysis

3.1 Abstract

This study focused on analyzing active pathways and the metabolic flux distribution in human neuronal AGE1.HN cells, which is a desirable basis for a rational design and optimization of producing cell lines and production processes for biopharmaceuticals. ^{13}C -labeling experiments and ^{13}C metabolic flux analysis were conducted using glucose, glutamine, alanine, and lactate tracers in parallel experiments. Connections between cytosolic and mitochondrial metabolite pools were verified, e.g., flux from TCA cycle metabolite ^{13}C to glycolytic metabolites. It was also found that lactate and alanine are produced from the same pyruvate pool and that consumed alanine is mainly directly metabolized and secreted as lactate. Activity of the pentose phosphate pathway was low being around 2.3% of the glucose uptake flux. This might be compensated in AGE1.HN by high mitochondrial malic enzyme flux producing NADPH. Mitochondrial pyruvate transport was almost zero. Instead, pyruvate carbons were channeled via oxaloacetate into the TCA cycle, which was mainly fed via α -ketoglutarate and oxaloacetate during the investigated phase. The data indicate that further optimization of this cell line should focus on the improved substrate usage which can be accomplished by an improved connectivity between glycolytic and mitochondrial pyruvate pools or by better control of the substrate uptake.

This chapter was published as

Niklas J, Sandig V, Heinzle E. Metabolite channeling and compartmentation in the human cell line AGE1.HN determined by ^{13}C labeling experiments and ^{13}C metabolic flux analysis. *J Biosci Bioeng*. DOI: 10.1016/j.jbiosc.2011.07.021.

3.2 Introduction

In the last decade, the pharmaceutical industry has put much effort into developing and establishing efficient cell culture processes for the production of biopharmaceuticals to fulfill the increasing demand of a global market with a projected size of USD 70 billion by 2010 (O'Callaghan and James 2008; Pavlou and Reichert 2004; Walsh 2006). The rapid growth and success of the biologics sector is driven by high success rates of therapeutic proteins, especially monoclonal antibodies (O'Callaghan and James 2008; Reichert et al. 2005).

The applied cellular production systems and cell culture processes must be capable of generating high product yields. Commonly used cell lines are CHO (Chinese hamster ovary), BHK (baby hamster kidney), or hybridoma cells (Dinnis and James 2005; Sandig et al. 2005). However, increasing the product yields by optimizing culture conditions is limited (Fogolin et al. 2004; Kumar et al. 2007; Oh et al. 2005; Trummer et al. 2006). Due to demands for higher productivity, efficiency, product quality (e.g., glycosylation), and robustness, new designer cell lines are developed and are entering the market (Rose et al. 2008; Sandig et al. 2005). The human cell line AGE1.HN (ProBiogen AG, Berlin, Germany) represents such a relatively new cell line which is well suited for the production of challenging biopharmaceuticals requiring complex human-type glycosylation (Blanchard et al. 2011). The rational improvement of the cell line can be facilitated by a thorough knowledge of growth and metabolism of the cells. In the area of systems biology research, the possibility is increasing of combining huge amounts of information with appropriate models enabling detailed knowledge and prediction of the investigated system (Kitano 2005; Westerhoff and Palsson 2004). A very powerful systems biology method represents metabolic flux analysis (Niklas et al. 2010; Sauer 2006; Wittmann 2007; Niklas and Heinzle 2011). Those flux distributions or *in vivo* reaction rates represent functional end points of genome, proteome, and metabolome interactions providing detailed information of the investigated system (Sauer 2006). While metabolic flux analysis, especially using ^{13}C labeled substrate, is widely applied in microbial biotechnology (Kiefer et al. 2004; Kim et al. 2008; Wittmann and Heinzle 2002), it is still less established in mammalian cells (Niklas et al. 2010). Due to complex nutrient requirements and usually unbalanced growth behavior, metabolic flux analysis in mammalian cells is much more complicated. Therefore, most studies applying metabolic flux analysis to mammalian cells were pure metabolite balancing (Niklas et al. 2009; Wahl et al. 2008). However, there are possibilities to investigate the metabolism under nearly steady state conditions applying ^{13}C metabolic flux analysis using special media in which the cellular metabolism is kept constant during a longer period (Deshpande et al. 2009).

An interesting aspect in eukaryotic cells that needs further investigation is metabolic compartmentation and the *in vivo* dynamics of key metabolic reactions that take place in cytosol as well as mitochondria. This can be accomplished by using ^{13}C metabolic flux analysis (^{13}C MFA). In order to perform a ^{13}C MFA, a thorough knowledge of the active enzymes and the connections in the metabolism of the system of interest is necessary, which enables the construction of a realistic carbon atom transition network. In this study, we performed labeling experiments using ^{13}C tracers of glucose, glutamine, lactate, and alanine to

unravel metabolic connections and active pathways in AGE1.HN. A carbon atom transition network was constructed taking into account metabolic compartmentation. In a recent publication on the metabolism and its dynamics during batch cultivation of the AGE1.HN cell line, distinct metabolic phases were observed (Niklas et al. 2011d). The first phase in the cultivation is characterized by overflow metabolism and energy spilling. It was proposed that one reason for this metabolic inefficiency might be the connectivity between glycolysis and TCA cycle resulting in a wasting of pyruvate produced intracellularly and, ultimately, energy. However, the metabolic flux distribution around the pyruvate node and, in particular, the compartmentation of the metabolism cannot be determined just by metabolite balancing as applied in our previous study (Niklas et al. 2011d). In this study, ^{13}C tracers and, subsequently, ^{13}C metabolic flux analysis were applied to get insights into these normally underdetermined parts of the metabolism. A detailed analysis of the metabolic fluxes during overflow metabolism in AGE1.HN sheds light on the metabolic reasons underlying the observed metabolic inefficiency in the first growth phase of this cell line. It additionally provides valuable hints for (i) further improvement of the cultivation process or (ii) genetic modifications improving the metabolic phenotype. To ensure reliable metabolic profiling, only mass isotopomer distributions of lactate were used for metabolic flux analysis. A powerful tracer combination was applied in parallel labeling experiments using differently labeled glucose and $[\text{U-}^{13}\text{C}_5]$ glutamine. We observed that the fluxes in the compartmented metabolic network can be resolved using the applied methodology revealing interesting aspects concerning the compartmentation of the cellular metabolism and the flux distribution in AGE1.HN during overflow metabolism.

3.3 Materials and Methods

3.3.1 Cell line

The cell line AGE1.HN[®] (ProBioGen AG, Berlin, Germany) was developed from primary cells from a human brain tissue sample which were immortalized with an expression plasmid containing the adenoviral E1 A and B genes of human adenovirus type 5 driven by the human pGK and the endogenous E1B promoter, respectively. E1A induces progression of the cell cycle, whereas E1B proteins prevent apoptosis caused by E1A through interaction with p53 and bax. The cell line was further modified to express the structural and regulatory protein pIX from human adenovirus type 5 which changes cell metabolism, enhances productivity for secreted proteins, and modulates susceptibility to a variety of viruses. The cell line was adapted to robust growth in suspension in both serum/protein-free and chemically defined culture media. In this study, parental AGE1.HN cell line was used to analyze connections in the metabolism as well as its compartmentation unaffected by the production of a particular therapeutic protein.

3.3.2 Labeling experiments

Different tracer experiments were conducted to analyze the connections between key metabolites in the central metabolism. The applied tracers were $[1,2\text{-}^{13}\text{C}_2]$ glucose (99%, Cambridge Isotope Laboratories,

Andover, MA, USA), [U-¹³C₆] glucose (99%, Euriso-Top, Saarbrücken, Germany), [U-¹³C₅] glutamine (99%, Cambridge Isotope Laboratories), [U-¹³C₃] alanine (98%, Cambridge Isotope Laboratories), and [1-¹³C₁] lactate (20% w/w in water, Cambridge Isotope Laboratories). The glucose and glutamine tracer experiments were carried out as follows. The cells were cultured in baffled shake flasks (Corning, NY, USA) at 37°C on a shaker (2 inches orbit, ES-X, Kühner, Basel, Switzerland) enclosed in a 5% CO₂ supplied, humidified (80%) incubator (Mytron, Heilbad Heiligenstadt, Germany). The preculture was carried out in a 250 ml baffled shake flask in 42-Max-UB-medium (Teutocell, Bielefeld, Germany; substrate concentrations in the medium are given in Table S1). The cells were centrifuged (800 1/min, 7 min, 22°C, Megafuge, Heraeus Instruments, Hanau, Germany) and the supernatant discarded. The pellet was resuspended in 42-Max-UB-medium without glucose and glutamine. Four 125 ml baffled shake flasks were inoculated reaching an initial cell density of about 4×10^5 cells/ml. Glucose and glutamine were finally added. The final culture volume was 54 ml. Samples (1.6 ml) were taken every day. 500 µl were directly used for cell counting. The rest was centrifuged (1,500 1/min, 5 min, 22°C, Megafuge, Heraeus Instruments, Hanau, Germany), the supernatant transferred into fresh tubes and frozen (-20°C). The analysis of several cultivation parameters was carried out using an automated cell culture analyzer (Cedex AS20, Innovatis, Bielefeld, Germany). Dissolved oxygen was measured in an additional cultivation in the applied culture system using the OXY-4 mini system (PreSens-Precision Sensing GmbH, Regensburg, Germany) (Wittmann et al. 2003). It was always higher than 80% air saturation. The cultivation conditions for alanine and lactate tracer experiments were as described above using an incubator supplied with shaking unit as well as temperature and CO₂ control (Innova 4230, New Brunswick Scientific, Edison, NJ, USA; 2 inches orbit). The cells from the preculture were transferred in two separate tubes, centrifuged (500 1/min, 5 min, 25°C, Labofuge 400R Function Line, Heraeus Instruments, Hanau, Germany), the supernatant discarded, and the pellet resuspended in phosphate buffered saline (PBS). After another centrifugation, the pellets were resuspended in 42-Max-UB medium containing either 2.4 mM [U-¹³C₃] alanine or 9 mM [1-¹³C₁] lactate and not any anabolic amino acids which were determined using data obtained from the [U-¹³C₆] glucose experiment described above. The cell suspensions were transferred into 50 ml bioreactor filter tubes (TPP, Trasadingen, Switzerland). The culture volume was 19 ml. Samples of 500 µl were taken every day. Cell counting was performed using an automated cell counter (Countess, Invitrogen, Karlsruhe, Germany).

Metabolite concentrations and their labeling were analyzed as described below. The ¹³C labeling state of a molecule can be expressed in different ways, e.g., by using molar fractions or fractional abundances of single mass isotopomers (Kelleher 1999; Wittmann 2002). To describe the ¹³C labeling of the whole molecule the molar enrichment (Kelleher 1999) or summed fractional labeling (Christensen et al. 2000) can be used but also the so called fractional labeling (*FL*, mol ¹³C/mol total carbon) of the total molecule, which was also applied in other studies on cellular metabolism (Bonarius et al. 2001; Grotkjaer et al. 2004; Mancuso et al. 1994). The *FL* for each metabolite having *n* carbons was calculated as follows

$$FL = \sum_{i=1}^n \frac{i \times m_i}{n} \quad (1)$$

where m_i represents the fraction of a mass isotopomer having i ^{13}C atoms.

The concentration of labeled carbon atoms CLC (Unit C-mol/l) for each metabolite M having in total n carbon atoms was calculated using

$$CLC = FL \times [M] \times n \quad (2)$$

This is required for the analysis of the total carbon transfer from ^{13}C labeled substrates to products. The relative carbon atom transfer RCT from the respective tracer to a metabolite can finally be calculated.

$$RCT = \left| \frac{\Delta CLC_M}{\Delta CLC_{tracer}} \right| \quad (3)$$

3.3.3 Experiments applied for metabolic flux estimation

Parallel experiments in which the tracers $[1,2-^{13}\text{C}_2]$ glucose, $[\text{U}-^{13}\text{C}_6]$ glucose, and $[\text{U}-^{13}\text{C}_5]$ glutamine were applied were used for metabolic flux analysis. The details of the cultivation are described in the previous section.

3.3.4 Quantification of metabolites

Glucose, lactate, and pyruvate in the supernatant were analyzed using high-pressure liquid chromatography (HPLC) as described previously (Niklas et al. 2009). Quantification of proteinogenic amino acids was performed by another HPLC-method (Kromer et al. 2005). For metabolic rate calculation, the metabolite concentrations were corrected for evaporation and glutamine data was corrected for degradation as described recently (Niklas et al. 2011d).

3.3.5 Analysis of labeling patterns

^{13}C -labeling of extracellular metabolites was analyzed applying gas chromatography mass spectrometry (GC-MS). 100 μl of the supernatants were lyophilized. 50 μl N,N -dimethylformamide was added and incubated at 80°C for 30 min. The metabolites were derivatized into corresponding t-butyldimethylsilyl derivatives using 50 μl N -methyl- N -t-butyldimethylsilyl-trifluoro-acetamide (MBDSTFA) (Wittmann et al. 2002) followed by another incubation at 80°C for 30 min. The GC-MS measurements were carried out on a GC (HP 6890, Hewlett Packard, Palo Alto, CA, USA) equipped with an HP5MS capillary column (5% phenyl-methyl-siloxane diphenylpolysiloxane, $30 \text{ m} \times 0.25 \text{ mm} \times 0.25 \mu\text{m}$, Agilent Technologies, Waldbronn, Germany), electron impact ionization at 70 eV, and a quadrupole detector (Agilent Technologies). The conditions were as follows: 1 μl injected sample volume; helium carrier gas flow of 1.1 ml/min; temperature gradient: 135°C for 7 min, $10^\circ\text{C}/\text{min}$ up to 162°C , $7^\circ\text{C}/\text{min}$ up to 170°C , $10^\circ\text{C}/\text{min}$ up to 325°C , 325°C for 2.5 min; inlet temperature: 140°C and heating with $720^\circ\text{C}/\text{min}$ up to 320°C ; interface temperature 320°C ; quadrupole temperature 150°C . For later determination of the mass distribution vectors the m-57 fragments of the extracellular metabolites were used which contain the

complete carbon skeleton (Wittmann et al. 2002). Carbon mass isotopomers were determined from the analyte mass isotopomer distribution using the method of Yang et al. (Yang et al. 2009).

Mean mass isotopomer distributions for the experiments and the period considered for metabolic flux analysis were calculated. Fractions for each mass isotopomer m_i having i labeled carbons were calculated from yields on biomass BM using

$$f_{m_i} = \frac{d[m_i]/d[BM]}{\sum_{i=0}^n d[m_i]/d[BM]} \quad (4)$$

where f represents the fraction of each mass isotopomer m_i having n carbon atoms.

3.3.6 Calculation of specific rates

Specific rates (r) were calculated for each metabolite M using

$$r_M = \mu \frac{d[M]}{d[BM]} \quad (5)$$

where μ represents the specific growth rate.

Assuming that the cells are spherical, the volume of the cells was calculated from the determined cell diameter and finally the specific biomass production was calculated using the relationship determined earlier (Niklas et al. 2011d).

3.3.7 Anabolic demand of AGE1.HN

The anabolic demand of AGE1.HN calculated from the biomass composition which was also applied in another study on AGE1.HN (Niklas et al. 2011d) is illustrated in Table 3-1.

3.3.8 Flux estimation

Inputs used for flux estimation were the measured extracellular fluxes, anabolic fluxes, as well as the labeling patterns of lactate. Labeling in secreted extracellular amino acids could also be used theoretically for flux estimation. However, these amino acids are present in the beginning of the cultivation, and reversibility of production and uptake of these as well as their conversion would change the extracellularly present labeling distribution, which then no longer reflects the intracellular labeling state. In this study, labeling patterns of lactate were therefore used. The advantages are as follows. Lactate is not present in the beginning of the cultivation, it can be directly measured, and its production reflects immediately the current state of the cellular metabolism.

Fluxes were estimated in Matlab R2008 (The Mathworks, Natick, MA, USA) using the elementary metabolite unit concept (Antoniewicz et al. 2007). The defined biochemical reaction stoichiometry including carbon atom transition mechanisms was automatically compiled into the executable files required for carbon flux simulation and numerical flux estimation runs. A gradient-based hybrid algorithm is utilized for the numerical flux estimation (Yang et al. 2008). During the simulation, the measured and simulated variables were fitted by minimizing the sum of least squares (Wittmann and Heinzle 2002).

Maximum flux value was set to 500% of the glucose uptake flux. Error propagation was calculated applying Gaussian error propagation using Monte-Carlo simulation.

Table 3-1 Anabolic demand of AGE1.HN.

Precursor	Anabolic demand [mmol/g _{DCW}]
G6P	0.438
P5P	0.226
GAP	0.097
ACA	2.283
Ala	0.519
Asp	0.298
Glu	0.413
Gln	0.413
Gly	0.721
Ile	0.289
Leu	0.560
Pro	0.257
Ser	0.448
Val	0.395

The anabolic demand was calculated from the biomass composition which was described elsewhere (Niklas et al. 2011d). The demand for the biomass precursors included in the metabolic network (Fig. 4-2) is depicted. *DCW* dry cell weight, *G6P* glucose 6-phosphate, *P5P* pentose 5-phosphate, *GAP* glyceraldehyde 3-phosphate, *ACA* acetyl coenzyme A, standard abbreviations for amino acids.

3.4 Results

3.4.1 Metabolic connections in AGE1.HN

A number of tracer experiments were carried out followed by analysis of fractional labeling (*FL*) in extracellular metabolites and subsequent calculation of the relative carbon atom transfer (*RCT*) from tracers to extracellular metabolites in order to unravel relevant and active connections in the metabolism. Fig. 3-1 depicts the *RCT* from different tracers to extracellular metabolites after 72 h. It can be seen that glucose was metabolized mainly to lactate since 76% of glucose consumed was detected in lactate. Smaller amounts were channeled to alanine (5%) and serine (3%). In addition, glucose carbons were also entering TCA cycle which can be seen by an increase in *FL* of glutamate and proline. On the other hand, there was also reflux from TCA cycle which can be deduced by the observed labeling in lactate as well as alanine when using [U-¹³C₅] glutamine as tracer. Further interesting results were found by applying lactate and alanine tracers. It was observed that lactate was also taken up to a small extent, which can be deduced from a decrease in labeled extracellular lactate as well as an increase in labeled extracellular alanine (Fig. 3-1). This shows in addition that alanine and lactate and subsequently the pyruvate pools responsible for their synthesis are connected. By using [U-¹³C₃] alanine, it was found that alanine which was taken up was

mainly directly used for transamination entering the cytosolic pyruvate pool, converted to lactate, and secreted. However, another part was also entering the central metabolism, particularly the TCA cycle, which can be seen by an increase in labeled glutamate. This indicates, in addition, that generally most of the intracellular pyruvate was directly metabolized to lactate.

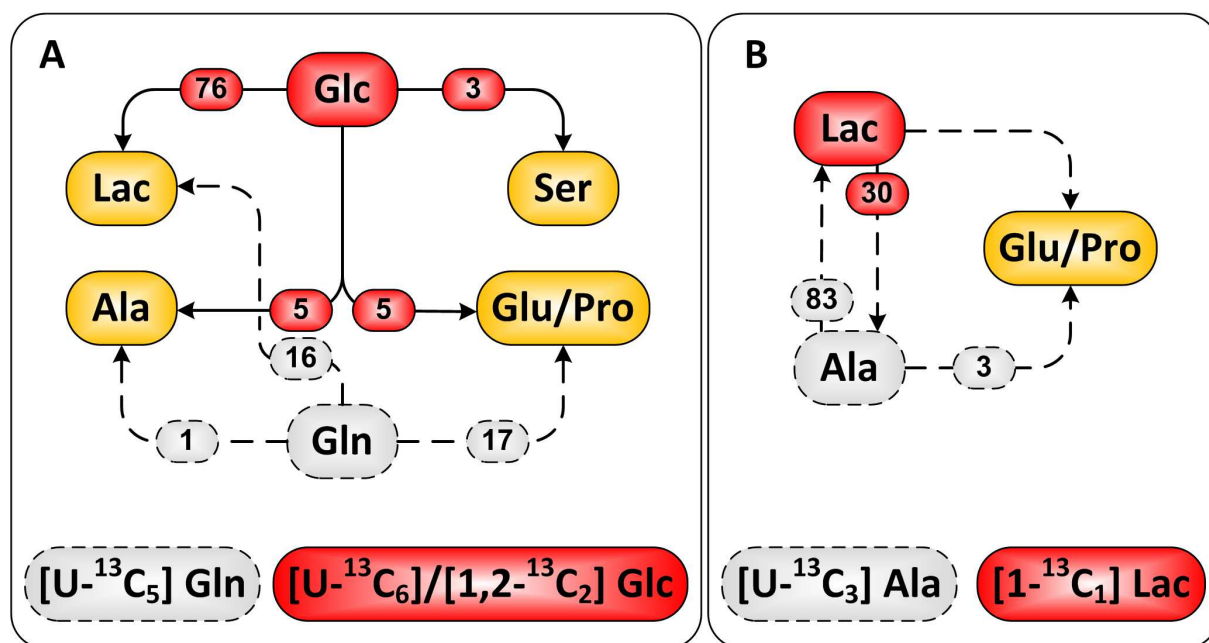


Fig. 3-1 Summary of the results obtained by different tracer experiments. Given are relative carbon atom transfers (RCT, [%]) from each tracer to extracellular metabolites after 72 h cultivation. The results from glucose labeling experiments using $[U-^{13}C_6]$ and $[1,2-^{13}C_2]$ glucose were averaged since these present the same information. A shows the results using glucose and glutamine tracers, B the results from alanine and lactate tracer experiments. *Glc* glucose, *Lac* lactate, standard abbreviations for amino acids.

3.4.2 Modeling

A metabolic carbon atom transition network of human central metabolism was set up (Fig. 3-2) using the genome information in the Kyoto Encyclopedia of Genes and Genomes (www.kegg.com), biochemistry books (Berg et al. 2003; Michal 1999), and the information obtained by tracer experiments (described above). Uptake fluxes of metabolites that do not contribute to the carbon atoms of the metabolites in the central metabolism are not important for ^{13}C metabolic flux analysis and were excluded allowing faster simulation and parameter estimation. These were taken as negligible if the uptake of a metabolite matched the anabolic demand. The reactions and carbon transfers of the model are shown in Table S2 of the supplementary material. Pyruvate and phosphoenolpyruvate pools as well as oxaloacetate and malate pools were lumped to one pyruvate pool and oxaloacetate pool in mitochondria and cytosol, respectively. As supported by the labeling experiments described before, reactions between cytosolic and mitochondrial pools of pyruvate and oxaloacetate as well as their transport reactions were modeled to be reversible. The model consisted in total of 13 extracellular fluxes, 13 anabolic fluxes, and 30 intracellular fluxes (16 defined as reversible). The anabolic demand (Table 3-1) for biomass precursors that are included in the

model was derived from the biomass composition which was also recently applied in another study (Niklas et al. 2011d).

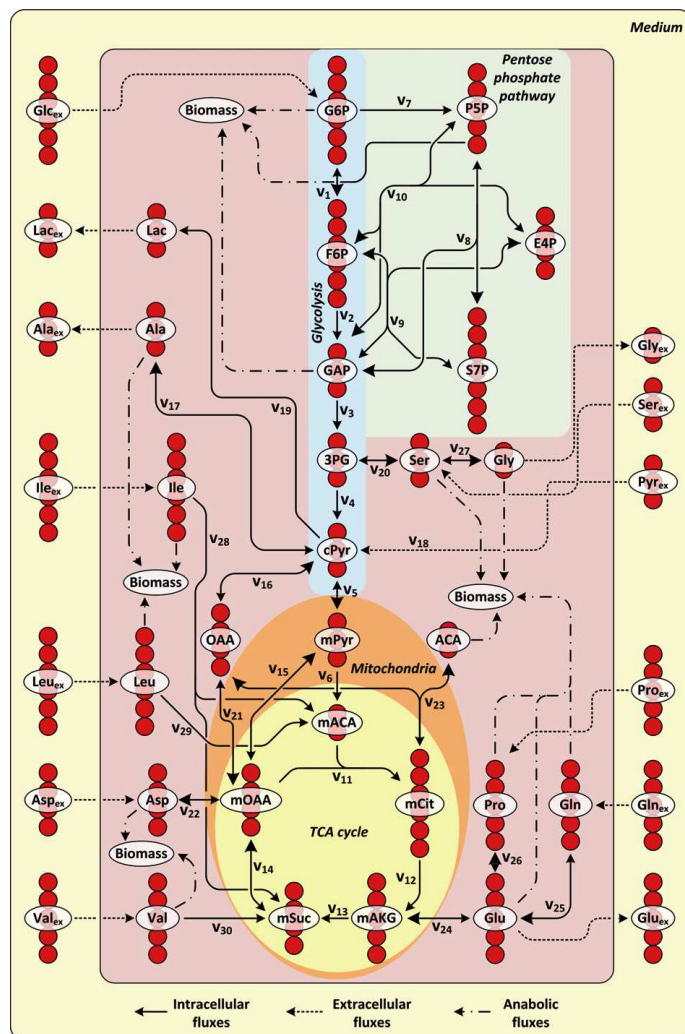


Fig. 3-2 Metabolic network for ^{13}C metabolic flux analysis in AGE1.HN. The carbon atom transition reactions of the network are given separately in Tab. S2. The reflux of a reversible reaction is indicated by the small line end of the arrow. Abbreviations: *3PG* 3-phosphoglycerate, *ACA* acetyl coenzyme A, *cPyr* cytosolic pyruvate, *E4P* erythrose 4-phosphate, *F6P* fructose 6-phosphate, *G6P* glucose 6-phosphate, *GAP* glyceraldehyde 3-phosphate, *Glc* glucose, *Lac* lactate, *mACA* mitochondrial acetyl coenzyme A, *mAKG* mitochondrial α -ketoglutarate, *mCit* mitochondrial citrate, *mOAA* mitochondrial oxaloacetate, *mPyr* mitochondrial pyruvate, *mSuc* mitochondrial succinate, *OAA* oxaloacetate, *P5P* pentose 5-phosphate, *Pyr* pyruvate, *S7P* sedoheptulose 7-phosphate, standard abbreviations for amino acids. Indices: *ex* extracellular.

3.4.3 Metabolic fluxes in AGE1.HN

Uptake and secretion rates for substrates and products (Table 3-2) were calculated for the growth phase between 18 and 72 h of the cultivation (see Fig. S1). In this phase, the cells exhibited overflow metabolism characterized by production of waste metabolites, e.g., lactate, alanine, and glutamate. Standard errors between the three cultivations were generally low (Table 3-2). Glutamine uptake rate was about 26% of the glucose uptake flux. Uptake of other amino acids was generally lower. However, the summed uptake of the branched chain amino acids leucine, isoleucine, and valine was comparable to the glutamine uptake. Serine, aspartate, and arginine uptake was also significantly higher compared to the remaining amino acid uptake rates.

Table 3-2 Extracellular rates in the exponential growth phase of AGE1.HN

	Rate [$\mu\text{mol/g/h}$]	SD [$\mu\text{mol/g/h}$]
r _{Glucose}	-144.6	5.3
r _{Lactate}	336.8	2.8
r _{Pyruvate}	-36.9	1.3
r _{Alanine}	20.1	2.4
r _{Arginine}	-10.9	3.3
r _{Asparagine}	-3.9	1.7
r _{Aspartate}	-14.0	3.5
r _{Cysteine}	-0.6	0.0
r _{Glutamate}	5.1	1.6
r _{Glutamine}	-38.3	1.4
r _{Glycine}	0.6	2.9
r _{Histidine}	-2.2	1.5
r _{Isoleucine}	-11.0	2.3
r _{Leucine}	-16.5	4.0
r _{Lysine}	-8.2	5.6
r _{Methionine}	-4.6	1.7
r _{Phenylalanine}	-4.6	1.9
r _{Proline}	-0.1	8.0
r _{Serine}	-16.8	5.4
r _{Threonine}	-5.9	2.2
r _{Tryptophan}	-1.5	0.9
r _{Tyrosine}	-3.9	1.2
r _{Valine}	-10.7	2.7

Metabolic rates for uptake (negative value) and production (positive value) of extracellular metabolites in the exponential growth phase of AGE1.HN (18-72 h). Mean values and standard deviations (SD) of three parallel cultivations in which different tracers ([1,2-¹³C₂] glucose, [U-¹³C₆] glucose, and [U-¹³C₅] glutamine) were applied.

By plotting metabolite (see Fig. S2) and lactate isotopomer (see Fig. S3) concentrations against glucose uptake, linear correlation was observed. This indicates that the pseudo steady state assumption during the exponential phase is valid and that the mean metabolism during this phase can be investigated using ¹³C MFA (Deshpande et al. 2009). Detailed ¹³C metabolic flux analysis was performed by including the labeling information stored in extracellular lactate resulting from three different parallel tracer experiments using [1,2-¹³C₂] glucose, [U-¹³C₆] glucose, and [U-¹³C₅] glutamine. The fit between simulated and measured extracellular fluxes as well as lactate labeling was very good (see Fig. S4). The resulting flux map is depicted in Fig. 3-3; detailed data including resulting errors in estimated rates is presented in Table S3 of the supplementary material.

Glucose which was taken up was mainly channeled through the glycolysis. Flux through the oxidative branch of the pentose phosphate pathway (PPP) was just around 2.3% of the glycolytic flux. The estimated flux through the non-oxidative branch of the PPP was very low.

The cytosolic pyruvate pool (cPyr) was mainly fed by the glycolytic flux. However, pyruvate uptake flux was about 20% of the glucose uptake (mol/mol) showing that extracellular pyruvate was also significantly contributing to intracellular pyruvate. The cytosolic pyruvate was almost exclusively converted to lactate and alanine and secreted. Just a very low amount was further used to produce energy. Flux between cytosolic oxaloacetate (OAA) and cPyr was estimated to be almost completely reversible having similar fluxes in both directions. Pyruvate transport between mitochondria and cytosol was very low having a higher flux from mitochondria to cytosol. Cytosolic oxaloacetate was entering mitochondria and feeding the mitochondrial oxaloacetate pool (mOAA). Flux from mOAA to mitochondrial pyruvate (mPyr) was relatively high and the only flux feeding mPyr pool.

The tricarboxylic acid (TCA) cycle was almost exclusively fed by substrates other than those derived from glucose. Glutamine uptake was about 27% (mol/mol) of the glucose uptake and glutamine was mostly metabolized to α -ketoglutarate feeding the TCA cycle. Other rates of anaplerotic reactions that significantly contributed to replenishing TCA cycle intermediates were the degradation of aspartate to mOAA as well as the degradation of the branched chain amino acids leucine, isoleucine, and valine. In total, carbon flux through the upper TCA cycle (citrate synthase) and lower TCA cycle (mAKG up to mOAA) was around 33% of the glucose uptake flux. Just the flux through the isocitrate dehydrogenase (mCit to mAKG) was lower which was caused by the citrate lyase catalyzed conversion of citrate producing cytosolic oxaloacetate and acetyl coenzyme A (ACA) that is needed for lipid biosynthesis.

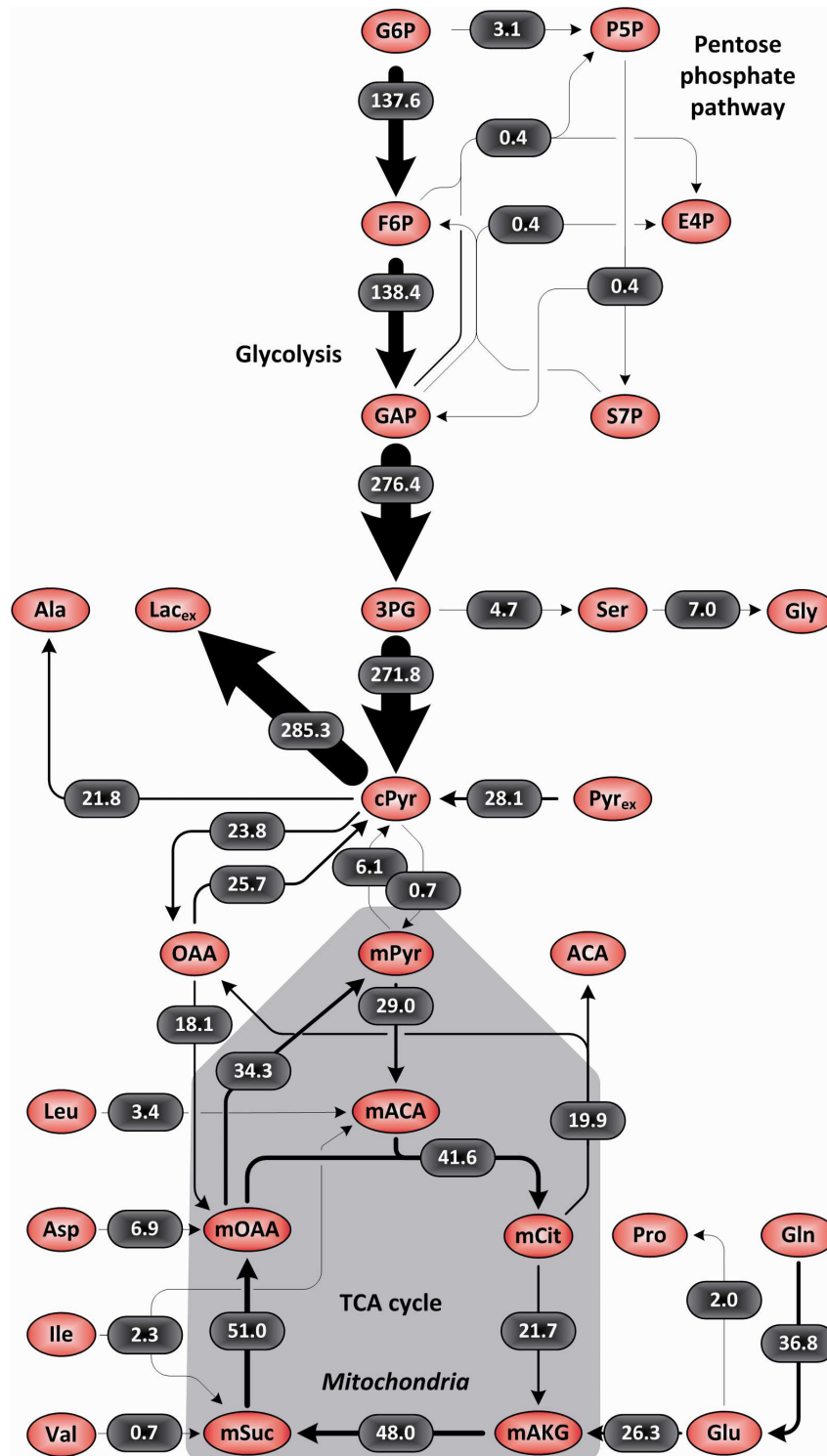


Fig. 3-3 Metabolic flux map for AGE1.HN during the first 3 days of batch cultivation. Fluxes are given in $\mu\text{mol}/\text{g}_{\text{biomass}}/\text{h}$. Flux strength is additionally indicated by the arrow width. Net fluxes could be determined very precisely in the metabolic network by using the applied tracer combination (Table S3). Fluxes to biomass and most extracellular fluxes are not depicted in this map. Abbreviations are defined in Fig. 3-2 (metabolic network). Reversibility for fluxes between cytosolic oxaloacetate (OAA) and cytosolic pyruvate (cPyr) as well as for exchange of cytosolic and mitochondrial pyruvate (cPyr-mPyr) is depicted. For other reversible fluxes the net fluxes could be determined precisely but not their reversibility (see Table S3). Therefore, just the net fluxes are presented for these reactions.

3.5 Discussion

3.5.1 Metabolic connections in AGE1.HN

In the first part of this study, labeling experiments were conducted to identify active pathways in AGE1.HN (Fig. 3-1). Channeling of glucose carbons mainly to lactate in permanent cell lines is commonly observed in mammalian cell culture (Altamirano et al. 2006; Bonarius et al. 2001; Sidorenko et al. 2008) and was also described for AGE1.HN in a recent study in which metabolic dynamics during growth were investigated (Niklas et al. 2011d). During the growth phase which was considered for metabolic flux analysis in this study, around 80% of the glucose carbons were channeled to the waste products lactate and alanine showing that the metabolism was not working efficiently (Fig. 3-1). This inefficient use of sugar carbons and energy which is stored in the wasted metabolites was already identified in the past as an optimization target and engineering approaches focused on optimizing this (Kim and Lee 2007). In AGE1.HN, only a very low amount of the glucose carbons were found later in the secreted amino acids glutamate and proline. This indicates, additionally, that glucose was not an important source for the TCA cycle during the investigated metabolic phase. On the other hand, a significant percentage of the consumed glutamine carbons were found later in lactate indicating reflux from the TCA cycle and a connection between mitochondrial and cytosolic metabolite pools. The lactate labeling experiment revealed that lactate production and uptake was to a certain extent reversible. This shows that it might also be possible in the future to design the cultivation process such that lactate, which is produced during a first phase, can be taken up again and be used as an energy source as it was presented for CHO cells (Altamirano et al. 2006). Alanine was also reversibly produced and taken up as unraveled by the alanine tracer experiment. Interestingly, the percentage of alanine carbons which were channeled to lactate was almost identical to the percentage of glucose carbons that were found later in lactate. This indicates that both metabolites, i.e., glucose and alanine, were feeding into the same pyruvate pool since the fate of their carbons seems almost identical. This is somehow in contrast to earlier reports in which a strict separation of the glycolytic pyruvate pool that only produces lactate and the pyruvate pool involved in alanine metabolism was proposed. Zwingmann et al. described the phenomenon of alanine uptake and direct conversion and secretion of lactate in astrocytes (Zwingmann et al. 2001). Their observation was that alanine which is taken up by the cells is only converted to lactate and nothing is channeled into central metabolism. Bouzier et al. analyzed lactate and glucose metabolism in C6 glioma cells and presented results that supported the concept of two separate pyruvate and lactate pools (Bouzier et al. 1998). This seems to be clearly not the case in AGE1.HN since all these metabolite pools are connected, and alanine carbons derived from consumed alanine were also entering central metabolism at a similar percentage as glucose carbons.

3.5.2 Metabolic fluxes in AGE1.HN

Metabolic flux distribution in AGE1.HN was computed by integrating data from glucose and glutamine tracer experiments. By applying different tracers in parallel experiments, a lot of information can already

be obtained solely from the labeling in lactate, as applied in this study, since it is directly derived from probably the most important metabolic hub in the cells, i.e., pyruvate. Similarly, the significance of information increase by parallel labeling experiments was shown for ^{13}C metabolic flux analysis using CO_2 label analysis (Yang et al. 2006b, 2006a). The metabolic flux distribution of AGE1.HN (18-72 h of the cultivation) shows some interesting differences compared to metabolic fluxes published for other cells. Relative pentose phosphate pathway (PPP) activity in AGE1.HN was low being around 2.3% of the glucose uptake flux (Fig. 3-3). In other mammalian cells, comparably low activities have been reported (Lee et al. 1998; Mancuso et al. 1994; Vo and Palsson 2006). Slightly higher relative PPP activity was presented in metabolic flux studies on HEK-293 cells (Le Ru et al. 2010) and hybridoma cells (Bonarius et al. 2001) being 15% and 20%, respectively. In some studies, surprisingly high PPP activities of even approximately 40% were reported (Goudar et al. 2010; Maier et al. 2008). Generally, PPP activity depends on the demand for NADPH, nucleotides, and specific sugars, which again depends on the growth conditions and growth rate of the cells. Additionally, the NADPH supply can also be accomplished by the activity of malic enzyme or transhydrogenases. Malic enzyme isoforms are differentially expressed in the cytosol and mitochondria having different isoforms that prefer NADH or NADPH (Pongratz et al. 2007). Especially in neuronal cells, it was reported that the malic enzyme and, in particular, the mitochondrial one might be highly enriched and play a key role in the mitochondrial metabolism of brain cells (McKenna 2007). In our study, relatively high activity of the mitochondrial flux from oxaloacetate (mOAA) to pyruvate (mPyr) was estimated indicating an important role of this flux in this neuronal cell line. This flux's principal contribution was to fill up the mitochondrial pyruvate pool, and it can also contribute to NAD(P)H supply in this cell line. The cytosolic fluxes between oxaloacetate (OAA) and pyruvate (cPyr) were estimated to be highly reversible and the net flux was very low. In other cells, this cytosolic flux was working in the same direction (OAA to cPyr) but was estimated to be higher (Bonarius et al. 2001; Goudar et al. 2010; Le Ru et al. 2010). In CHO and hybridoma cells, mitochondrial malic enzyme was working in the other direction compared to AGE1.HN converting pyruvate to oxaloacetate (Bonarius et al. 2001; Goudar et al. 2010). This might also explain the different PPP activities in AGE1.HN cells compared to CHO and hybridoma cells, since the malic enzyme flux contributes to the supply of NADPH for biosynthesis.

Another interesting finding in this study was that the TCA cycle was almost exclusively fed by substrates other than glucose. Pyruvate transport between cytosol and mitochondria was almost zero. Total TCA cycle activity was approximately 30% (mol/mol) of the glucose uptake flux. In other cells, e.g., in MDCK or CHO cells, very low TCA cycle activity was found compared to the glycolytic flux (Sidorenko et al. 2008), especially, during the exponential growth phase (Altamirano et al. 2006). However, in other cells, the feeding of the TCA cycle was mostly accomplished through the entry of glycolytic pyruvate into mitochondria (Bonarius et al. 2001; Goudar et al. 2010; Le Ru et al. 2010); other anaplerotic fluxes played a minor role (Bonarius et al. 2001; Goudar et al. 2010). In HEK-293 cells, the anaplerotic fluxes feeding the TCA cycle were approximately similar compared to the mitochondrial pyruvate transport (Le Ru et al.

2010). In spite of almost no pyruvate transport from cytosol to mitochondria, the flux through pyruvate dehydrogenase was high in AGE1.HN being around 20% (mol/mol) of the glucose uptake flux (Fig. 3-3).

3.5.3 Targets for improvement of metabolic efficiency

The metabolic phase that was investigated is characterized by an overflow of substrates and high production of waste metabolites resulting in spilling of carbon energy. The inefficient use of glucose and pyruvate carbons is, therefore, an optimization target for the AGE1.HN cell line. In particular, the connectivity between the pathways glycolysis and TCA cycle is very low. Fluxes into the cytosolic pyruvate pool were high but the pyruvate could not be efficiently channeled into mitochondria. Pyruvate transport between the compartments seems one of the major problems of this cell line under the applied conditions since it was almost zero. This could be solved in the future by genetic engineering approaches focusing on improved pyruvate transport into mitochondria or further conversion of pyruvate to oxaloacetate which might facilitate its transport and usage. Insertion of an additional pyruvate carboxylase gene might be an interesting option to improve flux from cytosol to mitochondria of AGE1.HN, as it was also tried in other cell lines (Elias et al. 2003; Irani et al. 1999). In particular, the finding that the main metabolic connection between cytosol and mitochondria in AGE1.HN cells seems to be the transport of oxaloacetate/malate makes this engineering strategy really interesting. The other possibility, which was also proposed earlier (Niklas et al. 2011d), is the reduction of substrate uptake minimizing the flow into the intracellular cytosolic pyruvate pool, which would most probably lead to a more efficient use of the nutrients. This can be done, e.g., by using efficient feeding strategies restricting substrate uptake or by applying genetic engineering strategies focusing on reduction of substrate uptake or waste product formation (Noguchi et al. 2000; Paredes et al. 1999; Wlaschin and Hu 2007).

The presented metabolic network and experimental platform for AGE1.HN cells also provides an important basis for further experiments to understand the effects of different environmental or genetic perturbations on cellular metabolism and its compartmentation as well as for the comparison of different producer cell lines.

3.6 Acknowledgements

This work has been financially supported by the BMBF project SysLogics - Systems biology of cell culture for biologics (FKZ 0315275A-F). We thank the Institute of Cell Culture Technology (University of Bielefeld, Germany) headed by Prof. Dr. Thomas Noll and especially Eva Schröder for most valuable help and experimental support. We thank Michel Fritz for valuable support for the HPLC and GC-MS analysis.

3.7 Supplementary material

The supplementary material for this chapter is available online:

<http://www.sciencedirect.com/science/article/pii/S1389172311002982>.

4 Primary metabolism in the new human cell line AGE1.HN at various substrate levels: increased metabolic efficiency and α_1 -antitrypsin production at reduced pyruvate load

4.1 Abstract

Metabolic responses of the new neuronal human cell line AGE1.HN to various substrate levels were analyzed in this study showing that reduced substrate and especially pyruvate load improves metabolic efficiency, leading to improved growth and α_1 -antitrypsin (A1AT) production. The adaptation of the metabolism to different pyruvate and glutamine concentrations was analyzed in detail using a full factorial design. The most important finding was an increasingly inefficient use of substrates as well as reduction of cell proliferation with increasing pyruvate concentrations in the medium. Cultivations with different feeding profiles showed that the highest viable cell density and A1AT concentration (167% of batch) was reached in the culture with the lowest glucose level and without pyruvate feeding. Analysis of metabolic fluxes in the differently fed cultures revealed a more efficient metabolic phenotype in the cultures without pyruvate feeding. The measured *in vitro* enzyme activities of the selected enzymes involved in pyruvate metabolism were lower in AGE1.HN compared with CHO cells, which might explain the higher sensitivity and different adaptation of AGE1.HN to increased pyruvate concentrations. The results indicate on the one hand that increasing the connectivity between glycolysis and the TCA cycle might improve substrate use and, ultimately, the production of A1AT. On the other hand, a better balanced substrate uptake promises a reduction of energy spilling which is increased with increasing substrate levels in this cell line. Overall, the results of this study provide important insights into the regulation of primary metabolism and into the adaptation of AGE1.HN to different substrate levels, providing guidance for further optimization of production cell lines and applied process conditions.

This chapter was published as

Niklas J, Priesnitz C, Rose T, Sandig V, Heinzle E. Primary metabolism in the new human cell line AGE1.HN at various substrate levels: increased metabolic efficiency and α_1 -antitrypsin production at reduced pyruvate load. *Appl Microbiol Biotechnol*. 2011. DOI: 10.1007/s00253-011-3526-6.

4.2 Introduction

Mammalian cells represent nowadays the predominant system for the production of recombinant proteins for clinical applications because of their ability to secrete properly folded and glycosylated proteins. Around 70% of recombinant therapeutic proteins are produced using cell culture processes, and this number is further increasing (O'Callaghan and James 2008). Intensive research in the past led to enormous improvement of the performance of mammalian cells (Wurm 2004). This was mainly enabled through better understanding and modification of parameters that influence productivity like cell growth, gene expression (Korke et al. 2004), metabolism (Bonarius et al. 2001; Cruz et al. 1999), protein secretion (Omasa et al. 2008), or repression of apoptosis (al-Rubeai and Singh 1998; Arden and Betenbaugh 2006; Nivitchanyong et al. 2007). For specific therapeutic glycoproteins with complex glycosylation, human cell lines may have an advantage compared to animal-derived cell lines since these human cells have a genuine human glycosylation system. The engineered cell line AGE1.HN represents such a very promising human-derived production system. In some initial studies, it was shown that these cells are well suited for the production of complex glycoproteins (Blanchard et al. 2011).

The neutrophil elastase inhibitor α_1 -antitrypsin (A1AT) represents a glycoprotein requiring N-glycosylation at three sites (Carrell et al. 1981). In the clinic, A1AT is required to treat patients having A1AT deficiency, an inherited disease that can result in lung emphysema and liver dysfunction (Kelly et al. 2010; Petrache et al. 2009). Patients with lung disease can be treated with A1AT augmentation therapy decreasing the mortality risk (A1AT-Group 1998). In spite of the fact that recombinant A1AT was produced in different prokaryotic and eukaryotic expression systems, there are currently only plasma-derived products licensed by the US FDA for intravenous treatment of A1AT deficiency (Karnaukhova et al. 2006). An alternative source for A1AT would be highly desirable since A1AT augmentation therapy is currently very expensive and not cost-effective (Gildea et al. 2003). A1AT derived from AGE1.HN cells has similar anti-inflammatory activity as commercial A1AT from human plasma (Blanchard et al. 2011), showing that the AGE.HN cell line is an alternative and favorable expression system for large-scale production of recombinant human A1AT.

The final product titer in a therapeutic protein production process in cell culture is related to high viable cell density and culture longevity (Kumar et al. 2007). In order to obtain high cell densities in a targeted development process, detailed knowledge of the metabolism of the producing cell system is desirable (Niklas et al. 2010). Metabolism of cells can be analyzed by metabolic profiling where, e.g., time courses of metabolites are interpreted or by different methods of metabolic flux analysis where intracellular reaction rates are analyzed (Niklas and Heinzle 2011; Niklas et al. 2010). Analysis of the cellular fluxome has shed light on the metabolism and its regulation not only in several mammalian cells (Bonarius et al. 2001; Gambhir et al. 2003; Niklas et al. 2009; Niklas et al. 2011d; Sidorenko et al. 2008; Teixeira et al. 2008) but also in microorganisms (Selvarasu et al. 2009a; Wittmann and Heinzle 2002) or plants (Heinzle et al. 2007).

In a metabolic flux study on parental AGE1.HN cells, changes in the metabolic fluxes during batch cultivation of the parental AGE1.HN cell line were analyzed (Niklas et al. 2011d). It was found that during cultivation, the metabolism in AGE1.HN was switching from an inefficient metabolic state characterized by waste product formation to a very efficient metabolic state with minimum energy spilling. The main event that was triggering this change in the metabolism was concluded to be the reduction in extracellular substrate levels including the depletion of pyruvate. Reduction of the glutamine level and finally its depletion was another perturbation occurring during batch cultivation, which led again not only to a metabolic shift but also to a stop of growth and reduction of viability. It seems interesting to investigate the effects of pyruvate and glutamine on growth, metabolism, and glycoprotein production in more detail. In particular, pyruvate was often not considered and sometimes even not measured in metabolic studies on mammalian cells. However, it was shown that pyruvate can be used to introduce beneficial changes in the metabolism of several mammalian production cells (Genzel et al. 2005; Omasa et al. 2010). Genzel et al. (Genzel et al. 2005) showed that high pyruvate concentrations in the medium can be used to replace glutamine resulting in similar growth and lower ammonia production in cultivations of MDCK, BHK21, and CHO-K1 cells. These mammalian cells could even grow in media containing up to 37 mM pyruvate. Omasa et al. found that the addition of pyruvate to cultivations of CHO cells resulted in an increased tricarboxylic acid (TCA) cycle activity accompanied by increased ATP and antibody production rates (Omasa et al. 2010). The studies mentioned show that it is interesting to investigate the effects of different substrate levels and especially different pyruvate concentrations on the metabolism in order to acquire an improved understanding of the cellular utilization of the substrates and their influence on cell growth and productivity. This improved understanding can eventually lead to the identification of promising targets for further metabolic engineering and for rational improvement of the production process.

With the aim of understanding the influence of major substrates on the metabolism and growth of AGE1.HN, different substrate levels were examined. The effects of start concentrations of pyruvate and glutamine on growth and metabolism of AGE1.HN in batch cultivation were studied using a full factorial design experiment. Based on these results, feeding experiments were carried out in which glucose, pyruvate, and glutamine were fed during the cultivation in order to maintain the substrate levels in a certain concentration range. Metabolic flux analysis using the metabolite balancing method was additionally performed for the differently fed cultures in order to analyze the differences in substrate use. The results of the study lead directly to further engineering strategies for the improvement of biopharmaceutical production in the human AGE1.HN cell line.

4.3 Material and methods

4.3.1 Cell lines and cell culture

The AGE1.HN[®] cell line (ProBioGen AG, Berlin, Germany) was developed from primary cells from a human brain tissue sample. A more detailed description of the cell line was published recently (Niklas et

al. 2011d). In this study, the parental AGE1.HN cell line as well as a derived production cell line (AGE1.HN.AAT) which produces the therapeutic protein A1AT were applied. Parental AGE1.HN cells were transfected with an expression vector containing the human A1AT gene driven by a human CMV/EF1 hybrid promoter (ProBioGen AG). The high-producing AGE1.HN.AAT cell line was derived after selection with puromycin. AGE.HN cells were cultivated in the serum-free 42-Max-UB medium (Teutocell AG, Bielefeld, Germany). T-CHO ATIII cells producing recombinant anti-thrombin III were obtained from Helmholtz Center for Infection Research (Braunschweig, Germany) and were cultured using serum-free CHO-S-SFM II medium (GIBCO, Invitrogen, Darmstadt, Germany). Standard cultivations of all cell lines were carried out in shake flasks (125 or 250 ml; Corning, NY, USA) at 37°C in an incubator containing shaking unit (Innova 4230, New Brunswick Scientific, Edison, NJ, USA, 2-in. orbit) with constant 5% CO₂ supply at 185 rpm.

4.3.2 Analytical methods

Cell counting was performed using an automated cell counter (Countess, Invitrogen, Karlsruhe, Germany) or a hemocytometer. Viability was assessed by applying the Trypan blue exclusion method. The pH in the samples was determined using a MP 220 pH meter (Mettler-Toledo, Giessen, Germany). Sugars, lactate, and pyruvate in the supernatant were analyzed using high-pressure liquid chromatography (HPLC) as described previously (Niklas et al. 2009). For the feeding experiments, glucose concentration was additionally measured using the Glucose-UV Assay Kit (Roche, Darmstadt, Germany) according to the manual. Quantification of proteinogenic amino acids was performed by HPLC using the method of Kromer et al. (Kromer et al. 2005). Ammonia was quantified using the ammonia assay kit of Sigma-Aldrich (Steinheim, Germany) according to the kit's instructions. The measurement was performed in a photometer (Novaspec, Pharmacia Biotech, LittleChalfont, England). The concentration of active A1AT was determined using the trypsin inhibitory assay. Calibration was done using standards with different A1AT concentrations (0.5-0.001 mg/ml in phosphate buffered saline (PBS); A1AT from human plasma was acquired from Sigma-Aldrich). The samples were diluted with PBS (1:20 to 1:60). Of the samples and standard solutions 50 μ l was mixed with a trypsin solution (0.1 mg/ml in an activity buffer containing 15 mM Tris, 100 mM NaCl, 0.01% (*v/v*) Triton X-100 at pH 7.6) and incubated for 10 min at 37°C. Of these solutions 10 μ l was pipetted into the wells of a 96-well plate and 90 μ l of a BAPNA solution (*N* α -benzoyl-L-arginine 4-nitroanilide hydrochloride, Sigma-Aldrich) was added to each well. The BAPNA solution was prepared by mixing 11 μ l of BAPNA stock solution (500 mM in DMSO) with 1,989 μ l activity buffer. The plate was incubated at 37°C for 1 h and the absorption finally measured at 405 nm (iEMS Reader MF, Labsystems, Helsinki, Finland).

4.3.3 Study of the effects of pyruvate and glutamine concentrations

The effects of pyruvate and glutamine on the metabolism of parental AGE1.HN cells were analyzed in a three-level full factorial design for both factors (glutamine and pyruvate), resulting in 3² cultivations. The applied pyruvate concentrations were 2, 5, and 9 mM; the glutamine concentrations were 5, 7.5, and 10

mM. The preculture was performed in normal 42-Max-UB medium (2 mM pyruvate, 5 mM glutamine). The cells were harvested by centrifugation (500 rpm, 5 min, 25°C, Labofuge 400R Function Line, Heraeus Instruments, Hanau, Germany) and the supernatant discarded. The cell pellet was resuspended in the medium without glutamine and pyruvate. The cell suspension was uniformly distributed into 50-ml bioreactor filter tubes (TPP, Trasadingen, Switzerland) and the supplements (glutamine, pyruvate) were added. The culture volume was 20 ml. Samples of 300 μ l were taken every day. Of the samples, 50 μ l was used directly for cell counting. The rest was centrifuged (8,000 rpm, 5 min, 25°C, Biofuge Pico, Heraeus Instruments), the supernatant transferred into tubes and frozen (-20°C) for later exometabolome analysis.

4.3.4 Cultivation of AGE1.HN.AAT using different substrate feeding

The effects of different feeding profiles of glucose and pyruvate on growth, metabolism, and product formation (A1AT) were analyzed. The preculture (42-Max-UB medium; 2 mM pyruvate, 2 mM glutamine) was harvested by centrifugation (500 rpm, 5 min, 25°C, Labofuge 400R Function Line, Heraeus Instruments) and the supernatant discarded. The pellets were washed once with PBS (37°C, centrifugation as before) and the cells were finally resuspended in 42-Max-UB medium without glucose and glutamine. After cell counting, the cell suspension was transferred into 50-ml bioreactor filter tubes (TPP) and the supplements were added. Glutamine (stock solution 200 mM) was added to a final concentration of 2 mM in all cultures and glucose (stock solution 200 g/l) was supplemented such that the concentration was 1 g/l (feeds 1 and 2) or 2 g/l (feeds 3 and 4). The total cultivation volume was 16 ml. The following cultivations were carried out: (1) Control (Batch), normal batch cultivation using the standard cultivation conditions; (2) feed 1 (high Glc), glucose controlled at high level (up to 2 g/l and mostly above 0.2 g/l); (3) feed 2 (high Glc+Pyr), glucose controlled at high level (up to 2 g/l and mostly above 0.2 g/l) and when glucose was fed pyruvate was added such that the pyruvate concentration in the medium was increased by about 2 mM; (4) feed 3 (low Glc), glucose controlled at low level (up to 1 g/l and mostly above 0.1 g/l); (5) feed 4 (low Glc+Pyr), glucose controlled at low level (up to 1 g/l and mostly above 0.1 g/l) and when glucose was fed pyruvate was added such that the pyruvate concentration in the medium was increased by about 1 mM. In all cultivations, glutamine was fed to avoid limitation. Samples for metabolite analysis were taken every day. Glucose was measured in the cultures more often to avoid any limitation and to maintain the planned feeding profile by adjusting the feeding amount.

4.3.5 Metabolic flux analysis

Metabolic fluxes in AGE1.HN upon different substrate feeding were calculated for the phase between 72 and 169 h in which the main differences in the metabolism were observed. Stationary metabolic flux analysis was applied as described in detail in a recent publication (Niklas et al. 2011d). The metabolic network that was used recently to analyze metabolic shifts in the parental AGE1.HN cell line (Niklas et al. 2011d) was slightly modified and extended so that it contains additionally the production of A1AT and its precursor demand. The amino acid demand for A1AT was derived directly from its amino acid sequence. The average glycosylation of A1AT was taken from the literature (Kolarich et al. 2006). To glycosylate one

A1AT protein having three *N*-glycosylation sites, the following sugar combination is needed: average glycosylation (three sites) = 12.69 *N*-acetylglucosamine + 9 mannose + 6.69 galactose + 6.681 *N*-acetylneuraminic acid + 0.321 fucose. The stoichiometry to synthesize 1 mol of fully glycosylated and active A1AT was included into the metabolic network model and can be seen in the stoichiometric matrix which is presented in the supplementary material (Table S1). A scheme of the applied metabolic network is depicted in Fig. 4-1.

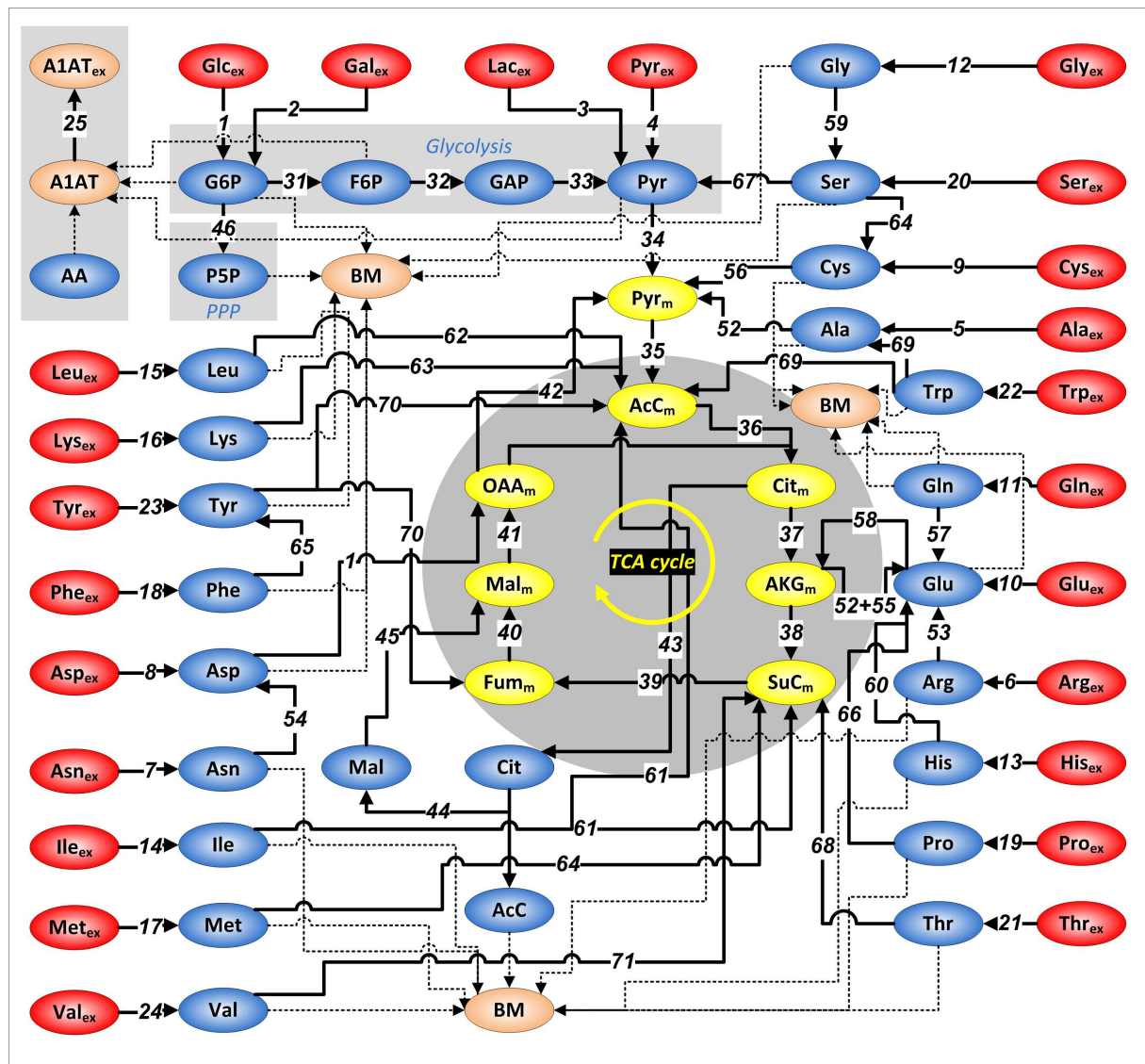


Fig. 4-1 Simplified scheme of the metabolic network model for calculation of metabolic fluxes in AGE1.HN (modified and extended version of a metabolic network model which was published previously (Niklas et al. 2011b)). Dotted lines indicate fluxes to biomass (BM), solid lines extracellular or intracellular fluxes. Flux numbers are depicted for extracellular and intracellular reactions. The stoichiometric matrix of the model is given in the supplementary material (Table S1). *PPP* pentose phosphate pathway, *TCA* tricarboxylic acid, *BM* biomass, *AA* all amino acids, *A1AT* α_1 -antitrypsin, *Glc* glucose, *Gal* galactose, *Lac* lactate, *Pyr* pyruvate, *G6P* glucose 6-phosphate, *P5P* pentose 5-phosphate, *F6P* fructose 6-phosphate, *GAP* glyceraldehyde 3-phosphate, *AcC* acetyl coenzyme A, *Cit* citrate, *AKG* α -ketoglutarate, *SuC* succinyl coenzyme A, *Fum* fumarate, *Mal* malate, *OAA* oxaloacetate, standard abbreviations for amino acids. Indices: *m* mitochondrial, *ex* extracellular.

4.3.6 Enzyme assays

Enzyme activity measurements were carried out in cuvettes using a UV/vis photometer (Helios α , Spectronic Unicam, Cambridge, England) set at 37°C. For performing enzyme assays, 50 μ l of cell suspension (10 μ l for lactate dehydrogenase (LDH) assay) was pipetted in each cuvette and 950 μ l of the respective assay solution (37°C) was added (990 μ l for LDH assay). Chemicals (analytical grade) were

purchased from Sigma-Aldrich, Fluka (Buchs, Switzerland), and Merck (Darmstadt, Germany). PBS buffer was acquired from PAA Laboratories (Pasching, Austria). The assay solutions for different enzymes were as follows. *Malic enzyme* (ME): 890 μ l PBS, 10 μ l MgCl_2 (200 mM), 10 μ l NADP^+ (100 mM), and 40 μ l malate (1 M). *LDH*: 960 μ l PBS, 25 μ l NADH (15 mM), and 5 μ l pyruvate (500 mM). *Pyruvate carboxylase* (PC): 830 μ l PBS, 10 μ l MgCl_2 (1 M), 15 μ l acetyl coenzyme A (50 mM), 10 μ l KHCO_3 (1 M), 40 μ l 5,5'-dithio-bis-(2-nitrobenzoic acid) (DTNB, 5 mM), 20 μ l pyruvate (2 M), 25 μ l ATP (100 mM), and 0.3 U citrate synthase. *Phosphoenolpyruvate carboxykinase* (PEPCK): 834 μ l PBS, 15 μ l NADH (10 mM) 1 μ l MgCl_2 (1 M), 10 μ l phosphoenolpyruvate (PEP) (100 mM), 75 μ l inosine diphosphate (20 mM), 10 μ l malate dehydrogenase (>12 U), and 5 μ l KHCO_3 (1 M). The cells were harvested in the exponential growth phase by centrifugation (5 min, 500 rpm, 25°C, Labofuge 400R, Heraeus Instruments). The supernatant was discarded and the pellet resuspended in PBS (37°C). This washing step was repeated and finally the pellet was resuspended in PBS and the cell density was determined. The cell suspension was diluted to yield a cell density of $\sim 5 \times 10^6$ cells/ml. The cells were disrupted by adding a Triton X-100 solution (5% v/v) such that the final concentration in the cell suspension was 0.05% (v/v) followed by incubation at 37°C for 10 min. This treatment was earlier found sufficient to permeabilize cellular and mitochondrial membranes (Niklas et al. 2011a). The cells were transferred into the cuvettes and the enzyme assay solution was added. The change in absorbance was finally monitored for 15 min. The specific enzyme activities per cell (SA) were calculated using

$$SA = \frac{\Delta A}{\Delta t \times \epsilon \times CD} \quad [1]$$

where A represents absorbance, CD the respective cell density, and t is time. For NAD(P)H-dependent measurements, the extinction coefficient, ϵ_{340} , of 6.22 l $\text{mmol}^{-1} \text{cm}^{-1}$ was used; for the DTNB-dependent measurements the extinction coefficient, ϵ_{412} , of 13.6 l $\text{mmol}^{-1} \text{cm}^{-1}$.

4.4 Results

4.4.1 Growth and metabolic profiles at different initial pyruvate and glutamine concentrations

AGE1.HN cells were grown in batch culture using media with different pyruvate (Pyr) and glutamine (Gln) concentrations in a full factorial design experiment to analyze the effects of both metabolites on growth and metabolism. Changes in cell density and in selected metabolite concentrations during cultivation are shown in the surface plots in Fig. 4-2 and in Table S2 of the supplementary material. The growth and metabolic profiles of all nine cultivations are depicted in the supplementary material (Fig. S1). Increasing Pyr concentrations led to a decrease in cell proliferation as well as total glucose and glutamine uptake and uptake of most amino acids (Fig. 4-2). Pyruvate uptake was highest in media having 5 mM Pyr as start concentration and was similar at high (9 mM) and low (2 mM) Pyr in the medium. Total lactate production was also highest in the 5 mM Pyr cultivations, but only slightly lower in the cultivations with 9 and 2 mM Pyr. The lactate/glucose quotient ($\Delta\text{Lac}/\Delta\text{Glc}$) that is also depicted in Fig. 4-2 as well as the

quotient of C-mol of produced lactate per C-mol of the consumed substrates glucose and pyruvate ($CLac/[CGlc+CPyr]$) indicate clearly a Pyr-dependent increase in the relative lactate production per consumed substrates. In the 9 mM Pyr cultivations, a $CLac/[CGlc+CPyr]$ quotient of even around 1 was observed. Additionally, glutamate and alanine production was influenced by an increasing Pyr concentration. An increase in the Gln concentration does not influence the cell proliferation, but led to an increase in the production of alanine, glutamate, and ammonia as well as a decrease in the uptake of asparagine and the branched chain amino acid isoleucine (Fig. 4-2, Table S2). Changes in extracellular metabolite concentrations per cell in the respective culture are depicted for some selected metabolites in Fig. 4-3. The data indicate that glucose and pyruvate uptake as well as the production of lactate per cell were increased depending on Pyr and were only little influenced by changing Gln concentration. Alanine and glutamate production as well as glutamine uptake per cell were increased with increasing Gln and Pyr consumption.

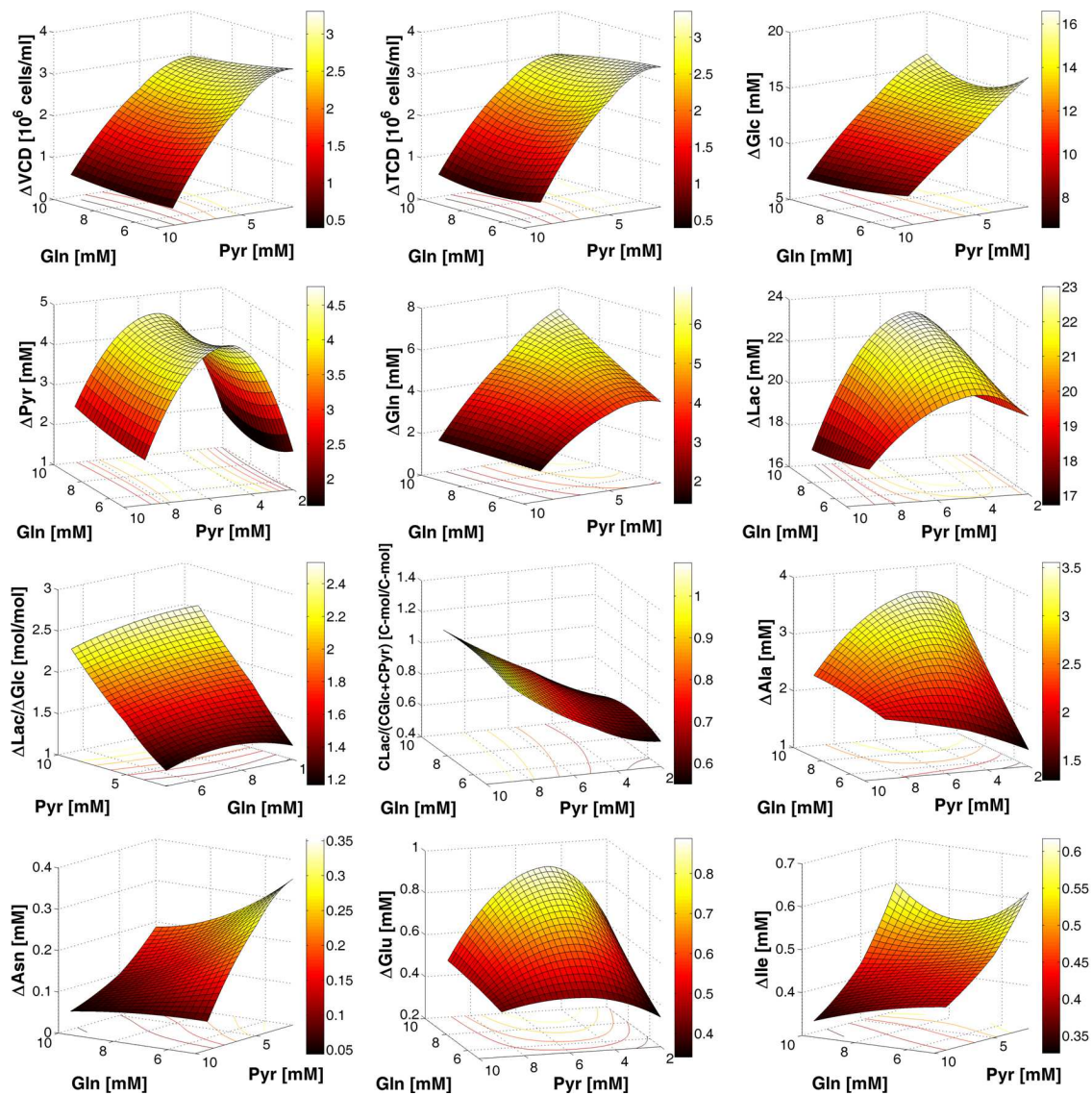


Fig. 4-2 Effects of different pyruvate (Pyr) and glutamine (Gln) concentrations in the medium on growth and extracellular metabolite levels (M) in AGE1.HN. Maximum changes, $\Delta M = |\text{Maximum (M)} - \text{Minimum (M)}|$, in

viable and total cell density (VCD, TCD) and extracellular metabolite levels (*Glc* glucose, *Lac* lactate, standard abbreviations for amino acids) are depicted. Additionally, the total Lac/Glc quotient ($\Delta\text{Lac}/\Delta\text{Glc}$) and the quotient of C-mol of produced lactate per C-mol of consumed glucose and pyruvate ($\text{CLac}/[\text{CGlc}+\text{CPyr}]$) in the different cultivations are presented. Detailed data are additionally given in Table S2. Growth and metabolic profiles are depicted in Fig. S1.

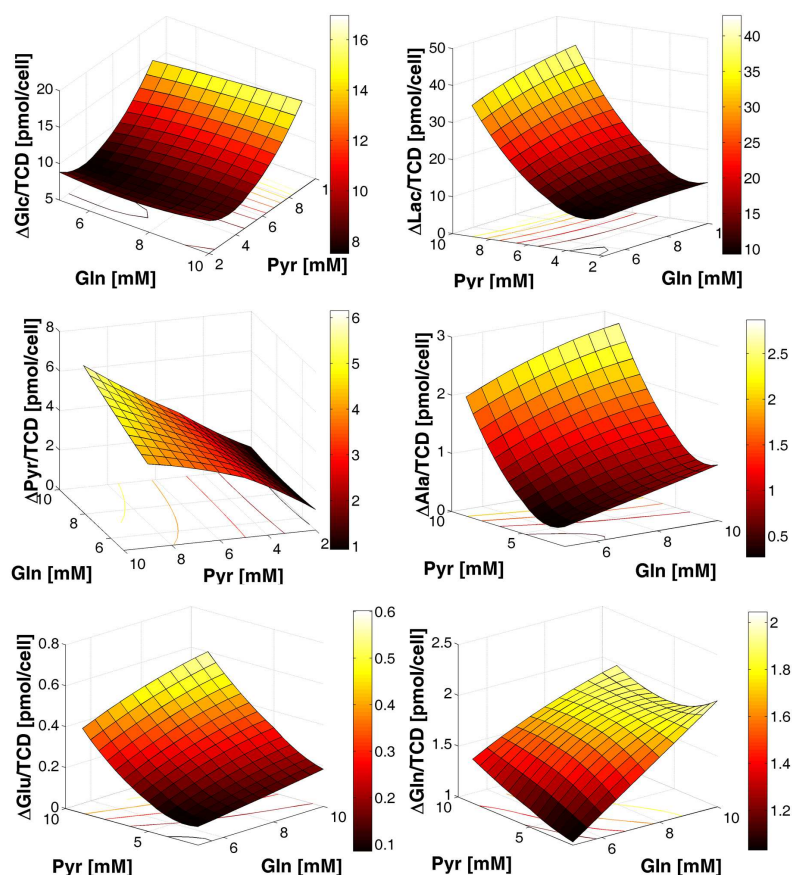
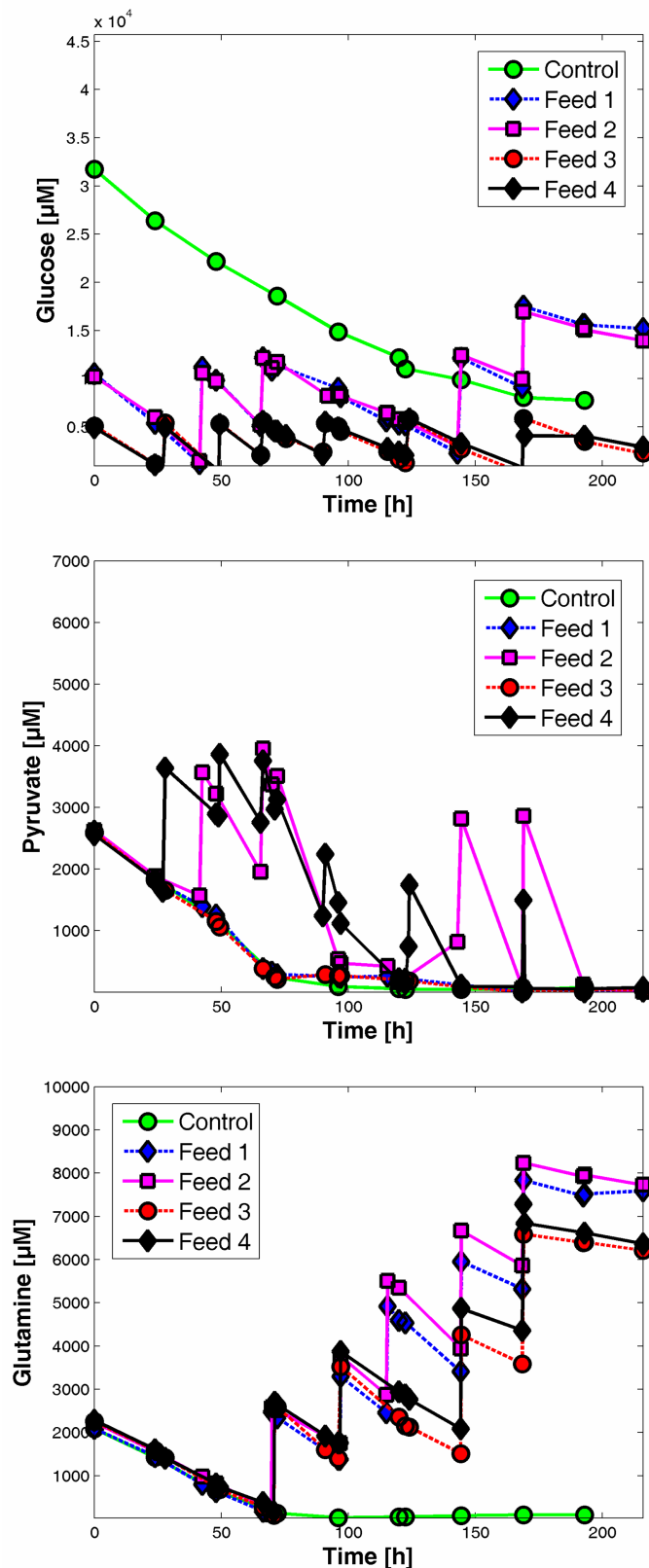


Fig. 4-3 Effects of different pyruvate (Pyr) and glutamine (Gln) concentrations in the medium on metabolite uptake or production per total cell density (TCD). Maximum changes, ΔM , in extracellular metabolite levels per total cell density in each cultivation are depicted (*Glc* glucose, *Lac* lactate, standard abbreviations for amino acids). Growth and metabolic profiles are depicted in Fig. S1.

4.4.2 Effects of different substrate feeding on growth and A1AT production

In the experiments described before with different pyruvate and glutamine concentrations, one of the most interesting aspects was the fact that increasing pyruvate concentrations led to low growth performance and high energy spilling, as indicated by high waste product formation. This effect of higher substrate load leading to energy wasting was further investigated by applying different feeding profiles. For these experiments, AGE1.HN cells producing the therapeutic glycoprotein A1AT were used to provide additional insights into the product formation under varying conditions of substrate supply. Different substrate feeding rates and different substrate concentrations in the medium might result in a different intracellular pyruvate supply and further changes in the cellular metabolism and product formation. The applied feeding profiles are depicted in Fig. 4-4. Different supplies of glucose and pyruvate were tested in the four feeding experiments. Growth and metabolite profiles (only most important metabolites) are

depicted in Fig. 4-5. Initially, growth and metabolism were similar in the fed-batch cultures and the batch cultivation. In a second phase after 72 h of cultivation, metabolism was clearly different depending on the applied feeding profile. The lower initial glucose concentration combined with feeding always resulted in higher cell density, increased culture longevity, and higher A1AT concentration compared with the batch cultivation. The highest viable cell density (146% of the batch cultivation) was achieved in the low-glucose culture without pyruvate feeding (Feed 3) in which also the highest A1AT concentration (167% of batch cultivation) was measured (Fig. 4-5). In the cultures that were also fed with pyruvate (feeds 2 and 4), lactate production was slightly higher after 72 h. Alanine and glutamate production were clearly increased compared with the cultures without the addition of pyruvate. Furthermore, A1AT production was lower



in the cultures which were additionally fed with pyruvate.

Fig. 4-4 Profiles of glucose (Glc), glutamine (Gln), and pyruvate (Pyr) concentrations during cultivations of the AGE1.HN.AAT cell line with different feeding profiles. Control (batch), normal batch cultivation using standard cultivation conditions; feed 1 (high Glc), glucose controlled at high level (up to 2 g/l and mostly above 0.2 g/l); feed 2 (high Glc+Pyr), glucose controlled at high level (up to 2 g/l and mostly above 0.2 g/l). When glucose was fed, pyruvate was added such that the pyruvate concentration in the medium was increased by about 2 mM; feed 3 (low Glc), glucose controlled at low level (up to 1 g/l and mostly above 0.1 g/l); feed 4 (low Glc+Pyr), glucose controlled at low level (up to 1 g/l and mostly above 0.1 g/l). When glucose was fed, pyruvate was added such that the pyruvate concentration in the medium was increased by about 1 mM. Glutamine was additionally fed to avoid limitation.

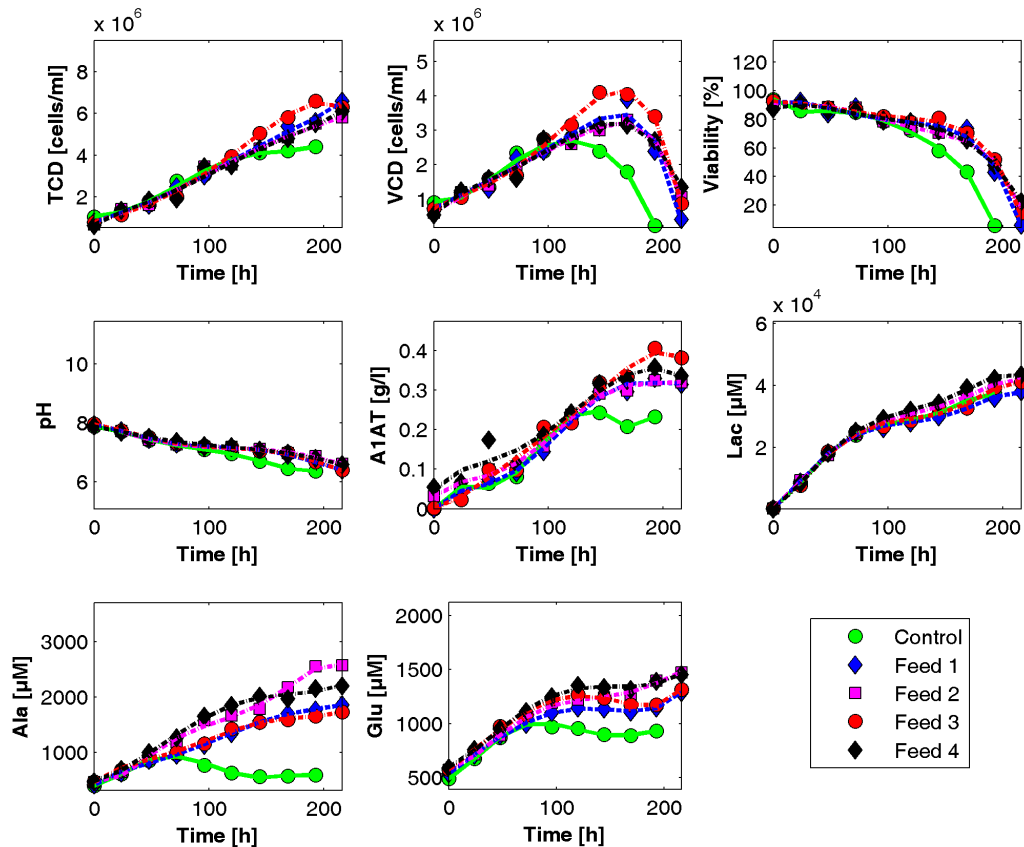


Fig. 4-5 Growth and metabolic profile of AGE1.HN.AAT cells during cultivation. The same experiment as in Fig. 4-4 where the applied feeding profiles are depicted. *TCD* total cell density, *VCD* viable cell density, *A1AT* α_1 -antitrypsin, *Lac* lactate, standard abbreviations for amino acids.

4.4.3 Metabolic changes upon different substrate feeding

In order to understand the main metabolic differences caused by different feeding of the substrates glucose and pyruvate, stationary metabolic flux analysis was performed for the phase between 72 and 169 h of the cultivation (Fig. 4-6, Table S3) in which the main differences in metabolite and growth profiles were observed (Fig. 4-5 and Fig. S2). It was found that the glucose uptake rate and glycolytic fluxes (v_{32} , Fig. 4-6) were only slightly reduced when pyruvate was fed as an additional carbon source (feed 2 and feed 4). Lactate production rate (v_3 , Fig. 4-6) was clearly increased in the cultures with pyruvate feeding. Mitochondrial pyruvate transport seemed to be slightly reduced with pyruvate feeding and with lower glucose concentration in the medium (v_{34} , Fig. 4-6). The activity of the upper and lower TCA cycle (v_{36} , v_{38} , Fig. 4-6) was unaffected by pyruvate feeding (feed 2 and feed 4) but was decreased in the cultures fed with low glucose levels (feed 3 and feed 4). The TCA cycle was mainly fed by pyruvate. Glutamate carbons were entering the TCA cycle to a lower extent and solely through transaminase-catalyzed conversion ($v_{52}+v_{55}$, Fig. 4-6). Glutamate dehydrogenase was working in the direction of glutamate (v_{58} , Fig. 4-6). This flux was clearly increased in the low-glucose cultures and slightly decreased when additionally pyruvate was fed. Net flux from glutamate to α -ketoglutarate ($v_{58}-[v_{52}+v_{55}]$) was increased with pyruvate feeding

(feed 2 and feed 4) and lower in the low-glucose cultures (feed 3 and feed 4) compared with the high-glucose cultures (feed 1 and feed 2). This flux was generally around 12% of the pyruvate transport flux (v_{34}). Glutamate and alanine production rates (v_5 and v_{10} , Fig. 4-6) were increased depending on pyruvate, as also observed for the lactate production rate. The highest A1AT production rate was found in the culture feed 3 in which glucose was maintained at a low level and pyruvate was not fed.

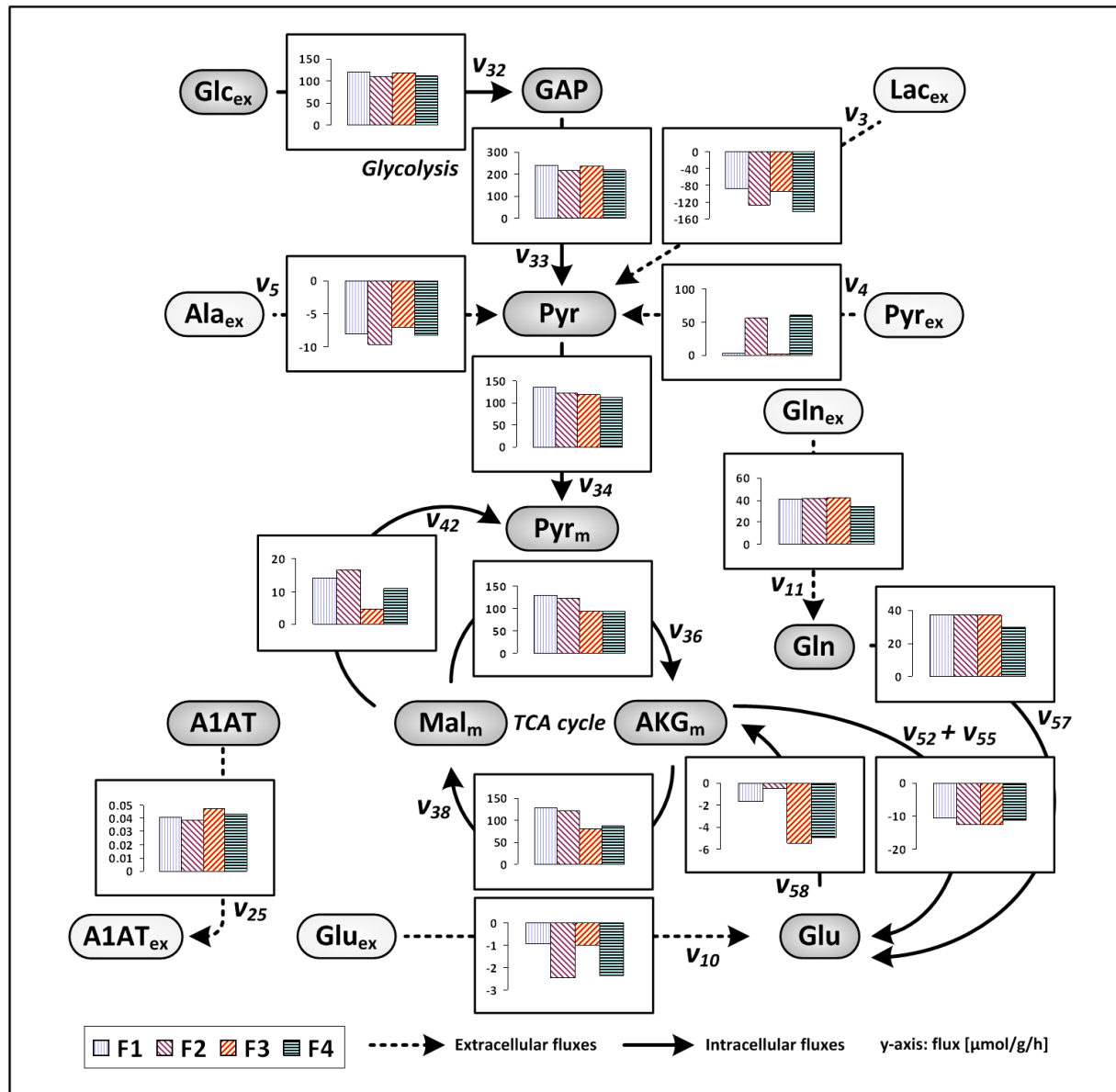


Fig. 4-6 Metabolic flux distribution of AGE1.HN during cultivations in which different feeding profiles (F1 – F4 correspond to feed 1-feed 4 of Fig. 4-4) were applied. The same experiment as shown in Figs. 4-4 and 4-5. Fluxes were calculated for the phase between 72 and 169 h. Negative values indicate fluxes in the opposite direction of the arrow. Detailed data are additionally presented in Table S3. The metabolic network including the flux numbers of the reactions and the abbreviations can be seen in Fig. 4-1.

4.4.4 Comparative analysis of *in vitro* activities of selected anaplerotic enzymes

In vitro activities of important enzymes of the pyruvate metabolism were measured in parental (AGE1.HN Par) and A1AT-producing (AGE1.HN.AAT) AGE1.HN cells and compared with the corresponding enzyme activity in a CHO cell line (T-CHO ATIII cells producing recombinant anti-thrombin III; Table 4-1). ME activity was slightly lower, whereas PC and PEPCK activities in AGE1.HN were by far lower than in CHO. LDH activity was slightly higher in AGE1.HN cell lines compared with CHO cells.

Table 4-1 *In vitro* activities of the enzymes malic enzyme (ME), pyruvate carboxylase (PC), phosphoenolpyruvate carboxykinase (PEPCK), and lactate dehydrogenase (LDH) in parental (AGE1.HN Par) and A1AT producing (AGE1.HN.AAT) AGE1.HN cells as well as in T-CHO ATIII cells.

	ME		PC		PEPCK		LDH	
AGE1.HN Par	81.5	±8.4	77.0	±9.4	2,582.9	±32.5	14,337.8	±510.4
AGE1.HN.AAT	97.7	±2.3	183.0	±15.9	2,676.7	±25.4	14,255.9	±403.0
T-CHO ATIII	143.3	±5.5	515.3	±20.8	7,143.5	±284.2	12,504.1	±337.6

Activities were measured in the exponential growth phase of the cells. Mean values and standard deviations of two measurements. Specific enzyme activities are given in fmol/cell/h.

4.5 Discussion

In the first part of this study, growth and metabolic profiles of AGE1.HN cells cultured with increasing pyruvate and glutamine concentrations were analyzed. In a recent study on metabolic dynamics, it was proposed that pyruvate and glutamine supply might induce characteristic changes in the metabolism of AGE1.HN (Niklas et al. 2011d). This was based on flux changes analyzed during batch cultivation. In order to investigate the influence of both substrate metabolites in detail, increased pyruvate and glutamine concentrations were applied in a full factorial design experiment and growth and metabolite concentrations were monitored. The dependency of the production and uptake of other metabolites on extracellular pyruvate and glutamine levels could be determined.

Increased glutamine concentrations did not cause significant changes in cell proliferation, but led to specific changes in the uptake and production of other amino acids and amino group donors as well as an increase in ammonia production (Table S1). Increased alanine production caused by increased glutamine concentration in the medium aids reducing ammonia intoxication. Transamination reactions, transferring amino groups from aspartate or glutamate to pyruvate, yielding alanine, may play a role in ammonia detoxification. Also, in other studies, increased alanine production in the presence of high ammonia concentrations was reported (Hansen and Emborg 1994; Miller et al. 1988; Ozturk et al. 1992). In AGE1.HN, it was additionally found that glutamine depletion is associated with a direct decrease in viability, showing its importance for this cell line (Niklas et al. 2011d). After glutamine depletion, the metabolism tries to compensate this by a higher uptake of the amino group donors glutamate and alanine, but this is not enough to sustain the growth rate and viability (Niklas et al. 2011d). Glutamine feeding

seems essential to maintain the viability and growth of AGE1.HN, as will also be outlined later in the discussion.

The cell interior of mammalian cells is compartmentalized and highly organized. To overcome diffusive barriers in the cell, enzymes of a metabolic pathway are sometimes associated physically and build static multienzyme complexes, so-called metabolons, resulting in a channeling of the metabolites through this pathway (Ovadi and Saks 2004). Glycolytic channeling and the association of glycolytic enzymes has been reported earlier (Graham et al. 2007). This might result in a direct conversion of glucose down to lactate, preventing an efficient use of glucose-derived pyruvate in the mitochondria. Additional cytoplasmic pyruvate pools could exist (Zwingmann et al. 2001), and this pyruvate might be transported more efficiently into mitochondria and might be further metabolized in oxidative decarboxylation and TCA cycle. Omasa et al. found that the ATP and antibody production rates of hybridoma cells could be increased by adding specific metabolites, i.e., pyruvate, malate, and citrate (Omasa et al. 2010). In particular, pyruvate enrichment caused an improvement of the energy metabolism (e.g., increase in TCA cycle fluxes) and a significant increase in product formation. In AGE1.HN cells, it seems that pyruvate has an opposite effect since growth and energy metabolism became less efficient with increasing pyruvate supply in the medium. In particular, lactate production per consumed substrate (glucose and pyruvate) increased. This indicates that pyruvate taken up from the medium is not differently and not more efficiently used than pyruvate derived through glycolysis. The performance of AGE1.HN is not improved by using additional pyruvate in the medium. Increasing pyruvate concentrations led to a less efficient metabolic phenotype with increased production of the waste metabolites lactate, alanine, and glutamate. This influence of pyruvate on the waste metabolite production was also proposed in a dynamic analysis of the metabolism of this cell line (Niklas et al. 2011d). Interestingly, an increase in the pyruvate supply was directly accompanied by an increase in lactate production per substrate that was taken up, resulting in an almost complete conversion of the substrates to lactate when 9 mM pyruvate was used in the medium (Fig. 4-2). This might also explain the almost complete stop of proliferation at the highest pyruvate concentration. The cells were not proliferating but were metabolizing the substrates, almost not producing any biomass but just waste metabolites. This indicates clearly that a reduction in the pyruvate load is beneficial for the growth of AGE1.HN and most probably also for later recombinant protein production. However, the pyruvate load and especially intracellular pyruvate load is dependent not only on the pyruvate concentration in the medium and its uptake but also on the cellular glucose uptake and the glucose amount which is metabolized through glycolysis. Generally, substrate level reduction seems beneficial to improve the efficiency of metabolism of AGE1.HN. Since pyruvate is efficiently taken up by the cells (Niklas et al. 2011d), the high pyruvate concentrations applied in this experiment (Fig. 4-2) mimic also the situation in which the cell has to cope with high intracellular pyruvate concentrations. It can be clearly seen in this study that the cells are not able to use the additional substrates efficiently by adapting their uptake or by increasing pyruvate flux into the TCA cycle which could result in better growth. Increased channeling of pyruvate into the TCA cycle depends on the possibility of increasing pyruvate transport, pyruvate dehydrogenase activity, anaplerotic reactions, and respiration activity. However, this

does not seem possible since the growth performance of the cells was clearly decreasing with increased substrate availability.

Another interesting application of high pyruvate concentrations in the medium was published by Genzel et al. (Genzel et al. 2005). It was reported that the replacement of glutamine by high pyruvate concentrations (e.g., 10 mM) seems to be an interesting strategy to reduce ammonia formation for some mammalian cell lines. However, when we tried to culture the human cell line AGE1.HN in media without glutamine, the cells did not grow even when increased concentrations of pyruvate were supplied (data not shown). Cultivation of the cells in media in which glutamine was replaced by glutamate was also not successful (data not shown). This might be caused by low or absent glutamine synthetase activity that was reported for other human cells (Bell et al. 1995; Street et al. 1993).

The strong influence of pyruvate on the energy spilling in AGE1.HN might also partly be explained by the lower activity of anaplerotic enzymes, e.g., malic enzyme, pyruvate carboxylase, and phosphoenolpyruvate carboxykinase compared with CHO cells (Table 4-1). As shown by Genzel et al. (Genzel et al. 2005) other mammalian cells (but not human cells) grow comparably well in media having low or high pyruvate concentrations, which might be explained by a higher enzymatic capacity to convert pyruvate and channel its carbons into TCA cycle associated with a higher respiratory activity. In a subsequent metabolic flux study on MDCK cells in normal medium or medium having high pyruvate concentration and no glutamine, it was suggested that most of the glucose consumed was excreted as lactate under high pyruvate conditions whereas pyruvate seemed to directly enter TCA cycle (Sidorenko et al. 2008). This is also different compared with AGE1.HN. The results of the feeding experiment (Fig. 4-4 and 4-5) and especially the metabolite balancing flux analysis (Fig. 4-6) showed that additional pyruvate does not lead to an increase in TCA cycle fluxes and was not beneficial for A1AT production. As mentioned before, anaplerotic reactions connecting glycolysis and the TCA cycle, the pyruvate dehydrogenase activity, or respiratory capacity might be the bottleneck resulting in the observed phenotype. The low *in vitro* activities of the measured anaplerotic enzymes (Table 4-1) and inefficient pyruvate use can be an indication that a genetic engineering strategy, as was applied in other mammalian cells, might also be interesting for the improvement of the AGE1.HN cell line, namely, the introduction of an additional pyruvate carboxylase gene (Elias et al. 2003; Irani et al. 1999). However, this will only lead to a significant improvement if oxidative phosphorylation is not the limiting step.

The results of this study led to another strategy. A reduction in the substrate load (decrease in glucose concentration and no pyruvate feeding) resulted in improved culture longevity, more efficient metabolism, and finally higher product concentration. Substrate feeding should be balanced in fed-batch processes of AGE1.HN to maintain a most efficient metabolism. However, according to the data of the feeding experiments in which waste product formation was also just partially reduced even at lowest glucose feeding, strategies focusing on inhibition/reduction of substrate uptake should be considered. This may lead to lower accumulation of toxic waste products, higher cell densities, and product concentrations in the cultivation. Some genetic engineering in the past on mammalian cells focused also on the reduction of excessive substrate uptake, leading to an improved metabolism in the modified cells (Altamirano et al.

2000; Wlaschin and Hu 2007). Based on the results of this contribution, we have worked out a targeted engineering strategy for this cell line which focuses on a more efficient substrate usage, and work is underway showing the influence of this strategy on glycoprotein production in AGE1.HN.

Regarding the general findings concerning primary metabolism in AGE1.HN, it can be concluded that certain aspects are similar compared with the metabolic behavior of other mammalian cells, e.g., overflow metabolism in the beginning of the cultivation with high waste product formation, whereas other important metabolic parameters are completely different. In particular, pyruvate utilization and pyruvate metabolism are different in AGE1.HN compared with, e.g., CHO or MDCK cells, as was outlined before in the discussion.

Differences in the metabolism and in the metabolic machinery of different production cell lines might also originate from their specific origin. Enzyme and transporter properties as well as metabolic requirements of the cells depend on the tissue from which they originate (Wang et al. 2010). The cells in these tissues have a certain enzyme expression, e.g., different glucose transporters (Elsas and Longo 1992; Thorens and Mueckler 2010) or different expression of glycolytic and gluconeogenic enzymes (Lawrence et al. 1986), which depends also on their nutritional environment present in the respective part of the body (Mather and Pollock 2011). Different substrate levels in different tissues and even parts of tissues (Mather and Pollock 2011) result in cells adapted to their environment fulfilling specific tasks (Gebhardt 1992). Cells derived from different tissues might have therefore different metabolic properties, and their enzyme expression as well as the ability to adapt the enzyme expression to varying situations might differ. However, one has to keep in mind that production cells are immortalized and their metabolic behavior changes compared with the tissue situation. Nevertheless, these changes might be constrained to a certain extent depending on the tissue type from which the cells originate, e.g., by epigenetic mechanisms.

In summary, the following conclusions can be drawn from the different experiments which were performed in this study. Pyruvate enrichment in the medium leads to an inefficient metabolism characterized by high energy spilling and lowered cell proliferation. Reduced substrate levels and no pyruvate feeding resulted in higher efficiency of substrate use as well as higher viable cell densities and A1AT concentrations. Pyruvate addition does not increase TCA cycle fluxes in AGE1.HN, contrary to reports using other mammalian cells. Generally, pyruvate utilization in AGE1.HN cells as well as fluxes around the pyruvate node seem to be significantly different compared with the other mammalian cells currently employed in biopharmaceutical production. The *in vitro* activity of the measured anaplerotic enzymes in AGE1.HN is lower compared with CHO cells and can be an interesting genetic engineering target for the improvement of AGE1.HN since pyruvate is not efficiently entering the TCA cycle. However, the most promising strategy in our opinion is the engineering of the cells toward a more balanced substrate uptake. Work is underway showing the effects of this engineering strategy on the production in AGE1.HN cells. The findings of this study provide a rational basis for further targeted improvement of the cellular metabolism and the cultivation process conditions for production cells.

4.6 Acknowledgements

This work has been financially supported by the BMBF project SysLogics - Systems biology of cell culture for biologics (FKZ 0315275A-F). We thank Armin Melnyk for performing enzyme assays, Michel Fritz for valuable support for the HPLC analysis, as well as Judith Wahrheit for fruitful discussions.

4.7 Supplementary material

The supplementary material for this chapter is available online:

http://www.springerlink.com/content/g671458385788v17/253_2011_Article_3526_ESM.html.

5 Metabolic flux rearrangement in the amino acid metabolism reduces ammonia stress in the α_1 -antitrypsin producing human AGE1.HN cell line

5.1 Abstract

This study focuses on metabolic changes in the neuronal human cell line AGE1.HN upon increased ammonia stress. Batch cultivations of α_1 -antitrypsin (A1AT) producing AGE1.HN cells were carried out in media with initial ammonia concentrations ranging from 0 to 5 mM. Growth, A1AT production, metabolite dynamics, and finally metabolic fluxes calculated by metabolite balancing were compared. Growth and A1AT production decreased with increasing ammonia concentration. The maximum A1AT concentration decreased from 0.63 g/L to 0.51 g/L. Central energy metabolism remained relatively unaffected exhibiting only slightly increased glycolytic flux at high initial ammonia concentration in the medium. However, amino acid metabolism was significantly changed. Fluxes through transaminases involved in amino acid degradation were reduced concurrently with a reduced uptake of amino acids. On the other hand, fluxes through transaminases catalyzing the formation of amino acids, i.e., alanine and phosphoserine, were increased leading to increased storage of excess nitrogen in extracellular alanine and serine. Glutamate dehydrogenase flux was reversed and increasingly fixing free ammonia with increasing ammonia concentration. Urea production additionally observed was associated with arginine uptake by the cells and did not increase at high ammonia stress. It was therefore not used as nitrogen sink to remove excess ammonia. The results indicate that the AGE1.HN cell line can adapt to ammonia concentrations usually present during the cultivation process to a large extent by changing metabolism but with slightly reduced A1AT production and growth.

This chapter was submitted as

Priesnitz C*, Niklas J*, Rose T, Sandig V, Heinzle E. Metabolic flux rearrangement in the amino acid metabolism reduces ammonia stress in the α_1 -antitrypsin producing human AGE1.HN cell line.

5.2 Introduction

In the last decades mammalian cell cultures have gained more and more importance in biotechnological and pharmaceutical industries. Apart from the use of mammalian cells in the prediction of toxicity (Noor et al. 2009), they have become increasingly popular for the production of biopharmaceuticals (Wurm 2004). This has been mainly due to their ability to introduce correct posttranslational modifications on the expressed proteins. Now, the number of therapeutic proteins produced in mammalian cells exceeds the number produced in bacteria (Walsh 2010). The most important posttranslational modifications are *N*- and *O*-linked glycosylation. Glycosylation plays an important role for protein stability, ligand binding, immunogenicity, and serum half-life (Walsh 2006). Much effort has been put into optimizing productivity and product quality by applying different strategies like engineering cell metabolism, protein secretion, apoptosis resistance, and glycosylation (Lim et al. 2010). One major factor that still limits productivity is the accumulation of toxic byproducts like lactate and ammonia in the cell culture medium. Ammonia results on the one hand from chemical decomposition of glutamine (Fritsch and Moore 1962), which is an important component in most cell culture media, and on the other hand from metabolic deamination reactions. The effects of increased ammonia concentrations on different mammalian cells were examined by several groups (Mirabet et al. 1997; Ozturk et al. 1992; Schneider et al. 1996). The large variation of the influence of ammonia on different cells described in the literature shows that it is important to analyze the effects of elevated ammonia levels for every cell line separately and that it is not possible to completely transfer results obtained for one cell line to another. The effects range from decreased cell growth and reduced productivity to alterations in the glycosylation pattern and inhibition of virus multiplication (Andersen and Goochee 1995; Borys et al. 1994; Hong et al. 2010; Koyama and Uchida 1989; Thorens and Vassalli 1986; Yang and Butler 2000, 2002) and are, at least, partly attributed to changes in the intracellular pH and changes in UDP-hexose levels (Ryll et al. 1994). To overcome these negative effects of ammonia on cell growth, productivity, and product quality, the reduction of the ammonia accumulation in the media is a major goal. To achieve this, a variety of different approaches was proposed including (over)expression of the glutamine synthetase (Bell et al. 1995; Cockett et al. 1990), controlled feeding of glutamine (Eyer et al. 1995; Glacken et al. 1986), feeding of glutamine according to the demand for biosynthesis (Xie and Wang 1994) or depending on the oxygen uptake rate (Eyer et al. 1995), co-culturing CHO cells with HepG2 cells (Choi et al. 2000), substitution of glutamine by glutamate, asparagine (Kurano et al. 1990), or α -ketoglutarate (Hassell et al. 1991), and adaptation of cells to high ammonia concentrations (Schumpp and Schlaeger 1992). Most of the investigations available deal with the effects of elevated ammonia levels in hybridoma and myeloma cells used for the production of monoclonal antibodies (McQueen and Bailey 1990; Miller et al. 1988; Ozturk et al. 1992; Reuveny et al. 1986), and comparatively few publications can be found about the effects in CHO cells (Yang and Butler 2000), BHK cells (Cruz et al. 2000), or other mammalian cell lines, although, they are among the most prominent cell lines for production of therapeutic proteins. In most publications, the investigated parameters were just cell growth and productivity, and only in some studies changes in extracellular metabolites were

additionally analyzed. Detailed studies on the effects of elevated ammonia concentrations on central metabolism and intracellular fluxes are hardly available (Bonarius et al. 1998a; Nadeau et al. 2000).

The main goal of the presented study was a detailed analysis of the effects of elevated ammonia concentrations on growth, metabolism, and glycoprotein production in the human cell line AGE1.HN (ProBioGen, Berlin, Germany) that was specifically designed for production of biopharmaceuticals requiring complex human-type glycosylation (Blanchard et al. 2011). In this study, an AGE1.HN cell line was used that is producing α_1 -antitrypsin (A1AT). This glycoprotein, which is produced *in vivo* in the human liver, has three N-glycosylation sites and requires complex glycosylation (Carrell et al. 1981; Kolarich et al. 2006). A1AT is an important biopharmaceutical that is required for augmentation therapy in A1AT deficiency, a hereditary disorder which may result in a shortened lifetime mainly caused by chronic respiratory insufficiency (Tonelli and Brantly 2010). So far, only plasma-derived human A1AT is approved for augmentation therapy, whereas the production of stable and active recombinant or transgenic A1AT in several non-human hosts was impeded by impurities or lower stability mainly caused by wrong glycosylation of the produced A1AT compared to the plasma-derived version (Karnaikhova et al. 2006).

In this study, the following questions were addressed: (i) what is the effect of ammonia on cell growth, A1AT formation, A1AT quality/activity, (ii) how does the metabolism of AGE1.HN change upon high ammonia supply and how is ammonia detoxified, and (iii) should further engineering focus on ammonia metabolism? The results are important for further rational improvement of human production cell lines based on a thorough understanding of cellular physiology.

5.3 Material and methods

5.3.1 Cell line

The AGE1.HN[®] cell line (ProBioGen AG, Berlin, Germany) was derived from a primary human tissue sample from the periventricular zone of a fetal brain. The cells were immortalized using an expression plasmid which contained the adenoviral genes E1 A and B of the human Adenovirus 5. These genes are driven by the human pGK and the endogenous E1B promoter, respectively. Furthermore, the cell line was improved by expressing the protein pIX of the human Adenovirus 5. This modification leads to changes in the metabolism, enhanced productivity of secreted proteins, and increased the susceptibility to various viruses. AGE1.HN cells were transfected with an expression vector containing human A1AT (ProBioGen AG) under the control of a specific CMV/EF1 hybrid promoter (ProBioGen AG). High producer cells were selected with puromycin. Recently, it was shown that the AGE1.HN cell line can produce fully active A1AT with its complex glycosylation pattern (Blanchard et al. 2011).

5.3.2 Cell culture and experimental procedure

The cells were cultured in shake flasks (Corning, NY, USA) or 50 ml bioreactors (TPP, Trasadingen, Switzerland) at 37°C in a 5% CO₂ supplied shake-incubator (185 1/min, 2 inch shaking orbit, Innova

4230, New Brunswick Scientific, Edison, NJ, USA). The preculture was carried out in a 250 ml shake flask in serum-free 42-Max-UB-medium (Teutocell AG, Bielefeld, Germany). The cells were centrifuged (500 1/min, 5 min, 22°C, Labofuge, Heraeus Instruments, Hanau, Germany) and the supernatant discarded. The pellet was resuspended in 30 ml PBS (37°C, PAA Laboratories, Pasching, Austria) and centrifuged again. After discarding the supernatant, the pellet was resuspended in 42-Max-UB-medium supplemented with 2 mM glutamine. Three 50 ml bioreactors were inoculated yielding an initial cell density of about 9×10^5 cells/ml. Through the addition of PBS or PBS containing NH_4Cl (125 mM and 250 mM), ammonium concentrations of 0 mM, 2.5 mM, and 5 mM were achieved. The final culture volume was 18 ml. Samples (300 μl) were taken every day. 30 μl were used for cell counting. The rest was centrifuged (10,000 1/min, 5 min, 22°C, Biofuge pico, Heraeus Instruments, Hanau, Germany) and the supernatant transferred into fresh tubes. Of the samples 70 μl were used for pH determination (MP 220 pH meter, Mettler-Toledo, Giessen, Germany), 20 μl were used for ammonia measurements, and the rest was frozen (-20°C). The analysis of cultivation parameters was carried out using an automated cell counter (Countess, Invitrogen, Karlsruhe, Germany) which determines cell density, viability (Trypan Blue exclusion method), and cell size.

5.3.3 Quantification of metabolites

Glucose, lactate, and pyruvate in the supernatant were analyzed using high-pressure liquid chromatography (HPLC) as described previously (Niklas et al. 2009). Quantification of proteinogenic amino acids was performed by another HPLC-method (Kromer et al. 2005). Glutamine data was corrected for degradation as described recently (Niklas et al. 2011d).

5.3.4 Quantification of ammonia and α_1 -antitrypsin

Ammonia was quantified using an ammonia assay kit (Sigma-Aldrich, Steinheim, Germany) according to the instructions. The sample volume was 20 μl and the absorption was measured in a spectrophotometer at 340 nm (iEMS Reader MF, Labsystems, Helsinki, Finland). The produced α_1 -antitrypsin was quantified using an activity assay. The assay is based on the inhibition of trypsin by α_1 -antitrypsin. The unbound trypsin was quantified via the cleavage of BAPNA (*N* α -benzoyl-L-arginine 4-nitroanilide hydrochloride, Sigma-Aldrich, Steinheim, Germany) that releases benzoyl-arginine and p-nitroaniline that was quantified photometrically. The assay was carried out as follows. For the trypsin working solution, 50 μl of trypsin (1 g/l in phosphate buffered saline (PBS); Sigma-Aldrich, Steinheim, Germany) were diluted with 450 μl activity buffer (15 mM Tris, 100 mM NaCl, 0.01% Triton-X 100, pH 7.6). For the BAPNA working solution, 11 μl of BAPNA (500 mM in DMSO; Sigma-Aldrich, Steinheim, Germany) were diluted with 1,989 μl activity buffer. The samples were diluted twenty to sixtyfold with PBS. In a 96-well plate, 50 μl of the diluted samples were mixed with 15 μl of trypsin working solution and the plate was incubated for 10 min at 37°C. 10 μl of the sample-trypsin mixtures were transferred into the wells of a new 96-well plate. 90 μl BAPNA working solution was added. The plate was incubated for 60 min at 37°C. For quantification, a standard curve was recorded using α_1 -antitrypsin (derived from human plasma; Sigma-

Aldrich, Steinheim, Germany) solutions having concentrations between 0.5 g/l and 0.001 g/l. The absorption was measured at 414 nm (iEMS Reader MF, Labsystems, Helsinki, Finland). Samples and standards were measured in triplicates.

5.3.5 Quantification of urea

Urea was quantified using an HPLC method described by Clark et al (Clark et al. 2007). Samples were diluted with distilled water (1:10) and a calibration curve was recorded with samples of known urea concentration.

5.3.6 Metabolic flux analysis.

Metabolic rates, F_i , for each extracellular metabolite, M_i , were calculated from the specific growth rate, μ , and concentration changes of metabolites, ΔC_{M_i} , as well as of biomass, ΔC_{BM} , for the growth phase between 0 and 74 h using

$$F_i = \mu \frac{\Delta C_{M_i}}{\Delta C_{BM}} \quad [1]$$

where C denotes concentration. To get a realistic representation of the accuracy of the calculated extracellular fluxes, the standard deviation of F_i was estimated by using the determined average standard deviation of the metabolite analysis in Monte-Carlo simulation. Anabolic fluxes were calculated using the anabolic demand which was recently presented in another metabolic flux study on AGE1.HN cells (Niklas et al. 2011d). The metabolic network model (single cell, two compartment model (Niklas et al. 2010)) which was used for calculation of intracellular fluxes is schematically depicted in Fig. 5-1. The stoichiometry of the network can be seen in the stoichiometric matrix which is given in the supplementary material (Table S1). The network consists in total of 27 extracellular fluxes, 5 anabolic fluxes and 41 intracellular fluxes. The rank of the stoichiometric matrix is 42. The intracellular fluxes in the overdetermined system were calculated using Matlab 7.5.0 (Version R2007b, The Mathworks, Natick, MA, USA) assuming pseudo steady-state. Standard methods applying Monte-Carlo simulation to calculate error propagation in the network were used (Niklas and Heinzle 2011). Consistency check of the model and calculated fluxes which represent a least-square solution was done by calculation of the redundancy matrix (Quek et al. 2010; van der Heijden et al. 1994). The specific change of metabolic fluxes, FC , upon cultivation of AGE1.HN at increased ammonia concentrations was calculated by

$$FC = -\frac{\Delta F_i}{\Delta NH_4^+} \quad [2]$$

Sensitivity of metabolic fluxes, FS , to changing ammonia concentrations was finally calculated using equation 3

$$FS = \left| \frac{FC}{SD_{FC}} \right| \quad [3]$$

where SD_{FC} represents the standard deviation of FC calculated by Monte-Carlo simulation using Matlab. It was defined that $FS > 1$ indicates a significant change in metabolic flux. $FC > 0$ indicates higher substrate uptake or lower product secretion rates, $FC < 0$ reduced substrate uptake or increased product secretion rates.

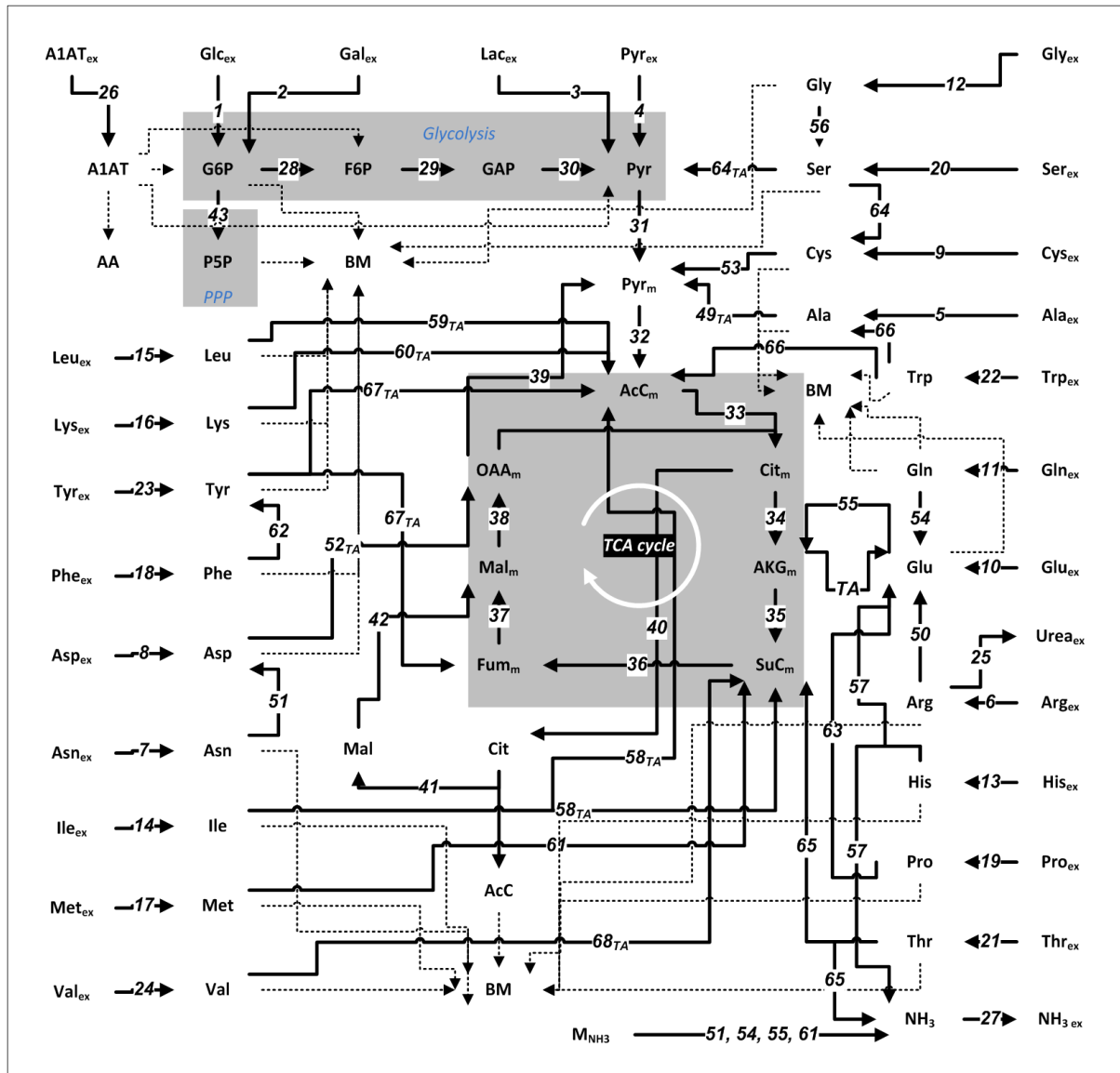


Fig. 5-1 Metabolic network model applied for metabolic flux analysis. The detailed stoichiometry of the model can be seen in the stoichiometric matrix, which is supplied in the supplementary material section. Flux numbers are given on the respective arrow. Direction of the arrow indicates in which direction the fluxes were defined. Dashed lines indicate anabolic fluxes. *BM* biomass, *PPP* pentose phosphate pathway, *TCA* tricarboxylic acid, *AA* all amino acids, *A1AT* α -1-antitrypsin, *Glc* glucose, *Gal* galactose, *Lac* lactate, *Pyr* pyruvate, *G6P* glucose 6-phosphate, *P5P* pentose 5-phosphate, *F6P* fructose 6-phosphate, *GAP* glyceraldehyde 3-phosphate, *AcC* acetyl coenzyme A, *Cit* citrate, *AKG* α -ketoglutarate, *SuC* succinyl coenzyme A, *Fum* fumarate, *Mal*, malate, *OAA* oxaloacetate, standard abbreviations for amino acids. Indices: *ex* extracellular, *TA* transaminase reaction, *m* mitochondrial. Flux numbers are defined in Table 5-1 and Table 5-2.

5.4 Results

5.4.1 Influence of ammonia on growth and A1AT production

Growth of AGE1.HN cells was influenced by the ammonia concentration in the medium (Fig. 5-2). Start concentrations of 2.5 mM ammonia did not affect the growth rate but clearly reduced the maximum cell density whereas ammonia concentrations of 5 mM reduced the growth rate as well as maximum cell density. With increasing ammonia start concentrations the viability dropped earlier. The ammonia secretion itself was also influenced by the ammonia concentration in the media. The higher the ammonia start concentration, the lower was the net ammonia secretion. In the cultivation starting with no ammonia, the ammonia concentration reached 6.5 mM after 10 days whereas in the 2.5 mM and in the 5 mM ammonia cultivation only 4.5 mM and 4.3 mM ammonia were produced in the same time period, respectively. The A1AT production decreased with increasing ammonia concentrations in the medium. In the control cultivation, 0.63 g/l A1AT were produced, which is a high concentration for such a complex glycoprotein in a batch process. At 5 mM initial ammonia concentration, this value was reduced by nearly 20% to 0.51 g/l.

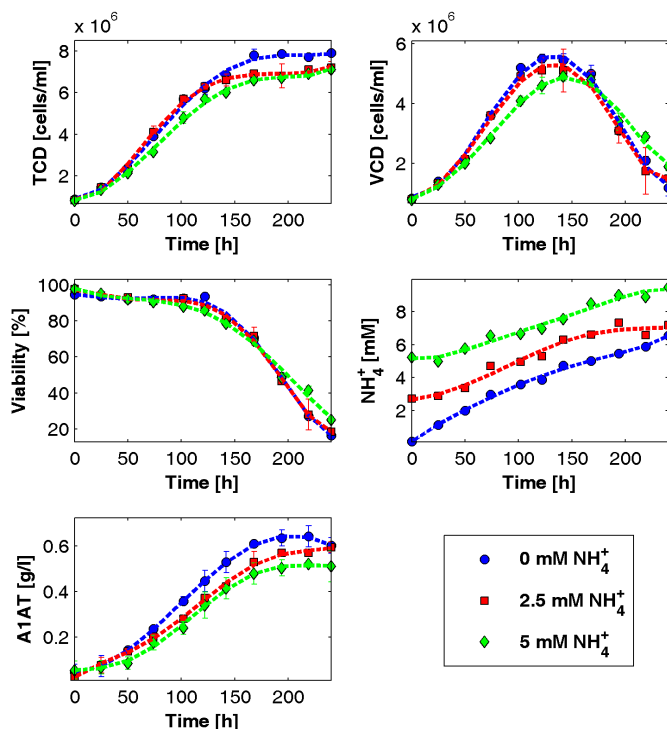


Fig. 5-2 Growth profile of AGE1.HN.AAT cells in media with different ammonia start concentrations. *TCD* total cell density, *VCD* viable cell density, *A1AT* α_1 -antitrypsin.

5.4.2 Dynamics of extracellular metabolite concentrations

The metabolism of the AGE1.HN cell line under normal batch cultivation conditions can be divided into distinct phases (Niklas et al. 2011d). This also applies for the cultivation with different ammonia start concentrations. The time courses of the most important metabolites are depicted in Fig. 5-3 and additional

ones in Fig. S1 of the supplementary material. In the presented cultivations, generally, two main metabolic phases can be distinguished. The first one is lasting from 0-74 h and is characterized by the presence of all substrates and resulting overflow metabolism. The second phase (after 74 h) starts with depletion of glutamine and pyruvate and is characterized by decreased growth but also less waste product formation. Taking into account the slightly decreased proliferation in the cultivations with higher ammonia start concentrations, no clear difference can be observed directly in the time courses for most extracellular amino acids. However, the decrease of extracellular glucose was similar in all three cultivations indicating higher glucose uptake per cell at high ammonia conditions. Total lactate concentration was slightly higher in the control cultivation compared to the 2.5 mM and 5 mM ammonia cultivations. Total extracellular alanine concentration was increased with increasing start concentration of ammonia. Production of alanine took place only in the first metabolic phase (0-74 h); in the second phase (after 74 h), in which glutamine and pyruvate were consumed, alanine was taken up by the cells. Similarly, glutamate was produced in phase I and consumed in phase II. The extracellular glutamate concentration was clearly increased with increasing ammonia levels in the medium (Fig. 5-3). The specific production rates in phase I were, however, not significantly changed (Table 5-1). The production of the C5 amino acid proline, which can be synthesized from glutamate, was increased with increasing initial ammonia concentration. Interestingly, we also observed relatively high production of urea in the AGE1.HN cell line. Urea production was, however, not increased with increasing ammonia and seems to be correlated with the respective cell number in the cultivation.

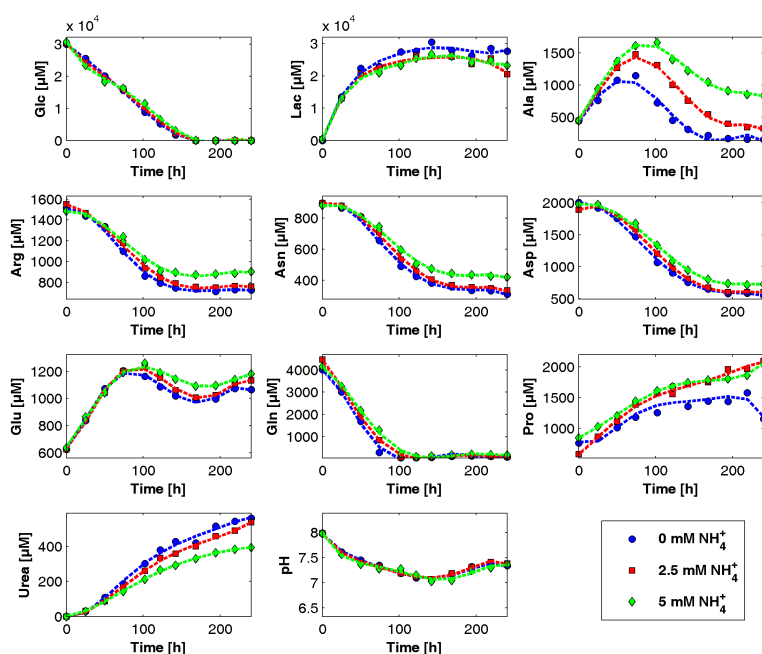


Fig. 5-3 Metabolic profiles of AGE1.HN.AAT cells in media with different ammonia concentrations. Time courses of selected metabolites and pH are depicted. Profiles of additionally measured metabolites are provided in Fig. S1 of the supplementary material. *Glc* glucose, *Lac* lactate, standard abbreviations for amino acids

5.4.3 Metabolic flux changes upon perturbation with increased ammonia concentrations

Metabolic fluxes were calculated for the growth phase between 0 and 74 h. For phase II, no fluxes were calculated since due to different growth rates in phase I different starting conditions were prevalent at the beginning of phase II. The balances around the metabolites were zero in the range of the standard deviation indicating a good fit between data and model. Uptake and secretion rates for all measured metabolites are depicted in Table 5-1. Sensitivities of metabolic fluxes (FS) to increasing ammonia concentrations were calculated to identify significant changes in the metabolism (Eq. 3). $FS > 1$, i.e., flux change larger than standard deviation of that flux, was defined as significant change in metabolic flux. Most significant changes were found in the extracellular rates of alanine ($FS = 6.06$) followed by asparagine ($FS = 3.01$) and the branched chain amino acids isoleucine ($FS = 2.72$) and leucine ($FS = 2.37$). The rates of tyrosine ($FS = 1.90$), phenylalanine ($FS = 1.84$), valine ($FS = 1.68$), serine ($FS = 1.58$), glycine ($FS = 21.51$), and threonine ($FS = 1.35$) were also significantly reduced with increasing ammonia concentration in the medium. Specific glucose uptake rates were similar in the cultivations starting with 0 and 2.5 mM ammonia, but in the 5 mM ammonia cultivation this rate was significantly higher. Specific production rates of urea and ammonia but also of A1AT were decreased with increasing ammonia concentration in the medium with $FS \sim 1$.

Intracellular fluxes in the central energy metabolism of AGE1.HN were mostly similar in the different cultivations and seemed to be uninfluenced by the extracellular ammonia concentration as indicated by flux sensitivities below 1 (Table 5-2). However, glycolytic fluxes were slightly higher in the 5 mM ammonia cultivation compared to the other cultivations with FS close to 1. Selected fluxes taking part in the ammonia metabolism are additionally depicted in Fig. 5-4. It was observed that metabolic fluxes through different transaminases that require α -ketoglutarate as amino group acceptor were reduced with increasing ammonia concentration in the medium. On the other hand fluxes through alanine and phosphoserine transaminases (v_{49} and v_{64}) catalyzing the formation of the respective amino acids were increased with increasing ammonia stress. Glutamate dehydrogenase (v_{55} , Glu-AKG_m) was working in the direction of α -ketoglutarate under reference conditions whereas in the cultivations with 2.5 mM and 5 mM ammonia start concentration in the medium this flux was reversed and increased with increasing initial ammonia concentration.

Table 5-1 Average specific extracellular rates in the first 74 h of the cultivation of AGE1.HN.AAT with different ammonia start concentrations (0 mM, 2.5 mM, 5 mM).

No.	Metabolite	Flux [$\mu\text{mol g}^{-1} \text{h}^{-1}$]						<i>FS</i>	<i>FC</i>	<i>SD_{FC}</i>
		0 mM NH_4^+		2.5 mM NH_4^+		5 mM NH_4^+				
		Flux	SD	Flux	SD	Flux	SD			
1	Glc	-429.17	56.90	-377.19	30.91	-479.06	39.99	1.07	10.21	9.55
2	Gal	-37.56	6.06	-36.08	3.96	-36.54	4.65	0.09	-0.11	1.23
3	Lac	639.75	2.84	546.76	45.56	682.46	56.90	0.58	-9.66	16.60
4	Pyr	-76.52	2.48	-64.73	5.53	-81.07	6.06	0.59	1.05	1.78
5	Ala	20.57	0.51	27.39	2.16	39.29	2.84	6.06	-3.74	0.62
6	Arg	-12.39	4.35	-10.77	2.06	-9.04	2.48	1.03	-0.66	0.64
7	Asn	-7.26	1.01	-5.53	0.52	-4.87	0.51	3.01	-0.48	0.16
8	Asp	-16.23	1.54	-10.12	3.20	-11.54	4.35	0.79	-0.90	1.13
9	Cys	-0.21	6.55	1.11	0.79	-0.30	1.01	0.06	-0.02	0.27
10	Glu	16.98	3.55	15.78	1.58	18.56	1.54	0.64	-0.30	0.47
11	Gln	-95.45	0.83	-88.64	6.64	-89.24	6.55	0.68	-1.31	1.92
12	Gly	6.76	1.37	6.88	2.74	13.33	3.55	1.51	-1.35	0.90
13	His	-3.23	1.56	-3.47	0.68	-2.32	0.83	0.76	-0.17	0.22
14	Ile	-14.73	5.41	-10.21	1.21	-10.33	1.37	2.37	-0.89	0.38
15	Leu	-23.76	0.81	-18.89	1.60	-17.72	1.56	2.72	-1.21	0.44
16	Lys	-16.63	0.74	-14.83	4.18	-11.27	5.41	0.68	-1.00	1.47
17	Met	-6.55	4.48	-5.62	0.70	-5.28	0.81	1.07	-0.26	0.24
18	Phe	-6.27	2.92	-4.81	0.58	-4.26	0.74	1.84	-0.39	0.21
19	Pro	13.37	1.26	22.22	3.35	19.81	4.48	1.09	-1.26	1.16
20	Ser	-33.41	0.63	-29.21	2.84	-27.06	2.92	1.58	-1.25	0.79
21	Thr	-7.98	0.97	-4.99	1.07	-5.53	1.26	1.35	-0.47	0.35
22	Trp	-0.79	1.85	-0.76	0.55	-0.55	0.63	0.29	-0.05	0.18
23	Tyr	-5.52	0.42	-3.45	0.86	-2.79	0.97	1.90	-0.53	0.28
24	Val	-14.15	0.02	-9.21	1.65	-9.88	1.85	1.68	-0.86	0.51
25	Urea	6.11	24.67	5.05	0.38	5.40	0.42	1.14	-0.15	0.13
26	A1AT	0.10	0.02	0.09	0.02	0.07	0.02	0.99	0.01	0.01
27	NH_3	91.67	11.32	66.67	16.03	56.37	24.67	1.34	-7.54	5.63

Standard deviation (SD) was calculated using Monte Carlo simulation. Negative values indicate uptake. *FS* flux sensitivity (Eq. 3), *FC* flux change (Eq. 2), *SD_{FC}* standard deviation of *FC*, *Glc* glucose, *Gal* galactose, *Lac* lactate, *Pyr* pyruvate, *A1AT* α_1 -antitrypsin, standard abbreviations for amino acids.

Table 5-2 Average specific intracellular fluxes in the first 74 h of the cultivation of AGE1.HN.AAT with different ammonia start concentrations (0 mM, 2.5 mM, 5 mM).

No.	Reaction	Flux [$\mu\text{mol g}^{-1} \text{h}^{-1}$]						FS	FC	SD_{FC}
		0 mM NH_4^+		2.5 mM NH_4^+		5 mM NH_4^+				
		Flux	SD	Flux	SD	Flux	SD			
28	G6P-F6P	456.72	31.68	399.78	29.85	505.52	38.43	0.91	9.51	10.50
29	F6P-GAP	453.79	31.69	397.21	29.93	503.39	38.41	0.98	9.90	10.15
30	GAP-Pyr	905.70	63.37	792.48	59.85	1,005.12	76.82	0.97	18.46	19.12
31	Pyr-Pyr _m	299.15	86.92	260.42	76.23	341.45	96.14	0.27	7.28	27.00
32	Pyr _m -AcC _m	350.82	88.23	283.38	77.26	377.35	97.51	0.24	6.31	26.83
33	OAA/AcC _m -Cit _m	377.07	89.37	294.58	80.02	393.25	101.17	0.14	3.57	26.30
34	Cit _m -AKG _m	330.69	89.49	247.10	80.13	352.61	101.18	0.20	5.60	27.47
35	AKG _m -SuC _m	362.37	89.81	270.75	80.57	379.38	103.12	0.20	5.61	28.53
36	SuC _m -Fum _m	375.73	90.68	273.59	81.35	387.84	104.17	0.15	4.06	27.50
37	Fum _m -Mal _m	376.32	90.85	272.64	81.79	387.43	105.04	0.07	2.05	28.15
38	Mal _m -OAA _m	371.03	88.77	297.15	79.41	392.18	101.19	0.19	5.04	26.62
39	Mal _m -Pyr _m	51.67	8.08	22.96	9.22	35.90	13.18	1.00	-3.16	3.17
40	Cit _m -Cit _{cc}	46.38	2.38	47.48	0.96	40.64	0.81	2.29	-1.14	0.50
41	Cit-AcC/Mal	46.38	2.38	47.48	0.96	40.64	0.81	2.15	-1.09	0.51
42	Mal-Mal _m	46.38	2.38	47.48	0.96	40.64	0.81	2.22	-1.14	0.51
43	G6P-P5P	4.39	0.19	4.52	0.07	3.88	0.06	2.70	-0.10	0.04
44	NADH-OP	1,705.02	447.11	1,281.32	396.81	1,789.98	507.03	0.14	18.64	135.65
45	FADH ₂ -OP	390.60	91.77	278.23	82.69	397.73	105.84	0.07	2.05	29.80
46	OP-ATP	4,848.44	1,254.90	3,620.64	1,115.40	5,071.53	1,425.34	0.25	85.58	344.04
47	ATP _{wOP}	726.13	152.19	508.85	145.37	939.17	173.29	0.86	38.85	45.36
48	ATP _{tot}	5,574.57	1,395.21	4,129.48	1,252.97	6,010.70	1,589.99	0.20	83.05	419.11
49	Ala-Pyr	-37.66	2.35	-42.49	2.55	-52.15	3.72	3.34	-2.85	0.85
50	Arg-Glu	-1.44	2.15	-1.10	2.15	-2.28	2.62	0.28	-0.17	0.62
51	Asn-Asp	-0.34	0.87	-2.14	0.68	-1.63	0.65	1.27	-0.26	0.21
52	Asp-OAA _m	6.04	3.89	-2.58	3.59	1.07	4.73	0.79	-0.98	1.23
53	Cys-Pyr _m	-0.09	1.20	-2.47	1.13	-0.35	1.33	0.15	-0.05	0.36
54	Gln-Glu	84.87	5.69	79.95	6.00	82.15	6.09	0.38	-0.61	1.60
55	Glu-AKG _m	7.05	9.65	-11.67	13.35	-24.27	19.54	1.41	-6.00	4.24
56	Gly-Ser	-23.67	3.21	-23.02	2.62	-27.24	3.52	0.80	-0.77	0.97
57	His-Glu	-1.98	1.71	0.07	1.81	-0.20	2.32	0.59	0.32	0.54
58	Ile-AcC _m /SuC _m	6.50	1.63	2.92	1.47	4.23	1.61	0.97	-0.44	0.46
59	Leu-AcC _m	7.05	2.04	3.41	2.03	4.78	2.04	0.77	-0.44	0.58
60	Lys-AcC _m	2.58	3.68	2.78	3.98	1.32	4.93	0.21	-0.26	1.19
61	Met/Ser-SuC _m /Cys	3.48	0.89	2.52	0.78	2.67	0.83	0.59	-0.14	0.24
62	Phe-Tyr	-1.61	1.03	-1.89	1.06	-1.18	1.41	0.20	0.07	0.36
63	Pro-Glu	-20.95	3.31	-28.75	3.42	-25.41	4.38	0.80	-0.92	1.16
64	Ser-Pyr	-5.43	4.34	-7.47	4.09	-12.20	4.84	1.02	-1.26	1.24

65	Thr-SuC _m	-1.82	1.36	-3.72	1.38	-1.58	1.84	0.14	0.06	0.46
66	Trp-AcC _m /Ala	-3.87	0.98	-2.81	1.09	-2.25	1.31	0.93	0.31	0.34
67	Tyr-AcC _m /Fum _m	0.60	1.94	-0.95	1.93	-0.40	2.65	0.26	-0.18	0.68
68	Val-SuC _m	5.20	2.02	1.13	1.70	3.13	2.20	0.64	-0.38	0.60

Standard deviation (SD) was calculated using Monte Carlo simulation. Negative values indicate reversed flux. *FS* flux sensitivity (Eq. 3), *FC* flux change (Eq. 2), SD_{FC} standard deviation of *FC*, *Pyr* pyruvate, *G6P* glucose 6-phosphate, *P5P* pentose 5-phosphate, *F6P* fructose 6-phosphate, *GAP* glyceraldehyde 3-phosphate, *AcC* acetyl coenzyme A, *Cit* citrate, *AKG* α -ketoglutarate, *SuC* succinyl coenzyme A, *Fum* fumarate, *Mal* malate, *OAA* oxaloacetate, *NADH* nicotinamide adenine dinucleotide, *FADH₂* flavine adenine dinucleotide, *ATP* adenosine triphosphate, *ATP_{wOP}* ATP production without oxidative phosphorylation, *ATP_{tot}* total ATP production, *OP* oxidative phosphorylation, standard abbreviations for amino acids. Indices: *m* mitochondrial.

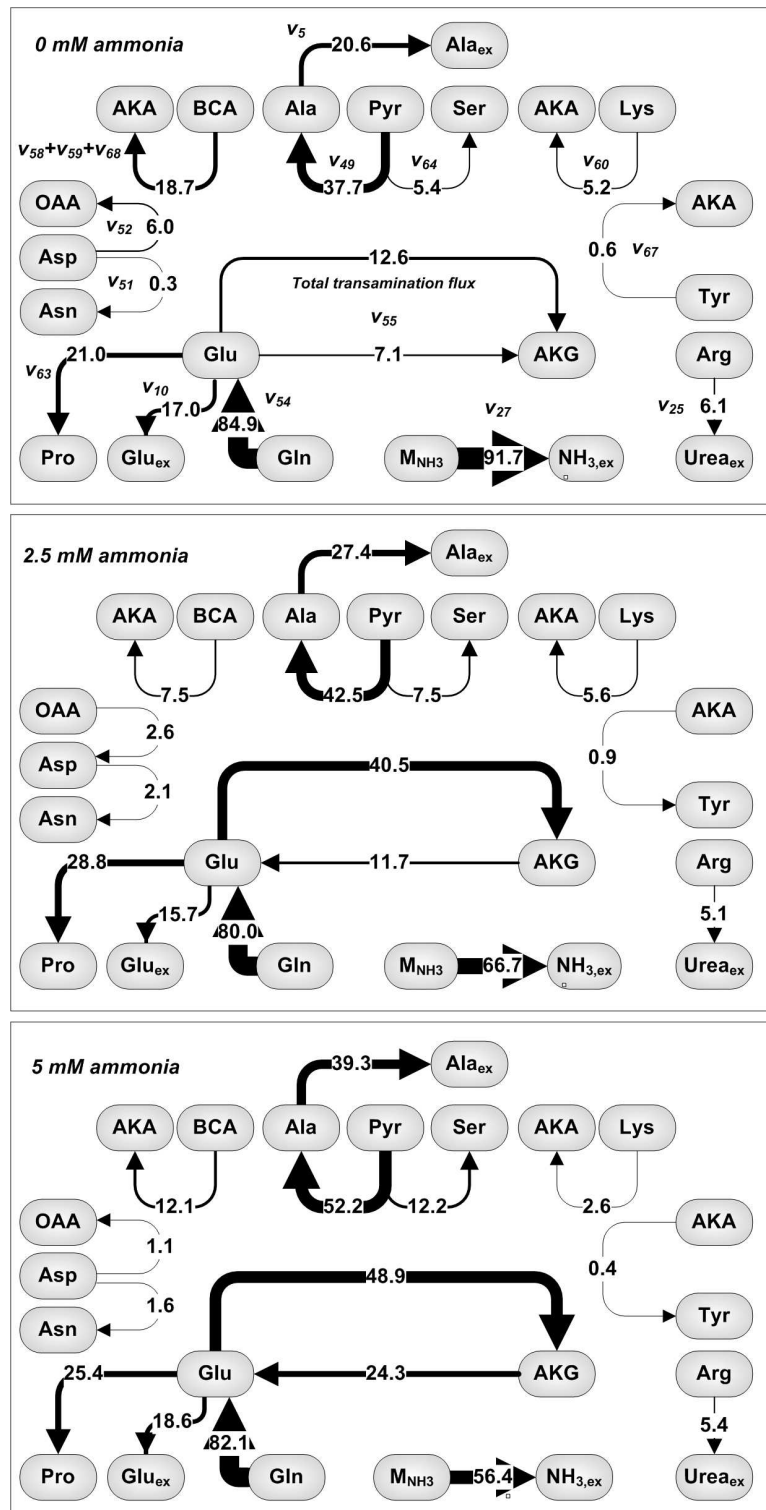


Fig. 5-4 Metabolic fluxes in the ammonia metabolism of AGE1.HN upon perturbation with different ammonia concentrations in the medium. Metabolic fluxes are given in $\mu\text{mol g}^{-1} \text{h}^{-1}$ and the flux strength is additionally indicated by the arrow width. The total transamination flux ($v_{49}+v_{52}+v_{58}+v_{59}+2v_{60}+v_{64}+v_{67}+v_{68}$) represents the total net flux from glutamate (Glu) to α -ketoglutarate (AKG) which was required for transamination reactions. Flux numbers are given in the upper figure. *AKA* α -ketoacids, *BCA* branched-chain amino acids (Ile, Leu, Val), *OAA* oxaloacetate, M_{NH_3} total ammonia produced from intracellular reactions, standard abbreviations for amino acids. Indices: *ex* extracellular.

5.5 Discussion

In this study, the specific effects of elevated extracellular ammonia levels on growth, A1AT production, and metabolism of the new human cell line AGE1.HN were analyzed. Initial ammonia concentrations of 2.5 mM and 5 mM as well as 0 mM as control were chosen because in reference cultivations of AGE1.HN ammonia concentrations of almost 5 mM were found at the end of the cultivation.

5.5.1 Increased ammonia stress reduces growth rate and production of ammonia and A1AT

It was found that initial concentrations of 2.5 mM ammonia already led to decreased maximum cell densities and that 5 mM ammonia slowed down growth significantly. Similar observations were made by Butler and Spier (Butler and Spier 1984) and Cruz et al. (Cruz et al. 2000) for BHK cells, where ammonia concentrations of 1 mM were found to reduce growth significantly. For channel catfish ovary (CCO) cells, similar values were found (Slivac et al. 2010) showing that 2.5 mM ammonia reduced growth by 44% and that 5 mM stopped growth almost completely. In contrast, for other cell lines like, e.g., some CHO cell lines, much higher ammonia concentrations up to 25 mM were tested and found to reduce growth only by 25% (Yang and Butler 2000). Additionally, specific protein production rates were influenced by extracellular ammonia concentrations. In our study, it was observed that 2.5 mM ammonia did only slightly decrease specific productivity. 5 mM ammonia led to reduced specific A1AT production rates of about 30% (Table 5-1). The total amount of A1AT produced during the cultivation depends, amongst other factors, on specific productivity and on viable cell density. Therefore, even 2.5 mM ammonia reduced the final A1AT titer primarily through significant reduction of maximal viable cell density. For CHO TF-70 cells expressing t-PA, concentrations of 8 mM ammonia were found to reduce the t-PA production significantly (Hansen and Emborg 1994). In contrast, it was shown for another CHO cell line producing G-CSF that ammonia concentrations up to 25 mM did not reduce protein secretion indicating a high ammonia tolerance for this cell line (Andersen and Goochee 1995). Similar observations were made for BHK cells by Cruz et al. where it was shown that concentrations as high as 20 mM ammonia reduced the specific productivity by 50% (Cruz et al. 2000).

Generally, the presented standard batch cultivation resulted in active titers of 0.63 g/l for the complex glycoprotein A1AT which was around 30% of the total cell biomass (~2 g/l) matching the expectations for an industrially relevant pharmaceutical producer cell line. The maximum product titer was reduced by nearly 20% when 5 mM ammonia was added at the beginning.

5.5.2 Central energy metabolism remains robust with increasing ammonia stress

The analysis of the metabolism of the AGE1.HN cell line under conditions of elevated extracellular ammonia concentrations revealed that the cell line's central energy metabolism is quite robust against increased extracellular ammonia concentrations since no significant changes in glycolysis and TCA cycle were observed under the analyzed conditions. Only in the 5 mM ammonia cultivation, glycolytic fluxes seemed to be slightly higher than in the control cultivation. In contrast to many other cell lines like BHK

(Cruz et al. 2000), CHO K1 (Yang and Butler 2000), and hybridoma cells (Ozturk et al. 1992), only a slight increase in specific glucose and no change in the glutamine consumption rate were observed in the AGE1.HN cell line. This indicates that the applied extracellular ammonia concentrations, which are usually not higher in the cultivation process, do not increase energy demand in AGE1.HN cells as was proposed by Martinelle et al. (Martinelle et al. 1998) for myeloma and hybridoma cells to maintain pH homeostasis. These two findings indicate that the cells are able to maintain energy supply even under ammonia stress conditions.

5.5.3 Ammonia stress results in global flux rearrangements in the amino acid metabolism of AGE1.HN

In contrast to the relatively uninfluenced fluxes in the central energy metabolism of the cells, several interesting adaptations to increased ammonia stress were observed in the metabolism of amino acids. Under standard conditions, the glutamate dehydrogenase (GDH) was catalyzing the formation of α -ketoglutarate producing ammonia (v_{55} in Table 5-2, Fig. 5-4). The net transamination flux was low and also produced α -ketoglutarate (Fig. 5-4). This flux direction was accomplished by the reaction of transaminases using pyruvate (alanine transaminase) or 3-phosphoglycerate (phosphoserine transaminase) as acceptor for the glutamate amino group producing, finally, the amino acids alanine and serine in the respective metabolic pathways. Fluxes through other transaminases involved in amino acid degradation pathways were high. The total flux distribution resulted in a relatively high ammonia production rate under standard conditions.

Increased ammonia stress (2.5 mM and 5 mM start concentration in the medium) resulted in a global rearrangement of the amino acid metabolism to reduce ammonia production and, eventually, ammonia accumulation in the medium. This was accomplished through changes in different metabolic reactions involved in ammonia metabolism. Glutamate dehydrogenase flux was reversed consuming ammonia and resulting in an increased production of glutamate from α -ketoglutarate (AKG). This was compensated by a large increase in the net transamination flux from glutamate to AKG. Fluxes of transamination reactions transferring amino groups to AKG, e.g., branched-chain amino acid transaminase or aspartate transaminase catalyzed reactions, were reduced, whereas the metabolic fluxes through transaminases catalyzing the formation of amino acids, i.e., alanine and phosphoserine transaminase, were increased with increasing initial ammonia concentration. Miller et al. also reported changes in transaminase activities upon raised ammonia concentrations in hybridoma cells (Miller et al. 1988). Commensurate with the increased transaminase fluxes, the production rate of alanine was increased and uptake rate of serine decreased. In the 5 mM ammonia cultivation, alanine production rate was doubled compared to the control cultivation showing the importance of alanine in the detoxification of ammonia. The reduction of the fluxes through transaminases involved in amino acid degradation pathways is actually accomplished by reduced uptake of the respective amino acids. As denoted before, the change in the glutamate dehydrogenase flux direction at higher ammonia load was compensated by increased transamination to AKG with a corresponding transfer of the amino group to alanine or serine and of the carbons into the

TCA cycle. Glutamate production rate was not increased significantly (Fig. 5-4, Table 5-1) with increased ammonia stress indicating that this flux is not used by the cells to remove excess glutamate. Proline production flux was, however, slightly increased. In effect, the flux changes led to reduced ammonia production and showed that the cell can react to increased ammonia concentration in the environment. Bonarius et al. described the adaptation mechanism of hybridoma cells to toxic levels (10 mM) of ammonia (Bonarius et al. 1998a). They also found that ammonia accumulation was reduced by a change in the glutamate dehydrogenase flux and that the additionally produced glutamate is further metabolized by aminotransferases. Increased production rates of alanine and proline, both used as nitrogen sinks, were also observed by the same authors as well as by other groups (Hansen and Emborg 1994; Ozturk et al. 1992; Schumpp and Schlaeger 1992). However, in hybridoma cells no changes in uptake rates of other amino acids were observed, e.g., branched chain amino acids that transfer intracellularly amino groups to AKG during their degradation. Additionally, we did not find any metabolic flux study investigating ammonia effects in which all transamination reactions taking place in amino acid degradation pathways were included in the metabolic flux model. However, as shown in this study, it is important to include and analyze these reactions since cells change fluxes through these amino acid degradation pathways as a response to increased ammonia stress thereby reducing the production of glutamate through transamination. It was very interesting to observe that the AGE1.HN cell line seems to be able to regulate the uptake rates of several amino acids and to adapt these to anabolic requirements. Under standard conditions, uptake of several amino acids, e.g., branched-chain amino acids, was higher than the anabolic demand for these biomass precursors. Higher ammonia concentration in the medium led to reduced uptake rates of amino acids getting closer to the demand for synthesis of biomass and A1AT production having lower fluxes through degradation pathways.

5.5.4 Adaptation mechanism of AGE1.HN cells to increased ammonia concentrations

A possible mechanistic explanation for the adaptive behavior described above is depicted in Fig. 5-5. Increased extracellular ammonia concentration leads to increased intracellular ammonia concentration. This might lead to a shift in the reaction equilibria of reactions where ammonia is involved towards fixation of free ammonia (e.g., α -ketoglutarate + ammonia \rightarrow glutamate). The resulting increased glutamate concentration would shift the reaction equilibrium of selected transaminase reactions towards production of amino acids, e.g., alanine, recycling glutamate to α -ketoglutarate. In contrast, the equilibria of ammonia/glutamate producing reactions in some amino acid degradation pathways are shifted towards the amino acids leading to reduced degradation. The increased production or reduced degradation of several amino acids leads to increased secretion and/or reduced uptake of these amino acids as observed during the experiment. Hypothetically, these changes in uptake and secretion of certain amino acids might lead to changes in the intracellular concentrations which could be an explanation for reduced biomass and A1AT production based on amino acid limitation.

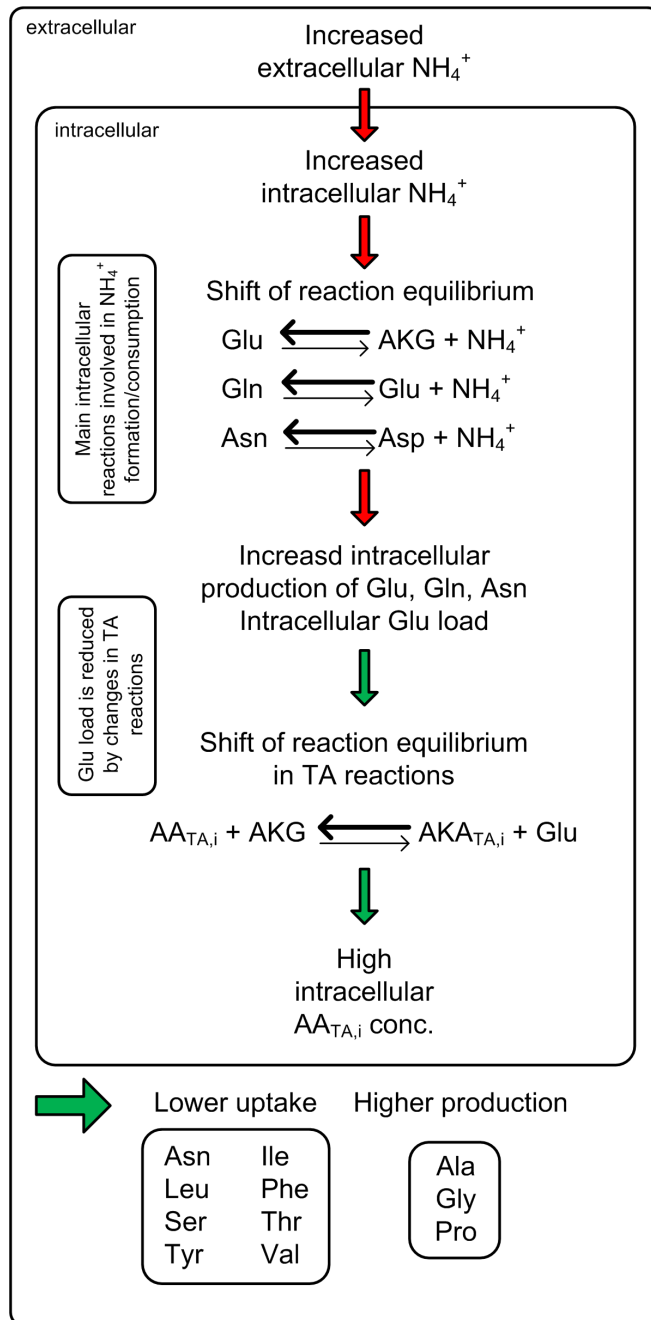


Fig. 5-5 Mechanistic explanation for the observed adaptation phenomena of the AGE1.HN cell line to increased extracellular ammonia concentrations. *AKG* α -ketoglutarate, *AKA* α -ketoacids, *AA* amino acid, standard abbreviations for amino acids, *TA* transaminase. Indices: *TA* amino acids produced by transamination.

5.5.5 Urea production in AGE1.HN cells is not altered by increased addition of ammonia

Interestingly, we found another possible nitrogen depository, i.e., urea. To our knowledge, this has not been reported or analyzed for any production cell line derived from non-liver tissue. A possible explanation for these findings in the neuronal cell line AGE1.HN is provided by the results from Braissant et al. and from Gotoh et al. who found that arginase II is expressed in almost all parts of the human brain (Braissant et al. 1999; Gotoh et al. 1997). Since the enzyme arginase catalyzes the degradation of arginine to ornithine and urea, this might be an explanation for the increasing urea concentrations found in the medium. The observation that the urea concentration is not increased with increasing ammonia supply in the medium indicates that urea is not used as nitrogen sink in AGE1.HN. This is

further supported by the fact that arginine which is taken up in excess and not needed for anabolic purposes is just converted via the enzyme arginase to urea and ornithine. The urea cycle seems to be inactive in AGE1.HN showing that urea is not used to remove excess ammonia. However, these findings might open up new possibilities to engineer this cell line towards even more efficient ammonia detoxification with minimal carbon wasting. This may be achieved through genetic engineering introducing the genes necessary to create fully functional urea cycle. Park et al. have introduced carbamoyl phosphate synthetase I and ornithine transcarbamoylase genes in CHO cells and found only a slight reduction in the ammonia production and a small increase in viable cell density (Park et al. 2000). However, for AGE1.HN cells the success of this strategy to decrease ammonia production as well as to increase A1AT production has to be tested.

5.6 Concluding remarks

In summary, the adaptation mechanism of the neuronal cell line AGE1.HN to cope with high ammonia concentrations was unraveled. The cell line adapts to high ammonia concentration by rearranging its amino acid metabolism towards lower ammonia production and increased ammonia fixation in amino acids. This indicates that the cell line has a kind of “ $\text{NH}_3/\text{NH}_4^+$ sensor”, in the simplest case just representing equilibrium effects, which enables the cell to sense changing conditions and furthermore to convert this information into described physiological adaptations. These adaptations mainly take place in amino acid metabolism and are based on regulatory changes in selected physiologically relevant processes. The uptake rates for specific amino acids are downregulated. Transaminase activities involved in amino acid degradation pathways are reduced, whereas activities of transaminases catalyzing the formation of amino acids are increased. In combination with a change in the glutamate dehydrogenase flux direction leading to the fixation of free ammonia, these adaptations lead to reduced ammonia accumulation and storage of excess ammonia in extracellular amino acids, mainly alanine. The fact that urea production only depended on cell number and arginine excess indicates that urea is not used to remove excess ammonia but indicates that arginase is expressed in AGE1.HN. From an engineering point of view, it can be concluded that further engineering of the cell line with the aim of increasing resistance to high ammonia conditions is of interest, particularly, if product titers should be further increased leading to an anticipated higher ammonia production. Possible targets are enzymes transferring amino groups that could be down-regulated in the case of consumed amino acids and up-regulated in the case of alanine and serine.

5.7 Acknowledgements

This work has been financially supported by the BMBF project SysLogics - Systems biology of cell culture for biologics (FKZ 0315275A-F). We gratefully acknowledge the fruitful collaboration of all project partners. We thank Michel Fritz for most valuable support for the HPLC analysis as well as Saskia Müller for proofreading.

5.8 Supplementary material

The supplementary material for this chapter is given in the supplementary material section at the end of the thesis.

6 Metabolism and metabolic burden by α_1 -antitrypsin production in human AGE1.HN cells

6.1 Abstract

The goal of this study was a detailed analysis of the metabolic burden on AGE1.HN cells imposed by the production of recombinant α_1 -antitrypsin (A1AT). This was accomplished by comparing the properties of a selected high-producing clonal cell line with the parental cell line. By analyzing growth and biomass dynamics, it was observed that RNA and lipid fractions were higher in the producer cell line. The differences found in the macromolecular composition were also reflected in the metabolism. Specific changes observed were, e.g., increased glycine and glutamate production in the producer, which could be explained by using a model describing the whole protein synthesis process. By simulating the theoretical metabolite demand for production of mature A1AT, it was found that the differences in metabolic profiles between producer and parental cells match the increased C1 unit and nucleotide demand in the producer. Comparison of metabolic fluxes revealed that energy metabolism was similar in both cell lines whereas fluxes in C1 and amino acid metabolism were changed and adapted to the different anabolic demand. The data indicate that the main cellular properties distinguishing the high producer from the parental cell population are, apart from production of A1AT, high RNA and lipid content. The increased lipid content points to an expanded secretion machinery in the producer cell line which might be an adaptation to high level secretion of A1AT or the specific property of this cell clone and the reason for its selection. Lipid metabolism and protein secretion seem important targets for further improvement of AGE1.HN.

This chapter was submitted as

Niklas J, Priesnitz C, Rose T, Sandig V, Heinzle E. Metabolism and metabolic burden by α_1 -antitrypsin production in human AGE1.HN cells.

6.2 Introduction

Alpha₁-antitrypsin (A1AT) deficiency is an inherited disease characterized by low serum levels of A1AT which can result in lung emphysema and liver dysfunction (Kelly et al. 2010; Petrache et al. 2009). The lack of protection against neutrophil elastase usually provided by A1AT leads to destruction of lung parenchyma and finally emphysema in the respiratory tract. The mortality rate of patients can be decreased by A1AT augmentation which is achieved by intravenous infusion of a purified preparation of human A1AT (A1AT-Group 1998). However, only human plasma-derived products are licensed by the US-FDA for intravenous treatment of A1AT deficiency in spite of many attempts to produce recombinant A1AT in prokaryotic and eukaryotic hosts (Karnaukhova et al. 2006). This fact makes the therapy currently very expensive and not cost-effective (Gildea et al. 2003) showing that an alternative source of A1AT would be important. Recently, it was shown that A1AT derived from the novel human cell line AGE1.HN has similar anti-inflammatory activity as plasma-derived A1AT (Blanchard et al. 2011) indicating that this cell line is a useful expression system for large scale production of this biopharmaceutical. Recent studies on growth, metabolism (Niklas et al. 2011b; Niklas et al. 2011c; Niklas et al. 2011d), and glycosylation properties (Blanchard et al. 2011) of this cell line have shown that AGE1.HN seems a favorable cell line for the production of glycoproteins requiring human-type post-translational modifications. Further improvement of the productivity might be achieved by a detailed understanding of the cellular protein production process.

The development of mammalian cell lines suitable for the production of biopharmaceuticals typically requires an intense effort. This is mainly due to the low frequency of recombinant cell clones expressing high levels of the desired target protein. Therefore, identifying and understanding the physiological characteristics of a high producer cell offers great potential. Addressing the specific requirements of producer clones via genetic engineering or defined adjustment of media and feed compositions should simplify cell line development and generally enhance the yields in industrial production.

Selected cellular principles underlying varying productivity were analyzed using different omics-technologies (Alete et al. 2005; Hayduk and Lee 2005; Seth et al. 2007; Smales et al. 2004; Yee et al. 2009). In proteomic analyses of cells with varying secreted recombinant protein productivities, changes in, e.g., translation, energy metabolism, chaperones, and cytoskeletal proteins were observed (Alete et al. 2005; Hayduk and Lee 2005; Smales et al. 2004). Seth et al. analyzed changes in transcriptome and proteome in different producers and proposed that differences in protein synthesis and cell growth controlling networks might lead to high productivity (Seth et al. 2007). Another transcriptome study concluded that particularly vesicle trafficking, endocytosis, and cytoskeletal elements go along with increased specific productivity (Yee et al. 2009). Khoo et al. compared the transcriptome of producer and non-producer cell lines (Khoo et al. 2007). They found that the producer cells did not grow any slower indicating negligible metabolic burden in this case but, nevertheless, differences in metabolic activities were observed. It was concluded that slower growth, as a result of metabolic burden, might be negligible in cells that were

selected for high productivity as well as growth rate. To our knowledge, a detailed analysis on the metabolome level concerning differences in productivity has not yet been described.

In this study, we analyzed the metabolic burden of α_1 -antitrypsin production in AGE1.HN. The goal was to compare growth, dynamics of biomass constituents, metabolite dynamics, and metabolic fluxes in the A1AT producing cell line AGE1.HN.AAT and its parental cell line. The following questions were addressed: (i) what are the differences in growth and biomass composition of both cell lines, (ii) what is changed in the cellular metabolism, (iii) what particularly distinguishes this clonal A1AT producing cell line from the parental cell population enabling this cell line to produce large quantities of the product, and (iv) can we identify potential targets for further improvement of the cell line by understanding the metabolic requirements of A1AT production and the adaptation of the cell to high-level glycoprotein secretion?

6.3 Material and methods

6.3.1 Cell line

The cell line AGE1.HN® (ProBioGen, Berlin, Germany) originates from primary human brain cells. These were immortalized and improved using different adenoviral genes as described previously (Niklas et al. 2011d). The α_1 -antitrypsin (A1AT) producing cell line AGE1.HN.AAT was developed as follows. Parental cells were transfected with an expression vector containing the human A1AT gene driven by a human CMV/EF1 hybrid promoter (ProBioGen). High producing clones were established with puromycin drug selection. In a recent publication, it was shown that A1AT derived from AGE1.HN cells was highly active and showed a complex glycostructure (Blanchard et al. 2011).

6.3.2 Analytical methods

Cell counting was performed using an automated cell counter (Countess, Invitrogen, Karlsruhe, Germany).

Cell dry weight. Cell suspensions containing exactly 3 or 4 × 10⁶ cells were harvested (500 1/min, 5 min, 25°C, Labofuge 400R Function Line, Heraeus Instruments, Hanau, Germany) and the pellets resuspended in 2 ml 37°C PBS. The suspensions were transferred into preweighed Eppendorf tubes and again centrifuged (4000 1/min, 5 min, 20°C, Picofuge, Heraeus Instruments, Hanau, Germany). The supernatant was discarded. The pellets were frozen at -70°C, lyophilized, and finally weighed.

Intracellular and extracellular proteins. Cell pellets from the cell dry weight analysis were resuspended in 200 μ l CellLytic™ M solution (Sigma-Aldrich, Steinheim, Germany) and incubated for 15 min at 20°C on a shaker (400 1/min, MS1 Minishaker, IKA, Staufen, Germany). After centrifugation (13,000 1/min, 10 min, 4°C, Biofuge fresco, Heraeus Instruments, Hanau, Germany) the supernatants were transferred into new tubes. Proteins were quantified using Bradford assay (Bradford 1976) (reagent from Bio-Rad Laboratories, Munich, Germany). A series of BSA (bovine serum albumin) solutions was used for calibration. The absorption was measured at 540 nm (iEMS Reader MF, Labsystems, Helsinki, Finland).

The total extracellular protein concentration was directly analyzed in culture supernatants using the Bradford assay.

RNA content was determined using the TRI Reagent® Solution from Applied Biosystems/Ambion (Austin, TX, USA) according to the manual. The RNA concentrations were determined spectrophotometrically (Genesys 10 Bio, Thermo Fisher Scientific, Waltham, MA, USA).

Total lipid analysis. Cells were cultured in 250 ml shake flasks (Corning) and harvested in the exponential growth phase by centrifugation (1,200 1/min, 5 min, 20°C, Labofuge 400R Function Line, Heraeus Instruments, Hanau, Germany). The supernatant was discarded and lipids were extracted using a protocol published by Akopian et al. (Akopian and Medh, 2006). In brief, the pellet was resuspended in cyclohexane/isopropanol (3:2 *v/v*), vortexed, and incubated on ice. After another centrifugation (4500 1/min, 10 min, Labofuge 400R Function Line, Heraeus Instruments, Hanau, Germany) the supernatant was transferred to a glass tube. After evaporation of the solvents the vessel was placed for drying at 80°C over night and then cooled down in a desiccator. Total extracted lipids were finally weighed.

Alpha₁-antitrypsin concentration and activity. A1AT (α_1 -antitrypsin) concentration was determined using an activity assay based on the inhibition of trypsin by A1AT. Calibration was done using standards with different A1AT concentrations (0.5-0.001 mg/ml in PBS; A1AT from human plasma was acquired from Sigma-Aldrich, Steinheim, Germany). Samples were appropriately diluted with PBS. Of the samples and standard solutions 50 μ l were mixed with a trypsin solution (0.1 mg/ml in an activity buffer containing 15 mM Tris, 100 mM NaCl, 0.01% (*v/v*) Triton X-100 at pH 7.6) and incubated for 10 min at 37°C. 10 μ l of these solutions were pipetted into the wells of a 96-well plate. 90 μ l of a BAPNA solution (*N* α -Benzoyl-L-arginine 4-nitroanilide hydrochloride, Sigma-Aldrich; 11 μ l of BAPNA stock solution [500 mM in DMSO] were mixed with 1,989 μ l activity buffer) was added to each well. The plate was incubated at 37°C for 1 h and the absorption was measured at 405 nm (iEMS Reader MF, Labsystems, Helsinki, Finland).

Extracellular metabolites. Concentrations of extracellular metabolites were measured by different HPLC methods (Kromer et al., 2005; Niklas et al., 2009).

6.3.3 Cell culture and experimental procedure

The cells were cultured in an incubator supplied with a shaking unit (Innova 4230, New Brunswick Scientific, Edison, NJ, USA; 2 inches orbit) at 37°C and 5% CO₂. The precultures were carried out in 250 ml shake flasks (Corning, NY, USA). The cells from the precultures were transferred in Falcon tubes, centrifuged (500 1/min, 5 min, 20°C, Labofuge 400R Function Line, Heraeus Instruments, Hanau, Germany), the supernatant discarded, and the pellet resuspended in phosphate buffered saline (PBS). After another centrifugation, the pellets were resuspended in medium and the cell suspensions transferred in 125 ml shake flasks (Corning, NY, USA). The applied serum-free medium was 42-Max-UB medium (Teutocell, Bielefeld, Germany). Samples containing more than 4×10^6 cells were taken every day. Cell counting was performed. A part of the cell suspension was used for the analysis of cell dry weight and protein content. The rest was centrifuged and the supernatant transferred into fresh tubes. The samples were frozen and stored at -20°C for later analysis of extracellular components. Since higher cell amounts

were necessary for a reliable analysis of RNA dynamics, separate cultivations in 250 ml shake flasks (Corning) were performed using the same media and conditions as before. Samples containing more than 3×10^6 cells were taken every 24 h. A part of this suspension was used for cell counting and an exactly defined volume was immediately centrifuged (8000 1/min, 5 min, 20°C, Biofuge pico, Heraeus Instruments, Hanau, Germany). The supernatant was discarded, the pellet resuspended in TRI Reagent® Solution (Applied Biosystems/Ambion, Austin, TX, USA) and stored at -70°C for later determination of RNA concentrations.

6.3.4 Metabolic flux analysis

Metabolic fluxes in the growth phase (days 0-4) of both cell lines were calculated using Matlab R2007b (The Mathworks, Natick, MA, USA) applying stationary metabolic flux analysis using metabolite balancing as described in literature (Niklas and Heinzle 2011; Niklas et al. 2011d; Stephanopoulos et al. 1998). The applied metabolic network model (Fig. 6-1) was set up using the Kyoto Encyclopedia of Genes and Genomes pathway database (www.kegg.com) for Homo sapiens.

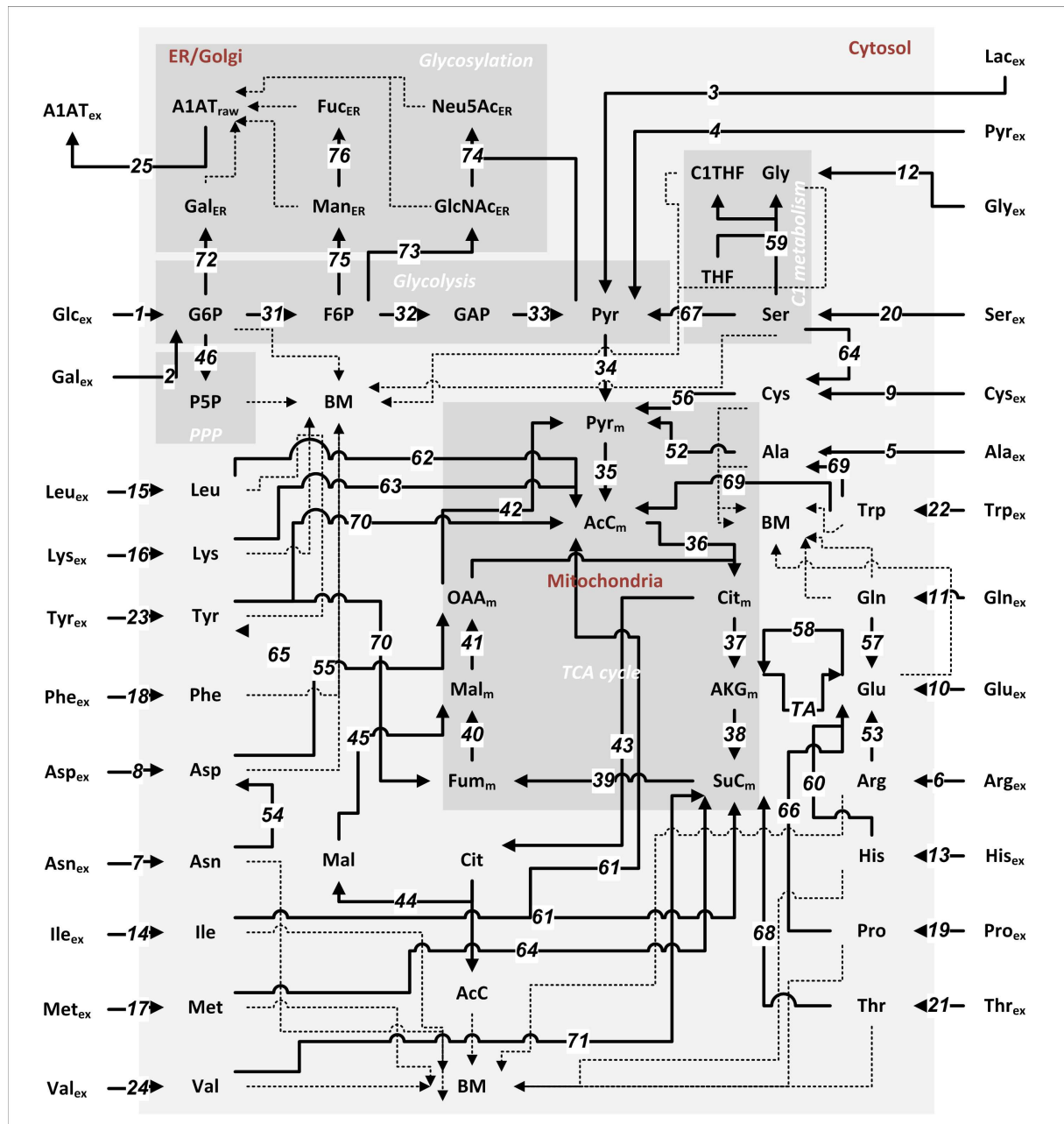


Fig. 6-1 Metabolic network model for metabolic flux analysis. Single cell, three compartment model distinguishing selected cytosolic and mitochondrial reactions as well as the α_1 -antitrypsin (A1AT) glycosylation that takes place in the endoplasmic reticulum (ER) and Golgi apparatus (Golgi). Anabolic fluxes are indicated by dashed lines. The stoichiometry of the model is given in the supplementary material (Table S1). Abbreviations: *BM* biomass, *Glc* glucose, *Gal* galactose, *Lac* lactate, *Pyr* pyruvate, *G6P* glucose 6-phosphate, *P5P* pentose 5-phosphate, *F6P* fructose 6-phosphate, *GAP* glyceraldehyde 3-phosphate, *AcC* acetyl coenzyme A, *Cit* citrate, *AKG* α -ketoglutarate, *SuC* succinyl coenzyme A, *Fum* fumarate, *Mal* malate, *OAA* oxaloacetate, *TA* transamination flux (TA = $v_{52} + v_{55} + v_{61} + v_{62} + 2v_{63} + v_{67} + v_{70} + v_{71}$), *Glc-NAc* N-Acetylglucosamine, *Man* mannose, *Fuc* fucose, *Neu5Ac* N-Acetylneuraminic acid, *THF* tetrahydrofolate, *C1THF* methylenetetrahydrofolate, standard abbreviations for amino acids. Indices, *ex* extracellular, *m* mitochondrial, *ER* localization in the ER or Golgi apparatus.

6.4 Results and discussion

6.4.1 Biomass dynamics in parental and A1AT producing AGE1.HN cells

The growth profiles of both cell lines are depicted in Fig. 6-2A. Cell growth and growth rate were similar in the first 120 h. After 120 h the A1AT producing AGE1.HN cells (AGE1.HN.AAT) were growing more slowly than the parental cell line (AGE1.HN) and the viability dropped faster in AGE1.HN.AAT. The time course of the dry weight was similar in both cell lines being initially slightly higher in AGE1.HN.AAT and after 48 h higher in the parental cell line. A1AT production was low in the first 48 h and then increasing up to a final concentration of ~ 0.4 g/l at the end of the cultivation. The time courses of selected biomass components were also analyzed (Fig. 6-2B). The total cell mass was increasing similarly in the first 96 h. After 96 h, AGE1.HN.AAT cell mass remained constant, whereas the extracellular protein concentration was increasing. This was different in the AGE1.HN cells where the cell mass was still increasing after 96 h and the increase in total extracellular protein mass was less. The total protein concentration in the culture (extracellular + cellular protein) remained almost constant after 96 h in AGE1.HN.AAT and after 120 h in AGE1.HN whereas cellular protein concentration was decreasing in AGE1.HN.AAT after 96 h. This indicates that specific cellular proteins might be degraded when there is a lack of protein building blocks to maintain the production of the recombinant glycoprotein A1AT which was high after 96 h. This was clearly different in the parental cell line where the total cellular protein concentration remained constant after 120 h. The total mass of the analyzed components at the end of the cultivation was similar in the cultivations of both cell lines being around 2.5 g/l. The final A1AT concentration, which was 0.4 g/l, was $\sim 22\%$ of the final cell mass and $\sim 30\%$ of the total protein in the culture.

The total cellular RNA fraction during the growth phase was higher in AGE1.HN.AAT than in AGE1.HN (Fig. 6-2C). This might be explained by the fact that the A1AT gene is driven by a strong CMV/EF1 hybrid promoter which results in high levels of A1AT mRNA transcripts in AGE1.HN.AAT. Generally, high mRNA levels of the gene of interest are desirable. In a study on CHO producer cell lines, it was found that high mRNA levels were characteristic for the high-producing cells (Chusainow et al. 2009).

We measured also total lipid content in both cell lines. It was observed that the cellular lipid fraction was increased in AGE1.HN.AAT compared with the parental cell line (Fig. 6-2D). This points to an increased intracellular secretion machinery in the producing cell, which can be caused by high flux of the protein product through the secretory pathway forcing the cell to provide more endoplasmic reticulum (ER) and Golgi apparatus (Golgi). It might be also a particular characteristic of this specifically selected clone and might, amongst other properties, have led to the high level of A1AT production in this particular clone and, therefore, its selection. Seth et al. also speculated that the transformation from a host cell to a high producing cell might entail an expanded protein secretion machinery (Seth et al. 2006). The same group discovered in a transcriptome and proteome study comparing high and low producers that expression of

genes involved in protein synthesis pathways is altered in high producers (Seth et al. 2007). In another transcriptome study, it was reported that increased specific antibody productivity is accompanied by a difference in the expression of genes involved in secretory pathway and cytoskeletal elements (Yee et al. 2009). In summary, increased secretion machinery might be one characteristic of a high producing cell.

The differences in the RNA level and lipid content resulted, consequently, in a different anabolic demand of the producing and parental cells (Table 6-1) which should also result in specific signatures in metabolism and metabolic fluxes.

Table 6-1 Anabolic demand of producer (AGE1.HN.AAT) and parental AGE1.HN cells.

	AGE1.HN.AAT	AGE1.HN
	Anabolic demand [$\mu\text{mol}/\text{g}_{\text{biomass}}$]	
Proteins	7,462.6	7,344.2
Lipids	202.9	170.7
RNA	176.9	116.3
DNA	45.3	45.3
Carbohydrates	438.3	438.3

RNA, lipid, and protein fractions in both cell lines were measured in this study. Carbohydrate and DNA data were taken from literature (Bonarius et al. 1996) and are therefore identical.

6.4.2 Metabolite dynamics in both cell lines

In order to explain the biomass and growth dynamics in both cell lines, time courses of extracellular substrate and product metabolites were analyzed (Fig. 6-3). In the growth phase from 0-96 h, similar time courses for most metabolites were observed. However, some specific differences were found. Glycine and glutamate production was higher in AGE1.HN.AAT compared to AGE1.HN whereas uptake of arginine and aspartate as well as alanine production was lower. Glutamine was depleted in the cultivations of both cell lines at ~ 96 h which resulted also in reduced growth (Fig. 6-2A). In particular, the increase in glycine and glutamate production points to an effect of the production of the glycoprotein A1AT on C1 metabolism and on the cellular nucleotide demand. This will be explained in more detail in the next section.

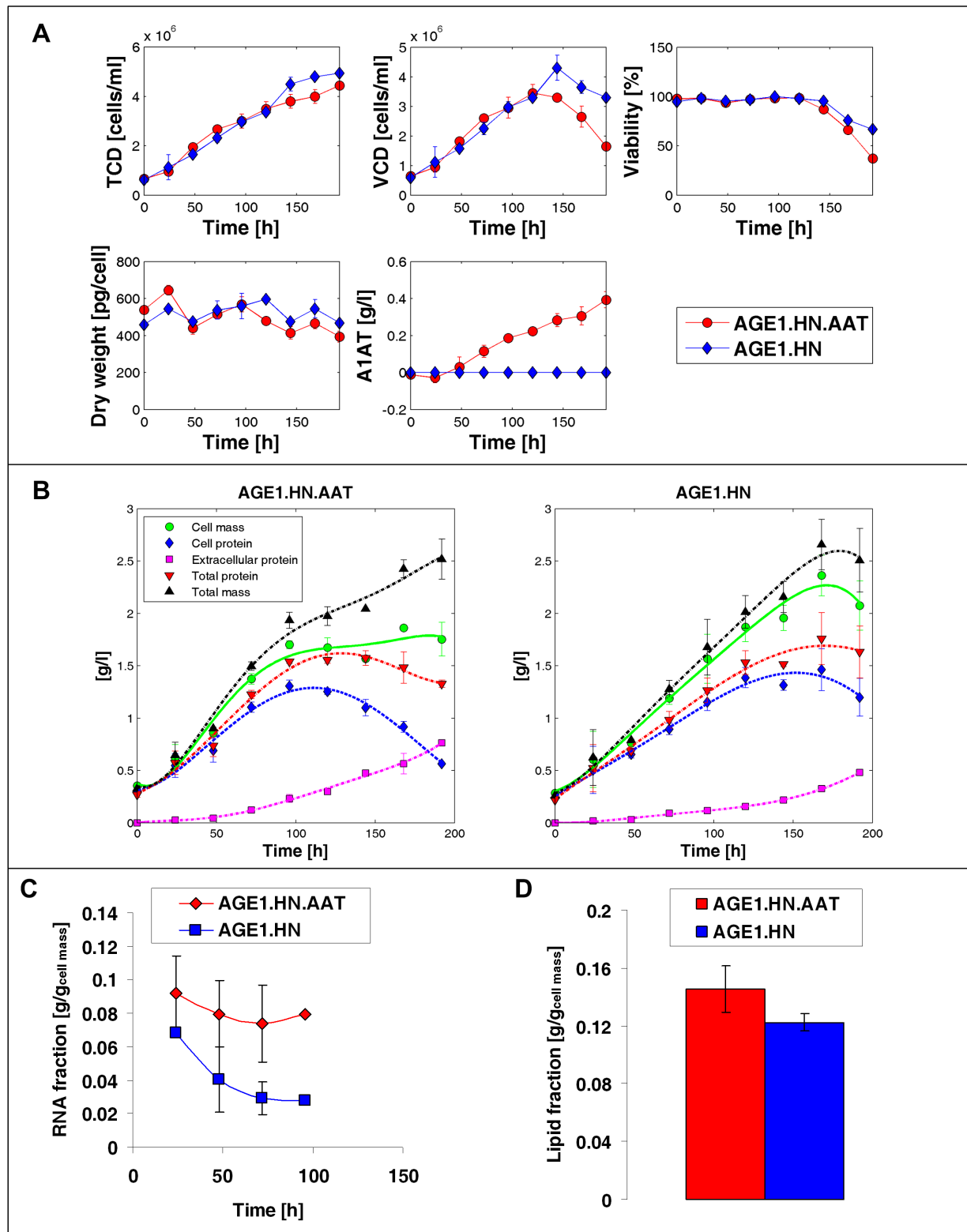


Fig. 6-2 Growth and biomass dynamics in α_1 -antitrypsin (A1AT) producing (AGE1.HN.AAT) and parental AGE1.HN cells. A. Growth profile of AGE1.HN.AAT and AGE1.HN cells. Mean values and standard deviations of two cultivations, respectively. *TCD* total cell density, *VCD* viable cell density. B. Dynamics of biomass components in both cell lines. Mean values and standard deviations of two cultivations. C. RNA fraction in both cell lines from day 1 to day 4 of the cultivation. Mean values and standard deviations of two cultivations. D. Total lipid fraction in AGE1.HN.AAT and AGE1.HN during growth phase. Mean values and standard deviations from five independent measurements using different biological samples.

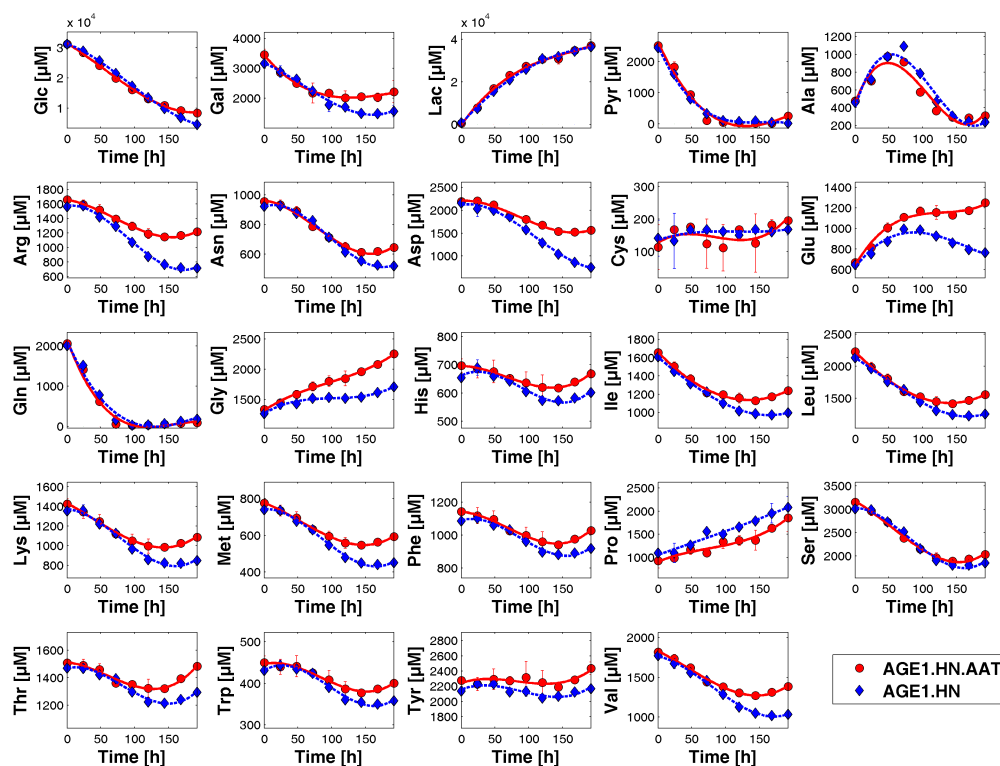


Fig. 6-3 Time course of extracellular metabolites during cultivation of AGE1.HN.AAT and AGE1.HN cells. Mean values and standard deviations of two cultivations. *Glc* glucose, *Gal* galactose, *Lac* lactate, *Pyr* pyruvate, standard abbreviations for amino acids.

6.4.3 Modeling of the theoretical metabolic burden of A1AT production

The differences that can be seen in the metabolism upon production of the glycoprotein can be best explained and understood by using an appropriate model of the theoretical anabolic demand that is needed to produce fully active α_1 -antitrypsin.

At first sight one might be puzzled to see an increase in the production of the amino acids glycine and glutamate upon A1AT production since both amino acids are needed in the amino acid chain of this particular protein. However, considering just the amino acids and energy needed for assembly of the amino acid chain is clearly underestimating the real anabolic demand of A1AT. The whole cellular production process of a glycoprotein includes expression (transcription), synthesis of the amino acid chain (translation), posttranslational modification in endoplasmic reticulum (ER) and Golgi apparatus (Golgi), and secretion of the mature protein. The modeling of this complex process comprises different parts of the cellular metabolism. Whereas the amount of building blocks needed to synthesize mature A1AT is fairly well known, some important parameters in the process are not that clear and their modeling is more challenging. Nucleotides are needed for the synthesis of mRNA and activated sugars. However, their turnover and stability are not known precisely which results in an unknown precursor demand. Nucleotides can be *de novo* synthesized or can be produced by reutilization and phosphorylation of

nucleoside monophosphates (NMPs). Since the reactions in the whole glycoprotein synthesis process take place in different compartments, transport reactions might play an important role and can also be limiting to a certain extent. Another parameter that is not known is the number of A1AT proteins that are translated from one mRNA molecule. Stability of the mRNA is another factor that can improve the protein production in a cell (Hung et al. 2011), as long as other factors are not limiting, reducing at the same time the burden on the transcription machinery. The total cellular content of glycosylated protein might also be significantly increased in a producing cell resulting in a significant increase in the glycosylation demand.

The biochemical equations of the different parts in the metabolism that are involved in the synthesis of the glycoprotein are presented below. The stoichiometry was taken from the Kyoto Encyclopedia of Genes and Genomes pathway database (www.kegg.com).

Depending on the mRNA stability, transcription of A1AT mRNA might be an additional metabolic burden for the cell since many NTPs are needed for mRNA synthesis. However, many proteins can be translated from just one mRNA. We don't know a priori how many mRNAs are synthesized and if this is really a significant burden for the cell. There is also the question of whether the cell will react by synthesizing more NTPs for RNA synthesis. In our simulations, we will assume different numbers of protein which can be synthesized per mRNA.

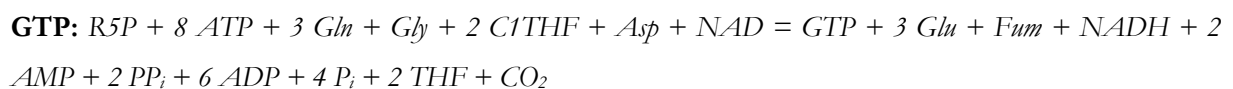
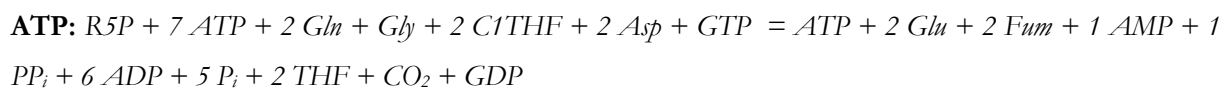
Translation of A1AT mRNA into raw protein is clearly a burden for the cell since the amino acids and energy that is needed to assemble the protein is an additional amount of substrates that cannot be used for synthesis of cell biomass. Protein biosynthesis is a most energy-intensive process.

The reactions of the glycosylation machinery take place in the endoplasmic reticulum and Golgi apparatus of the cell. In our model, both organelles were lumped and just the final glycosylation pattern was modeled. The stoichiometry that is needed to synthesize the glycans on the 3 N-glycosylation sites of A1AT was taken from literature (Kolarich et al. 2006). Transport of activated sugars into the Golgi apparatus is carried out by antiporters by an exchange with the corresponding nucleotide monophosphate, which requires no energy.

The model for the synthesis of A1AT derived from the biochemical equations is shown in Fig. 6-4.

6.4.3.1 Biochemical equations

Nucleotide biosynthesis



C1 metabolism



Transcription of A1AT mRNA

$$\mathbf{mRNA}_{A1AT}: 2543 \text{ UTP} + 2577 \text{ CTP} + 2514 \text{ ATP} + 2592 \text{ GTP} = \mathbf{mRNA}_{A1AT}$$

Translation of A1AT mRNA into raw protein

$$\mathbf{A1AT}_{\text{raw}}: 26 \text{ Ala} + 7 \text{ Arg} + 19 \text{ Asn} + 24 \text{ Asp} + 3 \text{ Cys} + 32 \text{ Glu} + 18 \text{ Gln} + 24 \text{ Gly} + 13 \text{ His} + 20 \text{ Ile} + 51 \text{ Leu} + 34 \text{ Lys} + 10 \text{ Met} + 27 \text{ Phe} + 19 \text{ Pro} + 25 \text{ Ser} + 30 \text{ Thr} + 27 \text{ Trp} + 3 \text{ Tyr} + 6 \text{ Val} + 1672 \text{ ATP} = \mathbf{A1AT}_{\text{raw}}$$

N-glycosylation of A1AT

Biosynthesis of activated sugars

$$\mathbf{UDP-GlcNAc}: \text{Gln} + \text{F6P} + \text{AcC} + \text{UTP} = \text{Glu} + \text{UDP-GlcNAc} + \text{CoA} + \text{PP}_i$$

$$\mathbf{CMP-Neu5Ac}: \text{UDP-GlcNAc} + \text{PEP} + \text{CTP} = \text{CMP-Neu5Ac} + \text{UDP} + \text{Pi} + \text{PP}_i$$

$$\mathbf{GDP-Man}: \text{F6P} + \text{GTP} = \text{GDP-Man} + \text{PP}_i$$

$$\mathbf{GDP-Fuc}: \text{GDP-Man} + \text{NADPH} = \text{GDP-Fuc} + \text{NADP}^+$$

$$\mathbf{UDP-Gal}: \text{G6P} + \text{UTP} = \text{UDP-Gal} + \text{PP}_i$$

N-glycosylation

$$\mathbf{A1AT}_{\text{mat}}: \mathbf{A1AT}_{\text{raw}} + 12.69 \text{ UDP-GlcNAc} + 9 \text{ GDP-Man} + 6.69 \text{ UDP-Gal} + 6.681 \text{ CMP-Neu5Ac} + 0.321 \text{ GDP-Fuc} = \mathbf{A1AT}_{\text{mat}} + 12.69 \text{ UDP} + 9 \text{ GDP} + 6.69 \text{ UDP} + 6.681 \text{ CMP} + 0.321 \text{ GDP}$$

The balance equations for the different parts of the model are presented in matrix form in the supplementary material (Table S2).

The nucleotide pools in the cell can be refilled by salvage nucleotides that are recycled from nucleoside diphosphates or monophosphates which needs just energy in the form of ATP. However, the cells are proliferating and the nucleotide pools have to be filled, additionally, with newly synthesized species. In our model, we included both possibilities. The relative fraction of new nucleotides and recycled ones is defined by the parameters f_1 and f_2 . The parameters t_{1-4} define the amount of the respective nucleotide that is needed to synthesize one mol of A1AT mRNA (\mathbf{mRNA}_{A1AT} , Fig. 6-4). Precursor metabolites required for the synthesis of nucleotides, sugars, activated sugars, and protein were included in the model. It is assumed in the model that all raw A1AT proteins ($\mathbf{A1AT}_{\text{raw}}$) are glycosylated and secreted. The parameters s_{1-5} define the amount of the respective activated sugar needed for glycosylation of A1AT (Fig. 6-4).

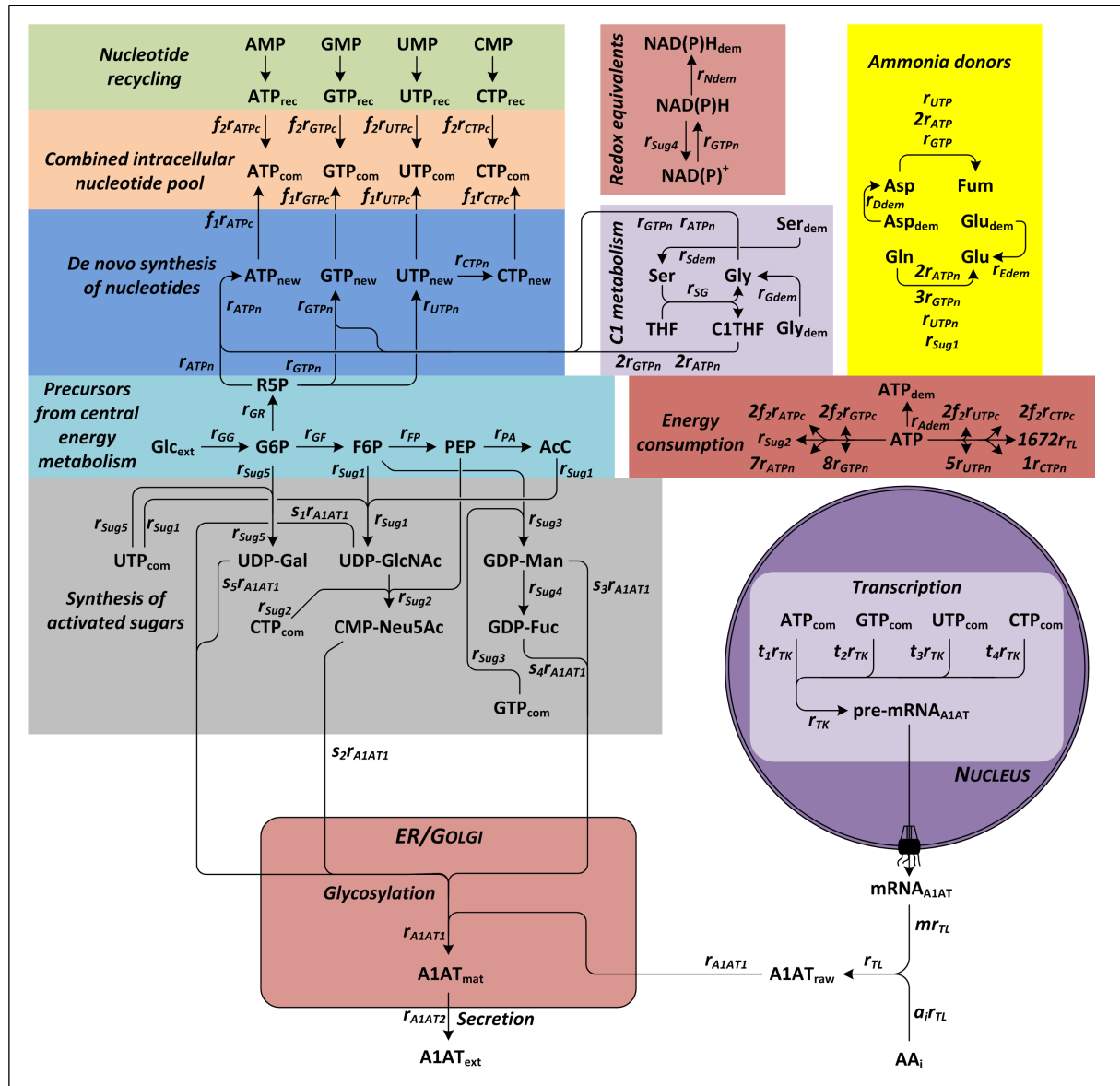


Fig. 6-4 Model to simulate the theoretical metabolic burden of A1AT production in human cells. This model describes in detail the theoretical metabolite demand that is needed to synthesize one mol of mature α_1 -antitrypsin (A1AT). The different parts of the model and the stoichiometry are described in the text. Abbreviations: Standard abbreviations for nucleotides and amino acids, NTP_{rec} recycled nucleoside triphosphate pool, NTP_{com} combined nucleoside triphosphate pool, NTP_{new} pool of newly synthesized nucleoside triphosphate, AA amino acid, Glc glucose, $G6P$ glucose 6-phosphate, $F6P$ fructose 6-phosphate, PEP phosphoenolpyruvate, AcC acetyl coenzyme A, $Glc-NAc$ N-Acetylglucosamine, Man mannose, Fuc fucose, $Neu5Ac$ N-Acetylneuraminic acid, Gal galactose, THF tetrahydrofolate, $C1THF$ methylenetetrahydrofolate. Specific metabolite indices, mat mature, ext extracellular, dem demand, raw raw. Rate names are given at the respective arrow. The stoichiometry of the model is additionally presented in the supplementary material (Table S2).

6.4.4 Simulated metabolite demand for A1AT production

Simulations were carried out using the model (Fig. 6-4) described in the previous section. Assuming metabolic steady state and using the average A1AT production rate, r_{A1AT2} , from two cultivations (Fig. 6-2) which was $0.0454 \mu\text{mol}/\text{g}_{\text{biomass}}/\text{h}$, the theoretical anabolic metabolite fluxes required for A1AT

synthesis were calculated. There are some parameters in the model that are not known. The first one is the relative fraction of new NTPs, f_1 , the second one the fraction of recycled NTPs, f_2 , and the third one the amount of mRNA per translated A1AT protein, m . These parameters were varied and the effects of changes were analyzed.

The calculated demand of selected metabolites depending on f_1 and m is depicted in Fig. 6-5. It was observed that glutamate and glycine are increasingly produced (negative demand) with increasing f_1 (fraction of new NTPs) and m (mRNA/A1AT). The demand for serine or aspartate rises with increasing nucleotide demand. These results indicate that one would expect an increase in the production of glutamate and glycine with increasing intracellular nucleotide demand, which was actually observed for AGE1.HN.AAT (Fig. 6-2). Aspartate and serine uptake was, however, not significantly higher in the producing cell line and even lower for aspartate. The applied model describes the theoretical metabolite demand and does not describe what might happen if, e.g., production of specific metabolites like glutamate or glycine is increased intracellularly. Increased intracellular production of glutamate has to be compensated by the cell. The adaptation might be an increased secretion of glutamate but also increased flux through transamination reactions might be an adaptation. Hereby, the glutamate amino group is transferred to an α -ketoacid producing an amino acid and α -ketoglutarate. This might be the case for aspartate but also for serine. Increased intracellular glutamate levels might lead, e.g., to higher intracellular production of aspartate from oxaloacetate leading to lower demand for extracellular aspartate. In order to understand the differences of producing and parental cell line on metabolic flux level, metabolic flux analysis using metabolite balancing was carried out as described in the next paragraph.

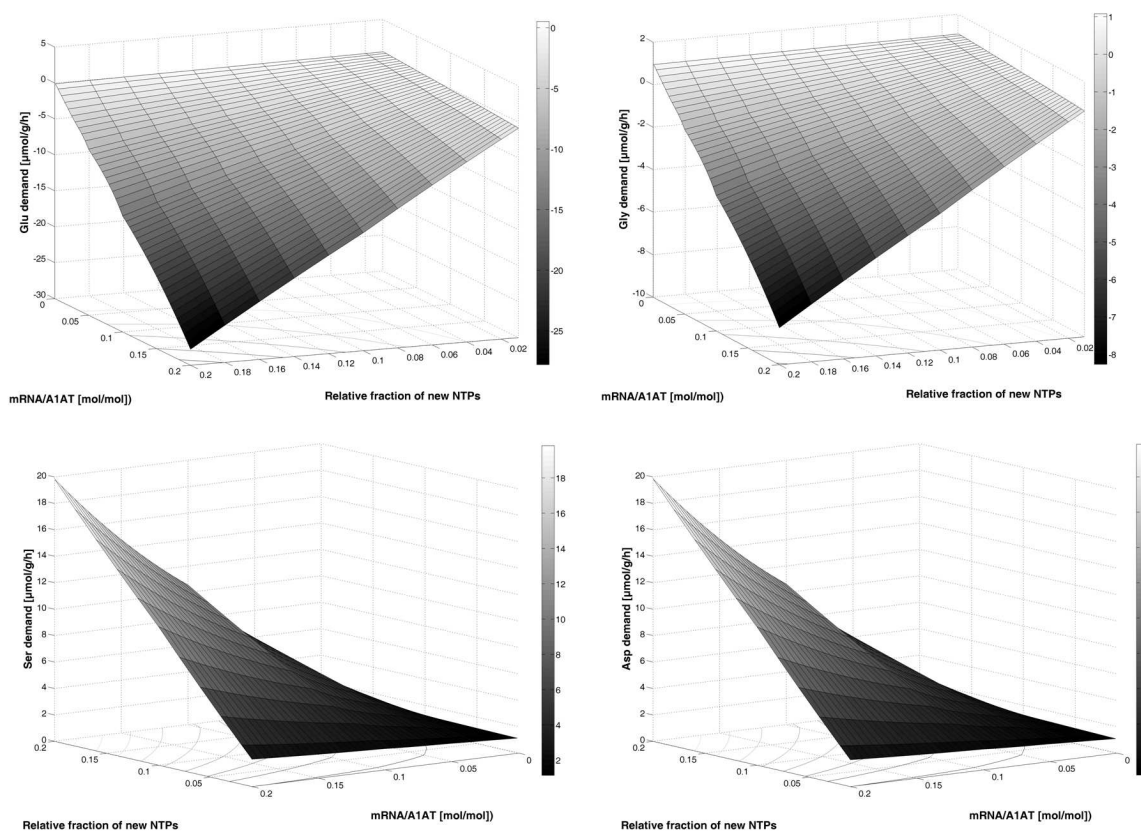


Fig. 6-5 Theoretical demand of selected metabolites upon A1AT production. The theoretical demand for selected metabolites depending on (i) the number of A1AT proteins that are translated per mRNA (mRNA/A1AT) and (ii) the relative intracellular fraction of newly synthesized nucleoside triphosphates (NTPs) is depicted. The demand is given as a theoretical rate in $\mu\text{mol/g/h}$ and was calculated using the observed mean A1AT production rate in the AGE1.HN.AAT cultivations (Fig. 6-2) which was $0.0454 \mu\text{mol/g/h}$.

6.4.5 Comparison of metabolic fluxes in parental and A1AT producing AGE1.HN cells

Selected metabolic fluxes are depicted in Fig. 6-6. A list of all fluxes is given in the supplementary material section (Table S3). It was observed that fluxes in the central energy metabolism (glycolysis, TCA cycle) were similar (Fig. 6-6). However, significant differences were found in other parts of the metabolism. The flux through glycine hydroxymethyltransferase (Fig. 6-6, GHMT, v_{59}) producing C1 units and glycine was higher in AGE1.HN.AAT concurrently with an increased glycine production rate (Fig. 6-6, v_{12}). Another change was observed in the glutamate metabolism and in the fluxes through different transaminases. Glutamate dehydrogenase was catalyzing the formation of glutamate in both cell lines, however, this flux was higher in AGE1.HN.AAT. This led to a higher flux into intracellular glutamate pool which was compensated in AGE1.HN.AAT by increased production of glutamate and increased transamination activity (TA). Aspartate and phosphoserine transaminases (Fig. 6-6, Table S3; v_{55} and v_{67} , respectively) were catalyzing the formation of the respective amino acid consuming excessive glutamate. On the other hand activities of other transaminases involved in amino acid degradation pathways, e.g., branched chain amino acid transaminases (Table S3, degradation of isoleucine, v_{61} , leucine, v_{62} , valine, v_{71}), were lower in

the producing cell resulting in lower glutamate production in these reactions. Alanine transaminase flux was, however, almost similar in both cell lines (Table S3, v_{52}) whereas alanine production was higher in the parental cell line (Fig. 6, v_5).

The sugar demand in ER/Golgi required for glycosylation was only calculated for A1AT production in the producing cell line. These fluxes were lower than 1% of the glucose uptake rate (Table S3) and sugar supply for glycosylation is presumably not a significant burden for the cell.

In summary, it was shown by the metabolic flux analysis that the differences in the anabolic demand of the producing cell line resulted in specific adaptations in intracellular fluxes in the amino acid metabolism and C1 metabolism whereas energy metabolism remained similar.

The higher RNA concentration of AGE1.HN.AAT is most likely due to the recombinant A1AT RNA itself and an increased pool of endogenous RNAs encoding for intracellular proteins directly or indirectly involved with high level A1AT expression. In addition, the higher lipid content can be interpreted as a specific adaptation of the cellular secretion machinery to the burden of processing and secreting high amounts of recombinant A1AT.

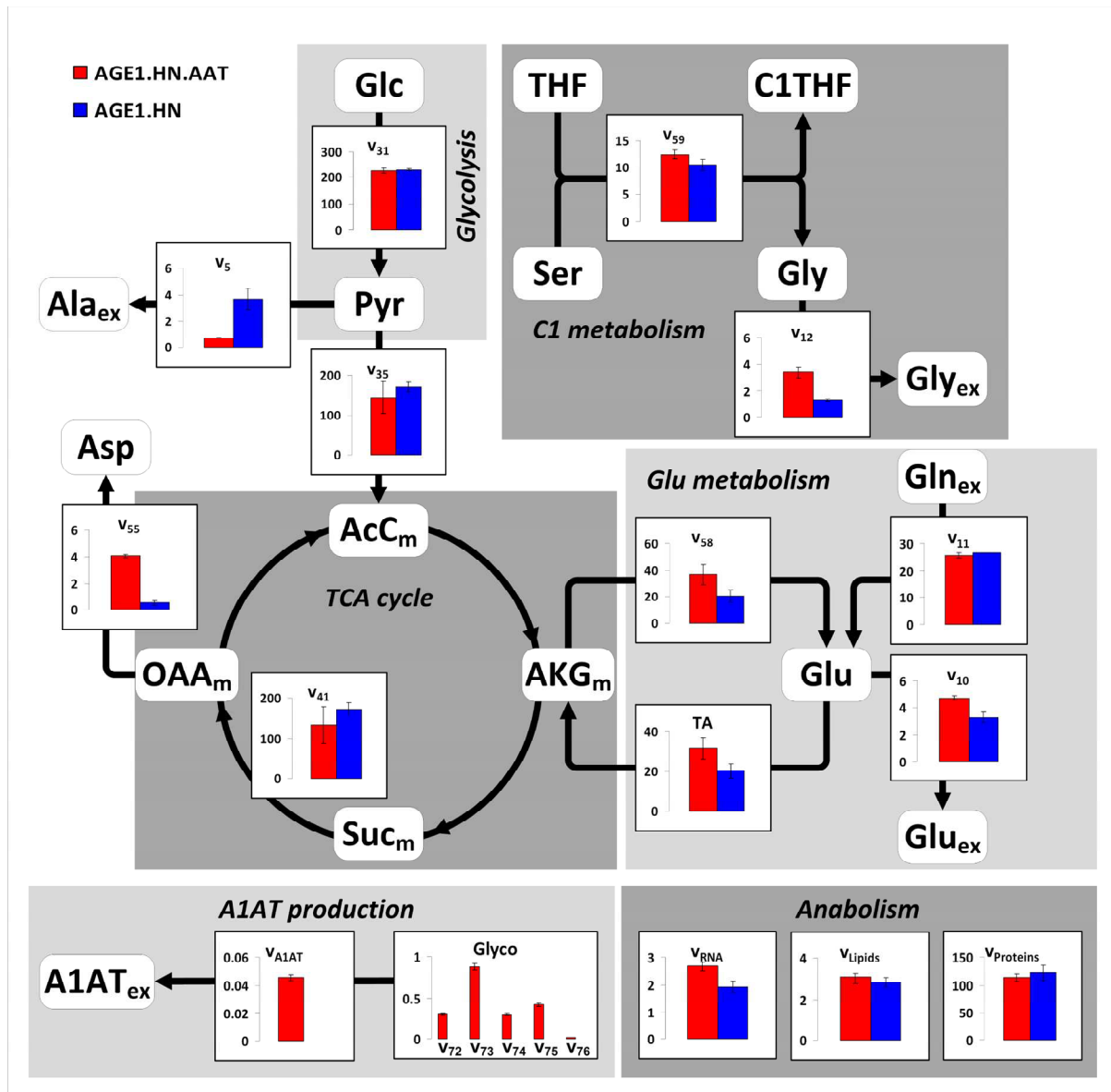


Fig. 6-6 Selected metabolic fluxes in AGE1.HN.AAT and AGE1.HN. Fluxes are given in $\mu\text{mol}/\text{g}_{\text{biomass}}/\text{h}$. Abbreviations and flux numbers as specified in the metabolic network model in Fig. 6-1 and in the representation of the stoichiometry of the metabolic network in the supplementary material (Table S1). *TA* transaminase flux. Glycosylation fluxes (*Glyco*) were only calculated for the product A1AT. In the parental cell (AGE1.HN) these were neglected. All calculated extracellular and intracellular fluxes are presented in Table S3 of the supplementary material.

6.4.6 Targets for improvement of biopharmaceutical production in AGE1.HN

Growth, metabolism, metabolic shifts, as well as metabolite channeling in AGE1.HN were analyzed and described in other recent publications (Niklas et al. 2011b; Niklas et al. 2011c; Niklas et al. 2011d) and promising targets for the improvement of energy metabolism and metabolic efficiency in the cells were identified, i.e., reduction of substrate load and improved connectivity between cytosolic and mitochondrial pyruvate pools. In this study, we will discuss other engineering possibilities which can be deduced from the specific differences between the selected producer and the parental cells.

Product titers in mammalian cell culture processes have tremendously increased in the past decades, which was mainly achieved by optimization of culture media and process control as well as genetic engineering of host cells. Engineering strategies applied in the past are summarized in several excellent reviews (Dinnis and James 2005; Kuystermans et al. 2007; Lim et al. 2010; Seth et al. 2006). The engineering of protein secretion and lipid metabolism represents one strategy to optimize the secretion of recombinant proteins (Lim et al. 2010; Seth et al. 2006). It is supposed that high level synthesis of glycoproteins is associated with a certain stress to the secretory machinery of the producer (Lim et al. 2010). In transcriptional analyses, several ER- and Golgi-localized proteins were found to be differently expressed and associated with enhanced productivity (Doolan et al. 2008). Translation or post-translational events like, e.g., modification and secretion via ER and Golgi, might be bottlenecks when the protein load exceeds the available capacity. In cells with high expression level, it was reported that productivity was not associated with mRNA level or transgene copy number indicating bottlenecks downstream in the process (Barnes et al. 2006; Ku et al. 2008; Lim et al. 2010). In particular, in cells where a secretory bottleneck was supposed, overexpression of XBP-1, a global regulator of the unfolded protein response, was enhancing productivity (Ku et al. 2008; Tigges and Fussenegger 2006). Earlier, it was suggested by Sriburi et al. that XBP-1 overexpression links the unfolded protein response to phospholipid biosynthesis and ER biogenesis (Sriburi et al. 2004). Shaffer et al. showed that XBP-1 induces expansion of the ER and other organelles in plasma cell differentiation leading to increased protein synthesis resulting in the characteristic phenotype of secretory cells (Shaffer et al. 2004). The specific differences between the selected clonal producer and the parental AGE1.HN cell population described in this study pointed to the fact that the most important cellular properties of the producer are high RNA levels and increased cellular lipid content. This resulted also in specific changes in the metabolism. While transcription and RNA level are not expected to limit A1AT expression when highly efficient promoters and selection strategies are applied, engineering of the secretion apparatus might be a promising strategy for further improving productivity in AGE1.HN. As shown in the aforementioned literature, overexpression of XBP-1 in AGE1.HN might push the cellular phenotype closer to the phenotype of a professional secretory cell and improve production. Engineering could be performed directly in parental AGE1.HN cells, which might lead to a new parental cell line with improved protein secretion properties and, presumably, later to better producers. Also, targeted feeding of specific lipid mixtures could further increase cellular phospholipid content leading to an expanded secretory apparatus in the cell, which might further enhance the yields. The effects of different lipid supplements in specific mammalian cell culture processes have also been analyzed and discussed in the literature (Jenkins et al. 1994; Nguyen et al. 1993; Seamans et al. 1994). Generally, we suggest genetic engineering of the lipid metabolism and the secretory pathway in AGE1.HN in order to further improve performance and productivity of this cell line.

6.5 Acknowledgements

This work has been financially supported by the BMBF project SysLogics - Systems biology of cell culture for biologics (FKZ 0315275A-F). We thank Michel Fritz for valuable analytical support.

6.6 Supplementary material

The supplementary material for this chapter is given in the supplementary material section at the end of the thesis.

7 Quercetin treatment changes fluxes in the primary metabolism and increases culture longevity and recombinant α_1 -antitrypsin production in human AGE1.HN cells

7.1 Abstract

Addition of the flavonoid quercetin to cultivations of the α_1 -antitrypsin (A1AT) producing human AGE1.HN.AAT cell line resulted in alterations of the cellular physiology and a remarkable improvement of the overall performance of these cells. In a first screening in 96-well plate format, toxicity and the effect of quercetin on the lactate/glucose ratio were analyzed. It was found that quercetin treatment reduced lactate/glucose ratio dose-dependently. An increase in culture longevity, viable cell density (160% of control), and A1AT concentration (195% of control) was observed in batch cultivation with 10 μ M quercetin compared to control. Detailed analysis of quercetin effects on primary metabolism revealed dose-dependent alterations in metabolic fluxes. Quercetin addition resulted in an improved channeling of pyruvate into mitochondria accompanied by reduced waste product formation and stimulation of TCA cycle activity. The observed changes in cellular physiology can be explained by different properties of quercetin and its metabolites, e.g., inhibition of specific enzymes, oxidation of cytoplasmic and mitochondrial NADH resulting in reduced NADH/NAD⁺ ratio, and cytoprotective activity. The present study shows that addition of specific effectors to the culture medium represents a promising strategy for improving the cellular metabolic phenotype and the production of biopharmaceuticals. The provided results contribute, additionally, to an improved understanding of quercetin action on the metabolism of human cells.

This chapter was submitted as

Niklas J, Nonnenmacher Y, Rose T, Sandig V, Heinzle E. Quercetin treatment changes fluxes in the primary metabolism and increases culture longevity and recombinant α_1 -antitrypsin production in human AGE1.HN cells.

7.2 Introduction

The human cell line AGE1.HN was specifically designed for the production of complex biopharmaceuticals requiring human-type glycosylation. One of these glycoproteins of interest is α_1 -antitrypsin (A1AT) which is required in the clinic to treat patients suffering from A1AT deficiency. This hereditary disorder can result in lung emphysema and liver dysfunction (Kelly et al. 2010; Petrache et al. 2009). The mortality risk can be significantly reduced by A1AT augmentation therapy (A1AT-Group 1998), however, this therapy is very expensive and not cost-effective (Gildea et al. 2003) particularly as so far all licensed A1AT-products are only derived from human plasma (Karnaukhova et al. 2006). Production of recombinant A1AT in several hosts was not successful. However, A1AT produced from AGE1.HN cells is biologically active and has similar anti-inflammatory activity as commercial A1AT (Blanchard et al. 2011) showing that AGE1.HN is a suitable expression system.

For further targeted improvement of the biopharmaceutical production in AGE1.HN, growth and metabolism of this cell line were analyzed in recent studies. In a first study of the metabolism and metabolic shifts of AGE1.HN during the cultivation, it was proposed that high substrate levels in the beginning of the cultivation might lead to energy spilling waste product formation (Niklas et al. 2011d). In a subsequent study, it was confirmed that reduced pyruvate load leads to improved metabolic efficiency and, ultimately, increased A1AT titers (Niklas et al. 2011b). Using detailed ^{13}C tracer studies and ^{13}C metabolic flux analysis, it was further revealed that mitochondrial pyruvate transport and the connectivity between TCA cycle and glycolytic metabolites is low during exponential growth in AGE1.HN (Niklas et al. 2011c). In summary, optimization of AGE1.HN's metabolism towards improved metabolic efficiency and balanced substrate use should be performed to improve biopharmaceutical production in this cell line. The optimization of cellular metabolism concerning efficient use of nutrients represents an issue that was addressed in several mammalian production cells in the past. Altamirano et al. showed that the replacement of the substrates glucose and glutamine by the slowly metabolized compounds galactose and glutamate resulted in a very efficient metabolism with minimal formation of the waste products lactate and ammonium (Altamirano et al. 2000). Genetic engineering of the sugar transport was another strategy that was successfully applied to decrease sugar uptake and waste product formation increasing final cell concentration (Wlaschin and Hu 2007).

Besides the modification of substrate availability and substrate concentrations and the targeted genetic engineering of producer cells, addition of specific substances having positive effects on growth, product titers, or specific productivity represents a very promising strategy for improving the cell culture process. It was reported that the addition of, e.g., DMSO, glycerol, or sodium butyrate can enhance the production of biopharmaceuticals in different mammalian cells (Cherlet and Marc 2000; Liu and Chen 2007; Oh et al. 2005; Rodriguez et al. 2005). Despite an increase in specific productivity in many producers, treatment with these chemicals results usually in a reduced growth rate which can reduce the final product titer compared to untreated cells (Rodriguez et al. 2005). It is likely that other substances can increase metabolic efficiency and can be used as media additives to reduce waste product formation and improve

culture longevity and productivity. Recently, it was reported that verapamil can almost completely stop lactate production in HL-1 cells without noticeably influencing cell growth (Strigun et al. 2011a) which is a sought-after cellular phenotype in cell culture processes.

In preceding work, we screened a number of compounds with a view to assessing their ability to increase metabolic efficiency or to improve α_1 -antitrypsin production in AGE1.HN cells. Quercetin was found to be one of the most promising candidates. This naturally occurring flavonoid, which is present in many plants, was reported to have many beneficial effects on human health, e.g., anti-tumor, anti-inflammatory, and anti-oxidant activity (Middleton et al. 2000). Additionally, quercetin was found to inhibit a number of enzymes and to modify important physiological parameters related to primary metabolism. It was reported that lactate dehydrogenase, pyruvate kinase (Grisolia et al. 1975), malate dehydrogenase (Seddon and Douglas 1981), or sugar transport (Martin et al. 2003; Salter et al. 1978; Shisheva and Shechter 1992) are inhibited by quercetin. Since the improvement of metabolic efficiency and a better balanced substrate use were optimization targets defined for AGE1.HN in recent publications (Niklas et al. 2011b; Niklas et al. 2011c; Niklas et al. 2011d), the reported beneficial and inhibitory activities of quercetin might be appropriate for improving the metabolism in AGE1.HN.

In this study, we analyze in detail the effects of quercetin on growth, metabolism, and α_1 -antitrypsin production in AGE1.HN. The results obtained are, on the one hand, useful for an improvement of biopharmaceutical production in mammalian cells and, on the other hand, important for an improved understanding of the effect of quercetin on the metabolism in human cells and on human health in general.

7.3 Material and methods

7.3.1 Cell line and cultivation

The α_1 -antitrypsin (A1AT) producing cell line AGE1.HN.AAT® (ProBioGen AG, Berlin, Germany) originates from primary human brain cells which were immortalized and engineered using selected adenoviral genes. The A1AT gene in this cell line is driven by a human CMV/EF1 hybrid promoter (ProBioGen AG). A more detailed description of the cells can be found in recent publications (Niklas et al. 2011b; Niklas et al. 2011c; Niklas et al. 2011d). Cultivations were carried out in an incubator supplied with a shaking unit (Innova 4230, New Brunswick Scientific, Edison, NJ, USA; 2 inches orbit) at 37°C and 5% CO₂ using 125 ml shake flasks (Corning, NY, USA) and serum-free 42-Max-UB medium (Teutocell AG, Bielefeld, Germany).

7.3.2 Analytical methods

Cell counting was performed using an automated cell counter (Countess, Invitrogen, Karlsruhe, Germany). Toxicity screening was performed using respiration measurements in 96-well OxoPlates (PreSens GmbH, Regensburg, Germany (Deshpande et al. 2005; John et al. 2003)) applying the equipment and procedures as described in recent publications (Niklas et al. 2009; Noor et al. 2009). A1AT (α_1 -

antitrypsin) concentration was measured as described recently (Niklas et al. 2011b) using an activity assay based on the inhibition of trypsin by A1AT. Concentrations of extracellular metabolites (sugars, organic acids, amino acids) were measured using different HPLC methods (Kromer et al. 2005; Niklas et al. 2009).

7.3.3 Screening in 96-well plates

Toxicity was assessed using respiration measurements in 96-well plates. Cells from the preculture were transferred into Falcon tubes, centrifuged (500 1/min, 5 min, 20°C, Labofuge 400R Function Line, Heraeus Instruments, Hanau, Germany), the supernatant discarded, and the pellet resuspended in medium. After cell counting and appropriate dilution, 198 µl of the cell suspension were pipetted into each well of the 96-well plate having a final cell density of 0.4×10^6 cells/ml. 100× stock solutions of the compounds were prepared in DMSO and 2 µl of the respective stock solution was finally added to the cells. Respiration was monitored for 24 h using a fluorescence reader (BMG Labtechnologies, Offenburg, Germany) with shaking unit (300 1/min) set at 37°C and enclosed in a chamber ensuring 5% CO₂ supply. After the respiration measurement, the cell suspension was centrifuged (8,000 1/min, 5 min, 20°C, Biofuge pico, Heraeus Instruments, Hanau, Germany), the supernatant transferred into fresh tubes, and frozen for later analysis of extracellular metabolites. EC₅₀ (effective concentration that elicits a half-maximal reduction of respiration) for quercetin was calculated as described recently (Niklas et al. 2009).

7.3.4 Study of effects of quercetin on growth, metabolism, and α₁-antitrypsin production in AGE1.HN

The cells were taken from the preculture and centrifuged (500 1/min, 5 min, 20°C, Labofuge 400R Function Line, Heraeus Instruments, Hanau, Germany). The supernatant was discarded and the pellet resuspended in fresh medium. After cell counting the cells were seeded into 50 ml bioreactor filter tubes (TPP, Trasadingen, Switzerland). Quercetin (CAS 117-39-5, Sigma-Aldrich, Steinheim, Germany; stock solution 1 mM in DMSO) was added to a final concentration of 10 µM. The control cultivation was performed with the same final DMSO concentration (1% *v/v*). Samples were taken every day. Cell counting was performed and extracellular metabolite concentrations as well as A1AT concentrations were measured in the culture supernatants.

7.3.5 Study of dose-dependent effects of quercetin on AGE1.HN

The experiment was started as described in the foregoing study having also the same materials. Tested quercetin concentrations were 0.1, 1, and 10 µM. 100× stock solutions were prepared in DMSO and added to the cultures. The control cultivation without quercetin was carried out with 1% (*v/v*) DMSO in the medium as it was also present in the quercetin cultivations. Growth was monitored for all cultivations. A1AT and extracellular metabolite concentrations in the culture supernatants were measured.

7.3.6 Metabolic flux analysis

Metabolic fluxes were calculated using Matlab R2007b (The Mathworks, Natick, MA, USA) applying stationary metabolic flux analysis using metabolite balancing as described in literature (Niklas and Heinzle 2011; Niklas et al. 2011d; Stephanopoulos et al. 1998). The stoichiometry of the applied metabolic network model (Fig. 7-1) for the AGE1.HN.AAT cell line is given as stoichiometric matrix in the supplementary material (Table S1).

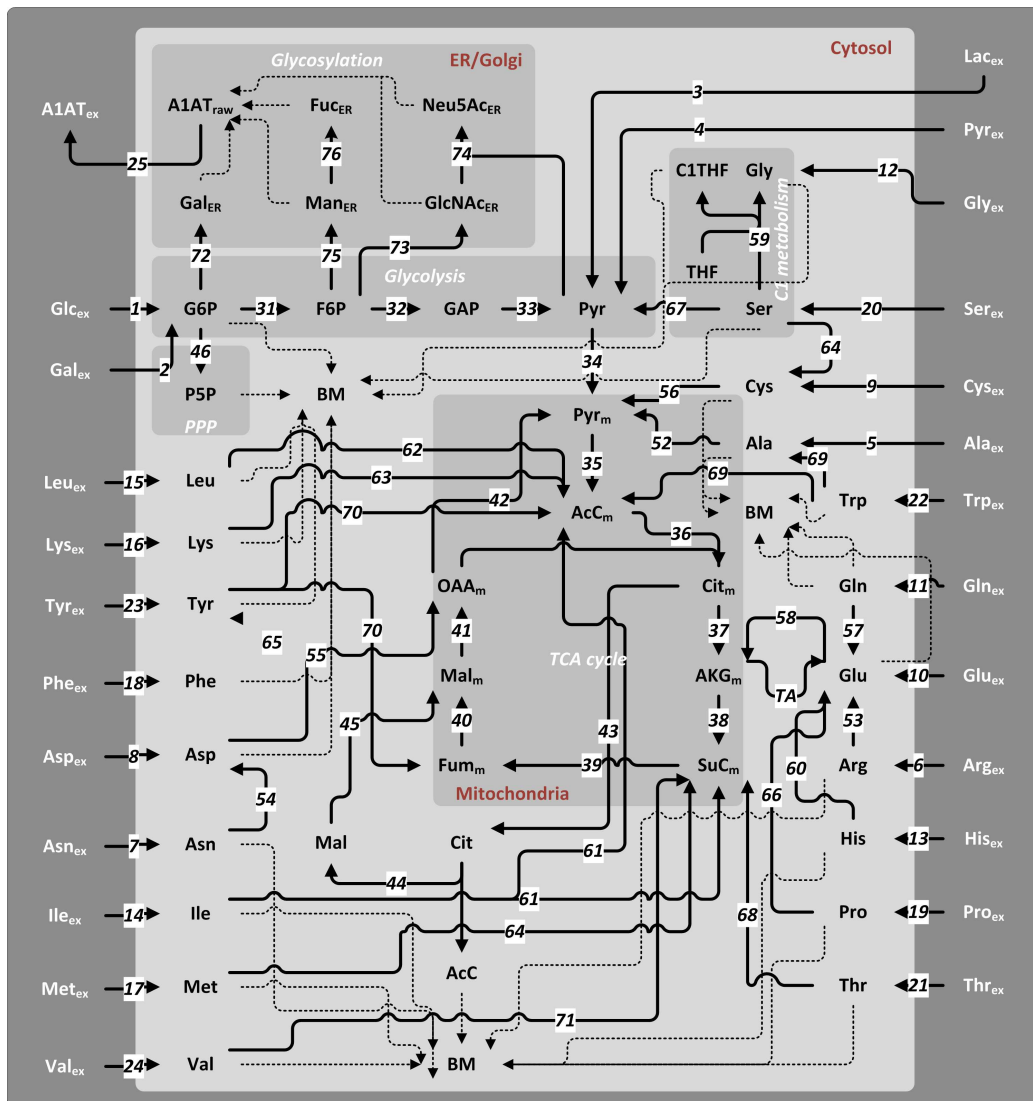


Fig. 7-1 Metabolic network model for metabolic flux analysis in AGE1.HN.AAT. The stoichiometric matrix of the model is given in Table S1 of the supplementary material. Dashed lines indicate fluxes to biomass. Abbreviations: *A1AT* α_1 -antitrypsin, *ER* endoplasmic reticulum, *Golgi* Golgi apparatus, *BM* biomass, *Glc* glucose, *Gal* galactose, *Lac* lactate, *Pyr* pyruvate, *G6P* glucose 6-phosphate, *P5P* pentose 5-phosphate, *F6P* fructose 6-phosphate, *GAP* glyceraldehyde 3-phosphate, *AcC* acetyl coenzyme A, *Cit* citrate, *AKG* α -ketoglutarate, *SuC* succinyl coenzyme A, *Fum* fumarate, *Mal* malate, *OAA* oxaloacetate, *TA* transamination flux ($TA = v_{52} + v_{55} + v_{61} + v_{62} + 2v_{63} + v_{67} + v_{70} + v_{71}$), *GlcNAc* N-Acetylglucosamine, *Man* mannose, *Fuc* fucose, *Neu5Ac* N-Acetylneuraminic acid, *THF* tetrahydrofolate, *C1THF* methylenetetrahydrofolate, standard abbreviations for amino acids. Indices *ex* extracellular, *m* mitochondrial ER localization in the ER or Golgi apparatus.

7.4 Results

7.4.1 Toxicity- and metabolic screening of effectors in 96-well plates

A number of chemicals influencing cellular glucose uptake, as reported in literature, were tested in different concentrations concerning toxicity on AGE1.HN.AAT cells (not shown). Additionally, metabolite profiling was carried out to identify promising candidates as well as the best concentrations fulfilling objectives that were defined as follows: (i) no toxic effects, (ii) reduction of lactate/glucose ratio. From a number of candidates quercetin was one of the most promising substances. In a respiration assay, an EC₅₀ value of 48 μ M (Fig. 7-2A) was observed. In the metabolite analysis, reduction of lactate/glucose ratio was detected for all tested concentrations showing a dose dependent decrease of the ratio (Fig. 7-2B).

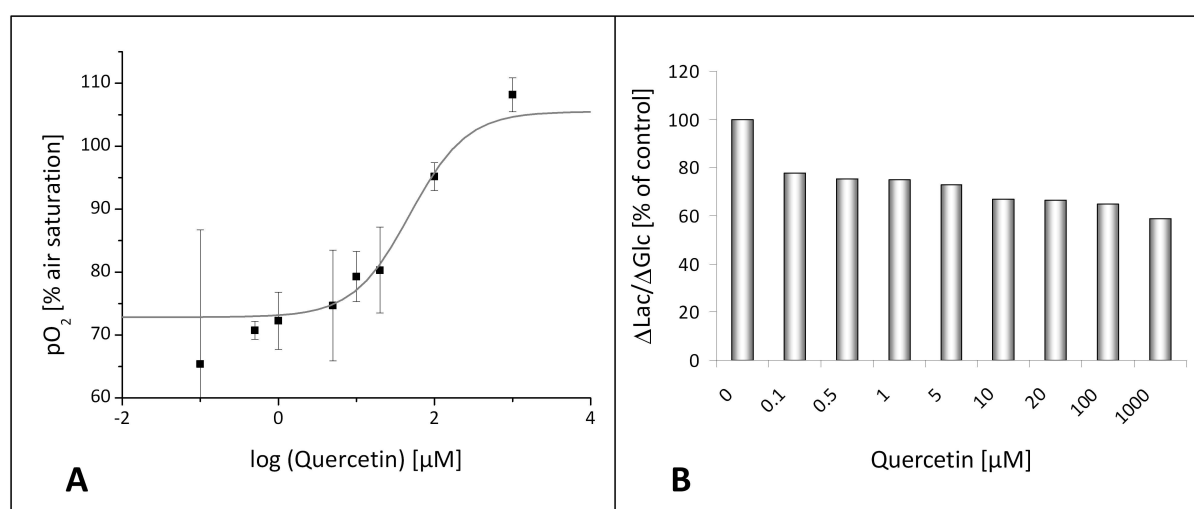


Fig. 7-2 Screening in 96-well plate. A. Concentration response curve for quercetin on AGE1.HN.AAT cells in respiration assay after 24 h (n=3). The dissolved oxygen (pO₂) is given as % air saturation. B. Lactate/glucose ratio (Δ Lac/ Δ Glc) after 24 h in AGE1.HN.AAT cells treated with different quercetin concentrations

7.4.2 Quercetin treatment increases culture longevity, maximal cell density, and A1AT production

Cultivations of AGE1.HN.AAT cells were carried out using selected subtoxic concentrations of the effectors as identified in the toxicity and metabolite screening. For quercetin, a concentration of 10 μ M was chosen which was clearly below EC₅₀ value showing at the same time a reduction in the Lac/Glc ratio. It was observed that the culture longevity was increased in the quercetin cultivation (Fig. 7-3). The maximal viable cell density that was reached during the process was much higher compared to the control with maximal viable cell densities of 5.5×10^6 cells/ml and 3.4×10^6 cells/ml for treated cells and control, respectively. The concentration of the product A1AT was 0.76 g/l at the end of the quercetin cultivation compared to an A1AT concentration of 0.39 g/l in the control (Fig. 7-4).

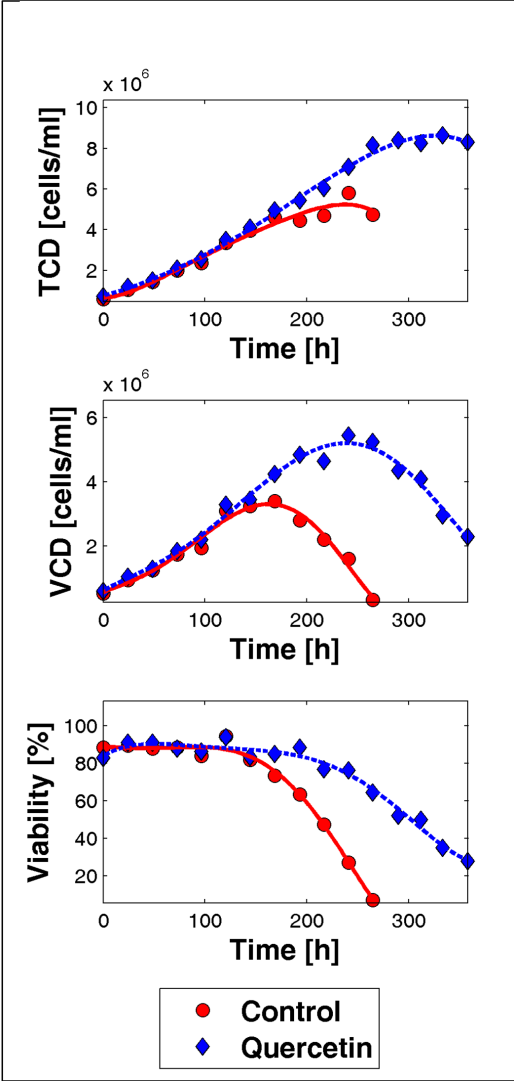


Fig. 7-3 Growth profile of AGE1.HN.AAT cells cultured without (control) and with 10 μ M quercetin. *TCD* total cell density, *VCD* viable cell density.

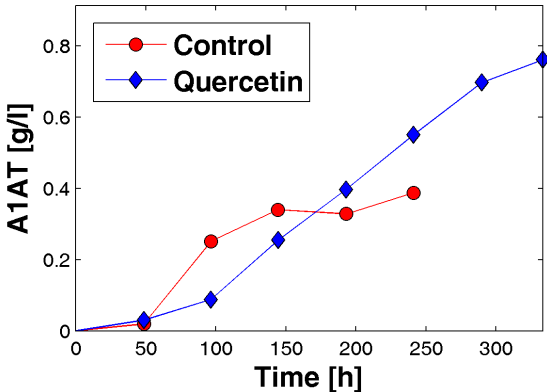


Fig. 7-4 Time course of α_1 -antitrypsin (A1AT) in the control cultivation and in the cultivation with 10 μ M quercetin in the medium. Same experiment as in Fig. 7-3.

7.4.3 Changes in extracellular metabolic profiles upon quercetin treatment

Time courses of extracellular metabolites during the cultivations are depicted in Fig. 7-5. Profiles for most metabolites were similar in the exponential growth phase until 120 h. Total alanine production was higher in the first 120 hours of the cultivation in quercetin treated cells. Lactate production as well as glucose uptake was only slightly reduced in the quercetin cultivation. After glutamine depletion at ~140 h, alanine was taken up in both cultivations. Glutamate was only taken up in the quercetin cultivation. In the control culture, reduced growth and decreasing viability were observed after glutamine depletion explaining the low substrate uptake. In contrast, increased culture longevity in the quercetin cultivation led to further consumption of substrates. Glucose and amino acids, like glutamate and aspartate, were completely consumed. Uptake of branched chain amino acids (e.g., Ile, Fig. 7-5) and asparagine remained high after glutamine was consumed.

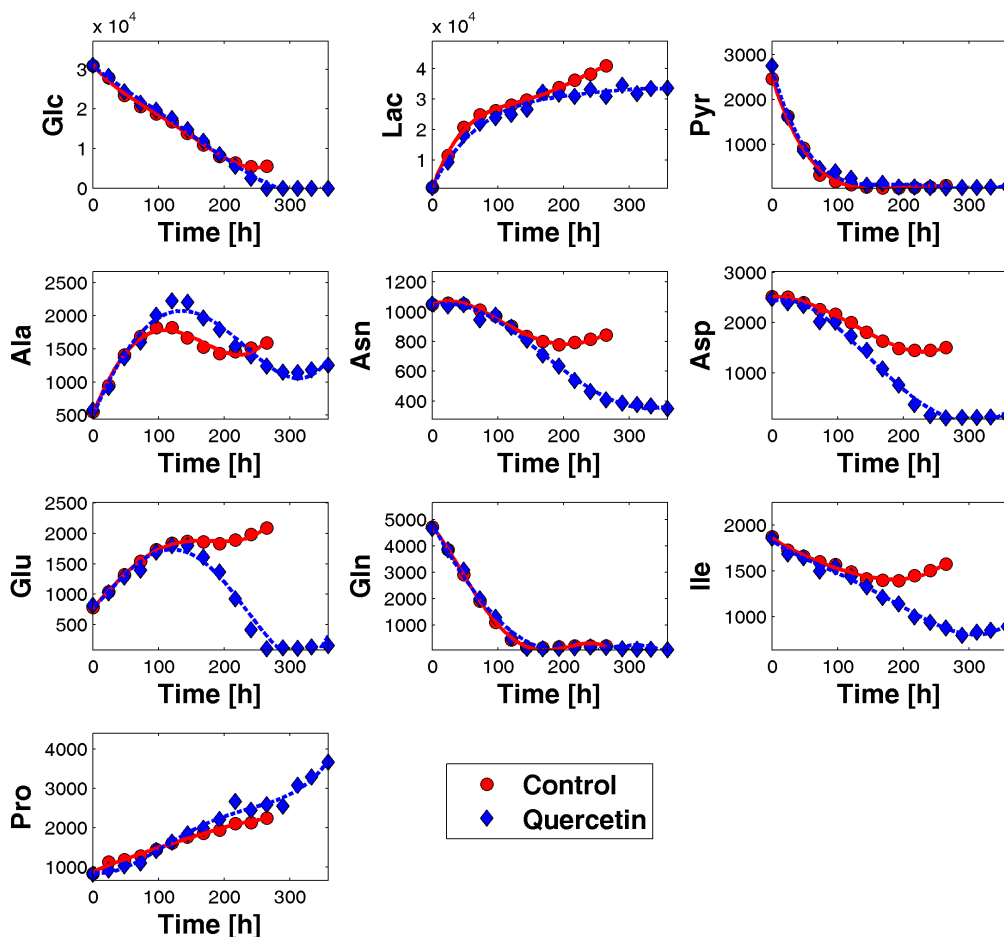


Fig. 7-5 Time courses of extracellular metabolites during the cultivations. Same experiment as in Figs. 7-3 and 7-4. *Glc* glucose, *Lac* lactate, *Pyr* pyruvate, standard abbreviations for amino acids

7.4.4 Quercetin treatment leads to metabolic flux changes in the beginning of the cultivation

For a detailed understanding of the influence of quercetin on the central metabolism in this cell line, metabolic flux analysis was carried out for different metabolic phases observed during cultivation. We divided the cultivations into the following phases. Phase 1 (0-72 h) is characterized by highest waste product formation and ends at 72 h where also pyruvate is consumed. Phase 2 (72-144 h) starts with the pyruvate depletion in the medium and ends when glutamine is consumed.

The most important fluxes calculated by stationary metabolic flux analysis for the different phases are depicted in Fig. 7-6.

In phase 1, the glucose uptake rate and glycolytic rates (e.g., v_{32} and v_{33}) were reduced upon quercetin treatment (86% of control) accompanied by reduced production rates for the waste metabolites lactate (83% of control, v_3) and alanine (84% of control, v_5). Flux of cytosolic pyruvate into TCA cycle was increased in the quercetin treated cells (231% of control, v_{34}). The increased flux through pyruvate dehydrogenase was supported by higher anaplerotic fluxes that were additionally feeding into TCA cycle intermediates. Flux from glutamate to α -ketoglutarate (v_{58} and TA) was higher in quercetin treated cells which was mainly accomplished by a reduction of the production and secretion of excess glutamate and proline (v_{10} and v_{19}). Degradation of branched chain amino acids (Ile, v_{61} ; Leu, v_{62} ; Val, v_{71}) to TCA cycle intermediates additionally contributed to replenishing the TCA cycle metabolite pools. In summary, metabolic efficiency, i.e., reduced waste product formation and increased TCA cycle activity, was increased by quercetin treatment.

In phase 2, metabolism of control and treated cells was almost identical in this experiment (Fig. 7-6).

7.4.5 Dose-dependent effects of quercetin on central metabolism in AGE1.HN

In order to verify the metabolic effects that were found for the cultivation with 10 μ M quercetin and to analyze which of these effects observed in the exponential growth phase are dose-dependent, we performed additional cultivations with different quercetin levels. Growth parameters and time courses of extracellular metabolites in the growth phase were measured and metabolic fluxes were calculated. The most important fluxes selected are shown in Fig. 7-7. It was observed that the glucose uptake rate and glycolytic rates (e.g., v_{32} and v_{33}) were slightly reduced compared to control (84-90% of control) at all applied quercetin concentrations ranging from 0.1 μ M to 10 μ M. Production of waste metabolites (lactate, v_3 ; alanine, v_5 ; glutamate, v_{10} ; proline, v_{19}) was decreased with increasing quercetin concentrations. In particular, lactate production rate (v_3) was dose-dependently decreased from 87% of control on 0.1 μ M quercetin to 79% and 74% of control on 1 μ M and 10 μ M quercetin treatment, respectively. According to the reduced channeling of pyruvate carbons to waste metabolites, flux of pyruvate into TCA cycle (v_{34}) was dose-dependently increased with increasing quercetin treatment (107%, 140%, 227% of control on 0.1 μ M, 1 μ M, and 10 μ M quercetin, respectively). Anaplerotic fluxes feeding the TCA cycle were higher when quercetin was applied as observed in the experiment described before (Fig. 7-6).

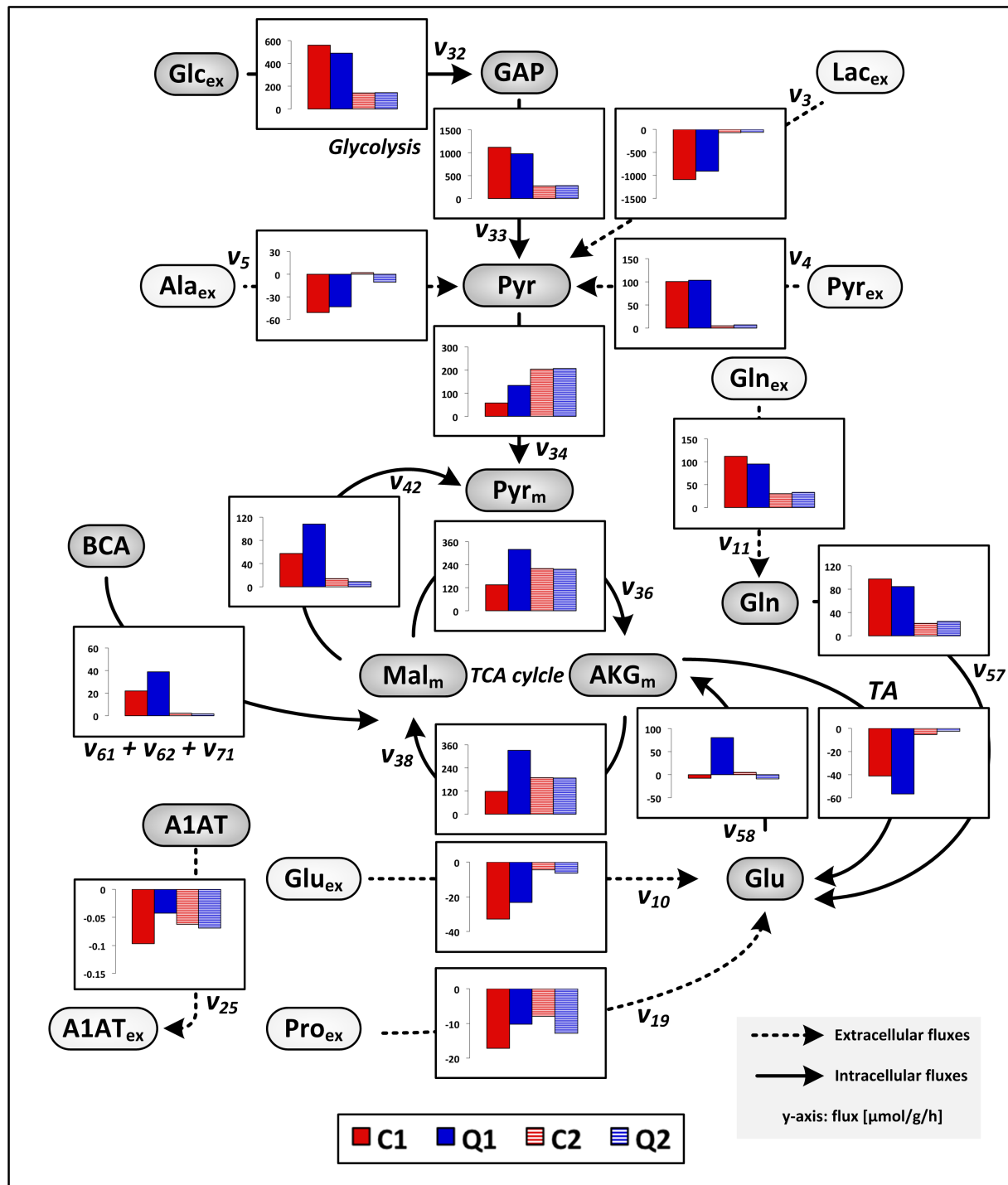


Fig. 7-6 Metabolic flux distribution of AGE1.HN.AAT cells in different growth phases and upon different treatment. The most important fluxes selected are depicted. Same experiment as in Figs. 7-3, 7-4, and 7-5. Growth of AGE1.HN.AAT was divided into distinct metabolic phases and fluxes were calculated for each phase. Phase 1 is ranging from 0-72 h, phase 2 from 72-144 h. C1, fluxes in phase 1 for the control cultivation; Q1, fluxes in phase 1 for the quercetin cultivation; C2, fluxes in phase 2 for the control cultivation; Q2, fluxes in phase 2 for the quercetin cultivation. Flux numbers and abbreviations are defined in Fig. 7-1 (metabolic network model) and in Table S1 of the supplementary material. *BCA* branched chain amino acid.

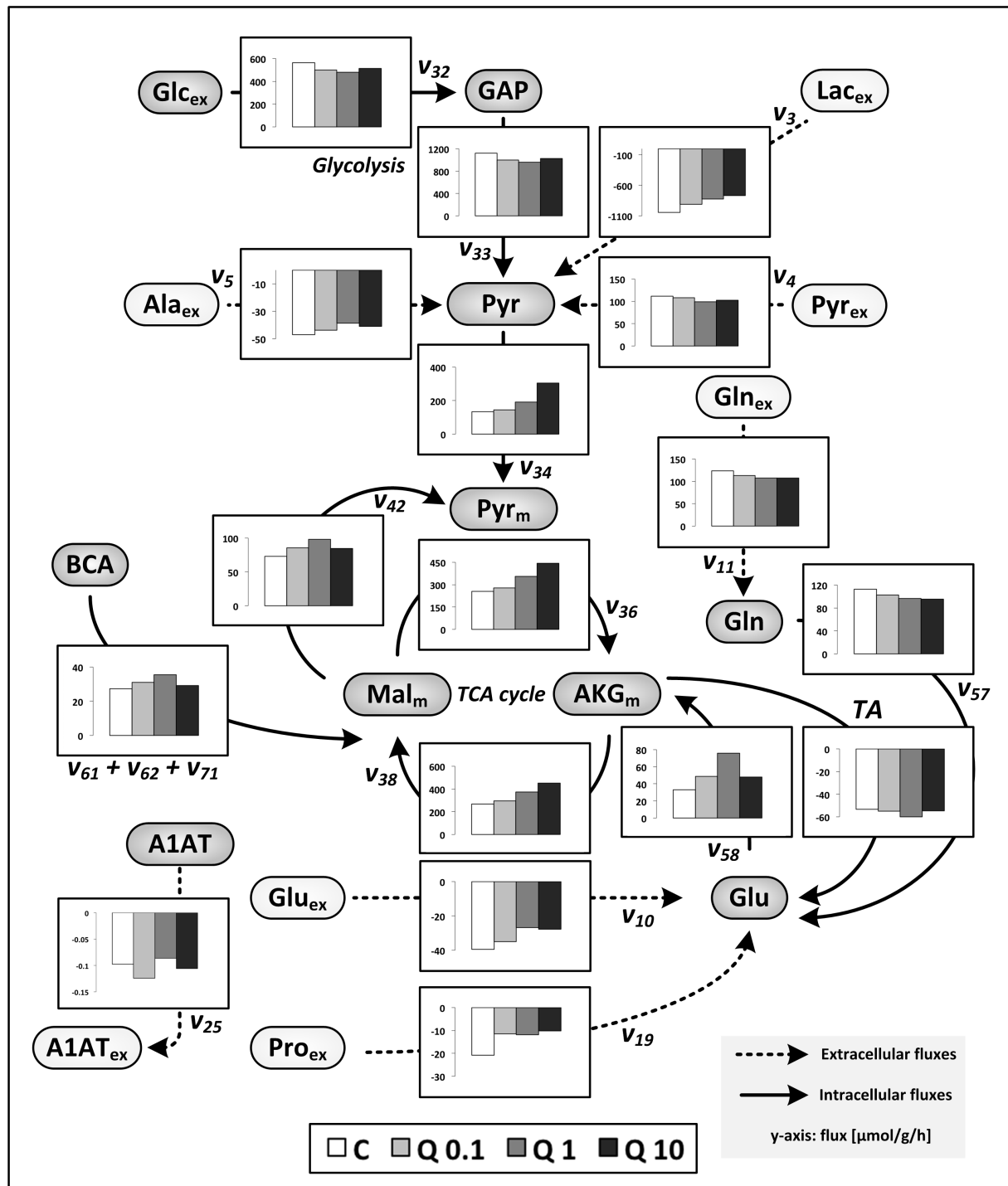


Fig. 7-7 Dose-dependent effects of quercetin on metabolic fluxes in AGE1.HN.AAT. Selected fluxes during the exponential growth phase are depicted. C, control cultivation; Q 0.1, cultivation with 0.1 μM quercetin; Q 1, cultivation with 1 μM quercetin; Q 10, cultivation with 10 μM quercetin. Flux numbers and abbreviations are defined in Fig. 7-1 (metabolic network model) and in Table S1 of the supplementary material. *BCA* branched chain amino acid.

7.5 Discussion

At the start of this study, we analyzed the toxicity of quercetin using a respiration assay (Noor et al. 2009) to determine the subtoxic concentration range. This procedure is similar to the one which was also applied recently to identify subtoxic effects of drugs (Niklas et al. 2009). The EC₅₀ for quercetin which was 48 μ M is similar to literature values for other human cells. In human lung embryonic fibroblasts and in human umbilical vein endothelial cells a 50% lethal concentration of 303 μ M and 61 μ M was reported, respectively (Matsuo et al. 2005). A 50% inhibitory concentration for inhibition of proliferation of 178 μ M was found for quercetin on pancreatic tumor cells (Harris et al. 2011).

The reported inhibitory activity of quercetin on cellular sugar transport (Martin et al. 2003; Salter et al. 1978; Shisheva and Shechter 1992) and, particularly, the inhibition of GLUT1 (Martin et al. 2003) as well as the inhibition of lactate dehydrogenase (Grisolia et al. 1975) were promising properties and the reason why we decided to test this compound on AGE1.HN. In recent studies on primary metabolism of AGE1.HN cells under various conditions, one of the conclusions was that a reduction of substrate uptake and an improvement of the connectivity between glycolysis and TCA cycle are promising optimization targets (Niklas et al. 2011b; Niklas et al. 2011c; Niklas et al. 2011d). It was suggested that changing these cellular properties might finally lead to higher metabolic efficiency and improved production. In the first screening of quercetin, we observed a dose dependent reduction of the lactate/glucose ratio (Fig. 7-2B) indicating an influence of quercetin on glucose transport or intracellular lactate production as reported in literature (Grisolia et al. 1975; Martin et al. 2003).

In the cultivation of AGE1.HN cells with 10 μ M quercetin, a remarkable increase in cell number and product titer at the end of the cultivation was observed. This shows that quercetin has beneficial effects for biopharmaceutical production in AGE1.HN. In the flux analysis, it was observed that quercetin treatment was improving the metabolic phenotype especially at the beginning of the cultivation (Fig. 7-6). While glucose and lactate uptake fluxes slightly decreased, the flux of pyruvate carbons into TCA cycle doubled. The fact that fluxes were mostly different in phase 1 of the cultivation points to a direct influence of quercetin at the beginning of the cultivation. It is possible that quercetin is rapidly taken up and metabolized by the cells. Boulton et al. examined the elimination of quercetin in HepG2 cells (Boulton et al. 1999). They observed that quercetin is rapidly metabolized. Quercetin itself and the different quercetin metabolites might have specific biological actions. This was also confirmed in other studies in which bioactivity and, in particular, cytotoxicity and cytoprotective effects of quercetin and its major *in vivo* metabolites were investigated (Spencer et al. 2003). Since it would be desirable to prolong the positive effect of quercetin on metabolic efficiency observed at the beginning of the cultivation, further studies investigating the metabolic effect of controlled quercetin feeding during cultivation would be interesting. However, as observed in this study, the improved metabolic phenotype and increased culture longevity for AGE1.HN upon a single dose of quercetin at the cultivation start was already remarkable.

The observed dose-dependent effect of quercetin on specific metabolic fluxes, i.e., decreased waste product formation rates and increased flux into TCA cycle, might be caused by an inhibitory effect of

quercetin on lactate dehydrogenase (Grisolia et al. 1975) or by other effects that this compound or derived metabolites exert inside the cell. It has been shown that quercetin can be transported and accumulated in mitochondria preventing mitochondrial damage (Fiorani et al. 2010), but it was also reported that active forms of this compound can oxidize mitochondrial as well as cytosolic NADH (Buss et al. 2005; Chan et al. 1999; Gasparin et al. 2003a; Metodiewa et al. 1999). This leads to a reduced NADH/NAD⁺ ratio and shifts the cellular conditions to a more oxidized state. In the isolated perfused rat liver, it was shown that quercetin stimulates TCA cycle activity which is probably caused by an increased mitochondrial NAD⁺ availability (Buss et al. 2005). Gasparin et al. reported that quercetin inhibits lactate production and decreases cytosolic NADH/NAD⁺ ratio (Gasparin et al. 2003b). Reduced lactate production was also observed in our study on neuronal AGE1.HN cells. An increased oxidation of cytosolic NADH and, therefore, increased NAD⁺ availability which can be induced by quercetin could lead to a shift in the reaction equilibrium of the lactate dehydrogenase catalyzed conversion in the direction of pyruvate. The cellular metabolism has to adapt to the situation which can be accomplished by increased channeling of pyruvate into mitochondria as observed for AGE1.HN upon quercetin treatment. This higher flux into mitochondria and, finally, TCA cycle might be even facilitated by specific changes in mitochondrial physiology induced by quercetin. Mitochondrial oxidation of NADH can reduce the efficiency of the TCA cycle and stimulate its overall activity since higher activity is necessary to provide the same energy level. This would consequently result in an increased metabolite demand for the TCA cycle and higher anaplerotic fluxes. Interestingly, this was exactly what was observed for AGE1.HN. Flux of pyruvate into mitochondria and into TCA cycle was increased in quercetin treated AGE1.HN cells accompanied by an increase in anaplerotic fluxes feeding the cycle.

The increase in culture longevity could be on the one hand due to the improved metabolism with reduced waste product formation. On the other hand, it is also possible that the reported cytoprotective activity of quercetin plays an important role in prolonging cell growth in the cultivation process keeping the viability high. Many studies reported protective effects of quercetin and excellent reviews explain the various functions of flavonoids including the flavonol quercetin in detail (Middleton et al. 2000; Ren et al. 2003). It was also shown that quercetin can be taken up and can accumulate in mitochondria and might help to prevent mitochondrial damage (Fiorani et al. 2010). Ishige et al. found that flavonoids can protect neuronal cells from oxidative stress by different mechanisms (Ishige et al. 2001). Quercetin alters glutathione metabolism and acts as antioxidant at the same time. This protective effect of quercetin might be another reason for the increased culture longevity of the neuronal AGE1.HN cell line when the compound is added to the medium.

7.6 Concluding remarks

In summary, we found that quercetin addition to the culture medium resulted in many beneficial effects on cultivation of the neuronal AGE1.HN cell line. An increase in culture longevity, viable cell density, and final A1AT titer was observed when quercetin was added to the medium accompanied by improved channeling of pyruvate into mitochondria having reduced waste product formation and increased TCA

cycle activity. We postulate that these effects might be induced by (i) inhibitory action of quercetin on specific enzymes, (ii) quercetin induced oxidized state with reduced NADH/NAD⁺ ratio, and (iii) cytoprotective activity. Testing of quercetin on other mammalian cells and testing of other flavonoids would be very interesting and might lead to the discovery of further interesting media additives for cell culture processes. The provided results in this study contribute, additionally, to an improved understanding of the effect of quercetin on human cells in general.

7.7 Acknowledgements

This work has been financially supported by the BMBF project SysLogics - Systems biology of cell culture for biologics (FKZ 0315275A-F). We thank Michel Fritz for valuable assistance with the analytics.

7.8 Supplementary material

The supplementary material for this chapter is given in the supplementary material section at the end of the thesis.

8 Outlook and future prospects

8.1 Improvement of biopharmaceutical production in the AGE1.HN cell line

The results presented in this thesis provide detailed insights into the primary metabolism of AGE1.HN and its adaptation to changing conditions. By interpreting the data, we were able to develop several ideas for improving the cell line or the cultivation conditions. Selected strategies, e.g., reduced substrate levels, were also tested in this thesis and the impact is described. Further genetic engineering of selected targets in AGE1.HN might lead to substantial improvement of the performance of this cell line. Generally, various cellular characteristics can be associated with high productivity (Seth et al. 2006), however, only specific engineering might be appropriate for a particular cell line.

We think that one interesting strategy for improving AGE1.HN may be increasing the connectivity of TCA cycle and glycolysis, as supported by the results presented in chapters 2-4. This might help lower overflow metabolism by reducing the cytosolic pyruvate load and increasing TCA cycle activity. As discussed earlier in the thesis, this strategy implies that additionally produced NADH/FADH₂ can be used and that oxidative phosphorylation activity is not the bottleneck. As shown in chapter 7, addition of quercetin resulted in reduced lactate production and increased channeling of pyruvate into mitochondria. However, we suggest that the increased TCA cycle activity might have been facilitated by prooxidant activity of quercetin which reduces NADH/NAD⁺ ratio. The energy level might have been similar in control and quercetin treated cells since cell growth was also similar. The effect of genetically modified connectivity between glycolysis and TCA cycle in AGE1.HN has still to be tested. Overexpression of a pyruvate carboxylase gene can be a promising strategy to increase pyruvate flux into mitochondria. This is further supported by the fact that we found low intercompartmental pyruvate transport and a high channeling of pyruvate carbons via oxaloacetate into TCA cycle (chapter 3).

Improving the substrate use and decreasing the energy spilling can also be accomplished by a reduction of substrate uptake, in an ideal scenario down to the uptake rate that is just needed for growth and product formation. This issue is discussed in detail in chapter 4, where we were able to show that a reduction in substrate levels improves metabolic efficiency. In fed-batch processes, low concentrations of the main carbon sources, i.e., glucose and glutamine, can be applied which might force the cellular metabolism to operate economically. Other possibilities include specific inhibition of the substrate uptake, e.g., by using inhibitors, genetic engineering of the cellular sugar transport (Wlaschin and Hu 2007), or specific alterations in the medium (Altamirano et al. 2000).

Resistance to high ammonia concentrations or lowering the ammonia formation during the cultivation are issues that have to be addressed mainly in fed-batch processes in which a high cell density and high ammonia concentration are reached. The adaptation of the cellular metabolism to increased ammonia stress is presented in detail in chapter 5. Generally, ammonia formation during fed-batch cultivation of AGE1.HN cells can be fairly well controlled through low feeding of glutamine. Therefore, engineering of AGE1.HN towards lower ammonia formation and increased ammonia fixation should not have priority

over the other strategies discussed in this chapter. However, if this engineering direction is of interest, specific manipulations in the amino acid metabolism might be promising. Ammonia formation could be lowered through increased fixation of free ammonia and storage in extracellular amino acids. Downregulation of the activity of amino acid consuming pathways and upregulation of the activity of transaminases producing amino acids would be a strategy leading to lowered ammonia formation in the process.

Engineering and improvement of protein secretion is another possibility of improving AGE1.HN. Shifting the cellular phenotype closer to one of a professional secretory cell might be accomplished by targeted genetic modifications. In earlier work on regulators of the unfolded protein response, phospholipid biosynthesis, and related ER biogenesis, it was shown, e.g., that overexpression of a global regulator of the unfolded protein response, i.e., X-box binding protein 1 (XBP-1), resulted in ER expansion and increased protein synthesis (Ku et al. 2008; Shaffer et al. 2004; Sriburi et al. 2004; Tigges and Fussenegger 2006). Similar modifications could also be performed in parental AGE1.HN cells which might lead to a new, improved parental cell line with better protein secretion properties and later to better producers. Another direction that would be interesting to follow may be the feeding of specific media additives with high lipid/phospholipid content. This might also facilitate ER biogenesis and, eventually, protein production and secretion.

8.2 Improved metabolic flux studies in mammalian cells

The available methods for metabolic flux analysis in mammalian cells can be applied to provide fascinating insights into numerous biological systems. However, there is still much room for improvement. The information about genomic sequences and the increasing availability of reconstructed genome scale metabolic networks tremendously improve metabolic flux studies and help to set up own models, also, for ^{13}C flux analysis. However, even if the reconstructed metabolic networks rely on accurate genomic information combined with a huge amount of published knowledge, it may still be necessary to study the network topology of a biological system of interest separately, since some genes might not be expressed and the expression of numerous genes might differ, e.g., caused by epigenetic mechanisms. To create a thorough knowledge of active enzymes and pathways, different methods can be applied, e.g., *in vitro* enzyme activity measurements, tracer studies, or proteomic analyses. The acquired information may also be combined to set up a relevant metabolic network model which comes as close as possible to the real situation. The fact that mammalian cells are compartmentalized is another issue so far only rudimentarily considered in metabolic flux studies. However, especially detailed ^{13}C metabolic flux analysis has the potential to unravel fluxes even in a system with several different compartments having different intracellular pools of the same metabolite. The development of new and improved methods makes it possible to determine enzyme activities in different compartments (Niklas et al. 2011a) and future methods might even enable to measure intracellular metabolite concentrations and their labeling in different cell compartments. These improved methods can facilitate in-depth insights into fluxes in and between different cellular compartments and in the underlying regulation (Wahrheit et al. 2011). The

measurement of intracellular metabolite concentrations as well as the labeling patterns of intracellular metabolites seems well established for adherent cells (Ahn and Antoniewicz 2011; Hofmann et al. 2008). For suspension cells, this is still an open question as it is doubtful whether the published methods for intracellular metabolite measurements are really robust enough to permit realistic studies uncorrupted by errors resulting, e.g., from insufficient quenching, cell leakage, or mixing of intracellular metabolites with extracellular species. Different results reported by different groups are confusing and hamper the choice of method (Dietmair et al. 2010; Sellick et al. 2011; Volmer et al. 2011). However, reliable methods for intracellular metabolite extraction would greatly contribute to obtaining further detailed insights into cellular metabolism of industrially relevant suspension cells by metabolic flux analysis. Another very interesting advance would be the aforementioned possibility of measuring metabolites and their labeling even in different cellular compartments. Suitable methods of measuring intracellular metabolite concentrations in different compartments are so far mainly established for plants (Krueger et al. 2011; Ratcliffe and Shachar-Hill 2001). Selective permeabilization (Niklas et al. 2011a) and the development of microfluidic devices (Wurm et al. 2010) might be promising starting points for developing methods for making this possible in suspension-cultured mammalian cells. Transient ^{13}C flux analysis represents a very promising approach to obtain flux estimates on a very short time scale and is, theoretically, well suited to characterize fluxes of mammalian cells in batch and fed-batch processes (Maier et al. 2008). However, reliable data of concentrations and labeling of intracellular metabolites would be required which is still challenging for suspension-cultured cells as discussed before and the computational and modeling part is much more sophisticated compared to the stationary ^{13}C based flux analysis methods.

8.3 Application of the presented metabolic flux analysis methods

The metabolic flux analysis methods that are described in this thesis can be applied to answer scientific questions related to cell metabolism not only in the biotechnological field but also in medical, toxicological, and pharmacological research.

Improved understanding of the metabolism of cell lines in cell culture processes should be a desirable goal since it can speed up and simplify the process development substantially. In general, the important variables in a cell culture process are cell line, media, and process parameters, and all influence productivity and yield. Ultimately, their optimal interplay determines the level of performance. Optimized processes can be achieved through a system-wide understanding, e.g., accomplished by integration of different omics data (Schaub et al. 2011) in which metabolic flux data plays an important role. This understanding and the ability to predict the consequences of specific perturbations on cell physiology and cell culture process can reduce time-consuming “trial and error-” strategy still commonly employed in the development of bioprocesses. Fluxome data for various conditions can be combined with other omics data to provide in-depth insights into cellular physiology and its regulation.

The combined analysis of calculated flux changes over time with measured changes of *in vitro* enzyme activities during cultivation represents an interesting application providing insights into the regulation of *in vivo* enzyme activities. Dynamic flux changes can be calculated by using the presented time resolved flux

analysis method (chapter 2) and subcellular enzyme activities can be determined, e.g., by applying the recently developed selective permeabilization methodology (Niklas et al. 2011a).

The dynamic flux analysis method described in chapter 2 may also be applied for studying dynamic responses of the cellular metabolism to specific perturbations. In this case, metabolite measurements should be performed in short time intervals ensuring reliable monitoring of the metabolic response. Interesting applications are, e.g., the dynamic response of the cellular metabolism to specific effectors or the alterations in the metabolism upon treatment with chemicals or drugs. The application of a time resolved method may be appropriate for many experimental setups in which the metabolism changes dynamically over time and metabolic steady state conditions are not fulfilled.

For detailed insights into cellular metabolism at metabolic steady state, the application of (i) ^{13}C tracers for monitoring the fate and distribution of substrate carbons in the cellular metabolism and (ii) ^{13}C flux analysis using multiple parallel labeling experiments is well suited as presented in chapter 3. Tracing of substrate carbons using ^{13}C labeled substrates can also be performed in situations in which the metabolism changes. In particular, the monitoring of concentration changes of single mass isotopomers is in this case very useful and specific information can be obtained depending on the tracer. Inherent challenges that limit the applicability of stationary ^{13}C metabolic flux analysis on suspension-cultured mammalian cells are attaining metabolic steady state and obtaining reliable and sufficient labeling information. The measurement of intracellular metabolite labeling would be desirable but the available methods of separating cells and medium as well as of quenching are not validated enough and are also not yet routinely applied. Measurement of the labeling in secreted, extracellular metabolites is, therefore, still a good option. However, industrially relevant media are very complex and also usually contain all amino acids severely reducing the number of extracellular metabolites of which the labeling information can be directly applied for stationary ^{13}C metabolic flux analysis, as discussed in chapter 3. Parallel labeling experiments and measurement of the labeling in extracellular metabolites that are not present at the beginning of the cultivation, e.g., lactate, is in this case a solution. Since lactate is derived from the central metabolic hub, i.e. pyruvate, its labeling is very valuable for ^{13}C flux analysis. The missing labeling information from other metabolites can be compensated for by applying parallel labeling experiments with multiple tracers, significantly increasing the information and reducing the uncertainties in calculated flux estimates. This approach has also been applied by Henry and colleagues to analyze the metabolism in HEK-293 cells (Henry and Durocher 2011; Henry et al. 2011).

The presented metabolic flux analysis methods and adapted versions of the metabolic network models have already been applied in additional studies. In particular, stationary ^{13}C flux analysis was well suited to unravel drug induced alterations in the central metabolism of HL-1 cells (Strigun et al. 2011a; Strigun et al. 2011b).

Summary

There is a growing recognition that systems biology studies combining large sets of experimental data with theoretical modeling can contribute tremendously to our understanding of how biological systems function. This integrative strategy can also be applied to improve mammalian cell culture processes based on a thorough understanding of cellular physiology and its regulation. The integration of different omics data and the development of integrated models of production cells might make it easier to predict how cells perform under varying conditions and to design optimized cell culture processes and cell lines in the future. This thesis focused on generating a detailed quantitative description of the primary metabolism of the novel human production cell line AGE1.HN with the aim of applying the acquired knowledge to improve biopharmaceutical production. To this end, experimental methods were developed and established, experimental data sets were generated, different methods for metabolic flux analysis including computational tools were developed and established, metabolic network models were set up, and metabolic fluxes were calculated and analyzed for various conditions. Overall, this thesis contains a broad and deep characterization of cell physiology and primary metabolism of the human cell line AGE1.HN and highlights future prospects for improved biopharmaceutical manufacturing. The main findings obtained and the conclusions drawn from the various studies can be summarized as follows.

The metabolism of mammalian cells in a cell culture process usually changes over time by adapting to different environmental conditions. Analyzing and understanding these metabolic dynamics is important for a targeted optimization of the process conditions or the production cell line. Metabolism of AGE1.HN and metabolic shifts during batch cultivation were quantitatively characterized in the study described in **chapter 2**. Stationary metabolic flux analysis was applied for calculating mean fluxes for distinct metabolic phases. Additionally, a time resolved flux analysis method was developed which makes describing metabolic flux changes over time possible. This method represents a valuable tool to support the development of cell culture media and processes in the future. For the AGE1.HN cell line, it was found that the primary metabolism switched from an inefficient overflow metabolism at the beginning of the cultivation to a very efficient metabolism with low energy spilling during the batch process. It was concluded that the high substrate levels result in a high channeling of pyruvate to lactate. This metabolic inefficiency might be improved, e.g., by the reduction of substrate levels or by genetic engineering.

Detailed insights into the channeling of metabolite carbons and into the metabolic fluxes during overflow metabolism were obtained by applying ^{13}C tracer experiments and ^{13}C metabolic flux analysis. The data are presented in **chapter 3**. The different tracer experiments made possible the unraveling of metabolic connections. Flux from TCA cycle metabolite carbons to glycolytic metabolites was observed. Additionally, we found that lactate and alanine originate from the same pyruvate pool, which is in contrast to certain published hypotheses. The applied ^{13}C metabolic flux analysis approach, in which the data from parallel tracer experiments were combined, proved effective in estimating fluxes in the applied compartmented metabolic network for AGE1.HN. We found that pentose phosphate pathway activity

was low being just around 2 % of the glycolytic flux. This might be compensated for by high malic enzyme flux producing NADPH. Direct transport of pyruvate into mitochondria was almost zero. The pyruvate carbons were mainly channeled via oxaloacetate into mitochondria entering the TCA cycle, which was mainly fed via α -ketoglutarate and oxaloacetate during the overflow metabolism phase investigated. The applied ^{13}C flux analysis method allows a detailed determination of metabolic fluxes in the primary metabolism of mammalian cells and can be used for studying related biological questions. In order to improve metabolic efficiency in the AGE1.HN cell line, engineering strategies focusing on improved metabolite transfer between cytosolic and mitochondrial pyruvate pools could be applied accompanied by improved control and targeted reduction of substrate availability and uptake.

The metabolism in standard batch processes was investigated in the studies presented in chapters 2 and 3. As discussed in chapter 2, the metabolism of AGE1.HN switched from an inefficient metabolic state with high waste product formation to a very efficient metabolic state with favorable flux distribution during the cultivation. It was proposed that the reduction in substrate levels including pyruvate depletion might be responsible for this metabolic shift. However the question was raised: what is the direct adaptation of the metabolism upon perturbation with different substrate load? Understanding the metabolic response of AGE1.HN to various substrate levels was the issue addressed in **chapter 4**. The adaptation of the metabolism to varying pyruvate and glutamine concentrations was investigated using full factorial design. Correlations between changed levels of these two metabolites and several other metabolic parameters were found. One of the most interesting findings was the increasingly inefficient substrate use accompanied by reduced cell growth when the pyruvate level in the medium was increased. In different fed-batch cultivations of an α_1 -antitrypsin producing AGE1.HN cell line, it was observed that the highest viable cell density and product titer were reached when the pyruvate load was minimized, which was accomplished by maintaining low glucose level and no feeding of pyruvate. By using metabolic flux analysis, we were able to show that reduced intracellular pyruvate load resulted in lower waste product formation and higher metabolic efficiency. The higher sensitivity to high pyruvate load and different adaptation of AGE1.HN compared to, e.g., CHO cells might be caused by the generally lower activity of enzymes involved in pyruvate metabolism, as measured in this study. The results presented in chapter 4 prove the hypotheses that have been developed in chapters 2 and 3. The efficiency of the metabolism and, ultimately, the overall performance of AGE1.HN were improved by reducing the substrate levels. Generally, specific differences in the metabolic behavior of AGE1.HN compared to other commonly employed production cell lines were observed, mainly, in the pyruvate metabolism. These differences in the metabolism and in the metabolic machinery of different production cell lines might derive from their specific origin. Depending on the organism and tissue type from which the cell lines are derived, enzyme and transporter properties as well as metabolic requirements might be constrained, e.g., by epigenetic mechanisms.

Another property that varies between cell lines is the response and resistance to high ammonia concentrations in the medium. This toxic metabolite accumulates during cell culture processes and can limit productivity and influence product quality. The alterations imposed by ammonia stress as well as the

adaptation mechanism of the α_1 -antitrypsin producing AGE1.HN cell line were analyzed in detail in the study described in **chapter 5**. Growth and product formation were slightly decreased with increasing ammonia concentration. By using metabolic flux analysis, it was observed that the fluxes in the central energy metabolism were similar at different levels of ammonia stress, whereas specific fluxes in the amino acid metabolism were significantly and dose-dependently changed. We were able to show that the AGE1.HN cell line adapts to high ammonia concentrations by rearranging its amino acid metabolism towards increased fixation of free ammonia and less ammonia production resulting, eventually, in reduced ammonia accumulation in the medium. Fluxes through transaminases in amino acid degradation pathways were reduced along with a reduced uptake of the respective amino acids. Activities of transaminases producing amino acids, e.g., alanine transaminase, were increased leading to the increased storage of excess nitrogen in extracellular amino acids. Glutamate dehydrogenase was increasingly catalyzing the formation of glutamate with increasing ammonia concentration in the medium leading to increased fixation of free ammonia. Additionally, urea production was observed in the AGE1.HN cell line, which is, presumably, solely carried out by arginase II and, therefore, not relevant to the removal of excess ammonia. In summary, the results indicate the existence of an “ammonia sensor” in these cells which might be, in the simplest case, just equilibrium effects leading to the observed adaptations in the metabolism. A mechanistic explanation for the metabolic behavior of this cell line is provided in that same chapter.

The development of high-producing cell lines for biopharmaceutical production is typically impeded by the low frequency of recombinant cell clones producing high levels of the target protein. Identifying the specific properties of the high producers as well as the metabolic and cellular requirements for high-level glycoprotein production might facilitate cell line development and help identify possible genetic engineering targets. This issue is addressed in **chapter 6** in which the changes in the metabolism and the metabolic burden imposed by α_1 -antitrypsin production in AGE1.HN were analyzed. In this study, we compared the properties of a specifically selected high-producing cell line with the parental cell line. By comparing time courses of cellular biomass, metabolites, and selected macromolecules, we were able to identify specific differences between both cell lines. In particular, RNA and lipid fractions were higher in the producer. These specific alterations result, as a consequence, in different anabolic requirements and in specific changes in the metabolism of the cells. Since the cellular glycoprotein synthesis is fairly complex, a network model was set up comprising the whole process. By performing simulations, it was observed that the simulated theoretical metabolite demand corresponds with the observed changes in metabolic profiles, e.g., increased glycine and glutamate production. The increased production of these specific amino acids can be explained by the increased C1 unit and nucleotide demand in the producer, which is due to higher lipid and RNA content in this cell line. Comparison of the metabolic fluxes in both cell lines revealed that the central energy metabolism was similar in both cell lines. However, fluxes in the amino acid metabolism and C1 metabolism were changed according to the altered anabolic demand. In summary, we were able to show that the main cellular properties distinguishing the producer from the parental cell line are increased lipid and RNA fractions resulting in specific metabolic adaptations. The increased RNA content in the

producer is probably due to high levels of the recombinant α_1 -antitrypsin mRNA and, presumably, an increased pool of RNAs encoding for proteins involved in high-level α_1 -antitrypsin production. The increased lipid content points to an expanded secretion machinery in the producer. This might be an adaptation to high-level glycoprotein production or a specific feature of this cell clone which might have led to its selection. This study indicates that the engineering of lipid metabolism and secretory apparatus might be a promising strategy for further improvement in the performance of this cell line.

The findings in chapters 2-4 highlight the possibility of improving biopharmaceutical production in AGE1.HN by optimizing the metabolism towards improved metabolic efficiency and balanced substrate use. In **chapter 7**, it is shown that treatment with the flavonoid quercetin induces changes in the primary metabolism of AGE1.HN resulting in lowered waste product formation, increased TCA cycle fluxes, and, ultimately, increased culture longevity and α_1 -antitrypsin titer. The improved channeling of pyruvate into mitochondria accompanied with a stimulation of TCA cycle activity upon quercetin treatment can be explained by different properties of quercetin and its metabolites. The results provided in chapter 7 show that the application of specific effectors might be a promising strategy for improving the metabolism and for enhancing the yields in cell culture processes.

Finally, an outlook for the future is provided in **chapter 8**. Possibilities of improving the performance of the AGE1.HN cell line are discussed and the future prospects for applying and improving metabolic flux analyses in mammalian cells are presented.

References

- A1AT-Group (1998) Survival and FEV1 decline in individuals with severe deficiency of alpha1-antitrypsin. The Alpha-1-Antitrypsin Deficiency Registry Study Group. *Am J Respir Crit Care Med* 158 (1):49-59
- Ahn WS, Antoniewicz MR (2011) Metabolic flux analysis of CHO cells at growth and non-growth phases using isotopic tracers and mass spectrometry. *Metab Eng* DOI:10.1016/j.ymben.2011.07.002
- Aiba S, Matsuoka M (1978) Citrate Production From n-Alkane by *Candida lipolytica* in Reference to Carbon Fluxes in vivo. *European J Appl Microbiol Biotechnol* 5:247-261
- Akesson M, Forster J, Nielsen J (2004) Integration of gene expression data into genome-scale metabolic models. *Metab Eng* 6 (4):285-293
- al-Rubeai M, Singh RP (1998) Apoptosis in cell culture. *Curr Opin Biotechnol* 9 (2):152-156
- Alberghina L, Westerhoff H (2005) *Systems Biology - Definitions and Perspectives*. Springer,
- Alete DE, Racher AJ, Birch JR, Stansfield SH, James DC, Smales CM (2005) Proteomic analysis of enriched microsomal fractions from GS-NS0 murine myeloma cells with varying secreted recombinant monoclonal antibody productivities. *Proteomics* 5 (18):4689-4704
- Altamirano C, Illanes A, Becerra S, Cairo JJ, Godia F (2006) Considerations on the lactate consumption by CHO cells in the presence of galactose. *J Biotechnol* 125 (4):547-556
- Altamirano C, Illanes A, Casablancas A, Gamez X, Cairo JJ, Godia C (2001) Analysis of CHO cells metabolic redistribution in a glutamate-based defined medium in continuous culture. *Biotechnol Prog* 17 (6):1032-1041
- Altamirano C, Paredes C, Cairo JJ, Godia F (2000) Improvement of CHO cell culture medium formulation: simultaneous substitution of glucose and glutamine. *Biotechnol Prog* 16 (1):69-75
- Altamirano C, Paredes C, Illanes A, Cairo JJ, Godia F (2004) Strategies for fed-batch cultivation of t-PA producing CHO cells: substitution of glucose and glutamine and rational design of culture medium. *J Biotechnol* 110 (2):171-179
- Amaral AI, Teixeira AP, Martens S, Bernal V, Sousa MF, Alves PM (2010) Metabolic alterations induced by ischemia in primary cultures of astrocytes: merging ¹³C NMR spectroscopy and metabolic flux analysis. *J Neurochem* 113 (3):735-748
- Andersen DC, Goochee CF (1995) The effect of ammonia on the O-linked glycosylation of granulocyte colony-stimulating factor produced by chinese hamster ovary cells. *Biotechnol Bioeng* 47 (1):96-105
- Antoniewicz MR, Kelleher JK, Stephanopoulos G (2007) Elementary metabolite units (EMU): a novel framework for modeling isotopic distributions. *Metab Eng* 9 (1):68-86
- Arden N, Betenbaugh MJ (2006) Regulating apoptosis in mammalian cell cultures. *Cytotechnology* 50 (1-3):77-92
- Audsley JM, Tannock GA (2008) Cell-based influenza vaccines: progress to date. *Drugs* 68 (11):1483-1491
- Balcarcel RR, Clark LM (2003) Metabolic screening of mammalian cell cultures using well-plates. *Biotechnol Prog* 19 (1):98-108
- Barnes LM, Moy N, Dickson AJ (2006) Phenotypic variation during cloning procedures: analysis of the growth behavior of clonal cell lines. *Biotechnol Bioeng* 94 (3):530-537
- Beard DA, Babson E, Curtis E, Qian H (2004) Thermodynamic constraints for biochemical networks. *J Theor Biol* 228 (3):327-333
- Becker J, Klopprogge C, Zelder O, Heinzle E, Wittmann C (2005) Amplified expression of fructose 1,6-bisphosphatase in *Corynebacterium glutamicum* increases in vivo flux through the pentose phosphate pathway and lysine production on different carbon sources. *Appl Environ Microbiol* 71 (12):8587-8596
- Beckers S, Noor F, Muller-Vieira U, Mayer M, Strigun A, Heinzle E (2010) High throughput, non-invasive and dynamic toxicity screening on adherent cells using respiratory measurements. *Toxicol In Vitro* 24 (2):686-694
- Bell SL, Bebbington C, Scott MF, Wardell JN, Spier RE, Bushell ME, Sanders PG (1995) Genetic engineering of hybridoma glutamine metabolism. *Enzyme Microb Technol* 17 (2):98-106
- Berg JM, Tymoczko JL, Stryer L (2003) *Biochemie*. 5 edn. Spektrum Akademischer Verlag, Berlin

- Blanchard V, Liu X, Eigel S, Kaup M, Rieck S, Janciauskiene S, Sandig V, Marx U, Walden P, Tauber R, Berger M (2011) N-glycosylation and biological activity of recombinant human alpha1-antitrypsin expressed in a novel human neuronal cell line. *Biotechnol Bioeng* 108 (9):2118-2128
- Boghigian BA, Seth G, Kiss R, Pfeifer BA (2010) Metabolic flux analysis and pharmaceutical production. *Metab Eng* 12 (2):81-95
- Bonarius HP, Hatzimanikatis V, Meesters KP, de Gooijer CD, Schmid G, Tramper J (1996) Metabolic flux analysis of hybridoma cells in different culture media using mass balances. *Biotechnol Bioeng* 50 (3):299-318
- Bonarius HP, Houtman JH, de Gooijer CD, Tramper J, Schmid G (1998a) Activity of glutamate dehydrogenase is increased in ammonia-stressed hybridoma cells. *Biotechnol Bioeng* 57 (4):447-453
- Bonarius HP, Houtman JH, Schmid G, de Gooijer CD, Tramper J (2000) Metabolic-flux analysis of hybridoma cells under oxidative and reductive stress using mass balances. *Cytotechnology* 32 (2):97-107
- Bonarius HP, Ozemre A, Timmerarends B, Skrabal P, Tramper J, Schmid G, Heinzle E (2001) Metabolic-flux analysis of continuously cultured hybridoma cells using $(13)CO_2$ mass spectrometry in combination with $(13)C$ -lactate nuclear magnetic resonance spectroscopy and metabolite balancing. *Biotechnol Bioeng* 74 (6):528-538
- Bonarius HP, Timmerarends B, de Gooijer CD, Tramper J (1998b) Metabolite-balancing techniques vs. ^{13}C tracer experiments to determine metabolic fluxes in hybridoma cells. *Biotechnol Bioeng* 58 (2-3):258-262
- Bonarius HPJ, Schmidt G, Tramper J (1997) Flux analysis of underdetermined metabolic networks: the quest for the missing constraints. *Trends Biotechnol* 15:308-314
- Borys MC, Linzer DI, Papoutsakis ET (1994) Ammonia affects the glycosylation patterns of recombinant mouse placental lactogen-I by chinese hamster ovary cells in a pH-dependent manner. *Biotechnol Bioeng* 43 (6):505-514
- Boulton DW, Walle UK, Walle T (1999) Fate of the flavonoid quercetin in human cell lines: chemical instability and metabolism. *J Pharm Pharmacol* 51 (3):353-359
- Bouzier AK, Goodwin R, de Gannes FM, Valeins H, Voisin P, Canioni P, Merle M (1998) Compartmentation of lactate and glucose metabolism in C6 glioma cells. A ^{13}C and 1H NMR study. *J Biol Chem* 273 (42):27162-27169
- Bradford MM (1976) A rapid and sensitive method for the quantitation of microgram quantities of protein utilizing the principle of protein-dye binding. *Anal Biochem* 72:248-254
- Braissant O, Gotoh T, Loup M, Mori M, Bachmann C (1999) L-arginine uptake, the citrulline-NO cycle and arginase II in the rat brain: an in situ hybridization study. *Brain Res Mol Brain Res* 70 (2):231-241
- Buss GD, Constantin J, de Lima LC, Teodoro GR, Comar JF, Ishii-Iwamoto EL, Bracht A (2005) The action of quercetin on the mitochondrial NADH to NAD(+) ratio in the isolated perfused rat liver. *Planta Med* 71 (12):1118-1122
- Butler M, Spier RE (1984) The effects of glutamine utilisation and ammonia production on the growth of BHK cells in microcarrier cultures. *Journal of Biotechnology* 1 (3-4):187-196
- Cakir T, Alsan S, Saybasili H, Akin A, Ulgen KO (2007) Reconstruction and flux analysis of coupling between metabolic pathways of astrocytes and neurons: application to cerebral hypoxia. *Theor Biol Med Model* 4:48
- Carrell RW, Jeppsson JO, Vaughan L, Brennan SO, Owen MC, Boswell DR (1981) Human alpha 1-antitrypsin: carbohydrate attachment and sequence homology. *FEBS Lett* 135 (2):301-303
- Chan T, Galati G, O'Brien PJ (1999) Oxygen activation during peroxidase catalysed metabolism of flavones or flavanones. *Chem Biol Interact* 122 (1):15-25
- Chen K, Liu Q, Xie L, Sharp PA, Wang DI (2001) Engineering of a mammalian cell line for reduction of lactate formation and high monoclonal antibody production. *Biotechnol Bioeng* 72 (1):55-61
- Cherlet M, Marc A (2000) Stimulation of monoclonal antibody production of hybridoma cells by butyrate: evaluation of a feeding strategy and characterization of cell behaviour. *Cytotechnology* 32 (1):17-29
- Choi S (2007) *Introduction to Systems Biology*. Humana Press, Totowa, New Jersey
- Choi YS, Lee DY, Kim IY, Kang S, Ahn K, Kim HJ, Jeong YH, Chun GT, Park JK, Kim IH (2000) Ammonia removal using hepatoma cells in mammalian cell cultures. *Biotechnol Prog* 16 (5):760-768

- Christensen B, Nielsen J (1999) Isotopomer analysis using GC-MS. *Metab Eng* 1 (4):282-290
- Christensen B, Thykaer J, Nielsen J (2000) Metabolic characterization of high- and low-yielding strains of *Penicillium chrysogenum*. *Appl Microbiol Biotechnol* 54 (2):212-217
- Chu L, Robinson DK (2001) Industrial choices for protein production by large-scale cell culture. *Curr Opin Biotechnol* 12 (2):180-187
- Chusainow J, Yang YS, Yeo JH, Toh PC, Asvadi P, Wong NS, Yap MG (2009) A study of monoclonal antibody-producing CHO cell lines: what makes a stable high producer? *Biotechnol Bioeng* 102 (4):1182-1196
- Clark S, Francis PS, Conlan XA, Barnett NW (2007) Determination of urea using high-performance liquid chromatography with fluorescence detection after automated derivatisation with xanthidol. *J Chromatogr A* 1161 (1-2):207-213
- Cockett MI, Bebbington CR, Yarranton GT (1990) High level expression of tissue inhibitor of metalloproteinases in Chinese hamster ovary cells using glutamine synthetase gene amplification. *Biotechnology (N Y)* 8 (7):662-667
- Cruz HJ, Freitas CM, Alves PM, Moreira JL, Carrondo MJ (2000) Effects of ammonia and lactate on growth, metabolism, and productivity of BHK cells. *Enzyme Microb Technol* 27 (1-2):43-52
- Cruz HJ, Moreira JL, Carrondo MJ (1999) Metabolic shifts by nutrient manipulation in continuous cultures of BHK cells. *Biotechnol Bioeng* 66 (2):104-113
- Dauner M, Sauer U (2000) GC-MS analysis of amino acids rapidly provides rich information for isotopomer balancing. *Biotechnol Prog* 16 (4):642-649
- Des Rosiers C, Lloyd S, Comte B, Chatham JC (2004) A critical perspective of the use of (13)C-isotopomer analysis by GCMS and NMR as applied to cardiac metabolism. *Metab Eng* 6 (1):44-58
- Deshpande R, Yang TH, Heinzle E (2009) Towards a metabolic and isotopic steady state in CHO batch cultures for reliable isotope-based metabolic profiling. *Biotechnol J* 4 (2):247-263
- Deshpande RR, Heinzle E (2009) Online monitoring of oxygen in spinner flasks. *Biotechnol Lett* 31 (5):665-669
- Deshpande RR, Koch-Kirsch Y, Maas R, John GT, Krause C, Heinzle E (2005) Microplates with integrated oxygen sensors for kinetic cell respiration measurement and cytotoxicity testing in primary and secondary cell lines. *Assay Drug Dev Technol* 3 (3):299-307
- Dietmair S, Timmins NE, Gray PP, Nielsen LK, Kromer JO (2010) Towards quantitative metabolomics of mammalian cells: development of a metabolite extraction protocol. *Anal Biochem* 404 (2):155-164
- Dinnis DM, James DC (2005) Engineering mammalian cell factories for improved recombinant monoclonal antibody production: lessons from nature? *Biotechnol Bioeng* 91 (2):180-189
- Doolan P, Melville M, Gammell P, Sinacore M, Meleady P, McCarthy K, Francullo L, Leonard M, Charlebois T, Clynes M (2008) Transcriptional profiling of gene expression changes in a PACE-transfected CHO DUKX cell line secreting high levels of rhBMP-2. *Mol Biotechnol* 39 (3):187-199
- Dorka P, Fischer C, Budman H, Scharer JM (2009) Metabolic flux-based modeling of mAb production during batch and fed-batch operations. *Bioprocess Biosyst Eng* 32 (2):183-196
- Duarte NC, Becker SA, Jamshidi N, Thiele I, Mo ML, Vo TD, Srivas R, Palsson BO (2007) Global reconstruction of the human metabolic network based on genomic and bibliomic data. *Proc Natl Acad Sci U S A* 104 (6):1777-1782
- Eagle H (1959) Amino acid metabolism in mammalian cell cultures. *Science* 130 (3373):432-437
- Elias CB, Carpentier E, Durocher Y, Bisson L, Wagner R, Kamen A (2003) Improving glucose and glutamine metabolism of human HEK 293 and *Trichoplusia ni* insect cells engineered to express a cytosolic pyruvate carboxylase enzyme. *Biotechnol Prog* 19 (1):90-97
- Elsas LJ, Longo N (1992) Glucose transporters. *Annu Rev Med* 43:377-393
- Europa AF, Gambhir A, Fu PC, Hu WS (2000) Multiple steady states with distinct cellular metabolism in continuous culture of mammalian cells. *Biotechnol Bioeng* 67 (1):25-34
- Eyer K, Oeggerli A, Heinzle E (1995) On-line gas analysis in animal cell cultivation: II. Methods for oxygen uptake rate estimation and its application to controlled feeding of glutamine. *Biotechnol Bioeng* 45 (1):54-62
- Ferrer-Miralles N, Domingo-Espin J, Corchero JL, Vazquez E, Villaverde A (2009) Microbial factories for recombinant pharmaceuticals. *Microb Cell Fact* 8:17

- Fiorani M, Guidarelli A, Blasa M, Azzolini C, Candiracci M, Piatti E, Cantoni O (2010) Mitochondria accumulate large amounts of quercetin: prevention of mitochondrial damage and release upon oxidation of the extramitochondrial fraction of the flavonoid. *J Nutr Biochem* 21 (5):397-404
- Fischer E, Zamboni N, Sauer U (2004) High-throughput metabolic flux analysis based on gas chromatography-mass spectrometry derived ^{13}C constraints. *Anal Biochem* 325 (2):308-316
- Fogolin MB, Wagner R, Etcheverrigaray M, Kratje R (2004) Impact of temperature reduction and expression of yeast pyruvate carboxylase on hGM-CSF-producing CHO cells. *J Biotechnol* 109 (1-2):179-191
- Follstad BD, Balcarcel RR, Stephanopoulos G, Wang DI (1999) Metabolic flux analysis of hybridoma continuous culture steady state multiplicity. *Biotechnol Bioeng* 63 (6):675-683
- Fong SS, Burgard AP, Herring CD, Knight EM, Blattner FR, Maranas CD, Palsson BO (2005) In silico design and adaptive evolution of *Escherichia coli* for production of lactic acid. *Biotechnol Bioeng* 91 (5):643-648
- Forbes NS, Clark DS, Blanch HW (2001) Using isotopomer path tracing to quantify metabolic fluxes in pathway models containing reversible reactions. *Biotechnol Bioeng* 74 (3):196-211
- Forbes NS, Meadows AL, Clark DS, Blanch HW (2006) Estradiol stimulates the biosynthetic pathways of breast cancer cells: detection by metabolic flux analysis. *Metab Eng* 8 (6):639-652
- Frame KK, Hu WS (1990) Cell volume measurement as an estimation of mammalian cell biomass. *Biotechnol Bioeng* 36 (2):191-197
- Gambhir A, Korke R, Lee J, Fu PC, Europa A, Hu WS (2003) Analysis of cellular metabolism of hybridoma cells at distinct physiological states. *J Biosci Bioeng* 95 (4):317-327
- Gasparin FR, Salgueiro-Pagadigorria CL, Bracht L, Ishii-Iwamoto EL, Bracht A, Constantin J (2003a) Action of quercetin on glycogen catabolism in the rat liver. *Xenobiotica* 33 (6):587-602
- Gasparin FR, Spitzner FL, Ishii-Iwamoto EL, Bracht A, Constantin J (2003b) Actions of quercetin on gluconeogenesis and glycolysis in rat liver. *Xenobiotica* 33 (9):903-911
- Gebhardt R (1992) Metabolic zonation of the liver: regulation and implications for liver function. *Pharmacol Ther* 53 (3):275-354
- Genzel Y, Dietzsch C, Rapp E, Schwarzer J, Reichl U (2010) MDCK and Vero cells for influenza virus vaccine production: a one-to-one comparison up to lab-scale bioreactor cultivation. *Appl Microbiol Biotechnol* 88 (2):461-475
- Genzel Y, Reichl U (2009) Continuous cell lines as a production system for influenza vaccines. *Expert Rev Vaccines* 8 (12):1681-1692
- Genzel Y, Ritter JB, König S, Alt R, Reichl U (2005) Substitution of glutamine by pyruvate to reduce ammonia formation and growth inhibition of mammalian cells. *Biotechnol Prog* 21 (1):58-69
- Gildea TR, Shermock KM, Singer ME, Stoller JK (2003) Cost-effectiveness analysis of augmentation therapy for severe alpha1-antitrypsin deficiency. *Am J Respir Crit Care Med* 167 (10):1387-1392
- Glacken MW, Fleischaker RJ, Sinskey AJ (1986) Reduction of waste product excretion via nutrient control: Possible strategies for maximizing product and cell yields on serum in cultures of mammalian cells. *Biotechnol Bioeng* 28 (9):1376-1389
- Godia F, Cairo JJ (2002) Metabolic engineering of animal cells. *Bioprocess Biosyst Eng* 24 (5):289-298
- Gotoh T, Araki M, Mori M (1997) Chromosomal localization of the human arginase II gene and tissue distribution of its mRNA. *Biochem Biophys Res Commun* 233 (2):487-491
- Goudar C, Biener R, Boisart C, Heidemann R, Piret J, de Graaf A, Konstantinov K (2010) Metabolic flux analysis of CHO cells in perfusion culture by metabolite balancing and 2D [^{13}C , ^1H] COSY NMR spectroscopy. *Metab Eng* 12 (2):138-149
- Goudar C, Biener R, Zhang C, Michaels J, Piret J, Konstantinov K (2006) Towards industrial application of quasi real-time metabolic flux analysis for mammalian cell culture. *Adv Biochem Eng Biotechnol* 101:99-118
- Graham JW, Williams TC, Morgan M, Fernie AR, Ratcliffe RG, Sweetlove LJ (2007) Glycolytic enzymes associate dynamically with mitochondria in response to respiratory demand and support substrate channeling. *Plant Cell* 19 (11):3723-3738
- Grisolia S, Rubio V, Feijoo B, Mendelson J (1975) Inhibition of lactic dehydrogenase and of pyruvate kinase by low concentrations of quercetin. *Physiol Chem Phys* 7 (5):473-475
- Grotkjaer T, Akesson M, Christensen B, Gombert AK, Nielsen J (2004) Impact of transamination reactions and protein turnover on labeling dynamics in (^{13}C)-labeling experiments. *Biotechnol Bioeng* 86 (2):209-216

- Hansen HA, Emborg C (1994) Influence of ammonium on growth, metabolism, and productivity of a continuous suspension Chinese hamster ovary cell culture. *Biotechnol Prog* 10 (1):121-124
- Harris D, Li L, Chen M, Lagunero F, Go V, Boros L (2011) Diverse mechanisms of growth inhibition by luteolin, resveratrol, and quercetin in MIA PaCa-2 cells: a comparative glucose tracer study with the fatty acid synthase inhibitor C75. *Metabolomics*:1-10
- Hassell T, Gleave S, Butler M (1991) Growth inhibition in animal cell culture. The effect of lactate and ammonia. *Appl Biochem Biotechnol* 30 (1):29-41
- Hayduk EJ, Lee KH (2005) Cytochalasin D can improve heterologous protein productivity in adherent Chinese hamster ovary cells. *Biotechnol Bioeng* 90 (3):354-364
- Heinzle E, Matsuda F, Miyagawa H, Wakasa K, Nishioka T (2007) Estimation of metabolic fluxes, expression levels and metabolite dynamics of a secondary metabolic pathway in potato using label pulse-feeding experiments combined with kinetic network modelling and simulation. *Plant J* 50 (1):176-187
- Heinzle E, Yuan Y, Kumar S, Wittmann C, Gehre M, Richnow HH, Wehrung P, Adam P, Albrecht P (2008) Analysis of ¹³C labeling enrichment in microbial culture applying metabolic tracer experiments using gas chromatography-combustion-isotope ratio mass spectrometry. *Anal Biochem* 380 (2):202-210
- Henry O, Durocher Y (2011) Enhanced glycoprotein production in HEK-293 cells expressing pyruvate carboxylase. *Metab Eng* 2011
- Henry O, Jolicoeur M, Kamen A (2011) Unraveling the metabolism of HEK-293 cells using lactate isotopomer analysis. *Bioprocess Biosyst Eng* 34 (3):263-273
- Henry O, Perrier M, Kamen A (2005) Metabolic flux analysis of HEK-293 cells in perfusion cultures for the production of adenoviral vectors. *Metab Eng* 7 (5-6):467-476
- Hofmann U, Maier K, Niebel A, Vacun G, Reuss M, Mauch K (2008) Identification of metabolic fluxes in hepatic cells from transient ¹³C-labeling experiments: Part I. Experimental observations. *Biotechnol Bioeng* 100 (2):344-354
- Hollemeier K, Velagapudi VR, Wittmann C, Heinzle E (2007) Matrix-assisted laser desorption/ionization time-of-flight mass spectrometry for metabolic flux analyses using isotope-labeled ethanol. *Rapid Commun Mass Spectrom* 21 (3):336-342
- Hong J, Cho S, Yoon S (2010) Substitution of glutamine by glutamate enhances production and galactosylation of recombinant IgG in Chinese hamster ovary cells. *Applied Microbiology and Biotechnology* 88 (4):869-876
- Hung F, Deng L, Ravnkar P, Condon R, Li B, Do L, Saha D, Tsao YS, Merchant A, Liu Z, Shi S (2011) mRNA stability and antibody production in CHO cells: improvement through gene optimization. *Biotechnol J* 5 (4):393-401
- Hyde R, Taylor PM, Hundal HS (2003) Amino acid transporters: roles in amino acid sensing and signalling in animal cells. *Biochem J* 373 (Pt 1):1-18
- Irani N, Wirth M, van Den Heuvel J, Wagner R (1999) Improvement of the primary metabolism of cell cultures by introducing a new cytoplasmic pyruvate carboxylase reaction. *Biotechnol Bioeng* 66 (4):238-246
- Ishige K, Schubert D, Sagara Y (2001) Flavonoids protect neuronal cells from oxidative stress by three distinct mechanisms. *Free Radic Biol Med* 30 (4):433-446
- Jang JD, Barford JP (2000) Effect of feed rate on growth rate and antibody production in the fed-batch culture of murine hybridoma cells. *Cytotechnology* 32 (3):229-242
- Jenkins N, Castro P, Menon S, Ison A, Bull A (1994) Effect of lipid supplements on the production and glycosylation of recombinant interferon-gamma expressed in CHO cells. *Cytotechnology* 15 (1-3):209-215
- John GT, Klimant I, Wittmann C, Heinzle E (2003) Integrated optical sensing of dissolved oxygen in microtiter plates: a novel tool for microbial cultivation. *Biotechnol Bioeng* 81 (7):829-836
- Jordan I, Vos A, Beilfuss S, Neubert A, Breul S, Sandig V (2009) An avian cell line designed for production of highly attenuated viruses. *Vaccine* 27 (5):748-756
- Kaplan RS (2001) Structure and function of mitochondrial anion transport proteins. *J Membr Biol* 179 (3):165-183
- Karnaukhova E, Ophir Y, Golding B (2006) Recombinant human alpha-1 proteinase inhibitor: towards therapeutic use. *Amino Acids* 30 (4):317-332
- Kelleher JK (1999) Estimating gluconeogenesis with [U-¹³C]glucose: molecular condensation requires a molecular approach. *Am J Physiol* 277 (3 Pt 1):E395-400

- Kelleher JK (2001) Flux estimation using isotopic tracers: common ground for metabolic physiology and metabolic engineering. *Metab Eng* 3 (2):100-110
- Kelly E, Greene CM, Carroll TP, McElvaney NG, O'Neill SJ (2010) Alpha-1 antitrypsin deficiency. *Respir Med* 104 (6):763-772
- Kessler N, Thomas-Roche G, Gerentes L, Aymard M (1999) Suitability of MDCK cells grown in a serum-free medium for influenza virus production. *Dev Biol Stand* 98:13-21; discussion 73-14
- Khoo SH, Falciani F, Al-Rubeai M (2007) A genome-wide transcriptional analysis of producer and non-producer NS0 myeloma cell lines. *Biotechnol Appl Biochem* 47 (Pt 2):85-95
- Kiefer P, Heinzle E, Zelder O, Wittmann C (2004) Comparative metabolic flux analysis of lysine-producing *Corynebacterium glutamicum* cultured on glucose or fructose. *Appl Environ Microbiol* 70 (1):229-239
- Kim HU, Kim TY, Lee SY (2008) Metabolic flux analysis and metabolic engineering of microorganisms. *Mol Biosyst* 4 (2):113-120
- Kim SH, Lee GM (2007) Down-regulation of lactate dehydrogenase-A by siRNAs for reduced lactic acid formation of Chinese hamster ovary cells producing thrombopoietin. *Appl Microbiol Biotechnol* 74 (1):152-159
- Kitano H (2005) International alliances for quantitative modeling in systems biology. *Mol Syst Biol* 1:2005 0007
- Koide T, Pang WL, Baliga NS (2009) The role of predictive modelling in rationally re-engineering biological systems. *Nat Rev Microbiol* 7 (4):297-305
- Kola I, Landis J (2004) Can the pharmaceutical industry reduce attrition rates? *Nat Rev Drug Discov* 3 (8):711-715
- Kolarich D, Weber A, Turecek PL, Schwarz HP, Altmann F (2006) Comprehensive glyco-proteomic analysis of human alpha1-antitrypsin and its charge isoforms. *Proteomics* 6 (11):3369-3380
- Korke R, Gatti Mde L, Lau AL, Lim JW, Seow TK, Chung MC, Hu WS (2004) Large scale gene expression profiling of metabolic shift of mammalian cells in culture. *J Biotechnol* 107 (1):1-17
- Koyama AH, Uchida T (1989) The effect of ammonium chloride on the multiplication of herpes simplex virus type 1 in Vero cells. *Virus Res* 13 (4):271-281
- Kramer JA, Sagartz JE, Morris DL (2007) The application of discovery toxicology and pathology towards the design of safer pharmaceutical lead candidates. *Nat Rev Drug Discov* 6 (8):636-649
- Kromer JO, Fritz M, Heinzle E, Wittmann C (2005) In vivo quantification of intracellular amino acids and intermediates of the methionine pathway in *Corynebacterium glutamicum*. *Anal Biochem* 340 (1):171-173
- Kromer JO, Wittmann C, Schroder H, Heinzle E (2006) Metabolic pathway analysis for rational design of L-methionine production by *Escherichia coli* and *Corynebacterium glutamicum*. *Metab Eng* 8 (4):353-369
- Krueger S, Giavalisco P, Krall L, Steinhauser MC, Bussis D, Usadel B, Flugge UI, Fernie AR, Willmitzer L, Steinhauser D (2011) A topological map of the compartmentalized *Arabidopsis thaliana* leaf metabolome. *PLoS One* 6 (3):e17806
- Ku SC, Ng DT, Yap MG, Chao SH (2008) Effects of overexpression of X-box binding protein 1 on recombinant protein production in Chinese hamster ovary and NS0 myeloma cells. *Biotechnol Bioeng* 99 (1):155-164
- Kumar N, Gammell P, Clynes M (2007) Proliferation control strategies to improve productivity and survival during CHO based production culture : A summary of recent methods employed and the effects of proliferation control in product secreting CHO cell lines. *Cytotechnology* 53 (1-3):33-46
- Kurano N, Leist C, Messi F, Kurano S, Fiechter A (1990) Growth behavior of Chinese hamster ovary cells in a compact loop bioreactor. 2. Effects of medium components and waste products. *J Biotechnol* 15 (1-2):113-128
- Kuystermans D, Krampe B, Swiderek H, Al-Rubeai M (2007) Using cell engineering and omic tools for the improvement of cell culture processes. *Cytotechnology* 53 (1-3):3-22
- Lawrence GM, Jepson MA, Trayer IP, Walker DG (1986) The compartmentation of glycolytic and gluconeogenic enzymes in rat kidney and liver and its significance to renal and hepatic metabolism. *Histochem J* 18 (1):45-53
- Le Ru A, Jacob D, Transfiguracion J, Ansoorge S, Henry O, Kamen AA (2010) Scalable production of influenza virus in HEK-293 cells for efficient vaccine manufacturing. *Vaccine* 28 (21):3661-3671
- Lee K, Berthiaume F, Stephanopoulos GN, Yarmush ML (1999) Metabolic flux analysis: a powerful tool for monitoring tissue function. *Tissue Eng* 5 (4):347-368

- Lee WN, Boros LG, Puigjaner J, Bassilian S, Lim S, Cascante M (1998) Mass isotopomer study of the nonoxidative pathways of the pentose cycle with [1,2-¹³C₂]glucose. *Am J Physiol* 274 (5 Pt 1):E843-851
- Lim Y, Wong NS, Lee YY, Ku SC, Wong DC, Yap MG (2010) Engineering mammalian cells in bioprocessing - current achievements and future perspectives. *Biotechnol Appl Biochem* 55 (4):175-189
- Liu CH, Chen LH (2007) Enhanced recombinant M-CSF production in CHO cells by glycerol addition: model and validation. *Cytotechnology* 54 (2):89-96
- Llaneras F, Pico J (2007) A procedure for the estimation over time of metabolic fluxes in scenarios where measurements are uncertain and/or insufficient. *BMC Bioinformatics* 8:421
- Maaheimo H, Fiaux J, Cakar ZP, Bailey JE, Sauer U, Szyperski T (2001) Central carbon metabolism of *Saccharomyces cerevisiae* explored by biosynthetic fractional (¹³C) labeling of common amino acids. *Eur J Biochem* 268 (8):2464-2479
- Maier K, Hofmann U, Bauer A, Niebel A, Vacun G, Reuss M, Mauch K (2009) Quantification of statin effects on hepatic cholesterol synthesis by transient (¹³C)-flux analysis. *Metab Eng* 11 (4-5):292-309
- Maier K, Hofmann U, Reuss M, Mauch K (2008) Identification of metabolic fluxes in hepatic cells from transient ¹³C-labeling experiments: Part II. Flux estimation. *Biotechnol Bioeng* 100 (2):355-370
- Mancuso A, Sharfstein ST, Tucker SN, Clark DS, Blanch HW (1994) Examination of primary metabolic pathways in a murine hybridoma with carbon-13 nuclear magnetic resonance spectroscopy. *Biotechnol Bioeng* 44 (5):563-585
- Martens DE (2007) Metabolic flux analysis of mammalian cells. In: Al-Rubeai M, Fussenegger M (eds) *Systems Biology*, vol 1. Springer, pp 275-299
- Martin HJ, Kornmann F, Fuhrmann GF (2003) The inhibitory effects of flavonoids and antiestrogens on the Glut1 glucose transporter in human erythrocytes. *Chem Biol Interact* 146 (3):225-235
- Martinelle K, Westlund A, Haggstrom L (1998) Saturable ammonium ion transport in myeloma and hybridoma cells is mediated by the Na⁺K⁺2Cl⁻-cotransporter. *Biotechnology Letters* 20 (1):81-86
- Martinez V, Gerdtzen ZP, Andrews BA, Asenjo JA (2010) Viral vectors for the treatment of alcoholism: use of metabolic flux analysis for cell cultivation and vector production. *Metab Eng* 12 (2):129-137
- Mather A, Pollock C (2011) Glucose handling by the kidney. *Kidney Int Suppl* (120):S1-6
- Matsuda F, Morino K, Miyashita M, Miyagawa H (2003) Metabolic flux analysis of the phenylpropanoid pathway in wound-healing potato tuber tissue using stable isotope-labeled tracer and LC-MS spectroscopy. *Plant Cell Physiol* 44 (5):510-517
- Matsuo M, Sasaki N, Saga K, Kaneko T (2005) Cytotoxicity of flavonoids toward cultured normal human cells. *Biol Pharm Bull* 28 (2):253-259
- McKenna MC (2007) The glutamate-glutamine cycle is not stoichiometric: fates of glutamate in brain. *J Neurosci Res* 85 (15):3347-3358
- McQueen A, Bailey JE (1990) Effect of ammonium ion and extracellular pH on hybridoma cell metabolism and antibody production. *Biotechnol Bioeng* 35 (11):1067-1077
- Melzer G, Esfandabadi ME, Franco-Lara E, Wittmann C (2009) Flux Design: In silico design of cell factories based on correlation of pathway fluxes to desired properties. *BMC Syst Biol* 3:120
- Metallo CM, Walther JL, Stephanopoulos G (2009) Evaluation of (¹³C) isotopic tracers for metabolic flux analysis in mammalian cells. *J Biotechnol*
- Metodiewa D, Jaiswal AK, Cenas N, Dickancaite E, Segura-Aguilar J (1999) Quercetin may act as a cytotoxic prooxidant after its metabolic activation to semiquinone and quinoidal product. *Free Radic Biol Med* 26 (1-2):107-116
- Michal G (1999) *Biochemical Pathways*. Spektrum Akademischer Verlag, Heidelberg
- Middleton E, Jr., Kandaswami C, Theoharides TC (2000) The effects of plant flavonoids on mammalian cells: implications for inflammation, heart disease, and cancer. *Pharmacol Rev* 52 (4):673-751
- Miller WM, Wilke CR, Blanch HW (1987) Effects of dissolved oxygen concentration on hybridoma growth and metabolism in continuous culture. *J Cell Physiol* 132 (3):524-530
- Miller WM, Wilke CR, Blanch HW (1988) Transient responses of hybridoma cells to lactate and ammonia pulse and step changes in continuous culture. *Bioprocess Engineering* 3 (1988) 113-122 3 (3):113-122
- Mirabet M, Navarro A, Lopez A, Canela EI, Mallol J, Lluís C, Franco R (1997) Ammonium toxicity in different cell lines. *Biotechnol Bioeng* 56 (5):530-537

- Modak J, Deckwer WD, Zeng AP (2002) Metabolic control analysis of eucaryotic pyruvate dehydrogenase multienzyme complex. *Biotechnol Prog* 18 (6):1157-1169
- Moseley HN (2010) Correcting for the effects of natural abundance in stable isotope resolved metabolomics experiments involving ultra-high resolution mass spectrometry. *BMC Bioinformatics* 11:139
- Nadeau I, Sabatie J, Koehl M, Perrier M, Kamen A (2000) Human 293 cell metabolism in low glutamine-supplied culture: interpretation of metabolic changes through metabolic flux analysis. *Metab Eng* 2 (4):277-292
- Nanchen A, Fuhrer T, Sauer U (2007) Determination of metabolic flux ratios from ¹³C-experiments and gas chromatography-mass spectrometry data: protocol and principles. *Methods Mol Biol* 358:177-197
- Neermann J, Wagner R (1996) Comparative analysis of glucose and glutamine metabolism in transformed mammalian cell lines, insect and primary liver cells. *J Cell Physiol* 166 (1):152-169
- Nguyen B, Jarnagin K, Williams S, Chan H, Barnett J (1993) Fed-batch culture of insect cells: a method to increase the yield of recombinant human nerve growth factor (rhNGF) in the baculovirus expression system. *J Biotechnol* 31 (2):205-217
- Nicholson JK, Connelly J, Lindon JC, Holmes E (2002) Metabonomics: a platform for studying drug toxicity and gene function. *Nat Rev Drug Discov* 1 (2):153-161
- Nielsen J (2003) It is all about metabolic fluxes. *J Bacteriol* 185 (24):7031-7035
- Nielsen LK, Reid S, Greenfield PF (1997) Cell cycle model to describe animal cell size variation and lag between cell number and biomass dynamics. *Biotechnol Bioeng* 56 (4):372-379
- Niittylae T, Chaudhuri B, Sauer U, Frommer WB (2009) Comparison of quantitative metabolite imaging tools and carbon-13 techniques for fluxomics. *Methods Mol Biol* 553:355-372
- Niklas J, Heinzle E (2011) Metabolic flux analysis in systems biology of mammalian cells. *Adv Biochem Eng Biotechnol*:DOI: 10.1007/1010_2011_1099
- Niklas J, Melnyk A, Yuan Y, Heinzle E (2011a) Selective permeabilization for the high-throughput measurement of compartmented enzyme activities in mammalian cells. *Anal Biochem* 416 (2):218-227
- Niklas J, Noor F, Heinzle E (2009) Effects of drugs in subtoxic concentrations on the metabolic fluxes in human hepatoma cell line Hep G2. *Toxicol Appl Pharmacol* 240 (3):327-336
- Niklas J, Priesnitz C, Rose T, Sandig V, Heinzle E (2011b) Primary metabolism in the new human cell line AGE1.HN at various substrate levels: increased metabolic efficiency and α 1-antitrypsin production at reduced pyruvate load. *Appl Microbiol Biotechnol* DOI: 10.1007/s00253-011-3526-6
- Niklas J, Sandig V, Heinzle E (2011c) Metabolite channeling and compartmentation in the human cell line AGE1.HN determined by (¹³C) labeling experiments and (¹³C) metabolic flux analysis. *J Biosci Bioeng* DOI: 10.1016/j.jbiosc.2011.07.021
- Niklas J, Schneider K, Heinzle E (2010) Metabolic flux analysis in eukaryotes. *Curr Opin Biotechnol* 21 (1):63-69
- Niklas J, Schrader E, Sandig V, Noll T, Heinzle E (2011d) Quantitative characterization of metabolism and metabolic shifts during growth of the new human cell line AGE1.HN using time resolved metabolic flux analysis. *Bioprocess Biosyst Eng* 34 (5):533-545
- Nivitchanyong T, Martinez A, Ishaque A, Murphy JE, Konstantinov K, Betenbaugh MJ, Thrift J (2007) Anti-apoptotic genes Aven and E1B-19K enhance performance of BHK cells engineered to express recombinant factor VIII in batch and low perfusion cell culture. *Biotechnol Bioeng* 98 (4):825-841
- Noguchi Y, Saito A, Miyagi Y, Yamanaka S, Marat D, Doi C, Yoshikawa T, Tsuburaya A, Ito T, Satoh S (2000) Suppression of facilitative glucose transporter 1 mRNA can suppress tumor growth. *Cancer Lett* 154 (2):175-182
- Noor F, Niklas J, Muller-Vieira U, Heinzle E (2009) An integrated approach to improved toxicity prediction for the safety assessment during preclinical drug development using Hep G2 cells. *Toxicol Appl Pharmacol* 237 (2):221-231
- Nyberg GB, Balcarcel RR, Follstad BD, Stephanopoulos G, Wang DI (1999a) Metabolic effects on recombinant interferon-gamma glycosylation in continuous culture of Chinese hamster ovary cells. *Biotechnol Bioeng* 62 (3):336-347

- Nyberg GB, Balcarcel RR, Follstad BD, Stephanopoulos G, Wang DI (1999b) Metabolism of peptide amino acids by Chinese hamster ovary cells grown in a complex medium. *Biotechnol Bioeng* 62 (3):324-335
- O'Callaghan PM, James DC (2008) Systems biotechnology of mammalian cell factories. *Brief Funct Genomic Proteomic* 7 (2):95-110
- O'Connell TM, Watkins PB (2010) The application of metabonomics to predict drug-induced liver injury. *Clin Pharmacol Ther* 88 (3):394-399
- Oh HK, So MK, Yang J, Yoon HC, Ahn JS, Lee JM, Kim JT, Yoo JU, Byun TH (2005) Effect of N-Acetylcystein on butyrate-treated Chinese hamster ovary cells to improve the production of recombinant human interferon-beta-1a. *Biotechnol Prog* 21 (4):1154-1164
- Omasa T, Furuichi K, Iemura T, Katakura Y, Kishimoto M, Suga K (2010) Enhanced antibody production following intermediate addition based on flux analysis in mammalian cell continuous culture. *Bioprocess Biosyst Eng* 33 (1):117-125
- Omasa T, Takami T, Ohya T, Kiyama E, Hayashi T, Nishii H, Miki H, Kobayashi K, Honda K, Ohtake H (2008) Overexpression of GADD34 enhances production of recombinant human antithrombin III in Chinese hamster ovary cells. *J Biosci Bioeng* 106 (6):568-573
- Ovadi J, Saks V (2004) On the origin of intracellular compartmentation and organized metabolic systems. *Mol Cell Biochem* 256-257 (1-2):5-12
- Ozturk SS, Riley MR, Palsson BO (1992) Effects of ammonia and lactate on hybridoma growth, metabolism, and antibody production. *Biotechnol Bioeng* 39 (4):418-431
- Paredes C, Prats E, Cairo JJ, Azorin F, Cornudella L, Godia F (1999) Modification of glucose and glutamine metabolism in hybridoma cells through metabolic engineering. *Cytotechnology* 30 (1-3):85-93
- Park H, Kim IH, Kim IY, Kim KH, Kim HJ (2000) Expression of carbamoyl phosphate synthetase I and ornithine transcarbamoylase genes in Chinese hamster ovary dhfr-cells decreases accumulation of ammonium ion in culture media. *J Biotechnol* 81 (2-3):129-140
- Patil KR, Rocha I, Forster J, Nielsen J (2005) Evolutionary programming as a platform for in silico metabolic engineering. *BMC Bioinformatics* 6:308
- Pau MG, Ophorst C, Koldijk MH, Schouten G, Mehtali M, Uytdehaag F (2001) The human cell line PER.C6 provides a new manufacturing system for the production of influenza vaccines. *Vaccine* 19 (17-19):2716-2721
- Pavlou AK, Reichert JM (2004) Recombinant protein therapeutics--success rates, market trends and values to 2010. *Nat Biotechnol* 22 (12):1513-1519
- Petersen S, de Graaf AA, Eggeling L, Mollney M, Wiechert W, Sahm H (2000) In vivo quantification of parallel and bidirectional fluxes in the anaplerosis of *Corynebacterium glutamicum*. *J Biol Chem* 275 (46):35932-35941
- Petrache I, Hajjar J, Campos M (2009) Safety and efficacy of alpha-1-antitrypsin augmentation therapy in the treatment of patients with alpha-1-antitrypsin deficiency. *Biologics* 3:193-204
- Pongratz RL, Kibbey RG, Shulman GI, Cline GW (2007) Cytosolic and mitochondrial malic enzyme isoforms differentially control insulin secretion. *J Biol Chem* 282 (1):200-207
- Puck TT, Cieciura SJ, Robinson A (1958) Genetics of somatic mammalian cells. III. Long-term cultivation of euploid cells from human and animal subjects. *J Exp Med* 108 (6):945-956
- Quek LE, Dietmair S, Kromer JO, Nielsen LK (2010) Metabolic flux analysis in mammalian cell culture. *Metab Eng* 12 (2):161-171
- Quek LE, Nielsen LK (2008) On the reconstruction of the *Mus musculus* genome-scale metabolic network model. *Genome Inform* 21:89-100
- Quek LE, Wittmann C, Nielsen LK, Kromer JO (2009) OpenFLUX: efficient modelling software for ¹³C-based metabolic flux analysis. *Microb Cell Fact* 8:25
- Ramakrishna R, Edwards JS, McCulloch A, Palsson BO (2001) Flux-balance analysis of mitochondrial energy metabolism: consequences of systemic stoichiometric constraints. *Am J Physiol Regul Integr Comp Physiol* 280 (3):R695-704
- Ratcliffe RG, Shachar-Hill Y (2001) Probing Plant Metabolism with Nmr. *Annu Rev Plant Physiol Plant Mol Biol* 52:499-526
- Reichert JM, Rosensweig CJ, Faden LB, Dewitz MC (2005) Monoclonal antibody successes in the clinic. *Nat Biotechnol* 23 (9):1073-1078
- Ren W, Qiao Z, Wang H, Zhu L, Zhang L (2003) Flavonoids: promising anticancer agents. *Med Res Rev* 23 (4):519-534

- Reuveny S, Velez D, Macmillan JD, Miller L (1986) Factors affecting cell growth and monoclonal antibody production in stirred reactors. *J Immunol Methods* 86 (1):53-59
- Ritter JB, Wahl AS, Freund S, Genzel Y, Reichl U (2010) Metabolic effects of influenza virus infection in cultured animal cells: Intra- and extracellular metabolite profiling. *BMC Syst Biol* 4:61
- Rodriguez J, Spearman M, Huzel N, Butler M (2005) Enhanced production of monomeric interferon-beta by CHO cells through the control of culture conditions. *Biotechnol Prog* 21 (1):22-30
- Rose T, Winkler K, Brundke E, Jordan I, Sandig V (2008) Alternative Strategies and New Cell Lines for High-level Production of Biopharmaceuticals. In: Knäblein J (ed) *Modern Biopharmaceuticals*. Wiley-VCH, Weinheim, Germany, Weinheim, Germany, pp 761-777
- Russell JB (2007) The energy spilling reactions of bacteria and other organisms. *J Mol Microbiol Biotechnol* 13 (1-3):1-11
- Ryll T, Valley U, Wagner R (1994) Biochemistry of growth inhibition by ammonium ions in mammalian cells. *Biotechnol Bioeng* 44 (2):184-193
- Salter DW, Custead-Jones S, Cook JS (1978) Quercetin inhibits hexose transport in a human diploid fibroblast. *J Membr Biol* 40 (1):67-76
- Sandig V, Rose T, Winkler K, Brecht R (2005) Mammalian Cells. In: Gellissen G (ed) *Production of Recombinant Proteins: Novel Microbial and Eukaryotic Expression Systems*. Wiley-VCH, Weinheim, Germany, Weinheim, Germany, pp 233-252
- Sanfeliu A, Paredes C, Cairo JJ, Godia F (1997) Identification of key patterns in the metabolism of hybridoma cells in culture *Enzyme Microb Technol* 21 (1):421-428
- Sauer U (2004) High-throughput phenomics: experimental methods for mapping fluxomes. *Curr Opin Biotechnol* 15 (1):58-63
- Sauer U (2006) Metabolic networks in motion: ¹³C-based flux analysis. *Mol Syst Biol* 2:62
- Sauer U, Bailey JE (1999) Estimation of P-to-O ratio in *Bacillus subtilis* and its influence on maximum riboflavin yield. *Biotechnol Bioeng* 64 (6):750-754
- Sauer U, Hatzimanikatis V, Bailey JE, Hochuli M, Szyperski T, Wuthrich K (1997) Metabolic fluxes in riboflavin-producing *Bacillus subtilis*. *Nat Biotechnol* 15 (5):448-452
- Savinell JM, Palsson BO (1992a) Network analysis of intermediary metabolism using linear optimization. I. Development of mathematical formalism. *J Theor Biol* 154 (4):421-454
- Savinell JM, Palsson BO (1992b) Network analysis of intermediary metabolism using linear optimization. II. Interpretation of hybridoma cell metabolism. *J Theor Biol* 154 (4):455-473
- Schaub J, Clemens C, Kaufmann H, Schulz TW (2011) Advancing Biopharmaceutical Process Development by System-Level Data Analysis and Integration of Omics Data. *Adv Biochem Eng Biotechnol* DOI: 10.1007/10_2010_98
- Schmidt K, Carlsen M, Nielsen J, Villadsen J (1997) Modeling isotopomer distributions in biochemical networks using isotopomer mapping matrices. *Biotechnol Bioeng* 55 (6):831-840
- Schmidt K, Marx A, de Graaf AA, Wiechert W, Sahm H, Nielsen J, Villadsen J (1998) ¹³C tracer experiments and metabolite balancing for metabolic flux analysis: comparing two approaches. *Biotechnol Bioeng* 58 (2-3):254-257
- Schneider M, Marison IW, von Stockar U (1996) The importance of ammonia in mammalian cell culture. *J Biotechnol* 46 (3):161-185
- Schumpp B, Schlaeger EJ (1992) Growth study of lactate and ammonia double-resistant clones of HL-60 cells. *Cytotechnology* 8 (1):39-44
- Seamans TC, Gould SL, DiStefano DJ, Silberklang M, Robinson DK (1994) Use of lipid emulsions as nutritional supplements in mammalian cell culture. *Ann N Y Acad Sci* 745:240-243
- Seddon AP, Douglas KT (1981) Photo-induced covalent labelling of malate dehydrogenase by quercetin. *Biochem Biophys Res Commun* 102 (1):15-21
- Segre D, Vitkup D, Church GM (2002) Analysis of optimality in natural and perturbed metabolic networks. *Proc Natl Acad Sci U S A* 99 (23):15112-15117
- Sellick CA, Hansen R, Stephens GM, Goodacre R, Dickson AJ (2011) Metabolite extraction from suspension-cultured mammalian cells for global metabolite profiling. *Nat Protoc* 6 (8):1241-1249
- Selvarasu S, Karimi IA, Ghim GH, Lee DY (2010) Genome-scale modeling and in silico analysis of mouse cell metabolic network. *Mol Biosyst* 6 (1):152-161
- Selvarasu S, Ow DS, Lee SY, Lee MM, Oh SK, Karimi IA, Lee DY (2009a) Characterizing *Escherichia coli* DH5alpha growth and metabolism in a complex medium using genome-scale flux analysis. *Biotechnol Bioeng* 102 (3):923-934

- Selvarasu S, Wong VV, Karimi IA, Lee DY (2009b) Elucidation of metabolism in hybridoma cells grown in fed-batch culture by genome-scale modeling. *Biotechnol Bioeng* 102 (5):1494-1504
- Sengupta N, Rose ST, Morgan JA (2010) Metabolic flux analysis of CHO cell metabolism in the late non-growth phase. *Biotechnol Bioeng*
- Seth G, Hossler P, Yee JC, Hu WS (2006) Engineering cells for cell culture bioprocessing--physiological fundamentals. *Adv Biochem Eng Biotechnol* 101:119-164
- Seth G, Philp RJ, Lau A, Jiun KY, Yap M, Hu WS (2007) Molecular portrait of high productivity in recombinant NS0 cells. *Biotechnol Bioeng* 97 (4):933-951
- Shaffer AL, Shapiro-Shelef M, Iwakoshi NN, Lee AH, Qian SB, Zhao H, Yu X, Yang L, Tan BK, Rosenwald A, Hurt EM, Petroulakis E, Sonenberg N, Yewdell JW, Calame K, Glimcher LH, Staudt LM (2004) XBP1, downstream of Blimp-1, expands the secretory apparatus and other organelles, and increases protein synthesis in plasma cell differentiation. *Immunity* 21 (1):81-93
- Shisheva A, Shechter Y (1992) Quercetin selectively inhibits insulin receptor function in vitro and the bioresponses of insulin and insulinomimetic agents in rat adipocytes. *Biochemistry* 31 (34):8059-8063
- Sidorenko Y, Wahl A, Dauner M, Genzel Y, Reichl U (2008) Comparison of metabolic flux distributions for MDCK cell growth in glutamine- and pyruvate-containing media. *Biotechnol Prog* 24 (2):311-320
- Slivac I, Blajic V, Radosevic K, Kniewald Z, Gaurina Srcek V (2010) Influence of different ammonium, lactate and glutamine concentrations on CCO cell growth. *Cytotechnology* 62 (6):585-594
- Smales CM, Dinnis DM, Stansfield SH, Alete D, Sage EA, Birch JR, Racher AJ, Marshall CT, James DC (2004) Comparative proteomic analysis of GS-NS0 murine myeloma cell lines with varying recombinant monoclonal antibody production rate. *Biotechnol Bioeng* 88 (4):474-488
- Sonntag K, Eggeling L, De Graaf AA, Sahm H (1993) Flux partitioning in the split pathway of lysine synthesis in *Corynebacterium glutamicum*. Quantification by ¹³C- and ¹H-NMR spectroscopy. *Eur J Biochem* 213 (3):1325-1331
- Spencer JP, Kuhnle GG, Williams RJ, Rice-Evans C (2003) Intracellular metabolism and bioactivity of quercetin and its in vivo metabolites. *Biochem J* 372 (Pt 1):173-181
- Sriburi R, Jackowski S, Mori K, Brewer JW (2004) XBP1: a link between the unfolded protein response, lipid biosynthesis, and biogenesis of the endoplasmic reticulum. *J Cell Biol* 167 (1):35-41
- Srivastava S, Chan C (2008) Application of metabolic flux analysis to identify the mechanisms of free fatty acid toxicity to human hepatoma cell line. *Biotechnol Bioeng* 99 (2):399-410
- Stephanopoulos GN, Aristidou AA, Nielsen J (1998) *Metabolic Engineering: Principles and Methodologies*. Academic Press, San Diego
- Street JC, Delort AM, Braddock PS, Brindle KM (1993) A ¹H/¹⁵N n.m.r. study of nitrogen metabolism in cultured mammalian cells. *Biochem J* 291 (Pt 2):485-492
- Strigun A, Noor F, Pironti A, Niklas J, Yang TH, Heinzle E (2011a) Metabolic flux analysis gives an insight on verapamil induced changes in central metabolism of HL-1 cells. *J Biotechnol* DOI:10.1016/j.jbiotec.2011.07.028
- Strigun A, Wahrheit J, Niklas J, Heinzle E, Noor F (2011b) Doxorubicin results in increased oxidative metabolism in HL-1 cardiomyocytes as shown by metabolic flux analysis. Submitted
- Sung YH, Song YJ, Lim SW, Chung JY, Lee GM (2004) Effect of sodium butyrate on the production, heterogeneity and biological activity of human thrombopoietin by recombinant Chinese hamster ovary cells. *J Biotechnol* 112 (3):323-335
- Suthers PF, Burgard AP, Dasika MS, Nowroozi F, Van Dien S, Keasling JD, Maranas CD (2007) Metabolic flux elucidation for large-scale models using ¹³C labeled isotopes. *Metab Eng* 9 (5-6):387-405
- Teixeira AP, Santos SS, Carinhas N, Oliveira R, Alves PM (2008) Combining metabolic flux analysis tools and ¹³C NMR to estimate intracellular fluxes of cultured astrocytes. *Neurochem Int* 52 (3):478-486
- Thorens B, Mueckler M (2010) Glucose transporters in the 21st Century. *Am J Physiol Endocrinol Metab* 298 (2):E141-145
- Thorens B, Vassalli P (1986) Chloroquine and ammonium chloride prevent terminal glycosylation of immunoglobulins in plasma cells without affecting secretion. *Nature* 321 (6070):618-620
- Tigges M, Fussenegger M (2006) Xbp1-based engineering of secretory capacity enhances the productivity of Chinese hamster ovary cells. *Metab Eng* 8 (3):264-272

- Tonelli AR, Brantly ML (2010) Augmentation therapy in alpha-1 antitrypsin deficiency: advances and controversies. *Ther Adv Respir Dis* 4 (5):289-312
- Toya Y, Ishii N, Hirasawa T, Naba M, Hirai K, Sugawara K, Igarashi S, Shimizu K, Tomita M, Soga T (2007) Direct measurement of isotopomer of intracellular metabolites using capillary electrophoresis time-of-flight mass spectrometry for efficient metabolic flux analysis. *J Chromatogr A* 1159 (1-2):134-141
- Trinh CT, Wlaschin A, Sreenc F (2009) Elementary mode analysis: a useful metabolic pathway analysis tool for characterizing cellular metabolism. *Appl Microbiol Biotechnol* 81 (5):813-826
- Tritsch GL, Moore GE (1962) Spontaneous decomposition of glutamine in cell culture media. *Exp Cell Res* 28:360-364
- Trummer E, Fauland K, Seidinger S, Schriebl K, Lattenmayer C, Kunert R, Vorauer-Uhl K, Weik R, Borth N, Katinger H, Muller D (2006) Process parameter shifting: Part I. Effect of DOT, pH, and temperature on the performance of Epo-Fc expressing CHO cells cultivated in controlled batch bioreactors. *Biotechnol Bioeng* 94 (6):1033-1044
- van der Heijden RT, Romein B, Heijnen JJ, Hellinga C, Luyben KC (1994) Linear constraint relations in biochemical reaction systems: II. Diagnosis and estimation of gross errors. *Biotechnol Bioeng* 43 (1):11-20
- van Winden WA, Wittmann C, Heinzle E, Heijnen JJ (2002) Correcting mass isotopomer distributions for naturally occurring isotopes. *Biotechnol Bioeng* 80 (4):477-479
- Velagapudi VR, Wittmann C, Schneider K, Heinzle E (2007) Metabolic flux screening of *Saccharomyces cerevisiae* single knockout strains on glucose and galactose supports elucidation of gene function. *J Biotechnol* 132 (4):395-404
- Villoslada P, Steinman L, Baranzini SE (2009) Systems biology and its application to the understanding of neurological diseases. *Ann Neurol* 65 (2):124-139
- Vo TD, Palsson BO (2006) Isotopomer analysis of myocardial substrate metabolism: a systems biology approach. *Biotechnol Bioeng* 95 (5):972-983
- Volmer M, Northoff S, Scholz S, Thute T, Buntmeyer H, Noll T (2011) Fast filtration for metabolome sampling of suspended animal cells. *Biotechnol Lett* 33 (3):495-502
- Vriezen N, van Dijken JP (1998) Fluxes and enzyme activities in central metabolism of myeloma cells grown in chemostat culture. *Biotechnol Bioeng* 59 (1):28-39
- Wahl A, Sidorenko Y, Dauner M, Genzel Y, Reichl U (2008) Metabolic flux model for an anchorage-dependent MDCK cell line: characteristic growth phases and minimum substrate consumption flux distribution. *Biotechnol Bioeng* 101 (1):135-152
- Wahl SA, Dauner M, Wiechert W (2004) New tools for mass isotopomer data evaluation in (^{13}C) flux analysis: mass isotope correction, data consistency checking, and precursor relationships. *Biotechnol Bioeng* 85 (3):259-268
- Wahrheit J, Nicolae A, Heinzle E (2011) Eukaryotic metabolism: Measuring compartment fluxes. *Biotechnol J* DOI: 10.1002/biot.201100032
- Walsh G (2006) Biopharmaceutical benchmarks 2006. *Nat Biotechnol* 24 (7):769-776
- Walsh G (2010) Biopharmaceutical benchmarks 2010. *Nat Biotechnol* 28 (9):917-924
- Wang Z, Ying Z, Bosty-Westphal A, Zhang J, Schautz B, Later W, Heymsfield SB, Muller MJ (2010) Specific metabolic rates of major organs and tissues across adulthood: evaluation by mechanistic model of resting energy expenditure. *Am J Clin Nutr* 92 (6):1369-1377
- Weber W, Fussenegger M (2007) Inducible product gene expression technology tailored to bioprocess engineering. *Curr Opin Biotechnol* 18 (5):399-410
- Weitzel M, Wiechert W, Noh K (2007) The topology of metabolic isotope labeling networks. *BMC Bioinformatics* 8:315
- Westerhoff HV, Palsson BO (2004) The evolution of molecular biology into systems biology. *Nat Biotechnol* 22 (10):1249-1252
- Wiechert W (2001) ^{13}C metabolic flux analysis. *Metab Eng* 3 (3):195-206
- Wiechert W, de Graaf AA (1996) In vivo stationary flux analysis by ^{13}C labeling experiments. *Adv Biochem Eng Biotechnol* 54:109-154
- Wiechert W, Mollney M, Isermann N, Wurzel M, de Graaf AA (1999) Bidirectional reaction steps in metabolic networks: III. Explicit solution and analysis of isotopomer labeling systems. *Biotechnol Bioeng* 66 (2):69-85
- Wiechert W, Mollney M, Petersen S, de Graaf AA (2001) A universal framework for ^{13}C metabolic flux analysis. *Metab Eng* 3 (3):265-283

- Winnike JH, Li Z, Wright FA, Macdonald JM, O'Connell TM, Watkins PB (2010) Use of pharmacometabonomics for early prediction of acetaminophen-induced hepatotoxicity in humans. *Clin Pharmacol Ther* 88 (1):45-51
- Wittmann C (2002) Metabolic flux analysis using mass spectrometry. *Adv Biochem Eng Biotechnol* 74:39-64
- Wittmann C (2007) Fluxome analysis using GC-MS. *Microb Cell Fact* 6:6
- Wittmann C, Hans M, Heinzle E (2002) In vivo analysis of intracellular amino acid labelings by GC/MS. *Anal Biochem* 307 (2):379-382
- Wittmann C, Heinzle E (1999) Mass spectrometry for metabolic flux analysis. *Biotechnol Bioeng* 62 (6):739-750
- Wittmann C, Heinzle E (2001a) Application of MALDI-TOF MS to lysine-producing *Corynebacterium glutamicum*: a novel approach for metabolic flux analysis. *Eur J Biochem* 268 (8):2441-2455
- Wittmann C, Heinzle E (2001b) MALDI-TOF MS for quantification of substrates and products in cultivations of *Corynebacterium glutamicum*. *Biotechnol Bioeng* 72 (6):642-647
- Wittmann C, Heinzle E (2002) Genealogy profiling through strain improvement by using metabolic network analysis: metabolic flux genealogy of several generations of lysine-producing corynebacteria. *Appl Environ Microbiol* 68 (12):5843-5859
- Wittmann C, Heinzle E (2008) Metabolic Network Analysis and Design in *Corynebacterium glutamicum*. In: Burkovski A (ed) *Corynebacteria: Genomics and Molecular Biology*.
- Wittmann C, Kim HM, Heinzle E (2004) Metabolic network analysis of lysine producing *Corynebacterium glutamicum* at a miniaturized scale. *Biotechnol Bioeng* 87 (1):1-6
- Wittmann C, Kim HM, John G, Heinzle E (2003) Characterization and application of an optical sensor for quantification of dissolved O₂ in shake-flasks. *Biotechnol Lett* 25 (5):377-380
- Wlaschin KF, Hu WS (2007) Engineering cell metabolism for high-density cell culture via manipulation of sugar transport. *J Biotechnol* 131 (2):168-176
- Wurm FM (2004) Production of recombinant protein therapeutics in cultivated mammalian cells. *Nat Biotechnol* 22 (11):1393-1398
- Wurm M, Schopke B, Lutz D, Muller J, Zeng AP (2010) Microtechnology meets systems biology: the small molecules of metabolome as next big targets. *J Biotechnol* 149 (1-2):33-51
- Xie L, Wang DI (1994) Applications of improved stoichiometric model in medium design and fed-batch cultivation of animal cells in bioreactor. *Cytotechnology* 15 (1-3):17-29
- Xie L, Wang DI (1996a) Energy metabolism and ATP balance in animal cell cultivation using a stoichiometrically based reaction network. *Biotechnol Bioeng* 52 (5):591-601
- Xie L, Wang DI (1996b) Material balance studies on animal cell metabolism using a stoichiometrically based reaction network. *Biotechnol Bioeng* 52 (5):579-590
- Xie L, Wang DI (1997) Integrated approaches to the design of media and feeding strategies for fed-batch cultures of animal cells. *Trends Biotechnol* 15 (3):109-113
- Yang M, Butler M (2000) Effects of ammonia on CHO cell growth, erythropoietin production, and glycosylation. *Biotechnol Bioeng* 68 (4):370-380
- Yang M, Butler M (2002) Effects of ammonia and glucosamine on the heterogeneity of erythropoietin glycoforms. *Biotechnol Prog* 18 (1):129-138
- Yang TH, Bolten CJ, Coppi MV, Sun J, Heinzle E (2009) Numerical bias estimation for mass spectrometric mass isotopomer analysis. *Anal Biochem* 388 (2):192-203
- Yang TH, Frick O, Heinzle E (2008) Hybrid optimization for ¹³C metabolic flux analysis using systems parametrized by compactification. *BMC Syst Biol* 2:29
- Yang TH, Wittmann C, Heinzle E (2006a) Respirometric ¹³C flux analysis--Part II: in vivo flux estimation of lysine-producing *Corynebacterium glutamicum*. *Metab Eng* 8 (5):432-446
- Yang TH, Wittmann C, Heinzle E (2006b) Respirometric ¹³C flux analysis, Part I: design, construction and validation of a novel multiple reactor system using on-line membrane inlet mass spectrometry. *Metab Eng* 8 (5):417-431
- Yee JC, Gerdtzen ZP, Hu WS (2009) Comparative transcriptome analysis to unveil genes affecting recombinant protein productivity in mammalian cells. *Biotechnol Bioeng* 102 (1):246-263
- Yoon SK, Song JY, Lee GM (2003) Effect of low culture temperature on specific productivity, transcription level, and heterogeneity of erythropoietin in Chinese hamster ovary cells. *Biotechnol Bioeng* 82 (3):289-298
- Yuan Y, Hoon Yang T, Heinzle E (2010) ¹³C metabolic flux analysis for larger scale cultivation using gas chromatography-combustion-isotope ratio mass spectrometry. *Metab Eng* 12 (4):392-400

- Zamboni N, Fischer E, Sauer U (2005) FiatFlux--a software for metabolic flux analysis from ^{13}C -glucose experiments. *BMC Bioinformatics* 6:209
- Zeng AP, Modak J, Deckwer WD (2002) Nonlinear dynamics of eucaryotic pyruvate dehydrogenase multienzyme complex: decarboxylation rate, oscillations, and multiplicity. *Biotechnol Prog* 18 (6):1265-1276
- Zupke C, Stephanopoulos G (1994) Modeling of Isotope Distributions and Intracellular Fluxes in Metabolic Networks Using Atom Mapping Matrices. *Biotechnol Prog* 10.:489-498
- Zupke C, Stephanopoulos G (1995) Intracellular flux analysis in hybridomas using mass balances and in vitro ^{13}C nmr. *Biotechnol Bioeng* 45 (4):292-303
- Zwingmann C, Leibfritz D (2003) Regulation of glial metabolism studied by ^{13}C -NMR. *NMR Biomed* 16 (6-7):370-399
- Zwingmann C, Richter-Landsberg C, Leibfritz D (2001) ^{13}C isotopomer analysis of glucose and alanine metabolism reveals cytosolic pyruvate compartmentation as part of energy metabolism in astrocytes. *Glia* 34 (3):200-212

Supplementary material

Supplementary material chapter 2

The supplementary material for this chapter is available online:

http://www.springerlink.com/content/b8373v8224272736/449_2010_Article_502_ESM.html.

Supplementary material chapter 3

The supplementary material for this chapter is available online:

<http://www.sciencedirect.com/science/article/pii/S1389172311002982>.

Supplementary material chapter 4

The supplementary material for this chapter is available online:

http://www.springerlink.com/content/g671458385788v17/253_2011_Article_3526_ESM.html.

Supplementary material chapter 5

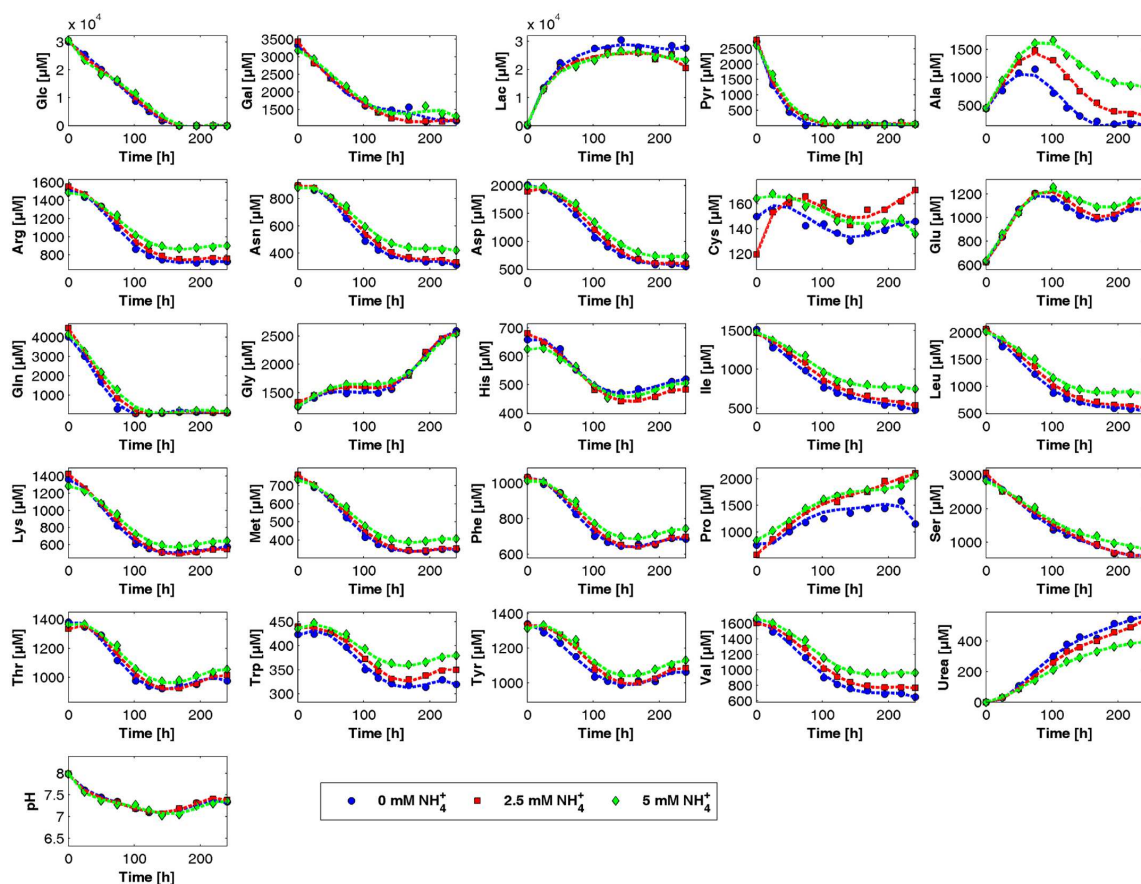


Fig. S1. Metabolic profile of all analyzed metabolites and pH in three different cultivations of AGE1.HNA.AT cells with different ammonia start concentrations (0 mM, 2.5 mM, 5 mM). *Glc* glucose, *Gal* galactose, *Lac* lactate, *Pyr* pyruvate, standard abbreviations for amino acids.

Table S2 Stoichiometric matrix of the model depicted in Fig. 6-4. Stoichiometric coefficients are related to the production of 1 mol A1AT. $f1$ fraction of newly synthesized NTP, $f2$ fraction of recycled NTP ($=1-f1$), m mRNA per translated A1AT protein [mol/mol].

	rA1AT2	rATPc	rUTPc	rCTPc	rATPn	rGTPn	rUTPa	rCTPa	rSug1	rSug2	rSug3	rSug4	rSug5	rSG	rTK	rTL	rA1AT1	rGG	rFP	rPA	rAdem	rNdem	rGdem	rSdem	rDdem	rEdem	rGR
mRNAA1AT	0	0	0	0	0	0	0	0	0	0	0	0	0	0	0	0	0	0	0	0	0	0	0	0	0	0	0
A1ATraw	0	0	0	0	0	0	0	0	0	0	0	0	0	0	0	0	0	0	0	0	0	0	0	0	0	0	0
A1ATmat	-1	0	0	0	0	0	0	0	0	0	0	0	0	0	0	0	0	0	0	0	0	0	0	0	0	0	0
A1Pcom	0	1	0	0	0	0	0	0	0	0	0	0	0	0	0	0	0	0	0	0	0	0	0	0	0	0	0
GTPcom	0	0	1	0	0	0	0	0	0	-1	0	0	0	0	0	0	0	0	0	0	0	0	0	0	0	0	0
UTPcom	0	0	0	1	0	0	0	0	0	0	0	0	-1	0	0	0	0	0	0	0	0	0	0	0	0	0	0
CTPcom	0	0	0	0	1	0	0	0	0	0	0	0	0	0	0	0	0	0	0	0	0	0	0	0	0	0	0
ATPnew	0	fl	0	0	0	0	0	0	0	0	0	0	0	0	0	0	0	0	0	0	0	0	0	0	0	0	0
GTPnew	0	0	0	fl	0	0	0	0	0	0	0	0	0	0	0	0	0	0	0	0	0	0	0	0	0	0	0
UTPnew	0	0	0	0	fl	0	0	0	0	0	0	0	0	0	0	0	0	0	0	0	0	0	0	0	0	0	0
CTPnew	0	0	0	0	0	fl	0	0	0	0	0	0	0	0	0	0	0	0	0	0	0	0	0	0	0	0	0
ATP	0	f2*2	f2*2	f2*2	-7	-8	-5	-1	0	0	-1	0	0	0	0	0	0	0	0	0	0	0	0	0	0	0	0
NAD(P)H	0	0	0	0	0	1	0	0	0	0	0	0	0	0	0	0	0	0	0	0	0	0	0	0	0	0	0
UDP-GlcNAc	0	0	0	0	0	0	0	0	1	-1	0	0	0	0	0	0	0	-12.69	0	0	0	0	0	0	0	0	0
CMP-Neut5Ac	0	0	0	0	0	0	0	0	0	0	0	0	0	0	0	0	-6.681	0	0	0	0	0	0	0	0	0	0
GDP-Man	0	0	0	0	0	0	0	0	0	0	1	-1	0	0	0	0	-9	0	0	0	0	0	0	0	0	0	0
GDP-Fuc	0	0	0	0	0	0	0	0	0	0	0	0	0	0	0	0	-0.321	0	0	0	0	0	0	0	0	0	0
UDP-Gal	0	0	0	0	0	0	0	0	0	0	0	0	1	0	0	0	-6.69	0	0	0	0	0	0	0	0	0	0
Ser	0	0	0	0	0	0	0	0	0	0	0	0	0	-1	0	-25	0	0	0	0	0	0	0	0	0	0	0
Gly	0	0	0	0	0	-1	-1	0	0	0	0	0	0	0	1	0	-24	0	0	0	0	0	0	0	0	0	0
Glu	0	0	0	0	0	2	3	1	0	0	0	0	0	0	0	0	-32	0	0	0	0	0	0	0	0	0	1
Asp	0	0	0	0	-2	-1	-1	0	0	0	0	0	0	0	0	0	-24	0	0	0	0	0	0	0	0	0	0
G6P	0	0	0	0	0	0	0	0	0	0	0	0	-1	0	0	0	0	0	0	0	0	0	0	0	0	0	-1
F6P	0	0	0	0	0	0	0	0	0	0	0	0	0	0	0	0	0	0	0	0	0	0	0	0	0	0	0
PEP	0	0	0	0	0	0	0	0	0	-1	0	0	0	0	0	0	0	0	0	0	0	0	0	0	0	0	0
AcC	0	0	0	0	0	0	0	0	0	0	-1	0	0	0	0	0	0	0	0	0	0	0	0	0	0	0	0
CITHF	0	0	0	0	0	0	0	0	0	0	0	0	0	0	0	0	0	0	0	0	0	0	0	0	0	0	0
R5P	0	0	0	0	0	-2	-2	0	0	0	0	0	0	0	0	0	0	0	0	0	0	0	0	0	0	0	0
	0	0	0	0	-1	-1	-1	0	0	0	0	0	0	0	0	0	0	0	0	0	0	0	0	0	0	0	0

Table S3 Metabolic fluxes in AGE1.HN.AAT and parental AGE1.HN cells.

		AGE1.HN.AAT		AGE1.HN	
Flux no.	Flux description	Flux [$\mu\text{mol/g/h}$]	SD [$\mu\text{mol/g/h}$]	Flux [$\mu\text{mol/g/h}$]	SD [$\mu\text{mol/g/h}$]
<i>Extracellular fluxes</i>					
1	Glc	216.14	6.27	217.32	0.83
2	Gal	19.08	3.43	21.83	2.18
3	Lac	-302.99	16.94	-299.39	0.65
4	Pyr	32.99	2.25	31.72	0.66
5	Ala	-0.70	0.02	-3.66	0.80
6	Arg	6.54	0.45	8.41	0.55
7	Asn	4.26	0.10	3.94	0.38
8	Asp	8.23	0.74	10.10	1.44
9	Cys	0.42	0.42	-0.02	0.78
10	Glu	-4.71	0.16	-3.29	0.40
11	Gln	25.68	0.85	26.57	0.12
12	Gly	-3.40	0.42	-1.32	0.12
13	His	1.70	0.14	1.67	0.15
14	Ile	7.67	0.02	8.41	0.50
15	Leu	11.02	0.41	11.33	0.44
16	Lys	6.38	0.44	6.82	0.12
17	Met	3.19	0.18	3.45	0.19
18	Phe	3.36	0.09	3.21	0.39
19	Pro	-2.79	0.55	-4.15	0.98
20	Ser	16.18	0.69	15.06	1.15
21	Thr	4.19	0.06	4.34	0.65
22	Trp	1.09	0.11	1.14	0.06
23	Tyr	2.76	0.70	4.01	0.85
24	Val	7.82	0.08	8.50	0.77
25	A1AT	0.05	0.00	0.00	0.00
<i>Anabolic fluxes</i>					
26	Carbo	6.65	0.39	7.27	0.82
27	DNA	0.69	0.04	0.75	0.08
28	RNA	2.68	0.16	1.93	0.22
29	Lip	3.08	0.18	2.83	0.32
30	Prot	113.17	6.67	121.77	13.75
<i>Intracellular fluxes</i>					
31	G6P-F6P	224.90	10.28	229.20	4.14
32	F6P-GAP	223.59	10.22	229.20	4.14
33	GAP-Pyr	444.69	20.59	456.13	8.54
34	Pyr-Pyr _m	152.14	37.64	166.14	10.87
35	Pyr _m -AcC _m	144.52	40.52	171.65	11.60
36	OAA/AcC _m -Cit _m	129.81	44.78	172.79	15.03
37	Cit _m -AKG _m	73.27	47.93	122.23	20.74
38	AKG _m -SuC _m	68.26	50.10	121.97	22.11
39	SuC _m -Fum _m	68.67	51.14	125.73	22.35

40	Fum _m -Mal _m	69.74	50.69	128.27	21.65
41	Mal _m -OAA _m	133.90	44.66	173.31	15.21
42	Mal _m -Pyr _m	-7.62	2.88	5.51	0.73
43	Cit _m -Cit _c	56.54	3.15	50.55	5.71
44	Cit _c -AcC/Mal	56.54	3.15	50.55	5.71
45	Mal-Mal _m	56.54	3.15	50.55	5.71
46	G6P-P5P	3.37	0.20	2.68	0.30
47	NADH-OP	451.64	237.57	679.88	91.21
48	FADH ₂ -OP	68.47	52.70	130.26	23.39
49	OP-ATP	1,231.80	672.97	1,895.11	263.10
50	ATP _{wOP}	-5.69	100.57	134.17	89.86
51	ATP _{tot}	1,226.10	773.55	2,029.28	352.96
52	Ala-Pyr	-12.38	0.63	-13.67	0.41
53	Arg-Glu	0.34	0.78	2.08	0.17
54	Asn-Asp	-1.80	0.36	-1.66	0.25
55	Asp-OAA	-4.09	0.13	-0.52	0.18
56	Cys-Pyr	-2.07	0.03	-2.05	0.35
57	Gln-Glu	11.73	1.59	14.10	1.53
58	Glu-AKG _m	-36.84	7.51	-20.44	4.84
59	Ser-Gly	12.47	0.79	10.43	1.04
60	His-Glu	-1.38	0.26	-1.01	0.15
61	Ile-AcC _m /SuC _m	1.67	0.24	2.93	0.11
62	Leu-AcC _m	-1.14	0.88	0.73	0.75
63	Lys-AcC _m	-3.65	0.87	-2.32	0.91
64	Met/Ser-SuC _m /Cys	0.81	0.27	1.38	0.04
65	Phe-Tyr	-1.93	0.28	-1.18	0.11
66	Pro-Glu	-8.18	0.32	-9.02	0.43
67	Ser-Pyr	-7.78	1.72	-6.60	0.96
68	Thr-SuC _m	-2.72	0.21	-1.63	0.02
69	Trp-AcC _m /Ala	-1.38	0.12	-0.20	0.10
70	Tyr-AcC _m /Fum _m	-1.46	0.30	0.52	0.48
71	Val-SuC _m	0.64	0.32	1.07	0.07
72	G6P-Gal _{ER}	0.30	0.01	0.00	0.00
73	F6P/AcC-GlcNAc _{ER}	0.88	0.04	0.00	0.00
74	GlcNAc _{ER} /PEP-Neu5Ac _{ER}	0.30	0.01	0.00	0.00
75	F6P-Man _{ER}	0.42	0.02	0.00	0.00
76	Man _{ER} -Fuc _{ER}	0.01	0.00	0.00	0.00
	TA AKG _m -Glu	-31.84	5.35	-20.18	3.47

Mean values and standard deviations (SD) of two cultivations. Abbreviations as described in Fig. 6-1. *NADH* nicotinamide adenine dinucleotide, *FADH₂* flavin adenine dinucleotide, *ATP* adenosine triphosphate. Fluxes through electron transport chain and oxidative phosphorylation (47-51, not specified in Fig. 6-1): *NADH-OP* (47), NADH flux into electron transport chain, *FADH₂-OP* (48) *FADH₂* flux into electron transport chain, *OP-ATP* (49) ATP produced in oxidative phosphorylation, *ATP_{wOP}* (50) ATP excess from pathways other than oxidative phosphorylation, *ATP_{tot}* (51) total cellular ATP excess.

Acknowledgements

First of all, I want to express my gratitude to Prof. Elmar Heinzle not only for offering me the opportunity to work on this topic, for being a great advisor and a driving force but also for providing the necessary freedom, for opening a lot of doors, and for the chance to take part in meetings, conferences, and workshops. I am very thankful to Prof. Manfred Schmitt for agreeing to review this thesis and for convincing me in a presentation in 2003 to study human and molecular biology in the Saarland.

Many thanks go to Thomas Rose and Volker Sandig from the ProBioGen AG for AGE1.HN and for their good cooperation. I really enjoyed the discussions and our work together. I am indebted to Eva Schröder and Prof. Thomas Noll from the Institute of Cell Culture Technology at the University of Bielefeld. The great, fruitful collaboration contributed very much to the fast progress of my work. I want to thank Stefan Northoff from Teutocell for providing excellent media and for his outstanding help with special orders. I acknowledge the financial support from the German Federal Ministry of Education and Research (BMBF). Thanks to Prof. An-Ping Zeng and Prof. Ralf Pörtner for the great coordination of the SysLogics project.

I have to express many thanks to my diploma, master, and bachelor students Armin Melnyk, Christian Priesnitz, Yannic Nonnenmacher, and Soumyaranjan Mohanty for their great work. Many thanks go to Armin not only for his work on permeabilized cells and enzyme assays but also for being a good friend that is always ready for sport and fun outside the lab. Similarly, I want to thank Christian for his experimental work, for proofreading, and for a lot of fun and laughter that always improved the climate at work. Thanks go to Yannic and Soumyaranjan for their enthusiasm and for performing excellent experiments.

Additionally, I want to thank the whole Biochemical Engineering group for the support, numerous discussions, and valuable help. I want to thank, especially, Michel Fritz for the support and help with different analytics, Robert Schmidt and Veronika Witte for technical support, Susanne Kohring for general help and for organizing and coordinating the institute, Klaus Hollemeyer for providing his expertise in chemistry and mass spectrometry, as well as for a lot of laughter, Konstantin Schneider for having an open ear for questions and for introducing me to the bioreactor. Thanks to Fozia Noor for giving me an introduction into the world of toxicology and cell culture, for a lot of support, and for managing the cell culture lab. Thanks to my co-workers Alexander Strigun and Judith Wahrheit. It was always nice to discuss matters with you and I really enjoyed working together. Special thanks to Judith for excellent proofreading. I want to thank Yongbo Yuan for the joint work, for the funny talks when we met at the weekend, and for his most important help and guidance when I visited China. Thanks to Georg Tascher for a lot of support with different methods for protein analysis, Daniel Müller for help with the GC-TOF instrument, and Saskia Müller for proofreading. I want to thank Averina Nicolae not only for many fruitful discussions about science but also about life in general and for a lot of fun. Thanks to Verena Schütz and Susanne Peifer for general help. I also have to thank, in particular, Verena and Judith

for initiating nice trips to the city after work. I want to express my gratitude to Andrew Cleeve for outstanding help and very important support. Many thanks also to Renate.

Thanks to my ski pals for the best days in the year and for giving me the necessary distraction from work. Special thanks go to Rouven for his infectious passion for the best sport in the world and for organizing great trips. I have to apologize for being unable to join every tour. I also want to thank Michael, Peter, Rouven, Dominik, and Martin for funny trips and evenings. Many thanks to my beloved partner Désirée for her daily support and encouragement, for keeping my feet on the ground, and for so many other things that are too many to mention. Special thanks go to my brother Peter not only for being the best brother ever but also for always helping me, for invaluable support, and for being a friend. I would like to express my deepest gratitude to my parents and grandparents who supported and encouraged me in every situation and aroused my interest in life sciences.

Curriculum vitae

Jens Niklas

Diplom-Biologe, geboren am 12.04.1983 in Neunkirchen Saar

<p>Projektleiter seit 10/2011</p>	<p>Insilico Biotechnology AG</p>
<p>Promotion 10/2008-10/2011</p>	<p>im Rahmen des BMBF-Projekts SysLogics (<i>Systems biology of cell culture for biologics</i>) in Kooperation mit der ProBioGen AG (Berlin) Institut für Technische Biochemie Universität des Saarlandes Titel: <i>“Primary metabolism and its regulation in the human cell line AGE1.HN – application of metabolic flux analysis for improved biopharmaceutical production”</i></p>
<p>Diplomarbeit 01/2008-09/2008</p>	<p>im Rahmen des EU-Projekts Vitrocellomics Institut für Technische Biochemie Universität des Saarlandes Titel: <i>„Physiologische Studien an der Hep G2-Zelllinie zur Testung pharmazeutischer Wirkstoffe“</i></p>
<p>Studium 10/2003-09/2008</p>	<p>Biologie mit Schwerpunkt Humanbiologie und Molekularbiologie Zentrum für Human- und Molekularbiologie Universitätsklinikum Homburg Saar und Universität des Saarlandes Abschluss mit Auszeichnung</p>
<p>Zivildienst 08/2002-06/2003</p>	<p>Ökumenische Sozialstation Kirkel</p>
<p>Schulbildung 07/1993-06/2002 07/1989-07/1993</p>	<p>Gymnasium Johanneum Homburg Grundschule Kirkel-Neuhäusel</p>

<p>Publikationen</p>	
<p>2009</p>	<p>Noor F, Niklas J, Muller-Vieira U, Heinzle E (2009) An integrated approach to improved toxicity prediction for the safety assessment during preclinical drug development using Hep G2 cells. <i>Toxicol Appl Pharmacol.</i> 237(2):221-31.</p> <p>Niklas J, Noor F, Heinzle E (2009) Effects of drugs in subtoxic concentrations on the metabolic fluxes in human hepatoma cell line Hep G2. <i>Toxicol Appl Pharmacol.</i> 240(3):327-36.</p>
<p>2010</p>	<p>Niklas J, Schneider K, Heinzle E (2010) Metabolic flux analysis in eukaryotes. <i>Curr Opin Biotechnol.</i> 21(1):63-9.</p>
<p>2011</p>	<p>Niklas J, Schröder E, Sandig V, Noll T, Heinzle E (2011) Quantitative characterization of metabolism and metabolic shifts during growth of the new human cell line AGE1.HN using time resolved metabolic flux</p>

analysis. *Bioprocess Biosyst Eng.* 34(5):533-45.

Niklas J, Heinzle E (2011)

Metabolic Flux Analysis in Systems Biology of Mammalian Cells. *Adv Biochem Eng Biotechnol.* DOI: 10.1007/10_2011_99.

Niklas J, Melnyk A, Yuan Y, Heinzle E (2011)

Selective permeabilization for the high-throughput measurement of compartmented enzyme activities in mammalian cells. *Anal Biochem.* 416(2):218-27.

Strigun A, Noor F, Pironti A, **Niklas J**, Yang TH, Heinzle E (2011)

Metabolic flux analysis gives an insight on verapamil induced changes in central metabolism of HL-1 cells. *J Biotechnol.* 2011. 20;155(3):299-307.

Niklas J, Sandig V, Heinzle E (2011)

Metabolite channeling and compartmentation in the human cell line AGE1.HN determined by ¹³C labeling experiments and ¹³C metabolic flux analysis. *J Biosci Bioeng.* DOI:10.1016/j.jbiosc.2011.07.021.

Niklas J, Hollemeyer K, Heinzle E (2011)

High-throughput phospholipid quantitation in mammalian cells using MALDI-TOF MS with N-trifluoroacetyl-phosphatidylethanolamine as internal standard. *Anal Biochem.* DOI: 10.1016/j.ab.2011.08.030.

Niklas J, Priesnitz C, Sandig V, Rose T, Heinzle E (2011)

Primary metabolism in the new human cell line AGE1.HN at various substrate levels: increased metabolic efficiency and α_1 -antitrypsin production at reduced pyruvate load. *Appl Microbiol Biotechnol.* DOI: 10.1007/s00253-011-3526-6.

Priesnitz C, **Niklas J**, Sandig V, Rose T, Heinzle E (2011)

Metabolic flux rearrangement in the amino acid metabolism reduces ammonia stress in the α_1 -antitrypsin producing human AGE1.HN cell line. Submitted.

Wahrheit J, **Niklas J**, Heinzle E (2011)

Evaluation of sampling and quenching procedures for the analysis of intracellular metabolites in CHO suspension cells. *BMC Proceedings.* In press.

Niklas J, Sandig V, Heinzle E (2011)

Compartmentation and channeling of metabolites in the human cell line AGE1.HN®. *BMC Proceedings.* In press.

Niklas J, Priesnitz C, Rose T, Sandig V, Heinzle E (2011)

Producer vs. parental cell – metabolic changes and burden upon α_1 -antitrypsin production in AGE1.HN®. *BMC Proceedings.* In press.

Strigun A, Wahrheit J, **Niklas J**, Heinzle E, Noor F (2011)

Doxorubicin results in increased oxidative metabolism in HL-1 cardiomyocytes as shown by metabolic flux analysis. Submitted.

Niklas J, Priesnitz C, Rose T, Sandig V, Heinzle E (2011)

Metabolism and metabolic burden by α_1 -antitrypsin production in human AGE1.HN cells. Submitted.

Niklas J, Nonnenmacher Y, Rose T, Sandig V, Heinzle E (2011)

Quercetin treatment changes fluxes in the primary metabolism and increases culture longevity and recombinant α_1 -antitrypsin production in human

| AGE1.HN cells. Submitted.

Konferenzbeiträge	
2008	<p>Noor F, Niklas J, Müller-Viera U, Mayer M, Heinzle E. A new approach to the improvement of hepatotoxicity prediction during preclinical drug testing. World Pharmaceutical Congress, 11.-14.05.2008, Philadelphia, Pennsylvania, USA.</p> <p>Noor F, Niklas J, Heinzle E. Metabolic flux analysis in Hep G2 cells indicates effects of drugs in subtoxic range. International Conference on Systems Biology (ICSB 2008), 23.-27.08.2008, Gothenburg, Sweden.</p> <p>Noor F, Niklas J, Strigun A, Beckers S, Heinzle E. Improved toxicity prediction for safety assessment of drugs during preclinical drug development using relevant hepatic and cardiac cell lines. 15th Congress on alternatives to animal testing, 19.-21.09.2008, Linz, Austria.</p> <p>Noor F, Strigun A, Niklas J, Beckers S, Heinzle E. Detection of toxic effects by monitoring metabolic processes. The 15th international congress on <i>in vitro</i> toxicology, 24.-28.09.2008, Stockholm, Sweden.</p> <p>Niklas J, Noor F, Heinzle E. Systems biology approach using multiple assay system on Hep G2 cells for safety evaluation in drug development. MipTec: the leading European event for drug discovery technologies, 14.-16.10.2008, Basel, Switzerland.</p> <p>Müller-Vieira U, Noor F, Mayer M, Niklas J, Heinzle E. A new approach to improve prediction of hepatotoxicity during preclinical drug testing. Miptec: the leading European event for drug discovery technologies, 14.-16.10.2008, Basel, Switzerland.</p>
2009	<p>Karschau J, Thiele M, Koch S, Niklas J, Heinzle E, Genzel Y, Kremling A, Reichl U, Marx U, Brecht R. Evaluation of a metabolic flux model for CHO cells to design highly effective fermentation processes. 21st meeting of the European Society for Animal Cell Technology, 7.-10.06.2009, Dublin, Ireland.</p> <p>Niklas J, Schröder E, Noll T, Sandig V, Heinzle E. Time resolved ¹³C metabolic flux analysis for detailed characterization of metabolic shifts in mammalian cells. International Conference Biosystems Analysis and Engineering (BioSys 2009), 15.-16.10.2009, Hamburg, Germany.</p> <p>Niklas J, Heinzle E. Stationary and time resolved ¹³C metabolic flux analysis for detailed characterization of the metabolism of mammalian producer cell lines. First conference of the SYSINBIO project - Systems biology as a driver for industrial biotechnology, 7.-10.12.2009, Istanbul, Turkey.</p>
2010	<p>Melnyk A, Yuan Y, Niklas J, Heinzle E. Determination of enzyme activities and study of subcellular enzyme networks using permeabilized mammalian cells. Analytica, 23.-26.03.2010, München, Germany.</p> <p>Niklas J, Priesnitz C, Sandig V, Heinzle E.</p>

- Quantitative analysis of metabolic dynamics of the new human designer cell line AGE1.HN. Metabolic Engineering VIII: Metabolic Engineering for Green Growth, 13.-18.06.2010, Jeju Island, South Korea.
- 2011 **Niklas J**, Sandig V, Heinzle E.
Metabolite channeling and compartmentation in the human cell line AGE1.HN determined by ¹³C labeling experiments and ¹³C metabolic flux analysis. 22nd ESACT Meeting 2011, 15.-18.05.2011, Vienna, Austria.
- Niklas J**, Priesnitz C, Sandig V, Rose T, Heinzle E.
Integrative analysis of metabolism and metabolic burden upon glycoprotein production in human cell line AGE1.HN. 22nd ESACT Meeting 2011, 15.-18.05.2011, Vienna, Austria.
- Wahrheit J, **Niklas J**, Heinzle E.
Evaluation of sampling and quenching procedures for the analysis of intracellular metabolites in CHO suspension cells. 22nd ESACT Meeting 2011, 15.-18.05.2011, Vienna, Austria.
- Schröder E, Scholz S, **Niklas J**, Rath A, Platas Barradas O, Jandt U, Rose T, Pörtner R, Reichl U, Zeng AP, Heinzle E, Noll T.
Characterization of cultivation of the human cell line AGE1.HN. 22nd ESACT Meeting 2011, 15.-18.05.2011, Vienna, Austria.
- Niklas J**, Priesnitz C, Sandig V, Rose T, Heinzle E.
A₁-antitrypsin for augmentation therapy in hereditary A1AT deficiency – a systems biology approach to optimize its production. International Conference on the Systems Biology of Human Disease, 22-24.06.2011, Boston, MA, USA.
- Wahrheit J, **Niklas J**, Heinzle E.
Metabolic flux dynamics and compartmental enzymes activities of CHO cells. International Conference on Systems Biology (ICSB 2011), 28.08.-01.09.2011, Mannheim/Heidelberg, Germany.
-